Reviving H-phosphonate Chemistry: Novel Methods for Sustainable Oligonucleotide Synthesis

James D. Thorpe

Department of Chemistry

McGill University

Montreal, QC, Canada

April 2023

A thesis submitted to McGill University in partial fulfillment of the requirements of the degree of

Doctor of Philosophy

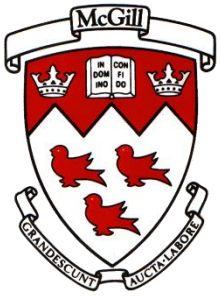

Dedicated to my grandparents Essie, Charlie, Anne, and Bill.

Although they didn't have the chance to be here for this, I hope they would have been proud.

Copyright Statements

Figure 1.3 includes images obtained from Blackburn, G. M.; Gait, M. J.; Williams, D. M.; Loakes, D. *Nucleic acids in chemistry and biology*; Royal Society of Chemistry, 2006.

Figures 1.4 and 1.5 includes images obtained from Deleavey, G. F.; Damha, M. J. Designing chemically modified oligonucleotides for targeted gene silencing. Chemistry & biology 2012, 19 (8), 937-954.

Figure 2.2 includes images obtained from Andrews, B. I.; Antia, F. D.; Brueggemeier, S. B.; Diorazio, L. J.; Koenig, S. G.; Kopach, M. E.; Lee, H.; Olbrich, M.; Watson, A. L. Sustainability challenges and opportunities in oligonucleotide manufacturing. The Journal of Organic Chemistry 2020, 86 (1), 49-61.

Figure 4.1 includes images obtained from Hope, K. S.; Lloyd, H. J.; Ward, D.; Michalchuk, A. A.; Pulham, C. R. Resonant acoustic mixing and its applications to energetic materials. New Trends in Research of Energetic Materials 2015, 134-143.

Preface and contributions

General guidance and troubleshooting throughout this thesis were provided by Dr. Masad J. Damha.

Dr. Tomislav Friščić and his group members (Dr. Davin Tan and Christopher Nickels) were instrumental in **Chapters 2** and **3** in providing access to vibrational ball milling instruments. Their encouragement and discussions and help with running those experiments is greatly appreciated. Dr. Tomislav Friščić (and Cameron Lennox) also graciously allowed us use of his resonant acoustic mixing instrument for work carried out in **Chapter 4**. Dr. Daniel O'Reilly was also instrumental in this work and helped to guide me in the early days of it.

Dr. Stefan Koenig and the rest of the American Chemical Society Green Chemistry Institute Pharmaceutical Roundtable provided valuable insight for the resonant acoustic mixing experiments carried out in **Chapter 4**.

Dr. Paolo Filipponi and Dr. Julien Haber from Novartis AG provided an initial push for the thermally controlled oligonucleotide synthesis strategy developed in **Chapter 4**. We remain eternally grateful to them for their faith and patience in us when pursuing this project.

All experiments contained in this thesis are the work of the author.

Abstract

The rapid growth of nucleic acid therapeutics has exponentially increased the demand for synthetic, chemically modified oligonucleotides. Solid-phase oligonucleotide synthesis (SPOS) using phosphoramidite chemistry is currently the gold-standard for the synthesis of therapeutic oligonucleotides at all scales. Despite regularly achieving very high (>99%) coupling yields and a simple purification process, SPOS relies on huge volumes of toxic and flammable organic solvents (acetonitrile, pyridine) which is a huge issue both economically and environmentally. This thesis focuses on the development of novel methods for the synthesis of oligonucleotides with an emphasis on improving the sustainability of the process.

Mechanochemistry has emerged over the past few decades as a valuable strategy to improve the sustainability of chemical processes. By using mechanical forces, such as grinding, milling, or shearing, chemical reactions can often be carried out completely solvent-free, or in the presence of stoichiometric amounts of solvents. In light of this, we have demonstrated the first use of vibration ball milling (VBM), a mechanochemical method, for the synthesis of short oligonucleotides. Using modified H-phosphonate chemistry, we were able to synthesize up to a DNA hexamer using VBM, as well as demonstrating the applicability to 2′-modified nucleosides, RNA, and both phosphodiester and phosphorothioate backbones in good yields. This method reduced the solvent consumption by up to 90% during reactions, but still relied on column chromatography for purification.

Resonant acoustic mixing (RAM), a highly efficient mixing process, has also recently found applications in driving chemical reactions. In a similar strategy to the VBM approach, we demonstrated the first synthesis of DNA dimers and trimers using RAM. The yield was improved as compared to VBM while also reducing solvent consumption by up to 90% during reactions and the method was demonstrated to be straightforward to scaleup.

SPOS relies on a solid, insoluble support, but many oligonucleotide synthesis strategies have also taken advantage of soluble supports for liquid-phase oligonucleotide synthesis (LPOS). However, most LPOS strategies require many operational steps (precipitations, filtrations, recrystallizations) and still consume large volumes of solvent. We developed a completely novel strategy for the synthesis of oligonucleotides on a soluble polyethylene glycol (PEG) support where reactions are controlled and purified by simple control of temperature. This thermally

controlled oligonucleotide synthesis (TCOS) strategy was applied to the synthesis of a trimer with high coupling yields (93-99%) while simultaneously reducing overall solvent consumption by up to 95%.

Analysis of the methods developed in this thesis compared to industry standards and literature protocols by comparison of process mass intensity (PMI) showed TCOS to greatly reduce solvent consumption, even at a small scale. VBM and RAM did not demonstrate the desired reduction in PMI due to the use of column chromatography, but a non-linear scaling of solvent consumption warranted another analysis. Should some metrics be improved, VBM and RAM could be viable for scaling up. The methods developed in this thesis offer new alternatives for the synthesis of oligonucleotides in a more sustainable manner.

Résumé

La croissance rapide des thérapies à base d'acides nucléiques a augmenté de manière exponentielle la demande d'oligonucléotides synthétiques et chimiquement modifiés. La synthèse d'oligonucléotides en phase solide (SOPS) utilisant la chimie des phosphoramidites est actuellement la norme de référence pour la synthèse d'oligonucléotides thérapeutiques à toutes les échelles. Malgré l'obtention régulière de rendements de couplage très élevés (>99%) et d'un processus de purification simple, le SOPS repose sur des volumes énormes de solvants organiques toxiques et inflammables (acétonitrile, pyridine), ce qui pose un énorme problème tant sur le plan économique qu'environnemental. Cette thèse se concentre sur le développement de nouvelles méthodes pour la synthèse d'oligonucléotides en mettant l'accent sur l'amélioration de la durabilité du processus.

La mécanochimie s'est imposée au cours des dernières décennies comme une nouvelle stratégie pour l'amélioration de la durabilité des processus chimiques. En utilisant des forces mécaniques, telles que le broyage, le fraisage ou le cisaillement, les réactions chimiques peuvent souvent être effectuées sans aucun solvant ou en présence de quantités stœchiométriques de solvants. Dans ce contexte, nous avons démontré la première utilisation du broyage à billes vibrant (BBV), une méthode mécanochimique, pour la synthèse d'oligonucléotides courts. En utilisant une chimie H-phosphonate modifiée, nous avons pu synthétiser jusqu'à un hexamère d'ADN en utilisant BBV, ainsi que démontrer l'applicabilité aux nucléosides 2'-modifiés, à l'ARN et aux squelettes phosphodiester et phosphorothioate avec de bons rendements. Cette méthode a permis de réduire la consommation de solvant jusqu'à 90% au cours des réactions, mais la purification reste tributaire de la chromatographie sur colonne.

Le mélange par résonance acoustique (RAM), un processus de mélange très efficace, a également récemment trouvé des applications dans la conduite de réactions chimiques. Dans une stratégie similaire à l'approche du BBV, nous avons démontré la première synthèse de dimères et de trimères d'ADN en utilisant le RAM. Le rendement a été amélioré par rapport au BBV tout en réduisant la consommation de solvant jusqu'à 90% au cours des réactions et la méthode s'est avérée simple à mettre à l'échelle.

La SOPS repose sur un support solide et insoluble, mais de nombreuses stratégies de synthèse d'oligonucléotides ont également tiré parti de supports solubles pour la synthèse

d'oligonucléotides en phase liquide (SOPL). Cependant, la plupart des stratégies de SOPL nécessitent de nombreuses étapes opérationnelles (précipitations, filtrations, recristallisations) et consomment toujours de grands volumes de solvant. Nous avons développé une stratégie entièrement nouvelle pour la synthèse d'oligonucléotides sur un support soluble en polyéthylène glycol (PEG) où les réactions sont contrôlées et purifiées par un simple contrôle de la température. Cette stratégie de synthèse d'oligonucléotides thermiquement contrôlée (SOTC) a été appliquée à la synthèse d'un trimère avec des rendements de couplage élevés (93-99%) tout en réduisant simultanément la consommation globale de solvant jusqu'à 95%.

L'analyse des méthodes développées dans cette thèse par rapport aux normes industrielles et aux protocoles littéraires par comparaison de l'intensité massique du processus (IMP) a montré que SOTC réduisait considérablement la consommation de solvant, même à petite échelle. Le BBV et le RAM n'ont pas démontré la réduction souhaitée du IMP en raison de l'utilisation de la chromatographie sur colonne, mais une échelle non linéaire de la consommation de solvant a justifié une autre analyse et nous avons constaté que si certains paramètres étaient améliorés, le BBV et le RAM pourraient être faisable pour une mise à l'échelle. Les méthodes développées dans cette thèse offrent de nouvelles alternatives pour la synthèse d'oligonucléotides de manière plus durable.

Acknowledgements

I first met Dr. Damha in 2014 when I was in my final semester at Dawson College. One of my final projects (for an English class) was to interview somebody and describe the organization of a company or department. Having been recently accepted into Chemistry at McGill, I emailed Dr. Damha, the chair of the department at the time, and asked to interview him. The fact that he took the time to sit down with me despite not even being a student at McGill yet, speaks volumes to who he is as a person. We met again in 2016 when he took a chance on me and allowed me to carry out research in his lab for a summer, even though I didn't have the best grades. From there, I did my honors project with him and then continued to do my PhD with him. For all the past years working with Dr. Damha, I am truly grateful to have had him as a supervisor. His laidback attitude and hands-off approach really let me grow as a scientist on my own, but he was always there to refocus me, offer words of encouragement, or get me to redraw a mechanism. His passion and genuine desire to see his students succeed are rare in this world. Dr Damha, thank you for all you have done for me.

To the Damha lab, thank you for welcoming me as an undergrad and seeing me out with a PhD. To Dan, Leonora, and Roberto, who became "us girls bffls", thank you for making the lab a great place to work, even when the work was slow. Dan, thank you teaching me the ins and outs of nucleic acid chemistry when I first joined the Damha lab as an undergrad. Despite the absolutely disgusting state of your fumehood, you still manage to teach me a few things and I'm proud of the work we've done together. Leonora, thanks for understanding the memes I made and encouraging me to post them on Twitter. I would also like to thank you for the wine glasses, which hold a special place in my heart. Roberto, thanks for the constant gossip and always keeping me in the loop. Truly, I aspire to not tolerate other people's garbage as little as you do.

To Danielle, thanks for all your help in the early days in learning H-phosphonate chemistry. Thank you (and Mitch) for also being great supervisors when I was a TA for you, I genuinely would not have wanted to TA for anybody else. To Sunit, thank you for teaching me to work smart and not hard and for all the good times we have had together. To Hala, thanks for the "bring sally up" challenges and inspiring me with your work ethic. To all the other members of the Damha lab past and present I had the pleasure of overlapping with: Maryam, Jovanka, Elise, Luisa, Israel, Ada, Adam, Halle, Julian, Zidi, Miguel, Henri, thank you all. Thank you also to the

Luedtke lab who we have had the pleasure of sharing space with for the past few years, your insight and expertise has been invaluable.

In the rest of the McGill Chemistry Department, I would like to thank a few people. Linda, for always giving us a head start when there was free food in the department, or saving us leftovers, you have no idea how much that meant to a hungry grad student and for always being so positive. To Alex, thank you for taking the time to analyze data with me and helping me to figure out what was going on in my reactions. And, when we weren't talking about science, it was always a pleasure to talk to you about travelling and Hawai'i. To Nadim, thank you also for taking the time to help me with my data and help with analyzing some complex samples. To Robin, thank you for keeping the NMR facility running in top shape during most of my PhD and fixing any problems quickly and efficiently. To Tomislav, who I had the pleasure of collaborating with on the mechanochemistry work, thanks for always thinking big and pushing us to aim high. To Sam, who I've known since I was an undergrad and though our hallway encounters slowly dwindled over the years, it was always nice to catch up with you. I would also like to thank my committee members: Dr. C. J. Li, thank you for your valuable insight and great fundamental chemistry questions and Dr. Youla Tsantrizos, thank you for always pushing me to think about the big picture and the applications of my work.

Outside of the lab, there are too many people who have made this process possible and bearable. To Nik, thanks for all the 30-minute seshes on the way home, skiing, biking, poker (with Ingrid) and all the other times we've hung out, or just spoke on the phone. Your friendship means the world to me. To Flu (Zach), I don't even know if we've hung out one on one? Maybe, but I've blacked it out. In all seriousness, thank you for all the laughs and the good times. To Kevin, thanks for always being willing to put in some work on the court when I needed to clear my mind. To Migs, thanks for being the most insane guy I know. You are the dog. To Max, thanks for being a bad guy. To my other high school friends: Aaron, Camille, Patrick, Annie, thank you for being a great group over the years.

To the original DBEC (Large Cheddar) squad, Sean and John, thanks for surviving that rough winter of 2017 with me. Thanks for the truly unhinged times between nights at Chez Serge, to Halo 3 rockets, bing bong, and everything in between. To Josh, thanks for taking those guys down a level when they needed it or gassing up Lucas at pub Antelo. Our ski nights were truly a

period of peace in times of chaos for me, we'll be hitting gainers in no time. To the rest of the Beters; Bennet, Sab, Kristi, Jenna, Savanna, Felicia, Carina, and Kayla, thanks for all the fun nights out and potlucks. To the Meatballs (Mitch, John, Ben, Egil), thanks for hooping and being one of the most fun basketball teams I've played on, let's bring home the 'chip. Finally, to the Yes Gang (of which there are too many to name), although we (Andrea and I) are relatively new to the crew, thank you for being so welcoming and always being down to do something.

To my family, thank you for being a constant source of support for me over the years. To my parents Janice and Ken, whether it was a homecooked meal, a delivery of leftovers, or helping with a much needed vacation thank you so much everything. Thank you for instilling in me a love of learning and a curiosity about the world around me. Without your support I never would have made it even half this far. To my brother Jono, and Megan. Thank you for always having something to do and encouraging us to hang out and relax a bit. Whether it was a night playing Betrayal, our many nights at trivia, or anything else, it was always a welcome distraction and helped me immensely. To the final member of my immediate family who has been there through thick and thin and is the best listener around, thank your Porkchop. I would also like to thank my aunts Charna (and Mark, Michael, and Mego) and Carole, for their words of encouragement over the years and genuine interest in my work.

I would like to thank my second family as well, my soon to be in-laws. To Michel and Reine, thank you for being like a second set of parents to me. Your help in every aspect has been amazing and I am grateful to be a part of your family. To Emilie & Matt and Gab & Michelle, it has been a pleasure seeing you almost every Friday night for the past five years and I hope we can continue the tradition moving forward. To Lauren and Nir, who welcomed me into their home time after time. Whether you just wanted a free babysitter or not for Sienna and Romy, I appreciate everything you have done for me and I never imagined I would care for your daughters so much. To the rest of the Lallouz and Kakon extended family of which there are far too many to name, thank you all for welcoming me with open arms.

Finally, I would like to thank Andrea from the bottom of my heart. Andy, I can say with 100% certainty I would not be here without you. You inspire me every day to be better, do better, and feel better, even when I don't want to. From talking through reactions that didn't work with me or helping me to format this very thesis, I can't even express how much I appreciate everything

you've done for me. I know it hasn't been easy for you during this time, but your ability to make me laugh and laugh with me through anything has made it all bearable. Knowing that I can come home to you every day for the rest of my life makes me all the more excited for the rest of it. There is genuinely nobody that knows me like you do and your unwavering faith in me despite my own self-doubts makes me feel like everything well be okay. I can't wait for our next adventure and look forward to whatever the next challenge is for us to overcome. You are my teammate forever and I love you.

Table of Contents

List of figures

List of schemes

List of tables

List of abbreviations

A	Adenine
Ac	Acetyl
Ac_2O	Acetic anhydride
ACN	Acetonitrile
AcOH	Acetic acid
AdaCl	Adamantane chloride
Ade	Adenine
ALE	Acetal levulinyl ester
ANA	Arabinonucleic acid
ASO	Antisense oligonucleotide
Bz	Benzoyl
C	Cytosine
CDN	Cyclic dinucleotide
CPG	Controlled pore glass
CPTP	*N*-[(4-Chlorophenyl)sulfanyl]phthalimide
CRISPR	Clustered regularly interspersed palindromic repeats
CTP	(2-Cyanoethyl)thiophthalimide
CTS	*N*-[(2-cyanoethyl)sulfanyl]succinimide
Cyt	Cytosine
DBU	1,8-Diazabicyclo[5.4.0]undec-7-ene
DCA	Dichloroacetic acid
DCC	Dicyclohexylcarbodiimide
DCE	1,2-Dichloroethane
DCM	Dichloromethane
DCPP	di-(2-chlorophenyl)phosphorochloridate
DIPEA	Diisopropylethylamine
DMAP	4-Dimethylaminopyridine
DMF	Dimethylformamide
DMTr	Dimethoxytrityl
DNA	Deoxyribonucleic acid

DPC	Diphenylphosphoryl chloride
DPCP	(*N*,*N*-Diisopropylamino)cyanoethyl phosphonamidic-Cl
DPHP	Diphenyl hydrogen phosphite
Et_2O	Diethyl ether
EtOH	Ethanol
ETT	5-(Ethylthio)-1*H*-tetrazole
F	Fluoro
FANA	2'-Fluoroarabinonucleic acid
G	Guanine
Gua	Guanine
HNA	Hexose nucleic acid
HPLC	High performance liquid chromatography
HRMS	High resolution mass spectrometry
iBu	Isobutyryl
IVT	*In vitro* transcription
LAG	Liquid-assisted grinding
LA-RAM	Liquid-assisted resonant acoustic mixing
Lev	Levulinyl
LNA	Locked nucleic acid
LPOS	Liquid-phase oligonucleotide synthesis
MeOH	Methanol
miRNA	Micro RNA
MMTr	Monomethoxytrityl
MOE	2'-Methoxymethyl
mRNA	Messenger RNA
MsCl	Mesyl chloride
MW	Molecular weight
NBO	2-Nitrobenzaldoxime
NCS	*N*-Chlorosuccinimide
NMI	*N*-Methylimidazole
NMR	Nuclear magnetic resonance

OMe	Methoxy
ONA	Oxepane nucleic acid
OSN	Organic solvent nanofiltration
PAc	Phenoxyacetyl
Pac_2O	Phenoxyacetic anhydride
PADS	Phenylacetyl disulfide
PEG	Polyethylene glycol
PMI	Process mass intensity
PMO	Phosphorodiamidate morpholino oligonucleotide
PNA	Peptide nucleic acid
PO	Phosphodiester
Pom	Pivaloyloxymethyl
PS	Phosphorothioate
PS_2	Phosphorodithioate
PTP	*N*-Phenylthiophthalimide
PvCl	Pivaloyl chloride
Pya	*N*-Methylpyrolidine-2-ylidenyl
Pyr	Pyridine
RAM	Resonant acoustic mixing
RISC	RNA induced silencing complex
RNA	Ribonucleic acid
RNAi	RNA interference
rRNA	Ribosomal RNA
siRNA	Small interfering RNA
SOSICS	Stereocontrolled oligonucleotide synthesis with iterative capping and sulfurization
SPOS	Solid-phase oligonucleotide synthesis
T	Thymine
TBAF	Tetra-*n*-butylammonium fluoride
TBDMS	*tert*-Butyldimethylsilyl
TBHP	*tert*-Butylhydroperoxide

TCA	Trichloroacetic acid
TCOS	Thermally controlled oligonucleotide synthesis
TES	Triethylsilane
TFA	Trifluoroacetic acid
THF	Tetrahydrofuran
Thy	Thymine
TIPS	Triisopropyl silyl
TLC	Thin-layer chromatography
TMG	*N,N,N′,N′*-Tetramethylguanidine
TREAT-HF	Triethylammonium hydrogen fluoride
tRNA	Transfer RNA
U	Uracil
Ura	Uracil
VBM	Vibration ball milling
VEGF	Vascular endothelial growth factor

Chapter 1:

Introduction

"Be strong in body, clean in mind, lofty in ideals."

- James Naismith

1.1: History of nucleic acids

We have learned about the ability of organisms to pass down traits to their progeny through the pioneering work of Charles Darwin's theory of evolution, followed shortly thereafter by Gregor Mendel's studies of pea plants[1]. While the basis for the study of genetics was laid by studying the phenotypes of finches and pea plants in the second half of the 19th century, the molecule responsible for information carrying and transfer was still unknown. The first isolation of such a material was carried out by Johann Friedrich Miescher in 1868 when he isolated a non-lipid, non-protein compound from the nucleus of cells which was aptly named "nuclein" [2]. Albert Kossel shortly thereafter was able to separate nuclein into a protein and non-protein, phosphorous-containing component which was termed "nucleic acid" in 1889 by Richard Altmann. Digestion of nucleic acids determined they were composed of three main structural components: a nitrogenous nucleobase, a ribose sugar, and a phosphate group[3]. Although the function of nucleic acid was not known at the time, later work by Fred Griffith in 1928 determined that this substance could alter a benign form of pneumococcus and render it deadly[4], suggesting it may play a role in the transmission of genetic information.

It was in 1944 that Oswald Avery, with Colin M. MacLeod and Maclyn McCarty, published their seminal work proposing that nucleic acids, or more specifically deoxyribonucleic acid (DNA), and not proteins, were the carriers of genetic information[5]. This work paved the way for the groundbreaking work by Rosalind Franklin and graduate student Raymond Gosling, and their analysis of the X-ray crystal structure of DNA, providing key evidence that the phosphate group of DNA was on the outside of the secondary structure[6]. Based on this work, James Watson and Francis Crick were able to deduce the correct and now universally known double-helix structure of DNA in 1953[7], which was further corroborated by Franklin's X-ray crystal structures[8]. This of course was one of the most important discoveries in biology to date, for which Watson, Crick and Wilkins won the Nobel Prize in Physiology and Medicine in 1962. Although Rosalind Franklin did not share in the Nobel Prize with Watson and Crick due to her tragic death in 1958 at the age of 37, her contributions to the field of molecular biology cannot be overstated.

1.2: Nucleic acid structure

1.2.1: Chemical composition of nucleic acids

Following the discovery of the DNA double helix, the study of nucleic acids as the information-bearing molecules of life began in earnest. Nucleic acids are long biopolymers composed of individual units known as nucleotides. As determined in the late 19th century, nucleotides are generally composed of three main structural components: the nitrogenous nucleobase, the ribose sugar, and a phosphate group (**Figure 1.1A**). Nucleosides, on the other hand, are the same as nucleotides, but without the phosphate group. The difference between nucleotides within a longer sequence comes down to the identity of the nucleobase, which form the basis of the information system of genetics. DNA is composed of four nucleobases: thymine (Thy or T), cytosine (Cyt or C), guanine (Gua or G), and adenine (Ade or A) (**Figure 1.1B**). Ribonucleic acid (RNA, **Figure 1.1A**) is composed of four nucleobases as well with Cyt, Gua, and Ade being the same, but Thy is replaced by uracil (Ura or U). These nucleobases further fall into two different categories: the monocyclic pyrimidines (Thy, Cyt, and Ura) and the bicyclic purines (Gua, Ade) and are attached at the anomeric position (C1′) of ribose (see **Figure 1.1A** for numbering of the ribose sugar). Pyrimidines are bonded through N1 of the nucleobase to the sugar and purines are bonded through N9 (see **Figure 1.1B** for numbering of nucleobases). The ribose sugar is also different between DNA and RNA, where in DNA the 2′-hydroxyl group is removed, hence the prefix deoxy. Finally, the phosphate group of nucleotides links the ribose sugars together through a negatively charged phosphodiester backbone between the 3′- and 5′ positions of sequential nucleotides (**Figure 1.1C**).

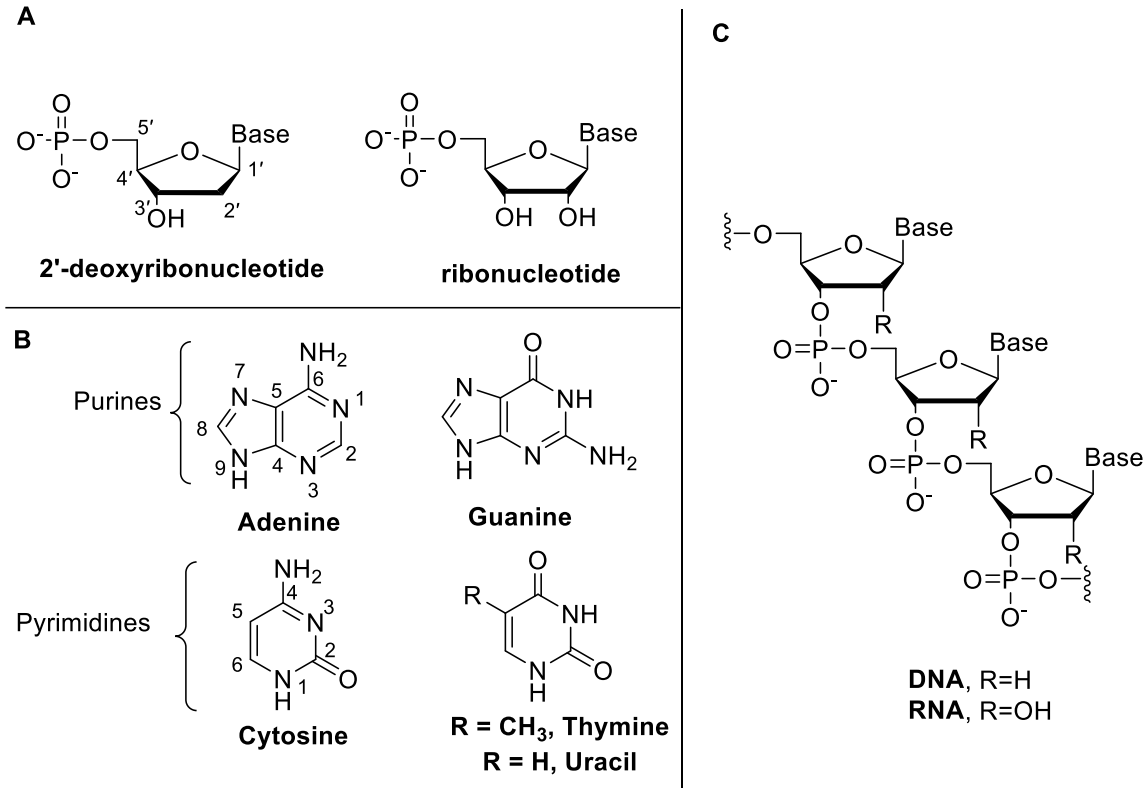

Figure 1.1: *Structure of nucleic acids:* ***A:*** *General structure of a nucleotide.* ***B:*** *Different nucleobases present in nucleic acids.* ***C:*** *3′-5′ linkage of nucleotides in naturally occurring nucleic acids.*

1.2.2: Nucleic acid conformation and secondary structure

As is the case with almost all cyclic, non-aromatic compounds, the ribose sugars of DNA and RNA exist in a 3-dimensional conformation and not in a single plane. The conformation (or sugar pucker) of ribose is well-studied and plays an important role in the secondary structure of nucleic acids as well. The full range of sugar puckers is represented by the pseudorotational wheel (**Figure 1.2**)[9], based on the phase angle value (P, in degrees) which indicates which portion of the ring is not within the same plane. In general, we describe the sugar pucker in relation to the C1′-O4′-C4′ plane with *endo* orientations coming above this plane and *exo* orientations coming below this plane. Based on this, we observe four possible energy minima in **Figure 1.2**, North (P≈0°, C3′-*endo*), East (P≈90°, O4′-*endo*), South (P≈180°, C2′-*endo*), and West (P≈270°, O4′-*exo*). In general, stereoelectronic effects determine which pucker is preferred, although in solution they exist in rapid equilibrium. The anomeric effect[10], where the nucleobase is pseudoaxial to O4′ (North) can help to stabilize this conformation due to hyperconjugation between the lone pair of O4′ and the σ* orbital of the bond between C1′ and the nucleobase.

However, this does not explain the difference that DNA sugars typically adopt a predominantly South conformation whereas RNA sugars typically favor the North conformation[11]. This is most often explained by the presence of the 2′-hydroxyl group of RNA which stabilizes the North conformation *via* the Gauche effect, where the σ C2′-H2′ bond can effectively donate to the σ* bond of the O4′-C1′ bond[12].

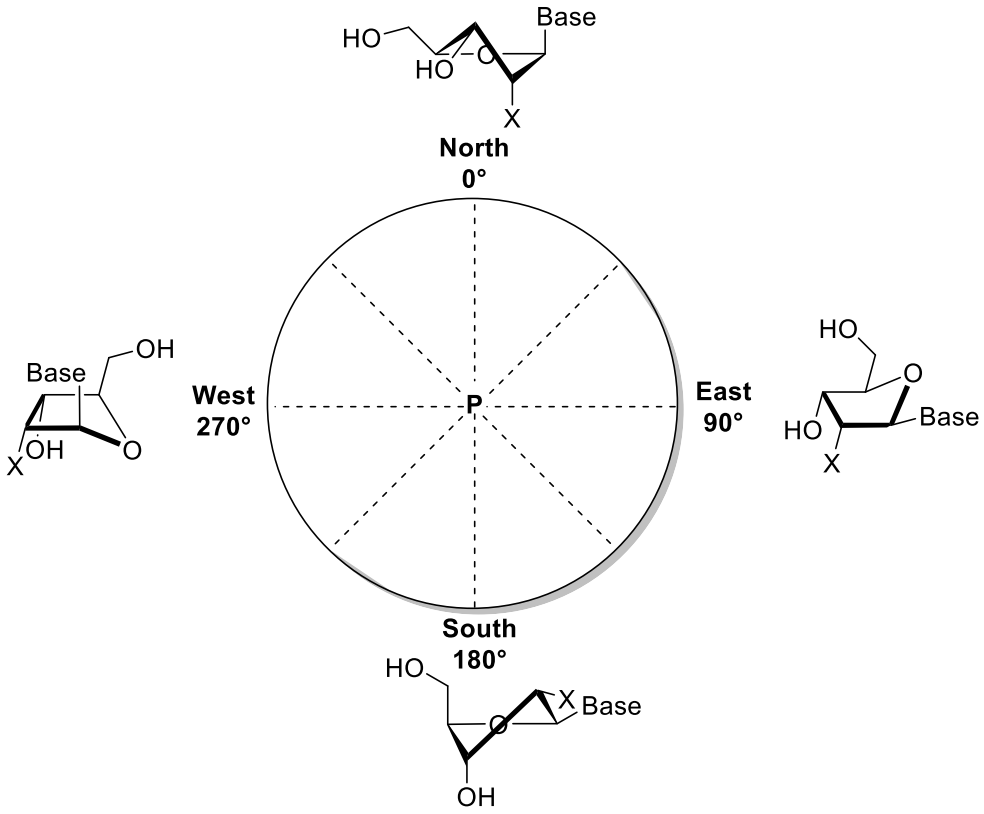

Figure 1.2: *Pseudorotational wheel and conformations of ribose sugars in nucleosides.*

As mentioned previously, natural DNA exists in the well-known double-helix structure[7]. The key features of the DNA double helix are the presence of two right-handed antiparallel strands which are held together predominantly by hydrogen-bonds (Watson-Crick base pairs, **Figure 1.3A**) and π-stacking interactions[13]. Franklin's findings that the phosphate group of DNA was present on the outside of the structure[8] led credence to the double helix structure, which minimized electrostatic repulsion of the negatively charged phosphates while also promoting favorable interactions with water. This also furthered the base-pairing scheme discovered by Watson and Crick with the aromatic nucleobases being on the inside of the structure where the hydrogen bonds between them could not be easily disrupted by water. Watson-Crick base pairs are defined by matches of hydrogen bond donors to acceptors, where pyrimidines pair with

purines. In general, A pairs with T (or U) and forms two hydrogen bonds, and G pairs with C and forms three hydrogen bonds (**Figure 1.3A**). However, other forms of base-pairing exist such as Hoogsteen[14] base pairs, but Watson-Crick base-pairs are by far the most common.

Not all nucleic acid double helixes are created equally. The famous DNA double helix exists predominantly in what known as a B-form[15] helix where the individual nucleotides are in the South conformation (**Figure 1.3C**). On the other hand, RNA when forming double helixes, tends to form an A-form[16] helix which exhibits a stockier structure than the B-form helix with the ribose sugars adopting the North conformation (**Figure 1.3B**). Indeed, one can see how the sugar conformation plays an important role in the secondary structure of nucleic acids. The form of the helix plays an important role in biology as well as different helical polymorphisms are better recognized by certain enzymes. Similarly to the variety of base-pairs possible with nucleic acids, there also exist a range of helical forms, such as left-handed Z-DNA[17], but most naturally occurring nucleic acids are A-form or B-form helices.

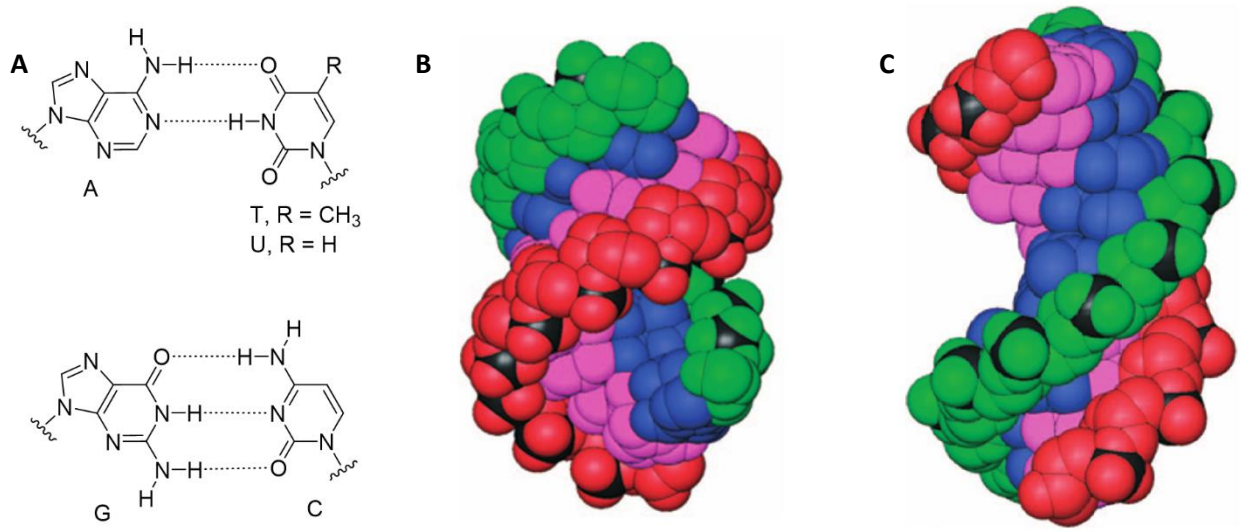

Figure 1.3: *Secondary structure of nucleic acids.* ***A:*** *Watson-Crick base pairing, A:T(U) on top, G:C on bottom.* ***B:*** *Van der Waals representation of A-form helix.* ***C:*** *Van-der Waals representation of B-form helix (right)* [18]*. Atoms of the sugar-phosphate backbone are represented in green and red for different strands, while atoms of nucleobases are represented in blue and purple.*

1.3: Biology of nucleic acids – the Central Dogma

The role of nucleic acids as information carriers has been well-documented since the 1940's. This forms the basis of the Central Dogma of molecular biology which describes the flow of genetic information more specifically. While DNA is the principal carrier of genetic

materials that is passed to offspring, the information contained within it as a genetic sequence does not directly code for proteins. Since DNA is stored in the nucleus of the cell and protein synthesis takes place in the cytoplasm, RNA acts as an intermediate in the transfer of information stored within DNA to the cytoplasm[19]. The transfer of information stored within DNA to RNA is known as transcription. The first step in this process converts DNA into single stranded RNA sequences known as precursor messenger RNA (pre-mRNA). After more enzymatic processing (capping[20], adenylation[21]) of the pre-mRNA, the non-coding regions (introns) are spliced out and the coding regions (exons) are ligated together, leading to the mature mRNA[22].

The mature mRNA sequence is then transported into the cytoplasm where the genetic information stored within can be converted into proteins in a process known as translation[23]. Large complexes composed of proteins and ribosomal RNA (rRNA) known as ribosomes read the mRNA three nucleotides at a time (codons) of which each of 64 (4^3) possible sequences corresponds to a different amino acid[24]. It should be noted that there are only 20 amino acids used during translation and many of the 64 codons are redundant. A separate RNA sequence known as transfer RNA (tRNA) bears a complementary three nucleotide sequence (anticodon) to the codon of the mRNA sequence being translated and helps to shuttle the specific amino acid to the ribosome, which is then added to the growing peptide[25]. The general flow of information from DNA to RNA during transcription and from RNA to proteins during translation constitutes the Central Dogma of molecular biology. Although there are some instances of a reversal of the flow of information, particularly from RNA to DNA *via* retroviruses[26], in general it flows from DNA to RNA to proteins.

1.4: Therapeutic oligonucleotides

Many diseases stem from naturally occurring errors during DNA replication or from mutation of DNA sequences. When errors or mutations occur, they often occur in non-coding regions of DNA, introns, or may have no effect, but occasionally they may lead to the synthesis of a non-functional protein or insufficient protein levels. In such cases, the genetic component of a disease can be hereditary and difficult to treat. Most traditional therapeutics are small molecules that target proteins either by tightly binding the active site or by allosteric binding, but based on the Central Dogma, in the case of diseases with genetic components, this can be thought of as treating the symptom and not the root cause. Thus, in recent years, nucleic acids

have emerged as a new class of informational drugs which can target DNA or mRNA sequences directly and prevent transcription or translation before a faulty protein causes a diseased state. By using naturally occurring Watson-Crick base pairing, the ability to theoretically target any disease with a genetic component has essentially created a new drug discovery platform.

1.4.1: Antisense oligonucleotides (ASOs)

One of the first class of nucleic acid drugs to emerge are the antisense oligonucleotides (ASOs). ASOs were discovered in 1978 when a singled stranded synthetic DNA oligonucleotide was shown to inhibit viral growth in the Rous sarcoma virus by binding to a complementary mRNA sequence[27]. ASOs are generally short oligonucleotides (~18-22 nucleotides) and operate by two different mechanisms (**Figure 1.4**) [28]. Steric block ASOs bind complementary mRNA sequences with very high affinity which prevents translation by the ribosome while some ASOs can recruit and enzyme known as RNase H which recognizes the DNA:RNA hybrid duplex and degrades it. Some ASOs can also modulate splicing[29] of certain mRNA molecules either leading to restoration[30] of the production of a protein or leading to truncation of a disruptive protein[31]. The first clinically approved nucleic acid drug was in fact an ASO, Vitravene, which was approved in 1998 for the treatment of cytomegalovirus retinitis and remains the only antiviral oligonucleotide brought to market[32]. Since then, nine more ASOs have been approved and research into their applications is only growing[33].

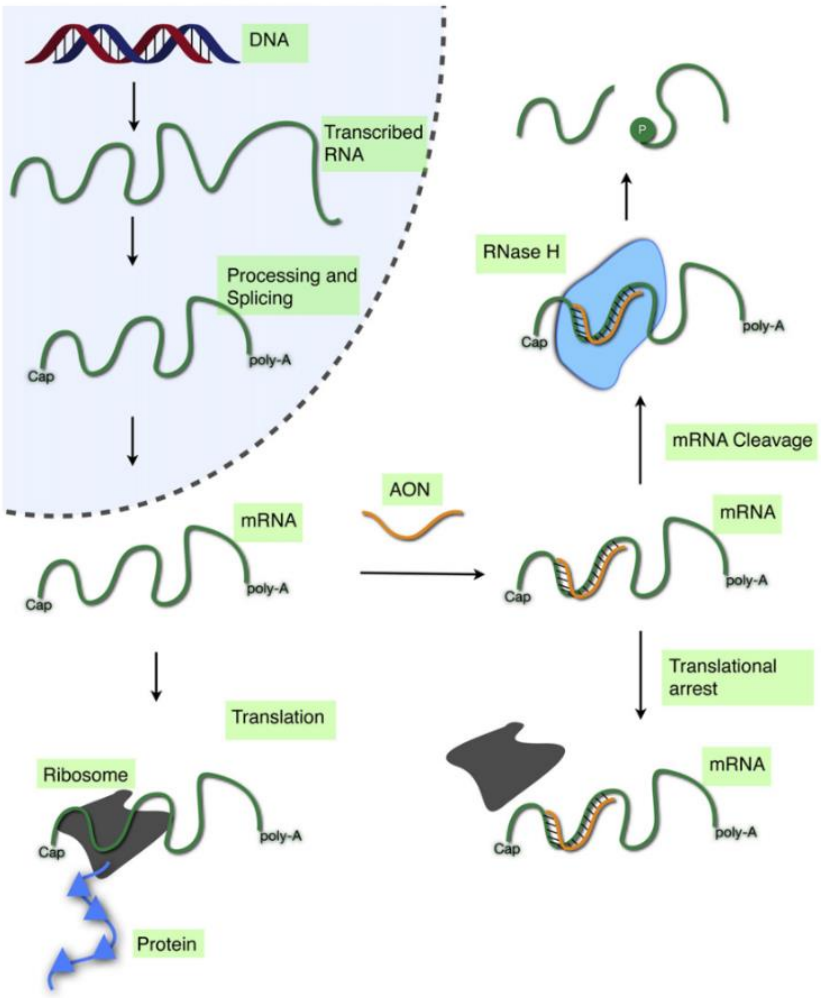

Figure 1.4: *Representation of the different mechanisms of ASOs via steric block or recruitment of RNase H*[28].

1.4.2: Small interfering RNAs (siRNAs)

Small interfering RNAs (siRNAs) are another important class of oligonucleotide therapeutics. In contrast to ASOs, which are typically single stranded DNA sequences, siRNAs are double stranded RNA sequences. siRNA takes advantage of the RNA interference (RNAi) pathway which was discovered in 1998 by Andrew Fire and Craig Mello, for which they won the 2006 Nobel Prize in Physiology or Medicine[34]. siRNAs also operate by complementary binding to the targeted mRNA sequence, but only one strand of the duplex, known as the guide strand (or antisense strand), is used for this. The guide strand is loaded into the RNA induced silencing complex (RISC) composed of multiple proteins, while the other strand, the passenger strand (or sense strand), is ignored[35]. The RISC can then use the guide strand to catalytically degrade mRNA sequences complementary to the guide strand (**Figure 1.5**) [28]. Despite the relatively

recent discovery of the RNAi pathway in 1998, the first siRNA therapeutic (Onpattro) was approved in 2018 for the treatment of hereditary transthyretin-mediated amyloidosis and since then four more have already been approved[32]. Given the catalytic nature of siRNA, they often require very small doses which can be effective for weeks or months at a time and this is evidenced by the rapid development of siRNA therapeutics in recent years[36].

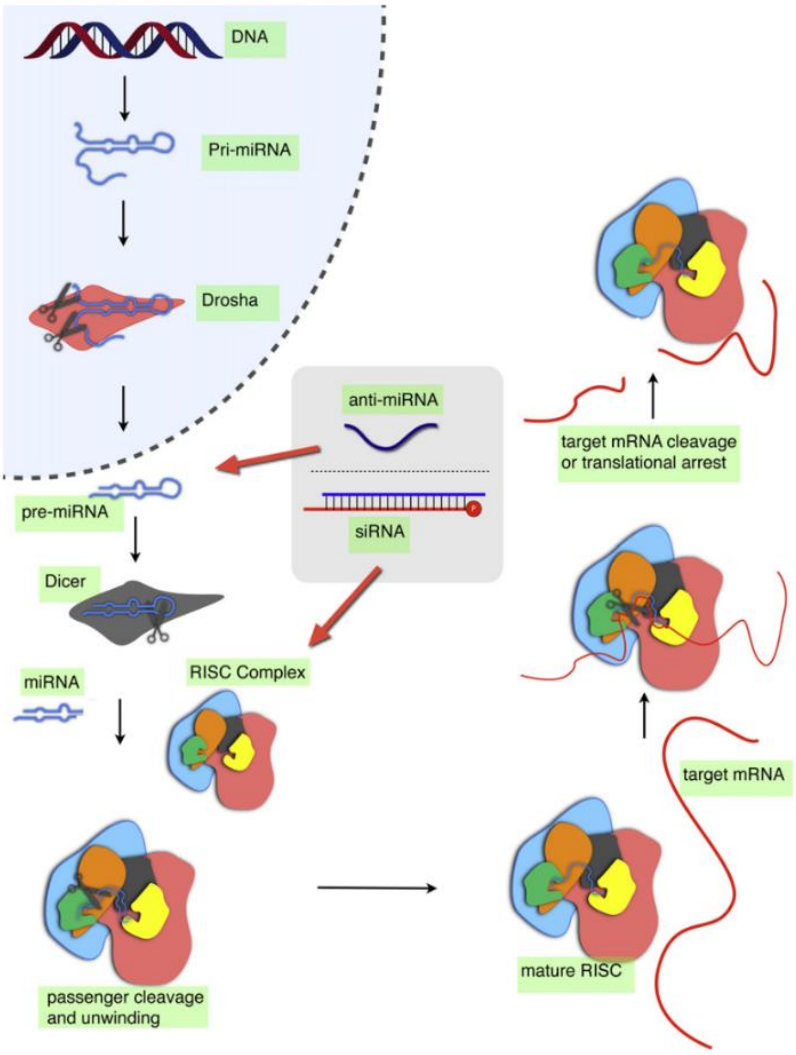

Figure 1.5: *Representation of the RNAi pathway resulting in mRNA cleavage by RISC[28].*

1.4.3: Other therapeutic oligonucleotides

While ASOs and siRNAs are the most widely studied oligonucleotide therapeutics, researchers have started taking advantage of new modes of action. The 2020 Nobel Prize in Chemistry was awarded to Emmanuelle Charpentier and Jennifer Doudna for their studies on the CRISPR-Cas system[37], which has enabled researchers to directly target DNA, rather than the

mRNA targets of ASOs and siRNAs[38]. The CRISPR-Cas system is rapidly growing into one of the most exciting tools in molecular biology and therapeutics by acting as "molecular scissors" of DNA[39]. Although there have not yet been any approved therapeutics taking advantage of the CRISPR-Cas mechanism, there are clinical trials under way in humans[40]. Other DNA targeting strategies such as prime editing[41] among others are also gaining attention for their versatility[42]. There has been one approved aptamer-based therapeutic that targets vascular endothelial growth factor (VEGF), a protein, but research into aptamer-based therapeutics is ongoing[43]. Other strategies such as miRNA[44], CpG oligonucleotides[45], and others[46] have also gained widespread attention. Of course, with the onset of the COVID-19 pandemic, mRNA vaccines have brought the use of oligonucleotides as therapeutics into the spotlight of the world[47]. In contrast with ASOs and siRNAs, mRNA vaccines are often long (hundreds to thousands of nucleotides) sequences and are generally composed of unmodified or natural RNA[48] and code for the sequence of a protein to stimulate an immune response.

1.4.4: Chemical modifications of therapeutic oligonucleotides

The success of ASOs, siRNAs, and other therapeutic oligonucleotides has relied on chemical modifications of nucleic acids[49]. In general, oligonucleotides are not very "drug-like" and stand in stark contrast to Lipinski's rules[50]. They are large, highly charged molecules which are readily degraded by endo- and exonucleoases[51]. Thus, chemical modifications are necessary to improve stability, binding affinity to target mRNA sequences, and to aid with delivery and targeting. Indeed, when looking at the structure of an approved siRNA such as Givosiran (**Figure 1.6**), we see that it contains no natural RNA in either strand with all sugar residues having their 2′-hydroxyl group replaced by either a fluorine or methoxy (OMe) group[52]. Additionally, there are certain residues at the ends of the strands which have a non-bridging oxygen of the phosphodiester (PO) backbone replaced by a sulfur atom yielding a phosphorothioate (PS)

backbone. Finally, the sense strand is conjugated to a GalNAc residue which aids in delivery to the liver[53].

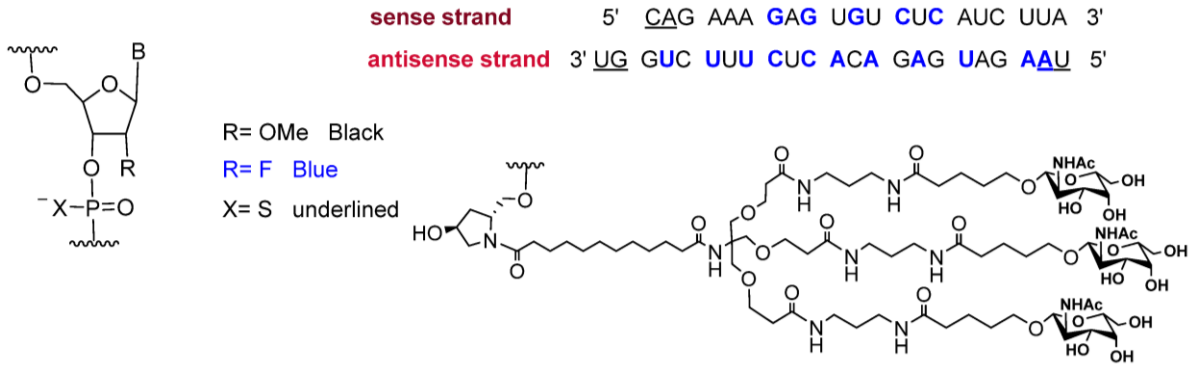

Figure 1.6: *Structure of Givosiran with chemical modifications highlighted.*

While the challenges associated with oligonucleotide therapeutics are many, the clever application of chemical modifications has alleviated many of these issues[49]. Additionally, the unique position of oligonucleotides as informational drugs allows researchers to separately optimize targeting and the pharmacokinetic properties of oligonucleotides (**Figure 1.7**). While the structure of small-molecule drugs both directly determines the target and metabolism of the drug, oligonucleotide targeting can be optimized by sequence selection while chemical modifications can drive favorable pharmacokinetic properties.

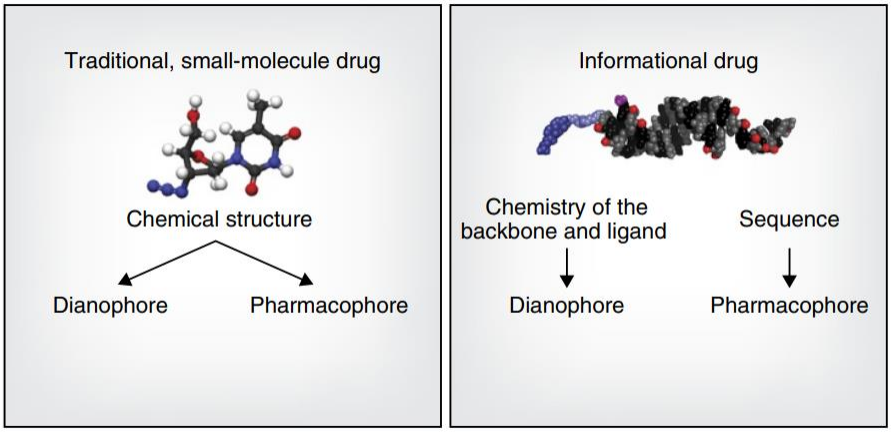

Figure 1.7: *Comparison of traditional, small-molecule drugs with informational drugs such as oligonucleotides[49].*

Thus, researchers have screened a huge range of chemical modifications of nucleic acids. The three main structural components of nucleotides are also the three areas where chemical modifications have been applied: the ribose sugar, the nucleobase, and the phosphodiester backbone (**Figure 1.8**). As shown above with Givosiran, common sugar modifications are

employed at the 2′ position which can help to tune the specific conformation at the level of the nucleotide, which in turn can affect the duplex. Common sugar modifications include the aforementioned 2′F and 2′OMe as well as arabino (ANA, epimer of RNA), 2′F arabino (FANA, epimer of 2′F), locked nucleic acid (LNA), 2′methoxyethyl (MOE), and ring expanded sugars such as hexose nucleic acid[54] (HNA) and oxepane nucleic acid, which has been linked through various hydroxyl groups[55] (ONA, **Figure 1.8A**). Sugar modifications generally increase duplex stability and can provide increased nuclease resistance.

Backbone modifications include the replacement of bridging or non-bridging atoms of the phosphodiester with other heteroatoms. The PS[56] backbone is by far the most widely adopted by greatly increasing nuclease resistance and enhancing cellular uptake and almost every approved oligonucleotide has at least one PS backbone. Other backbone modifications include phosphorodithioate (PS_2), phosphoramidate[57], and the more exotic peptide nucleic acid[58] (PNA) and phosphorodiamidate morpholino oligonucleotide[59] (PMO) backbones (**Figure 1.8B**). The crossover between sugar and backbone modifications becomes blurred when looking at PNA and PMO, but broadly speaking they modify the backbone of the sequence. The nucleobase has not been as extensively modified as the sugar and phosphate of nucleic acids, but some examples exist such as 5-methylcytosine and 5-methyluracil (or thymine). The modifications shown in **Figure 1.8** represent just a handful of the most widely studied chemical modifications applied to oligonucleotide therapeutics and is a non-exhaustive list, but this topic has been well-reviewed and we direct the reader there for further reading[60].

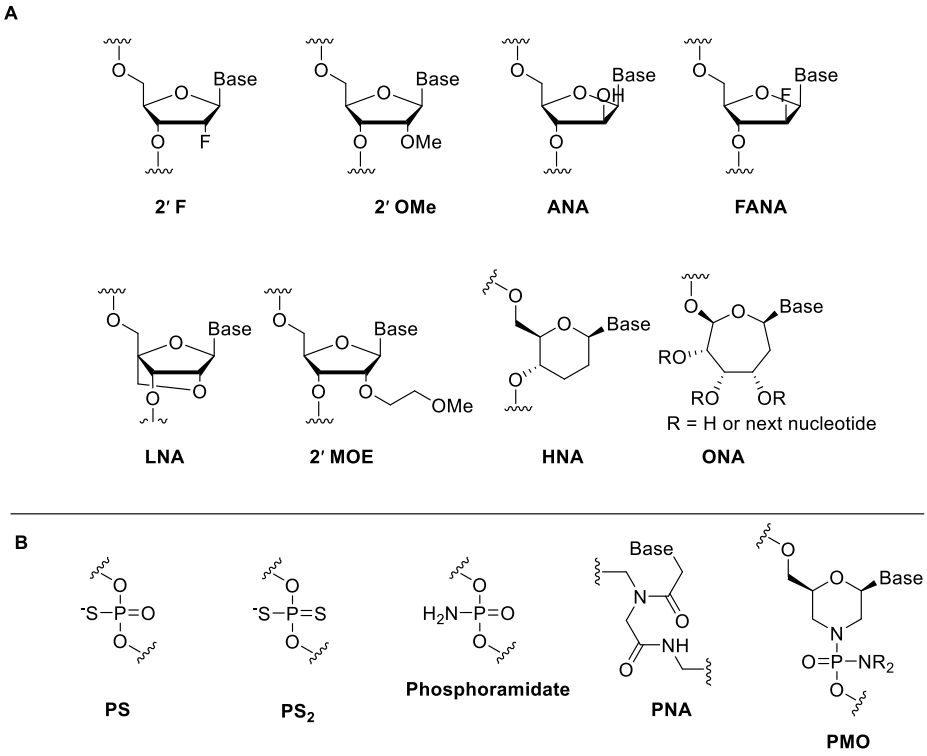

Figure 1.8: *Sample of chemical modifications used in oligonucleotide therapeutics.* ***A:*** *Sugar modifications.* ***B:*** *Backbone modifications.*

1.5: Chemical synthesis of nucleic acids

The wide range of chemical modifications used in oligonucleotides presents a unique challenge for the synthesis of specifically modified oligonucleotides. In contrast with mRNA vaccines, which are very long sequences composed mostly of natural RNA, ASOs and siRNAs contain many modifications in very specific positions, many of which may not be substrates for the polymerases used during *in vitro* transcription (IVT) for the synthesis of mRNA vaccines. This has led to the development of various chemical methods over the past 70 years for the synthesis of oligonucleotides of which a wide range of chemical modifications are tolerable and can be inserted at any position within the sequence. Although the history of the chemical synthesis is long and well-reviewed, we will summarize some of the early chemistry here, but direct the reader towards Colin Reese's excellent 2005 review for insights into the fundamental chemistry that was developed in the early years of oligonucleotide synthesis (of which much of the chemistry is still in use today) [61].

1.5.1: P(V) Chemistry: Todd, Khorana, and Letsinger

Initial efforts towards the chemical synthesis of nucleic acids containing natural 3′-5′ linkages focused on using P(V) chemistry as that is the oxidation state of phosphorous in naturally occurring DNA and RNA. The first chemical synthesis of a dinucleotide containing a natural 3′-5′ linkage was carried out in the lab of Alexander Todd in 1955 using what was later termed the phosphotriester approach[62]. His approach (**Scheme 1.1**) began by reaction of diphenyl chlorophosphonate **1** with benzyl H-phosphonate **2** to produce the mixed anhydride **3**[63]. Subsequent phosphorylation of **4** was carried out using **3** to produce **5**. Interestingly for later efforts using H-phosphonate chemistry, Todd noted the instability of the H-phosphonate diester (see **1.5.5** and **2.2.3**) product **5** and he immediately reacted the crude material with *N*-chlorosuccinimide (NCS) to yield the chlorophosphate **6**[62]. Crude **6** was reacted with **7** which yielded the phosphotriester intermediate, and after deprotection yielded the first chemically synthesized dinucleotide **8** bearing a 3′-5′ linkage. This effort essentially ended Todd's work towards chemical oligonucleotide synthesis as he turned his research focus elsewhere (winning the Nobel Prize for Chemistry in 1957), leaving the door open for other scientists to take up the challenge.

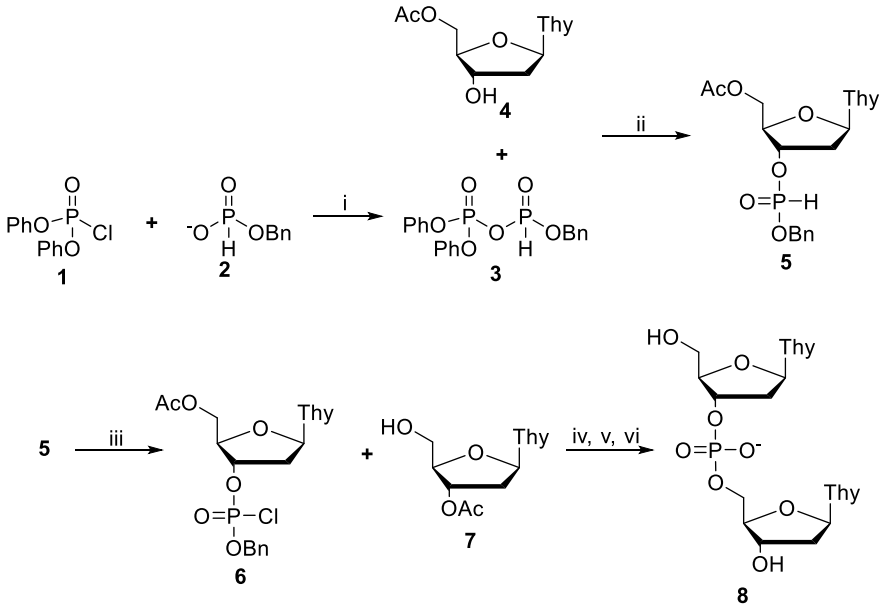

Scheme 1.1: *Todd's phosphotriester strategy for the first synthesis chemical synthesis of a dinucleotide. Reagents:* ***i****, Pyridine, benzene.* ***ii****, 2,6-lutidine, benzene.* ***iii****, NCS, ACN, benzene.* ***iv****, 2,6-lutidine, ACN.* ***v****, H_2SO_4, EtOH, H_2O.* ***vi****, $Ba(OH)_2$, H_2O.*

Shortly after Todd published his synthesis of a dinucleotide, Har Gobind Khorana started publishing his own work on the chemical synthesis of oligonucleotides using a different strategy

where the phosphodiester linkage was left unprotected during synthesis. Not surprisingly, this strategy was termed the phosphodiester approach, but similarly to Todd's phosphotriester strategy relied on P(V) chemistry. Khorana first published a short description on the synthesis of dinucleotides in 1957[64], but greatly expanded upon it in 1958[65]. Khorana's straightforward approach began with condensation of 3′-acetyl 5′-phosphate thymidine **9** and 5′-acetyl thymidine in the presence of dicyclohexylcarbodiimide (DCC) yielding the desired protected dinucleotide in 66% yield over 2 days[65]. Having optimized the reaction conditions, they then evolved the strategy by using a trityl protecting group at the 5′ position (**10**) and expanding the coupling to other nucleosides (**Scheme 1.2**) yielding mixed base dinucleotides **11** in good (60-70%) yields over 2 days followed by deprotection to yield **12**[65]. Importantly, differing from Todd's strategy, Khorana's introduction of the orthogonal 5′-trityl protecting group allowed for the possibility of chain elongation. Although Khorana initially used the trityl protecting group, partial cleavage of the glycosidic bond (particularly in the case of purines) under the harsh acidic conditions required for trityl deprotection (**Scheme 1.2, ii**) led him to develop the derivatized monomethoxytrityl (MMTr) and dimethoxytrityl (DMTr) 5′-protecting groups which are now ubiquitous in oligonucleotide synthesis due to their increased lability under acidic conditions as compared to trityl[66]. Although coming almost a decade later, Khorana's work in optimizing the nucleobase protecting groups also deserves mention, most of which are still commonly used today[67]. Despite the advantages of Khorana's phosphodiester approach over Todd's phosphotriester approach, the phosphodiester strategy was largely abandoned after Khorana's work, likely due to the difficulties encountered during purification of highly charged molecules and the relatively low yields of coupling reactions even after extended periods[61]. Khorana continued working in the field for decades and shared the Nobel Prize in Physiology or Medicine with Robert Holley and Marshall Nirenberg in 1968 for their efforts and contributions to cracking down the genetic code[68].

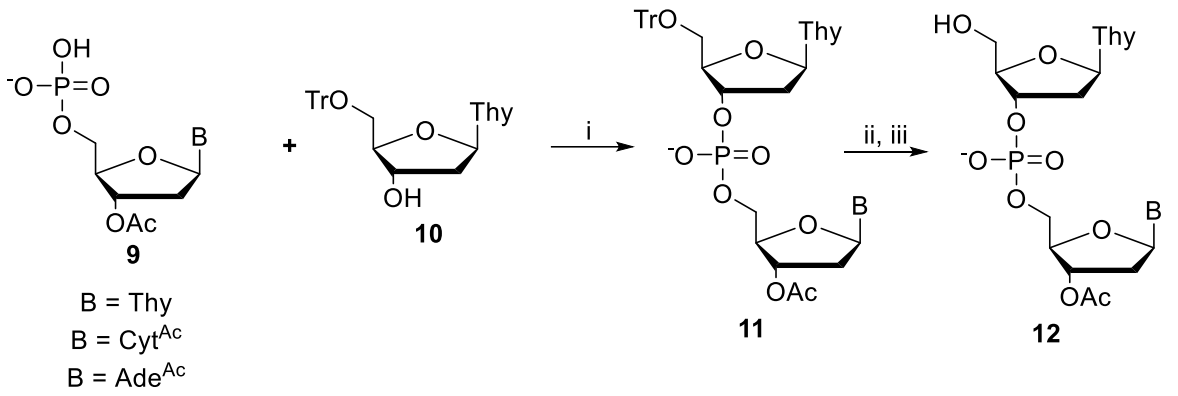

Scheme 1.2: *Khorana's phosphodiester strategy for dinucleotide synthesis. Reagents:* ***i****, DCC, pyridine.* ***ii****, 80% AcOH reflux.* ***iii****, NaOH, H_2O.*

Following the development of the phosphodiester chemistry by Khorona, there was a renaissance of the phosphotriester strategy in the late 1960s led by Robert Letsinger. Letsinger returned to the phosphotriester strategy in 1965 where he foreshadowed later advances in oligonucleotide synthesis by synthesizing a dinucleotide on a solid (polystyrene) support (**Scheme 1.3**) [69]. In contrast to modern solid-supports in use today, Letsinger began with 5′-trityl cytidine **13** which was coupled to the polymer at the exocyclic amine of the nucleobase to yield **14**. The free 3′-hydroxyl group of **14** was phosphorylated with β-cyanoethyl phosphate in the presence of DCC, which is analogous to the chemistry used by Khorana previously, to prepare phosphodiester **15**. The use of the β-cyanoethyl as a phosphate protecting group was a key finding in its own right, owing to the ease of synthesis[70], mild deprotection conditions, and its continued use today in solid-phase synthesis. Coupling of unprotected thymidine with **12** in pyridine for two days, followed by deprotection by sodium hydroxide treatment then acetic acid treatment, yielded the desired dinucleotide **16**[69]. Letsinger expanded this strategy in 1967 by migrating the support to the 3′-position, adopting the MMTr and DMTr groups developed by Khorana, and demonstrating an iterative synthesis of a trinucleotide[71]. This procedure laid the foundation for modern oligonucleotide synthesis, particularly Letsinger's finding that the reaction of a 5′-hydroxyl with an activated 3′-phosphate proceeded much more rapidly than the reaction of a 3′-hydroxyl with a 5′-phosphate[72]. Additionally, Letsinger and Ogilvie discovered that large quantities (up to 40g) of DNA dimers and trimers could be synthesized and purified by column chromatography, albeit with relatively low coupling yields (64% for dimer and 49% for trimer) [73]. Around the same time that Letsinger was publishing his work, Fritz Eckstein[74] and Colin Reese[75] were also synthesizing oligonucleotides using phosphotriester chemistry, albeit

with different phosphate protecting groups (trichloroethyl and aryl, respectively). While the cyanoethyl protecting group fell into the background for the foreseeable future, the aryl protecting groups developed by Reese came into their own during the 1970s for their tunability by modifying the aromatic ring[76]. Substitution of the aryl protecting group and careful selection of deprotection reagents led to highly selective and rapid deprotection conditions being developed[77]. During this time there was a marked increase in the capabilities of researchers to synthesize longer oligonucleotides and we once again direct the reader towards Reese's review for an excellent overview of the phosphotriester approach during this time[61].

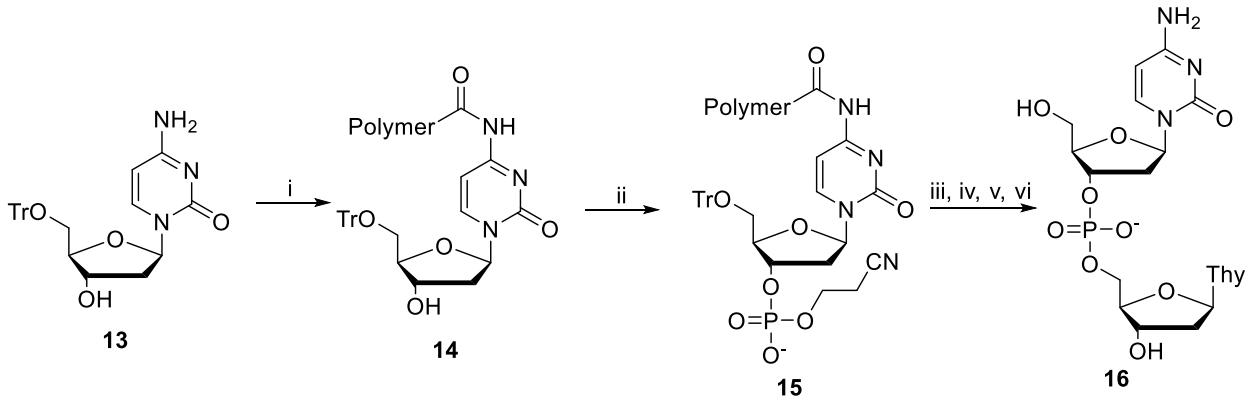

Scheme 1.3*: Letsinger's phosphotriester strategy for dinucleotide synthesis. Reagents:* ***i****, Polymer acid chloride, pyridine.* ***ii****, β-cyanoethyl phosphate, DCC, pyridine.* ***iii****, MsCl, pyridine.* ***iv****, thymidine, pyridine.* ***v****, NaOH, dioxane, ethanol.* ***vi****, 80% AcOH.*

1.5.2: P(III) Chemistry: Letsinger, Caruthers, and Beaucage

By the middle of the 1970s, many researchers had adopted the phosphotriester approach for oligonucleotide synthesis, but the next breakthrough came once again from Robert Letsinger in his studies of P(III) chemistry. In 1976, Letsinger reported the use of phosphorodichloridite with an aryl protecting group for the phosphitylation of a nucleoside at the 3′ position followed by subsequent coupling with a 5′-hydroxyl nucleoside and oxidation using iodine and water[78]. The immediate benefit of this approach was the greatly increased reactivity of the P(III) compounds, with reactions done within minutes as compared to the hours or days required for previous approaches relying on P(V) chemistry. Despite this, Letsinger's strategy using the bifunctional phosphorodichloridite **18** gave rise to undesired 5′-5′ and 3′-3′ linked nucleosides as impurities (**Scheme 1.4**). He attempted to circumvent this by using excess of 5′-phenoxyacetyl (PAc) nucleoside **17**, but this still resulted in the formation of 3′-3′ dimers (**20**) as impurities. Nonetheless, coupling of chlorophosphite **19** by addition of 3′-MMTr nucleoside **21** directly to

the solution, followed by iodine-water oxidation, yielded the desired phosphate triester **22** in 65% yield. This approach was later automated by Ogilvie in the early 1980's by combining the phosphite triester approach with solid-phase synthesis[79].

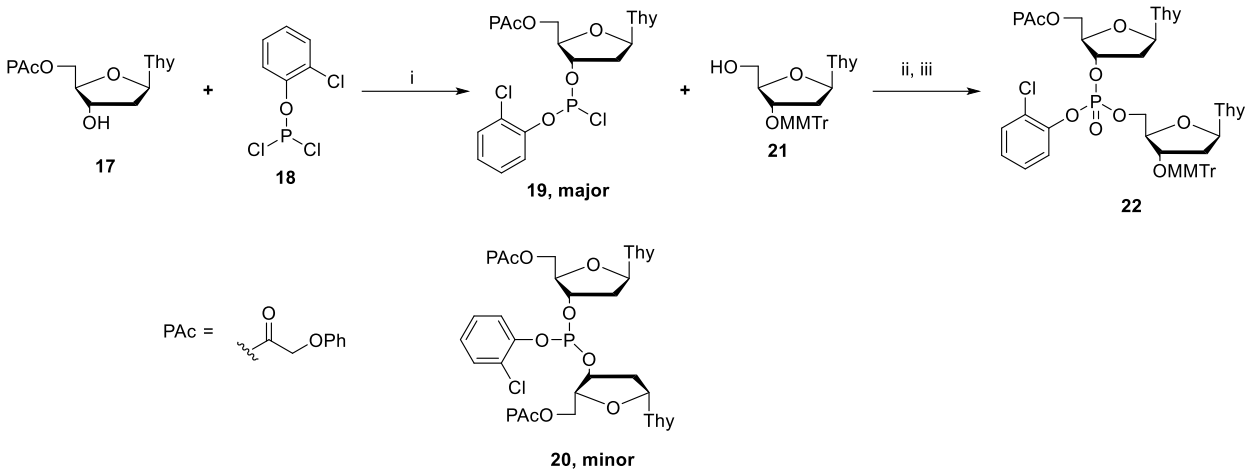

Scheme 1.4: *Letsinger's P(III) strategy for oligonucleotide synthesis. Reagents:* ***i****, 2,6-lutidine, THF, -78°C.* ***ii****, 2,6-lutidine, THF, -78°C.* ***iii****, I_2, H_2O, THF, -10°C.*

The P(III) chemistry introduced by Letsinger in 1976 increased interest in this type of chemistry in the following years, but in 1981 Serge Beaucage and Marvin Caruthers published their seminal paper on phosphoramidities for oligonucleotide synthesis[80]. Rather than using a bifunctional phosphitylating reagent as Letsinger used, Beaucage and Caruthers synthesized monofunctional **23** by addition of dimethylamine to methoxydichlorophosphine at -15°C (**Scheme 1.5**). The phosphoramidites **25a-d** were then synthesized in excellent yields (90-94%) by reacting **23** with a protected nucleoside **24** in the presence of diisopropylethylamine (DIPEA). Subsequent coupling of the phosphoramidites using *1H*-tetrazole as a weak acidic activator with **26** yielded phosphite triesters **27a-d** in excellent yields (93-97%) as measured by ^{31}P NMR. This work opened the door to P(III) chemistry, although later work perfected the phosphoramidite approach, namely by substituting the methyl groups of the phosphoramidite with isopropyl groups[81], and by reintroducing the β-cyanoethyl protecting group from Letsinger's phosphotriester strategy[82].

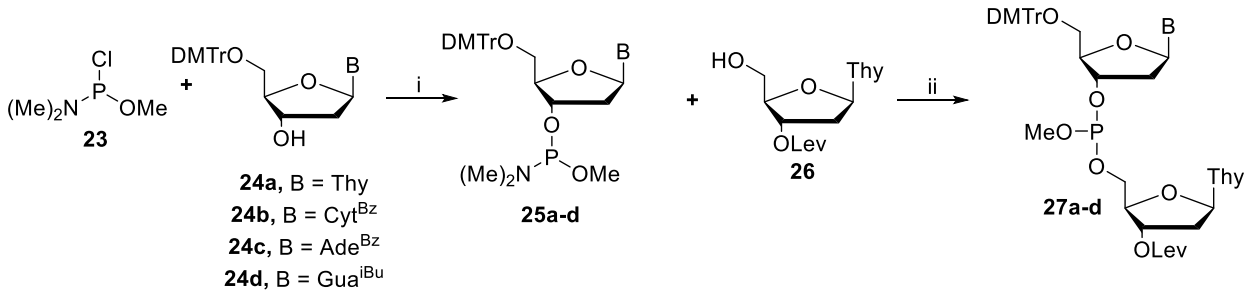

Scheme 1.5: *Beaucage and Caruther's phosphoramidite strategy for oligonucleotide synthesis. Reagents:* ***i****,* $CHCl_3$*, DIPEA.* ***ii****, ACN, 1H-tetrazole.*

1.5.4: Solid-phase oligonucleotide synthesis and automation

The high reactivity of P(III) phosphoramidites allowed for coupling yields that are routinely above 99% in minutes rather than hours or days and the success of solid-support synthesis was finding application in oligonucleotide synthesis (1984 Nobel Prize in Chemistry to Bruce Merrifield for solid-phase peptide synthesis). These discoveries rendered the phosphoramidite approach the most effective strategy by far for chemical synthesis of oligonucleotides at all scales and was later adapted to a solid-phase[83] strategy that was eventually automated. Careful attention was paid to the choice of protecting groups in the development of the automated solid-phase oligonucleotide synthesis (SPOS) cycle. Fortunately, work by Khorana optimized the amine protecting groups of the nucleobases[67], which are still commonly used today. Adenine is usually protected with a benzoyl group (Bz), guanine with an isobutyryl group (iBu), and cytosine with an acetyl group (Ac, **Figure 1.9A**). Uracil and thymine, which have no exocycle amine groups are usually left unprotected. Of course, other protecting groups are used for specialized applications, but the most common ones are shown. Following Letsinger's observation that the 5′-hydroxyl reacts much more rapidly with activated 3′-phosphates than the opposite reaction[72], oligonucleotide synthesis in general is carried out in the 3′ to 5′ direction. Thus, the use of the 5′-DMTr protecting group previously developed was suitable for automated synthesis as well. The choice of protecting groups for the 2′-hydroxyl groups of RNA was a more complicated issue, but in general the *tert*-butyldimethylsilyl (TBDMS) protecting group is the most commonly employed[84]. Other 2′ protecting groups have also been successful, such as levulinyl[85] (Lev) and acetal levulinyl ester[86] (ALE), to name just a few (**Figure 1.9B**).

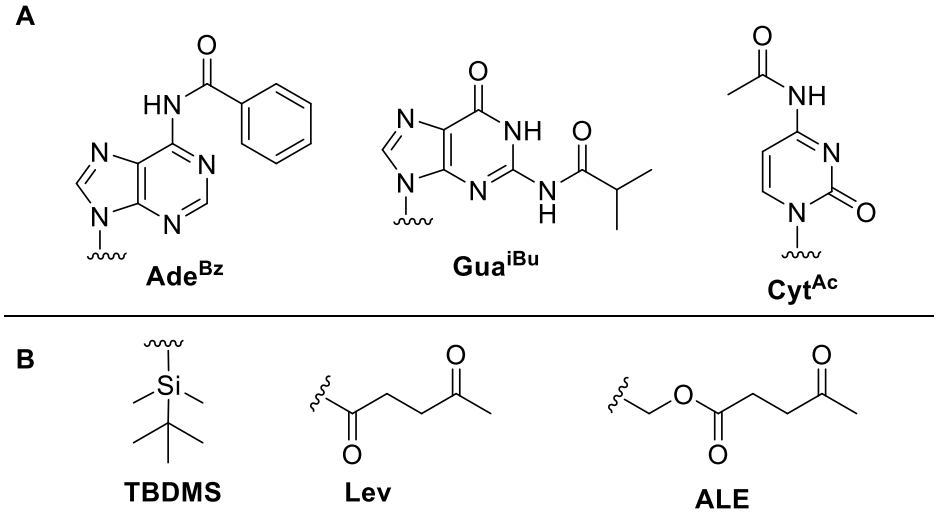

Figure 1.9*: Common protecting groups used in oligonucleotide synthesis.* ***A:*** *Nucleobase protecting groups.* ***B:*** *Some 2′-hydroxyl protecting groups for RNA chemical synthesis.*

Having optimized the chemistry behind oligonucleotide synthesis, the automation of the process brought the time required to synthesize oligonucleotides down from multiple days of manual labor to a few hours overnight. The synthesis cycle begins with removal of the 5′DMTr protecting group of a 3′-controlled pore glass (CPG) derivatized nucleoside using trichloroacetic acid (TCA) in dichloromethane (DCM) (**Figure 1.10**). Coupling of the incoming phosphoramidite is carried out using 5-(ethylthio)-1*H*-tetrazole (ETT) which is slightly more acidic than the previously used tetrazole. A capping step is required using acetic anhydride to protect any unreacted 5′-hydroxyl groups, thus minimizing any further reaction leading to impurities. The resulting P(III) phosphite triester linkage is then oxidized to the P(V) phosphate triester using aqueous iodine in pyridine/THF. Oxidation is required as phosphite triesters are unstable in the presence of acid and the linkage would degrade during detritylation in the next step of the synthesis cycle[87]. The cycle is repeated until the desired sequence is synthesized and is compatible with a range of chemically modified sugars and backbones. Once the synthesis is complete, the resulting oligonucleotide is cleaved from the solid support using ammonium hydroxide, which also removes any base protecting groups and cyanoethyl backbone protecting groups. If RNA is being synthesized, an extra deprotection step may be necessary depending on the 2′-protecting group, but silyl reagents are usually removed using triethylammonium hydrogen

fluoride (TREAT-HF) or tetra-n-butylammonium fluoride (TBAF). Importantly, automated SPOS is compatible with a wide range of chemically modified nucleotides and backbones.

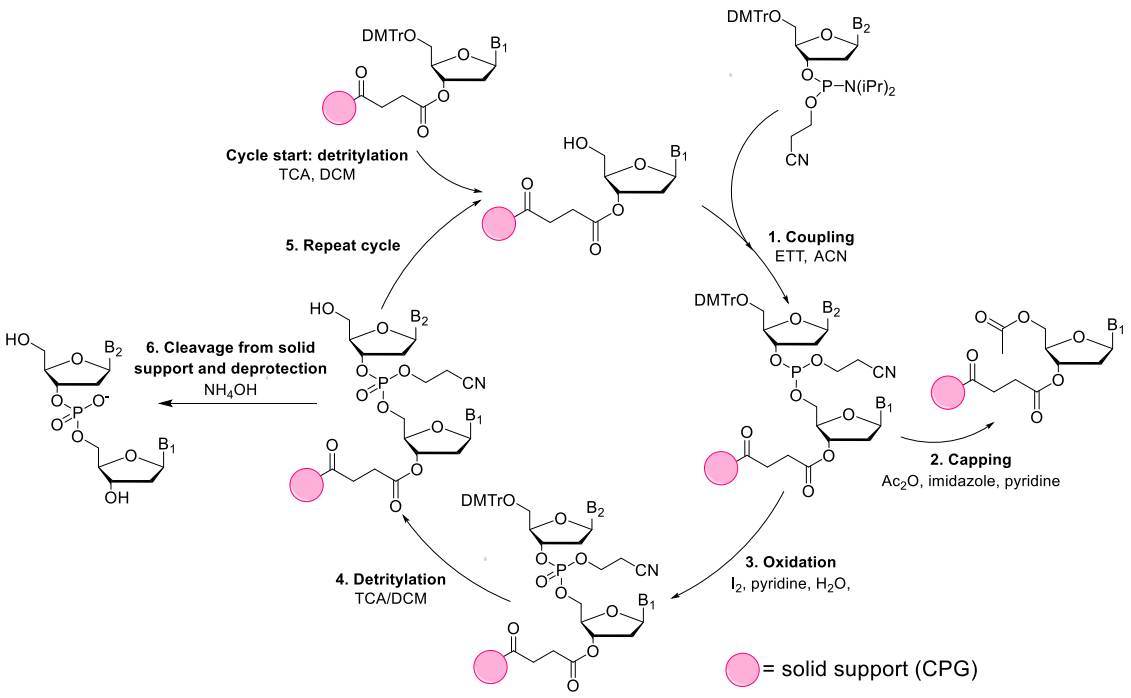

Figure 1.10: *General solid-phase synthesis cycle of DNA oligonucleotides.*

1.5.5: H-phosphonate chemistry: Stawiński and Reese

Despite the advancements of phosphoramidite chemistry during the 1980s, some researchers continued to work on other types of chemistry. In particular, Jacek Stawiński adopted H-phosphonate chemistry for oligonucleotide synthesis. Todd originally synthesized H-phosphonate diesters, but immediately converted them to chlorophosphates before completing his synthesis of dinucleotides (**Scheme 1.1**), but he never directly used H-phosphonates for coupling[63]. Stawiński found that H-phosphonates **28** (**Scheme 1.6**) possess some unique characteristics compared with other phosphorous chemistries. Despite being pentavalent like phosphotriesters or phosphodiesters, H-phosphonates are formally in the oxidation state of P(III) due to the slightly lower electronegativity of phosphorous than hydrogen. This allows for simple conversion of H-phosphonates *via* oxidation to a range of P(V) species, but lacking the lone pair of other P(III) species (such as phosphoramidites), they are much more stable to air and moisture[88]. Exploiting the interesting chemistry of H-phosphonates Stawiński was able to develop a simplified automated synthesis cycle for oligonucleotide synthesis (**Scheme 1.6**). They initially tested the coupling efficiency of H-phosphonate monoester **22** in the presence of various

coupling reagents[89], but settled on pivaloyl chloride (PvCl) as the reagent of choice. Thus, in the presence of PvCl, **28** was coupled with 3′-CPG nucleoside **29** in approximately 1 minute followed by detritylation to yield **30** with average coupling yield of 97-100%. The H-phosphonate method had a clear advantage at this phase, as capping was not performed at all and oxidation not performed until the end of the synthesis cycle. This is due to the stability of H-phosphonate diesters to acid, as compared to phosphite triesters which are very unstable in the presence of any acid[87]. Thus, oxidation and deprotection were performed at the end of the automated cycle yielding the desired dT dodecamer of the general structure **31** as a single band isolated by gel electrophoresis. Similarly, Stawiński applied this strategy to the automated synthesis of RNA oligonucleotides using TBDMS protecting groups and found similar efficiency[90]. While the single final oxidation step is attractive, it is only useful if the entire sequence is composed of PO backbones, if there are interspersed PS and PO linkages (or others), one must carry out each oxidation or sulfurization step at the appropriate time.

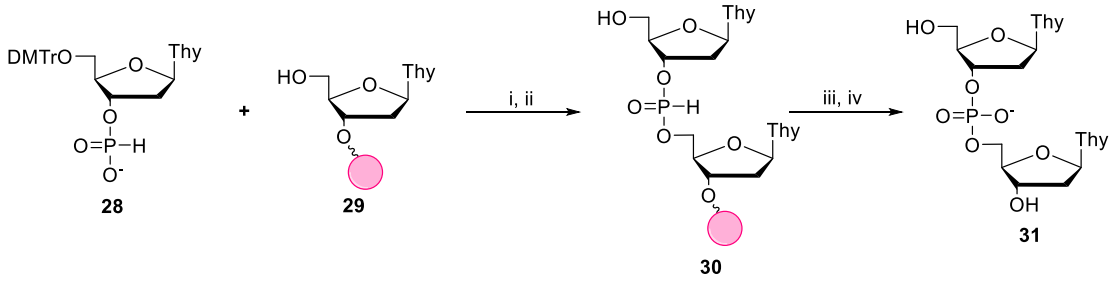

Scheme 1.6: *Stawiński's H-phosphonate strategy for oligonucleotide synthesis. Reagents:* ***i,*** *PvCl, ACN, pyridine.* ***ii,*** *DCA, DCM.* ***iii,*** *I_2, pyridine, H_2O.* ***iv,*** *NH_4OH.*

As mentioned above, H-phosphonates are readily converted into a range of P(V) species and given the array of internucleotide linkages used in oligonucleotide therapeutics, this allows H-phosphonates to be a versatile synthetic handle[91]. Oxidative conversion of H-phosphonate diesters to PO, PS, phosphoramidate[57], alkyl phosphonate, phosphoroselenoate, and other backbones have all been demonstrated (**Figure 1.11**)[88]. However, while H-phosphonate diesters themselves are stable to acidic conditions, they have been shown

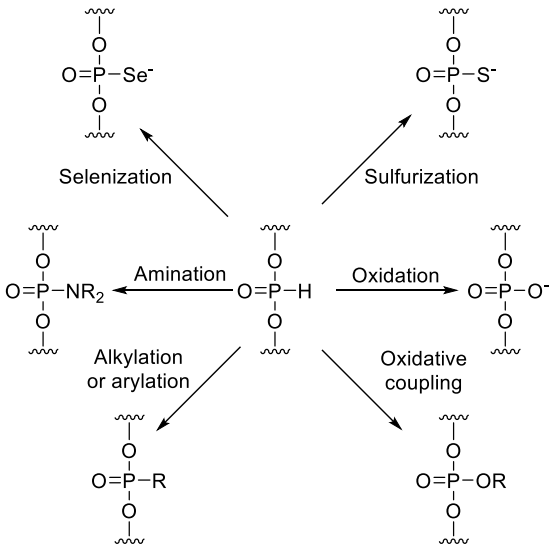

Figure 1.11*: Strategies to access a range of phosphorous backbones from H-phosphonates.*

to degrade in the presence of basic aqueous conditions, which will be further discussed in **Chapter 2**[87]. Additionally, while the strategy outlined by Stawiński is attractive, the yields obtained were still generally lower than those obtained by the phosphoramidite method and the use of H-phosphonate chemistry did not gain widespread use. Colin Reese developed a modified H-phosphonate approach that circumvented the instability of H-phosphonate diesters by oxidizing them to the corresponding phosphorothioate triester and used this strategy to synthesize the antisense oligonucleotide drug Vitravene on a multi-gram scale in solution[92]. This approach will also be discussed further in **Chapter 2**.

1.5.5: Stereocontrolled oligonucleotide synthesis

As discussed in section **1.4.4**, the PS backbone is one of the most important chemical modifications used in developing therapeutic oligonucleotides. However, the natural PO backbone of DNA and RNA is not a stereocenter, but the substitution of an oxygen by sulfur does confer chirality at this position (**Figure 1.12**). Despite this, approved oligonucleotide therapeutics with chiral phosphorous backbones are available as a mixture of all possible diastereomers which can number in the hundreds of thousands (2^{19} possible diastereomers for a 20-mer phosphorothioate oligonucleotide) [93]. In this regard, oligonucleotides are not held to the same standard as other therapeutics where absolute stereochemistry is essential and most drugs are available as single enantiomers or diastereomers. The importance of stereochemistry in drug development is perhaps best illustrated by thalidomide, one of the world's most notorious drugs due to the severe birth defects it induced in children between 1957 and 1962. One enantiomer of the drug caused birth defects, while the other provided the desired effects alleviating morning sickness[94]. Despite evidence that the stereochemistry at phosphorous does play a role in the pharmacology of oligonucleotides[95], it has widely been accepted that a mixture of diastereomers provides an acceptable therapeutic response. One can imagine that precise control of stereochemistry may lead to more effective therapies being developed. In fact, there have been numerous studies demonstrating the difference in biological activity and chemical properties of stereopure (or stereoenriched) PS oligonucleotides including modulation of RNase H activity[96], immune activation[97], siRNA activity[98], and chemical properties[99]. The difficulties in producing

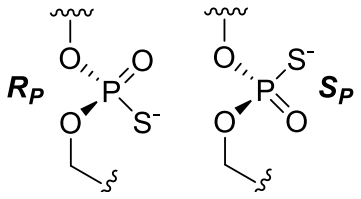

***Figure 1.12**: Different stereochemistries of a PS backbone.*

stereopure oligonucleotides have been historically compounded by the lack of efficient chemistry for stereospecific phosphorous coupling as well as the difficulties associated with purifying the many possible diastereomers.

Despite the introduction of the PS backbone during the infancy of oligonucleotide synthesis by Eckstein in 1967[56], the majority of the work done on stereocontrolled PS synthesis began during the 1980s. Wojciech Stec was one of the early pioneers of stereocontrolled PS synthesis, most notably due to his work on developing an oxathiaphospholane method. Initial mechanistic work found hydrolysis of oxathiaphospholane **32** (**Scheme 1.7A**) occurs exclusively via cleavage of the P-S bond followed by rapid elimination of the episulfide to yield **33** as the exclusive diastereomer[100]. This observation led to the development of nucleotide oxathiophospholane **34** which in the presence of DBU and a 3′-protected nucleoside **35**, followed by deprotection, yielded stereopure PS dimer **36** in high yield (>95%, **Scheme 1.6B**). Further elaboration of this strategy allowed for synthesis of a stereopure dodecamer of adenosine via solid-support synthesis and subsequent experiments showed that the all S_P sequence had a higher binding affinity than the all R_P sequence to a complementary strand[101]. This represented one of the first discoveries of significant changes in chemical properties of an oligonucleotide as determined by the stereochemistry of a PS backbone.

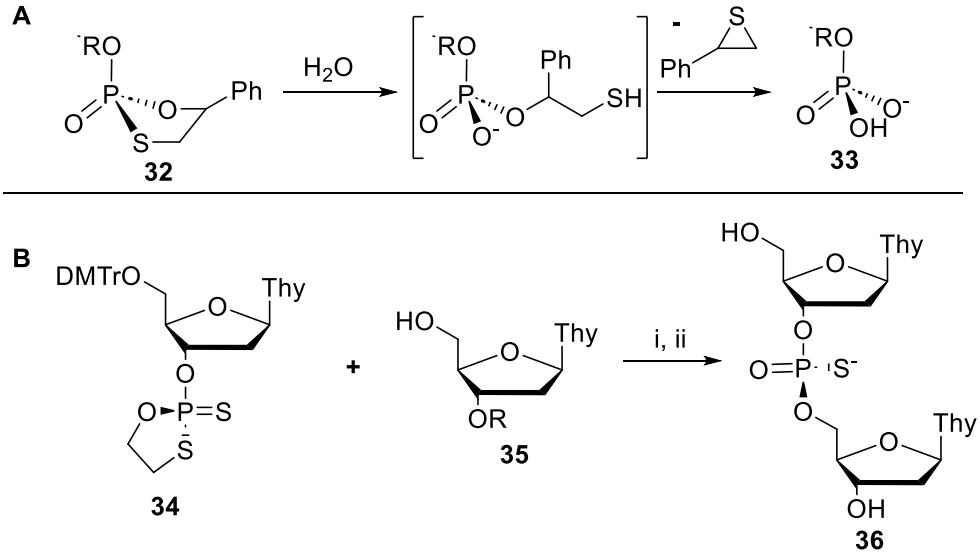

Scheme 1.7: *Stec's oxathiaphospholane strategy for stereocontrolled PS synthesis.* ***A:*** *Mechanistic studies into stereospecific hydrolysis followed by loss of episulfide of oxathiaphospholane.* ***B:*** *Stereospecific synthesis of dinucleotide bearing PS linkage. Reagents:* ***i****, DBU, ACN.* ***ii,*** *TCA in DCM then NH_4OH.*

Stec later evolved the strategy in 1998 by modifying the oxathiaphospholane ring into a spiro compound which facilitated separation of the diastereomeric monomers and further allowed them to introduce both stereocontrolled PS linkages and natural PO linkages[102]. Although some other strategies (H-phosphonate[103], indol-oxazaphosphorine[104], and others) emerged during this time, most were not highly diastereoselective or were not amenable to solid-phase synthesis. Stec's strategy was the most successful to emerge during this time, but he correctly noted[101] that there were still numerous challenges to be addressed with stereospecific PS oligonucleotide synthesis including low coupling yields (~92-96%) and difficulties in purification despite the improvements made in 1998. Additionally, in 1995 Sudhir Agrawal developed a chiral oxazaphospholidine strategy based on ephedrine which resulted in stereopure monomers, but stereoselectivity of 9:1 during sulfurization of the monomer[105]. While this represented an important step forward, the lack of 100% stereocontrol during sulfurization, coupled with their observations that stereoselectivity was lost during activation with acidic activators[106] (tetrazole) prevented this approach from being widely adopted. Agrawal further elaborated this strategy using a bicyclic oxazaphospholidine derivative for solid-phase synthesis which gave similar (9:1 stereoselectivity) as the previous approach, but allowed for easier purification of diastereomers[107].

The next major advancement came in 2000 with Beaucage's adaptation of phosphoramidite chemistry to stereocontrolled PS synthesis[108]. Beaucage's approach circumvented the rapid epimerization of activated P(III)[109] species previously reported by Agrawal by synthesizing cyclic acylphosphoramidites. Contrarily to standard phosphoramidite chemistry which is activated by weak acids with nucleophilic conjugate bases, this strategy relied on base-activation of the 5′OH of a 3′-protected nucleoside, likely due to the reduced basicity of the amide of **37** (**Scheme 1.8**) as compared to the amine of a typical phosphoramidite. Thus, in the presence of *N,N,N′,N′*-tetramethylguanidine (TMG), **37** was coupled with **38** to yield the phosphite triester **39** quantitatively as a single diastereomer. Sulfurization using Beaucage's reagent[110] yielded the PS triester **40** as a single product, as confirmed by ^{31}P NMR. Further elaboration of this strategy to solid-phase synthesis resulted in average coupling yields of 98% (calculated by DMTr absorbance at 498 nm) and stereopure trimers and tetramers were synthesized and analyzed by HPLC after deprotection with ammonia.

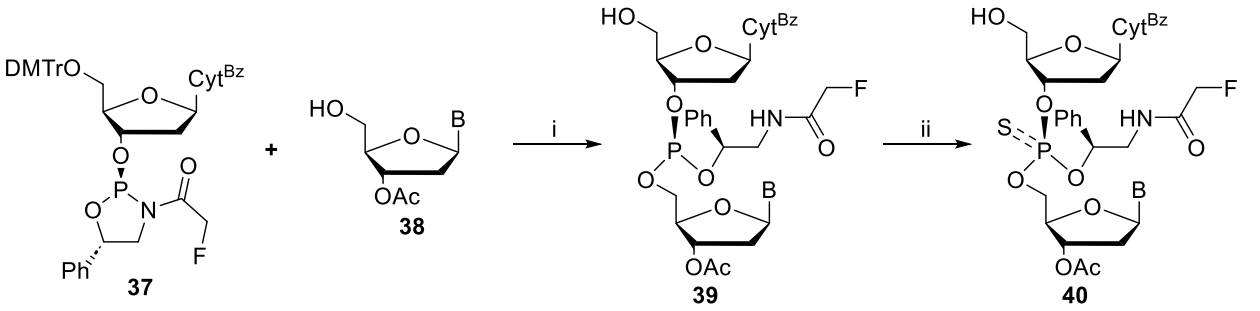

***Scheme 1.8**: Beaucage's cyclic phosphoramidite strategy for stereocontrolled PS synthesis. Reagents: **i**, TMG, ACN. **ii,** Beaucage's reagent, ACN.*

In a similar strategy adopted by both Agrawal and Beaucage's work, in 2002 Takeshi Wada developed a stereoselective oxaphospholidine strategy utilizing a non-nucleophilic acidic activator that would avoid the loss of stereoselectivity observed by Agrawal[111]. This strategy started by synthesis of diastereopure phosphoramidites **41** (**Scheme 1.9**) from PCl_3 and β-amino alcohols using the same approach adopted by Agrawal. The key work came in development of the novel activator **43**, which was easily synthesized from the corresponding amine and tetrafluoroboric acid etherate. It should be noted that two other similar activators were synthesized, but **43** produced the best results in terms of diastereoselectivity and reaction time. Coupling of **41** with **42** in the presence of 2 equivalents of **43** yielded phosphite triester **44** quantitatively with >99:1 diastereoselectivity for the R_P isomer in under 5 minutes. It should be noted that the reaction with the opposite diastereomer of **41** produced similar results, albeit with slightly lower diastereoselectivity (4:96) for the S_P isomer. Sulfurization of **44** with Beaucage's reagent produced PS triester **45** followed by deprotection and analysis by HPLC and ^{31}P NMR yielded PS dimer **46** as a single isomer. Importantly, acetylation after coupling was necessary to avoid side reactions of the amine of the chiral auxiliary during sulfurization. The same strategy was fine-tuned and applied to 5′DMTr phosphoramidites similar to **41** allowing for applications to solid-phase synthesis of longer (up to 10-mer) oligomers with excellent yields and diastereoselectivites[112].

During the 2000s Wada continued to pioneer stereoselective oligonucleotide synthesis as evidenced by his many publications including his adaptation of the oxophospholidine strategy to synthesize stereopure boranophosphates[113] and H-phosphonates[114]. While H-phosphonates themselves are not particularly useful due to their instability[87], they do offer a synthetic handle for transformation to a wide range of other functional groups including phosphoramidates[115],

alkyl phosphonates, phosphoroselenoates, and others[91]. His efforts culminated in the solid-phase oligonucleotide synthesis of longer stereopure DNA oligomers[116], RNA oligomers[117], and 2′-modified oligomers[118]. Additionally, Wada published an excellent review[119] in 2011 which covers much of the same stereoselective chemistry described here as well as elaborating on some other strategies that had less success.

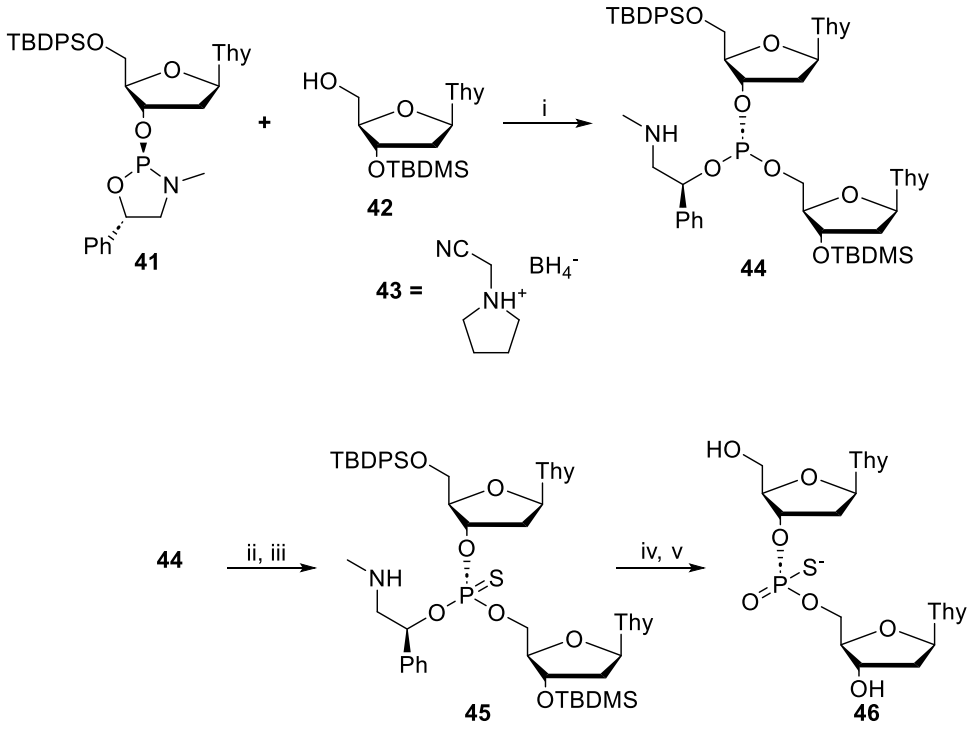

Scheme 1.9: *Wada's oxophospholidine strategy for stereocontrolled PS synthesis using non-nucleophilic acid activators. Reagents:* ***i, 43****, ACN.* ***ii****,* Ac_2O*, pyridine.* ***iii****, Beaucage's reagent.* ***iv,*** *DBU.* ***v,*** *TREAT-HF.*

Perhaps the best application of the oxophospholidine chemistry has been reported by Wave Life Sciences. Their 2017 publication detailed the important changes from Wada's work in their development of the stereocontrolled oligonucleotide synthesis with iterative capping and sulfurization (SOSICS) platform[120]. They used bicyclic phosphoramidites **47a-d** (**Scheme 1.10**) similar to those previously used by Wada[116] and changed the counterion of **43** to triflate to give activator **49**. Coupling of **47** with a solid-supported nucleoside **48** in the presence of **49** yielded phosphite triester **50** with inversion of stereochemistry. Capping with phenoxyacetic (PAc) anhydride yielded the key intermediate **51**. In contrast to Wada's strategy, sulfurization was achieved using *S*-cyanoethyl methylthiosulfonate which also led to spontaneous cleavage of the chiral auxiliary *via* an Arbuzov-type mechanism[121]. The retention of the chiral auxiliary during

synthesis had previously limited the length of oligonucleotides that could by synthesized by the oxophospholidine method to 12 nucleotides[116]. Addition of a methyl group at the α-position of the auxiliary of **51** allowed for an S_N1 type mechanism[121] to occur during sulfurization leading to the desired PS triester **52**. Detritylation of **52** under standard solid-phase conditions completes the synthesis cycle and after completion of the synthesis the oligonucleotide can be deprotected as normal.

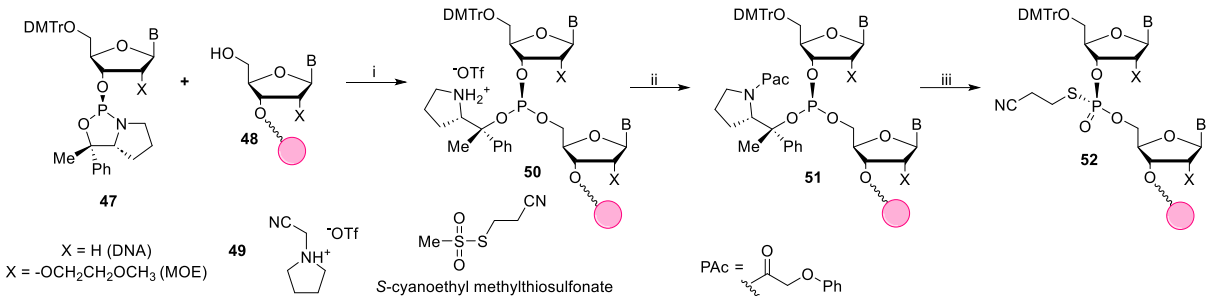

Scheme 1.10: *Wave Life Science's SOSICS platform. Reagents:* ***i****, 49, ACN.* ***ii****, Pac_2O, 2,6-lutidine, THF, then N-methylimidazole with the previous reagents.* ***iii****, S-cyanoethyl methylthiosulfonate, bis(trimethylsilyl)-trifluoroacetamide, ACN.*

Having developed a method for the synthesis of oligonucleotides with high yield and diastereoselectivity, the effects of various PS stereochemistries were explored within mipomersen, a 20-mer PS oligonucleotide gapmer with five 2′-methoxyethyl (MOE) residues at each end. Seven stereopure variants of mipomersen based on rational design were tested and compared against the stereorandom sequence. This study confirmed the previous observations[95] that the sequences containing higher R_P content had higher melting temperatures based on the amount of R_P incorporations (~0.5°C increase in T_m per R_P insertion). The all S_P oligonucleotide was more lipophilic as compared to the all R_P oligonucleotide as determined by elution time on a C18 reversed-phase HPLC column. When studying the stability of the oligonucleotides, it was found that increasing S_P content also increased stability in rat whole liver homogenates and the same trend was observed *in vitro* in rat serum. Perhaps most exciting about the stability assays was the ability of S_P PS linkages in the wings of an all DNA gapmer to provide similar stability as a gapmer with 2′MOE[122] residues and R_P linkages in the wings. Based on key protein interactions with the backbone as determined by the X-ray crystal structure of RNase bound to an RNA:DNA duplex, the authors designed sequences containing a 3′-$S_PS_PR_P$-5′ (*SSR*) motif in the central region of the gapmer to maximize those interactions. The sequence containing the

SSR motif displayed the highest cleavage activity of all sequences including mipomersen (stereorandom), although the sequence containing an *RRS* motif also displayed high activity. The *SSR* motif was also tested in an unrelated sequence to exclude sequence specific effects and they observed a similar increase in cleavage activity. Finally, they tested the sequences in mice and observed a similar suppression in protein levels after 17 days by mipomersen, the *SSR* sequence, and the *RRS* sequence. However, protein levels in mice administered the *SSR* sequence remained significantly lower for a much longer period, with statistically significant differences up to day 40. Similarly, a separate sequence in mice containing the *SSR* motif had increased activity as compared to the stereorandom sequence. This study represents the first systematic study of PS stereochemistry in therapeutically relevant sequences and demonstrated the power of stereocontrol to affect both physiochemical and pharmacological properties of an ASO.

Until recently, the oxophospholidine approach developed by Wada had been the most widely method for the synthesis of stereopure PS oligonucleotides in both industry[123] and academia[124]. However, Phil Baran developed a completely different strategy for stereocontrolled PS oligonucleotide synthesis using P(V) chemistry. Baran's strategy, initially published in 2018[125], is similar to Stec's oxathiaphospholane strategy, but relies on a limonene (**53**) derived scaffold to impart chirality. The reagent they developed, **ψ** (**Scheme 1.11A**), is prepared by epoxidation of **53** to yield **54** followed by ring-opening and subsequent closing with **55**. Stereochemistry of the PS linkage can be controlled as either S_P or R_P by using the corresponding **(+)-ψ** or **(-)-ψ**, respectively (derived from (-)-limonene or (+)-limonene). Nucleoside **56** (**Scheme 1.11B**) was loaded onto **ψ** to yield **53** with excellent yield (76-96%) in the presence of DBU. Subsequent coupling of **57** with nucleoside **58** in the presence of DBU yields dimer **59** with excellent yield (70-91%) as a single diastereomer. Additionally, they performed an unoptimized solid-phase synthesis using the **ψ** chemistry of a thymidine pentamer. Although the yield was low (23%), they obtained the desired pentamer a single diastereomer. Comparison with typical solid-phase phosphoramidite synthesis yielded the expected mixture of diastereomers, but in a much higher overall yield (63%).

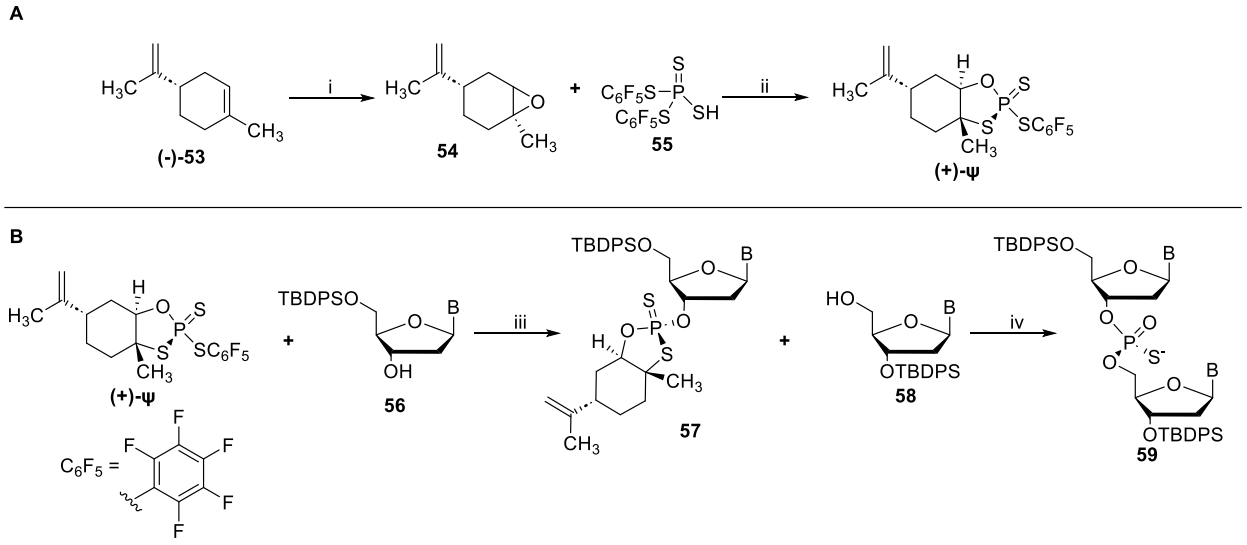

Scheme 1.11: *Baran's oxathiaphospholane strategy for stereocontrolled PS synthesis.* ***A:*** *Synthesis of P(V)* ***ψ*** *reagent.* ***B:*** *Nucleoside loading and coupling with* ***ψ.*** *Reagents:* ***i****, H_2O_2, phenylphosphonic acid, methyltrioctylammonium hydrogen sulfate, Na_2SO_4, sodium tungstate decahydrate, H_2O.* ***ii****, TFA, DCM.* ***iii****, DBU, ACN. i****v,*** *DBU, ACN.*

Baran further applied the **ψ** system to the synthesis of stereopure cyclic dinucleotides (CDNs), which have important biological implications[126]. Traditional strategies for CDN synthesis involve numerous protection and deprotection steps as well as providing a mixture of four diastereomers which are difficult to separate[127]. Baran's CDN synthesis began with coupling of **ψ**-loaded nucleoside **60** (**Scheme 1.12**) to solid-support bound nucleoside **61** with DBU. Cleavage of the resulting dimer from the solid-support yields stereopure dimer **62** and simultaneously liberates the 3′-hydroxyl of the nucleoside previously bound to the solid-support. To form the macrocycle, the authors devised two separate strategies: a stepwise approach or concerted approach. The stepwise approach is followed when R of **60** and **62** is **ψ**. This strategy offers complete stereocontrol resulting in synthesis of a single isomer of CDN **57**, but lower overall yield (14%). Although not explicitly addressed, the low yield is likely due to the competitive reaction of the 5′-hydroxyl of **61** with the 5′-**ψ** of **60** (undesired) versus reaction with the 3′-**ψ.** The concerted strategy is instead adopted when R of **62** is H. This reaction also involves a competitive reaction, but takes place during the macrocyclization step (**iv, Scheme 1.12**). The 5′ and 3′-hydroxyl groups of **62** can both competitively react with **ψ**, leading to poorer diastereoselectivity (3:1), but higher overall yield (44%) of **63**. Both strategies offer distinct advantages and reduce the number of steps for CDN synthesis by 4-5 as well as offering an avenue for stereospecific synthesis.

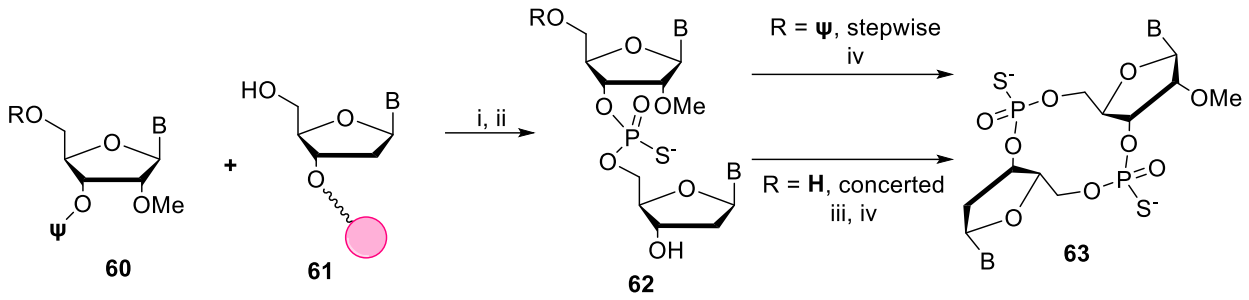

***Scheme 1.12**: Baran's stereocontrolled P(V) approach for CDN synthesis. Reagents: **i**, DBU, ACN. **ii**, NH_4OH. **iii**, **ψ**, DBU, ACN. **iv**, DBU, ACN.*

Baran continued to develop the **ψ** system by expanding it to include methods for synthesis of PS backbones, phosphodiester backbones, and phosphorodithioate backbones (PS_2) [128]. Besides the **(+)-ψ** and **(-)-ψ** reagents developed for stereocontrolled synthesis of S_P and R_P PS backbones respectively, they also developed ψ^2 for PS_2 synthesis, ***rac*-ψ** for racemic PS synthesis, and ψ^O for PO synthesis (**Figure 1.13**). Overall, the synthesis of these reagents followed a similar strategy as the system developed for the original **ψ** reagents. The synthesis of ψ^2 was directly inspired by Stec's[129] work, but circumvented some hazardous chemicals previously used and had no need of a chiral scaffold. Similarly, ψ^O had no need for a chiral scaffold and was designed in a similar way with a final desulfurization step using SeO_2. Finally, ***rac*-ψ** was synthesized very similarly to **(+)-ψ** and **(-)-ψ,** but used an achiral cyclohexene backbone rather than limonene, which imparts no stereocontrol on the coupling reactions. It should be noted that a significant amount of work was done in regard to optimizing the chemistry of these reagents and we direct the reader towards the publication for this information.

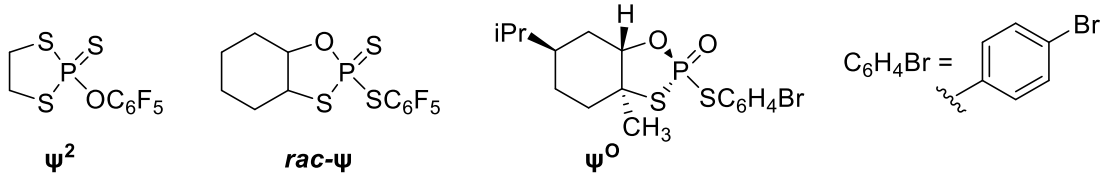

***Figure 1.13:** Baran's P(V) **ψ** reagents for the synthesis of oligonucleotides with different backbones.*

One of the issues the ψ^2 reagent circumvents is the inevitable formation of a small amount (7-10%) of PS backbone as inseparable impurities during the deprotection of PS_2 backbones[130]. Baran's strategy allowed access to PS_2 cleanly in one fewer step than the corresponding phosphoramidite approach, which resulted in the aforementioned impurities. Similarly, during oxidation of a mixed backbone (PO and PS) trimer they observed

desulfurization of the PS backbone when using phosphoramidite chemistry, but the P(V) approach using ψ^{O} to construct the PO backbone resulted in the desired product only. It should be noted that during typical phosphoramidite synthesis the PS backbone during such a synthesis would be protected with a cyanoethyl group and during this experiment they subjected an unprotected PS linkage to the oxidation conditions resulting in desulfurization. They also assessed the reaction rates of their P(V) platform with comparisons to phosphoramidite chemistry and the largely outdated phosphotriester approach previously described[70]. Their results confirmed the slow reaction rates of the traditional phosphotriester approach, but found their P(V) platform to have similar reaction rates to phosphoramidite chemistry, with all ψ reagent reactions complete within two minutes.

Having optimized the chemistry and assessed the reactivity of the P(V) system, they embarked on the challenge of developing an automated solid-phase synthesis cycle (**Figure 1.14**). They first had to develop a new universal linker for the solid support that would be stable to the basic conditions (DBU) required for loading and coupling. Additionally, alternative protecting groups from the typical amides used for the exocyclic amines of the nucleobases were also required (Pya[129] and Pom[131], **Figure 1.14**). They then set out to synthesize a small library of oligonucleotides bearing three locked nucleic acid (LNA) residues in the wings surrounding a DNA core with a range of backbone chemistries. Importantly, they synthesized a range of sequences and used the same synthesis cycle in each case in order to exclude any sequence specific results. They first synthesized stereopure PS gapmers of different sequences with both continuous S_P or R_P backbones as well as alternating S_P and R_P backbones. They then synthesized oligomers with PO and stereodefined PS backbones, as well as with PS_2 and stereodefined PS backbones. Impressively, they demonstrated the versatility of the platform by synthesizing an oligomer with stereodefined S_P and R_P PS backbones, PO backbones, and PS_2 backbones. Although the yields of the synthesis were generally lower than that of phosphoramidite chemistry solid-phase synthesis, this work represents the first example of a system in which

stereodefined PS, diastereomeric PS, PO, and PS_2 backbones can be synthesized within a single sequence and without modifications to the synthesis cycle.

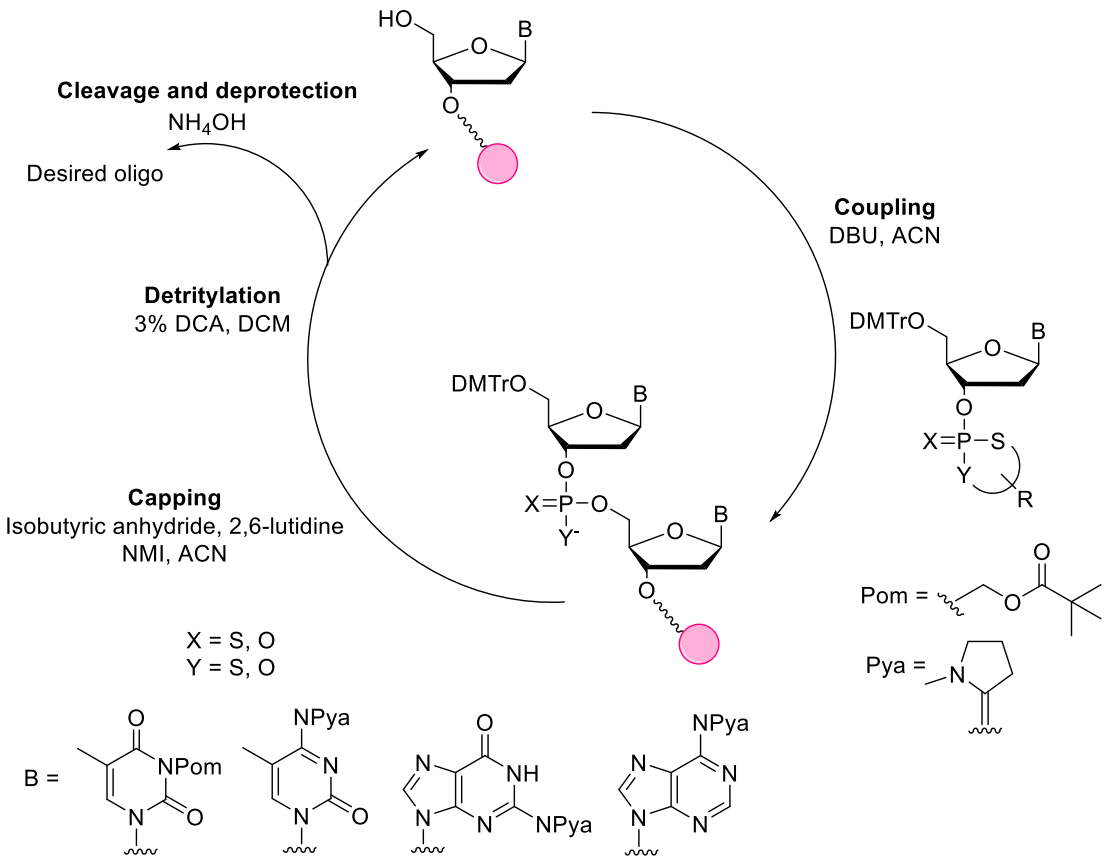

Figure 1.14: *Baran's automated solid-phase synthesis cycle using the* ***ψ*** *system.*

Some other strategies have emerged for stereocontrolled PS synthesis, but none have thus far been as reliable as the oxophospholidine strategy or the **ψ** system. For example, researchers at Alnylam Pharmaceuticals took advantage of the different retention times of R_P and S_P isomers of a PS dimer to isolate the pure diastereomers[132]. From these pure compounds they then synthesized dimer phosphoramidites which were then incorporated at the termini of siRNA molecules *via* solid-phase synthesis. While a relatively straightforward way to obtain stereopure compounds without developing new chemistry, this approach is limited in scope to compounds with few isolated PS linkages. Scott Miller, rather than previous works that relied on chiral auxiliaries, designed a chiral catalyst system based on either peptide-phosphonic acids or C2 symmetrical phosphonic acids to control PS stereochemistry[133]. Miller's strategy was only applied to the synthesis of 2′-5′ linked dimers with no strategy or demonstration for chain elongation and the yields (60-90%) and diastereoselectivities (up to 94:6, but mostly lower) were

generally insufficient to be applicable to longer sequences. However, the application of the chiral catalysts to CDN synthesis showed promise. Although the majority of work towards stereocontrolled oligonucleotide synthesis has explicitly been focused on PS backbones due to their ease of synthesis and powerful therapeutic effects, there are other backbone modifications that can impart chirality. However, the challenges of studying stereopure PS backbones have similarly limited the study of other chiral backbones. Some alternative stereopure backbones were synthesized by Wada as previously mentioned, but their application in longer oligonucleotides has been limited. However, Baran adapted his **ψ** towards stereoselective synthesis of methyl phosphonate dimers using a similar chiral auxiliary he termed **Π**[134]. The divergence from the **ψ** system involved transition to the *trans* isomer of limonene oxide (**54**) followed by loading with MeMgBr and subsequent coupling with a nucleoside. This strategy was applied to a wide range of substrates with excellent diastereoselectivity (>20:1) and generally good yields, but has yet to be applied to oligonucleotides longer than dimers.

While the physiochemical and pharmacological differences between the different isomers of PS oligonucleotides has been demonstrated *in vitro* and *in vivo*[120], there has yet to be convincing results in patients[93]. Further investigation towards these stereocontrolled oligonucleotides is required with simultaneous improvements in synthetic protocols.

1.5.6: Large-scale oligonucleotide synthesis

Due to the ever increasing number of oligonucleotide therapeutics on the market and in clinical trials, the capacity to synthesize oligonucleotides on large scales is a necessity for the industry moving forward. Although solid-phase oligonucleotide synthesis (SPOS) using phosphoramidite chemistry has remained the method of choice for large scale oligonucleotide synthesis, there are certain drawbacks. A recent analysis of eight different oligonucleotides in different phases of clinical development found a process mass intensity (PMI, defined as $\frac{\text{mass of raw materials (kg)}}{\text{mass of API (kg)}}$) of approximately 200 per nucleotide[135]. Furthermore, the authors found that of all the reagents used, up to 43% of them were

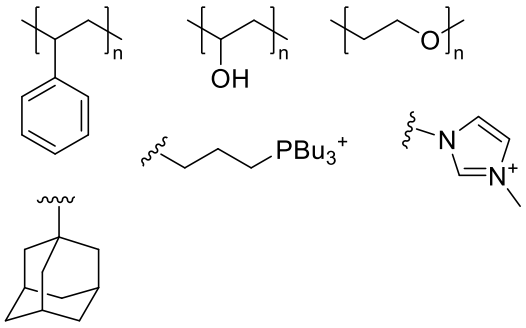

Figure 1.15*: A small sample of soluble supports used in LPOS. Clockwise from the top left: polystyrene, polyvinyl alcohol, PEG, imidazolium, phosphonium, and adamantyl.*

organic solvents which are notoriously toxic and hard to dispose of (**Figure 2.2**). A separate article also estimated that large scale oligonucleotide synthesis used on average 1320 liters of ACN and generated 4416 liters of waste per kilogram of oligonucleotide produced[136]. While current demands for synthetic oligonucleotides can be met by SPOS, should the need for a single oligonucleotide in huge quantities be required SPOS may not be the solution[137]. The loading capacity of solid-supports, excess of reagents required, and specialized equipment (rather than more typical batch reactors) required for SPOS have all been identified as potential issues, including the environmental concerns mentioned above. For these reasons, many researchers including our research group have turned towards liquid-phase oligonucleotide synthesis (LPOS) and other methods for both scalability and sustainability.

Liquid-phase oligonucleotide synthesis operates very similarly to SPOS, but with a key change from an insoluble support to a soluble support. Some examples of soluble supports are illustrated in **Figure 1.15** including polystyrene[138], polyvinyl alcohol[139], PEG[140], imidazolium[141], phosphonium[142], and adamantyl[131]. This change allows for homogeneous reaction conditions on a large scale in batch reactors with precipitation or extraction taking place in-between synthesis steps. LPOS has been the main avenue that researchers have explored towards developing larger scale oligonucleotide synthesis, and the impact of LPOS[143, 144] and soluble supports[145] have been reviewed in recent years. In general, most LPOS strategies have relied on very similar strategies to those outlined above with minimal changes to coupling chemistry (phosphoramidite) and the major changes coming from the use of different soluble supports. To that end, we direct the reader towards those reviews for comprehensive overviews of the field prior to 2019, but some more unique approaches will be highlighted here.

One of the more unique approaches to LPOS has been developed by Andrew Livingston and is based on organic solvent nanofiltration (OSN) [146]. Organic solvent nanofiltration generally operates by filtering compounds down to the molecular level with great precision based usually on size, geometry, or both[147]. Livingston's work initially attempted to use a PEG-supported strategy, but found the rejection rate (amount of the construct that did not pass through the membrane) to be too low resulting in inefficient purification. They eventually settled on trifunctional homostar linker (**64, Scheme 1.13**) which they hypothesized would improve the rejection rate. After also developing a new OSN membrane that would be compatible with

oligonucleotide synthesis, they functionalized **64** with 5′DMTr-2′OMe U **65** through a succinyl linker and following detritylation yielded **66**, ready for coupling. They coupled phosphoramidite **67** with **66** using 1.5 equivalents of **67** per branch of **66** (4.5 eq. total) followed by sulfurization using phenylacetyl disulfide (PADS) to yield phosphorothioate dimer **68** in 75% apparent yield. They repeated the synthesis cycle until a 9-mer was synthesized in decent crude purity (49%)[148]. While the initial coupling to dimer **68** resulted in a modest apparent yield of 75%, they found that the apparent yield increased with increasing length of the oligonucleotide up to a plateau of approximately 95%. The authors hypothesized that this was due to the increased rejection rate and therefore increased recovery of the oligonucleotide as the chain was extended. Besides the large volumes required during diafiltration steps, an additional precipitation step was also required after each detritylation reaction.

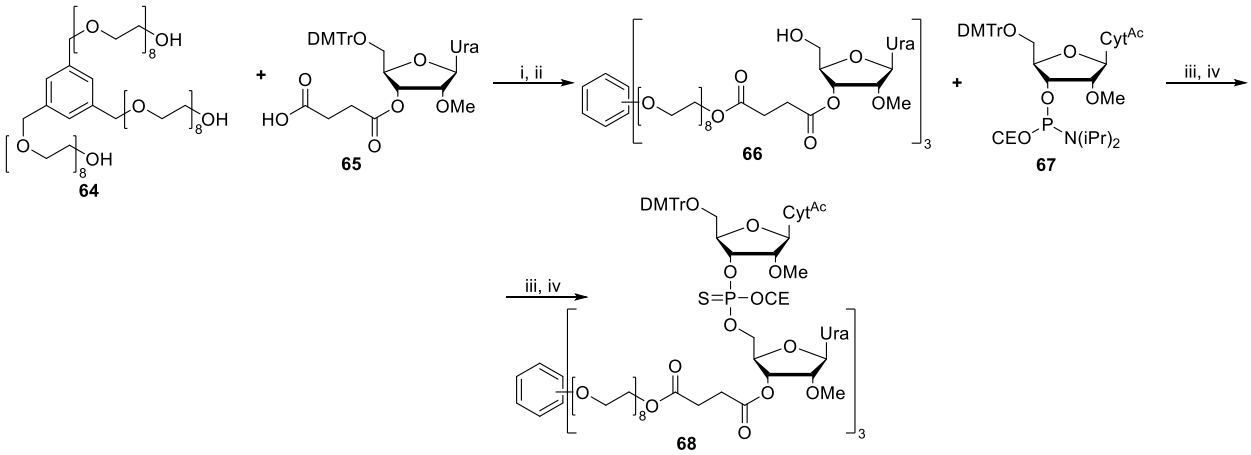

Scheme 1.13: *Livingston's organic solvent nanofiltration strategy for liquid-phase oligonucleotide synthesis. Reagents:* ***i****, 2,6-dichlorobenzoyl chloride, NMI, DCM.* ***ii****, DCA, pyrrole, DCM.* ***iii****, ETT, ACN.* ***iv****, PADS, pyridine.*

While not developed for the synthesis of therapeutic oligonucleotides, Andreas Walther reported a scalable LPOS strategy used for the construction of DNA hydrogels[149]. While most oligonucleotide synthesis strategies have focused on therapeutic applications, DNA-based hydrogels possess unique characteristics as non-toxic, stimuli-responsive materials[150]. Walther's strategy used a four-armed PEG support **69** (**Scheme 1.14**, for simplicity only one arm shown after **69**), inspired by previous work[151]. Although previous efforts had used a similar strategy[152], they only synthesized oligonucleotides up to pentamers with no real improvements on the synthetic strategy outlined by Bonora in 1993[140]. The present work thus began by coupling of phosphoramidite **70** with free hydroxyl groups of **69**. The use of phosphoramidite chemistry for this first loading of a nucleoside onto **69** rather than a linker (often succinyl) is possible in this strategy as there is no cleavage of the final oligonucleotide from **69.** One can imagine modifying

this approach slightly which would allow for cleavage from the support, liberating the desired oligonucleotide. Their approach differed from previous LPOS strategies by omitting precipitation after each step of the synthesis cycle and instead directly proceeding with oxidation using *meta*-chloroperbenzoic acid (mCPBA) in one-pot to yield **71**. They then proceeded directly with detritylation, once again in one-pot, using trichloroacetic acid (TCA) and triethylsilane (TES) as a trityl cation scavenger to yield **72**. Finally, instead of precipitation of the product from diethyl ether, they found precipitation after this three-step protocol from 2-propanol at -30°C yielded the desired product **73** in excellent yield and purity. Thus, their strategy reduced the number of precipitation steps significantly and was readily scaled up to 10 grams. They applied the synthesis cycle outlined in **Scheme 1.14** to synthesize dT and dA 20-mers. Additional optimization of detritylation conditions for the dA oligonucleotides were required to avoid depurination, and they eventually found that using a 70-fold excess (per each of four arms) of dichloroacetic acid (DCA) at 0°C resulted in efficient detritylation and minimal depurination after reacting for 100 minutes. Mixing of the dT and dA oligonucleotides and slow annealing resulted in hydrogels up to several cm^3 size with interesting properties.

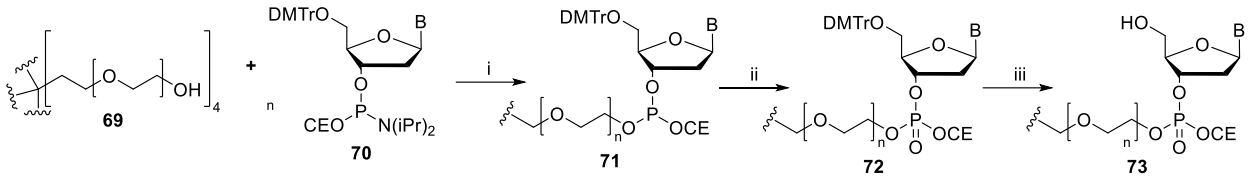

Scheme 1.14: *Walther's four-armed PEG synthesis cycle for the synthesis of DNA hydrogels. Reagents:* ***i****, ETT, ACN.* ***ii****, mCPBA.* ***iii****, TCA, DCM, TES (for dT) then precipitation from 2-propanol at -30°C. DCA, DCM, TES, 0°C (for dA) then precipitation from 2-propanol at -30°C.*

Biogen's recent work on LPOS is one of few examples of a successful scale-up of the strategy[153]. They applied a convergent strategy using tetra- and pentamer blocks to synthesize an 18-mer ASO gapmer on a ~200 gram scale and a 34-mer on a gram scale. They also synthesized a handful of the blocks used at a 3kg scale, demonstrating the ability to further scale up the process. While their work did not do much to fundamentally change the phosphoramidite chemistry used during LPOS, their use of a lower MW soluble support (**Figure 1.16**), successful scaleup, and comprehensive analysis of the impurity profile is commendable. Another successfully scaled up LPOS

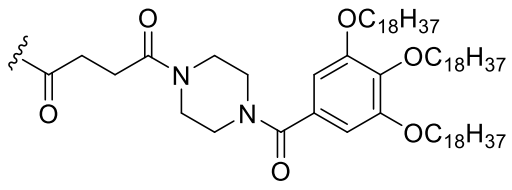

Figure 1.16*: Soluble support used by Biogen in their convergent LPOS strategy.*

used Ajiphase[154] to synthesize GMP phosphorodiamidate morpholino oligonucleotide (PMO) on a 10 kg scale[144]. In contrast to other LPOS strategies, the Ajiphase approach required only a single precipitation after reactions and yielded oligonucleotides in high yields and purities. However, long reaction times (60 minutes) are a significant drawback. In recent years, including Walther's approach, Biogen's approach, and the Ajiphase approach, researchers have leaned into telescoping reactions with minimal precipitations after synthesis cycles (rather than after each reaction) which has substantially reduced solvent usage.

Biocatalysis for oligonucleotide synthesis has emerged as a promising strategy and has been recently reviewed[155]. However, enzymatic synthesis of oligonucleotides comes with a few key challenges: substrate scope, challenges associated with triphosphate synthesis, and the template-dependent nature of most polymerases. Probably the simplest biocatalytic strategy that has been applied for oligonucleotide synthesis has relied on ligase enzymes to stitch together smaller fragments yielding the desired final product[156]. This strategy still relies on chemical methods (usually SPOS) for the synthesis of short oligonucleotides, which simplifies the overall process as more challenges are encountered when synthesizing longer sequences by SPOS. Use of a template during ligation has also been shown to ligate fragments containing 2′MOE modifications and PS backbones in 90% yield[157]. While this is a very high yield, the loss of even 10% of highly precious fragments with 5′-phosphate groups is problematic. More interestingly have been the template-free approaches using engineered polymerases for developing an enzymatic synthesis cycle for oligonucleotide synthesis[158]. While this is also a promising strategy, the large excess of nucleotide triphosphates presents issues for large-scale synthesis as well as the challenges mentioned above. Overall, the synthesis of oligonucleotides by enzymatic processes for therapeutic purposes, which contain many chemical modifications in very specific locations, is relatively underdeveloped when compared with chemical methods, but represents an exciting new direction for the field. It should be mentioned of course that the production of mRNA vaccines has been successfully scaled up by companies such as Moderna *via* IVT, but is not necessarily a suitable strategy for the synthesis of ASOs or siRNAs.

1.6: Thesis objectives

The aim of this thesis is to develop more sustainable methods for oligonucleotide synthesis using H-phosphonate chemistry. Emphasis is placed on reducing solvent consumption

during reactions and, in later chapters, during purification and the scalability of the methods. Finally, we benchmark the methods developed to traditional solution-phase and solid-phase methods.

Chapter 2 focuses on the use of mechanochemistry, specifically vibrational ball milling (VBM), for the synthesis of short DNA oligonucleotides. We optimized the chemical reactions of H-phosphonate chemistry by VBM and synthesized dimers and trimers and reduced solvent consumption by up to 90% during reactions.

Chapter 3 continues the work of the previous chapter, by expanding the strategy to longer sequences and chemically modified sequences. We achieved this by adopting a "block" coupling approach, where we coupled dimers together to eventually synthesize a hexamer. We also showed the compatibility of the method with RNA, 2′F, 2′OMe, and PS backbone oligonucleotides.

Chapter 4 demonstrates the development of two new strategies for sustainable oligonucleotide synthesis. The first, uses resonant acoustic mixing (RAM) to synthesize DNA dimers and trimers. We optimized the chemistry using RAM and H-phosphonate chemistry and similarly reduced solvent use during reactions by up to 90% and successfully demonstrated the scaleup of the method up to a multi-gram scale. The second method developed in this chapter takes advantage of the physical properties of a PEG-nucleoside conjugate in a process we have termed thermally controlled oligonucleotide synthesis (TCOS). We found that PEG-nucleosides retain similar melting temperatures to unconjugated PEG and that conducting of reactions where the PEG-nucleoside is melted (~75°C) followed by cooling of the mixture allows for selective precipitation of PEG-oligonucleotides. Addition of very small amounts of solvent left other reagents in solution allowing for isolation of pure PEG-oligonucleotides in high yield and recovery. This strategy reduced solvent consumption by up to 95% for the whole synthesis process as compared to similar methods.

Chapter 5 compares the three methods developed in previous chapters to solution-phase reactions as well as promising strategies from the literature. The PMI for the three methods developed in the previous chapters is calculated as well as for a comparable solution-phase reaction. PMI calculation of two strategies from the literature was also performed and all of the

above methods were compared to large-scale SPOS methods. Finally, the solvent choice was also examined for potential safety hazards and the feasibility of scaling each method.

1.7: References:

(1) Dahm, R. Friedrich Miescher and the discovery of DNA. *Developmental biology* **2005**, *278* (2), 274-288.

(2) Dahm, R. Discovering DNA: Friedrich Miescher and the early years of nucleic acid research. *Human genetics* **2008**, *122*, 565-581.

(3) Levene, P.; London, E. On the structure of thymonucleic acid. *Science* **1928**, *68* (1771), 572-573.

(4) Griffith, F. The significance of pneumococcal types. *Epidemiology & Infection* **1928**, *27* (2), 113-159.

(5) Avery, O. T.; MacLeod, C. M.; McCarty, M. *Studies on the chemical nature of the substance inducing transformation of pneumococcal types: induction of transformation by a desoxyribonucleic acid fraction isolated from pneumococcus type III*; Springer, 2017.

(6) Franklin, R. E.; Gosling, R. G. Molecular configuration in sodium thymonucleate. *Nature* **1953**, *171*, 740-741.

(7) Watson, J. D.; Crick, F. H. Molecular structure of nucleic acids: a structure for deoxyribose nucleic acid. *Nature* **1953**, *171* (4356), 737-738.

(8) Franklin, R. E.; Gosling, R. G. Evidence for 2-chain helix in crystalline structure of sodium deoxyribonucleate. *Nature* **1953**, *172*, 156-157.

(9) Altona, C. T.; Sundaralingam, M. Conformational analysis of the sugar ring in nucleosides and nucleotides. New description using the concept of pseudorotation. *Journal of the American Chemical Society* **1972**, *94* (23), 8205-8212.

(10) Juaristi, E.; Cuevas, G. The anomeric effect. **1994**.

(11) Rich, A. The double helix: a tale of two puckers. *Nature Structural & Molecular Biology* **2003**, *10* (4), 247-249.

(12) Plavec, J.; Tong, W.; Chattopadhyaya, J. How do the gauche and anomeric effects drive the pseudorotational equilibrium of the pentofuranose moiety of nucleosides? *Journal of the American Chemical Society* **1993**, *115* (21), 9734-9746.

(13) Hunter, C. A. Sequence-dependent DNA structure: the role of base stacking interactions. *Journal of molecular biology* **1993**, *230* (3), 1025-1054.

(14) Nair, D. T.; Johnson, R. E.; Prakash, S.; Prakash, L.; Aggarwal, A. K. Replication by human DNA polymerase-ι occurs by Hoogsteen base-pairing. *Nature* **2004**, *430* (6997), 377-380.

(15) Drew, H. R.; Wing, R. M.; Takano, T.; Broka, C.; Tanaka, S.; Itakura, K.; Dickerson, R. E. Structure of a B-DNA dodecamer: conformation and dynamics. *Proceedings of the National Academy of Sciences* **1981**, *78* (4), 2179-2183.
(16) Wang, A.; Fujii, S.; Van Boom, J. H.; Rich, A. Molecular structure of the octamer d (GGCCGGCC): modified A-DNA. *Proceedings of the National Academy of Sciences* **1982**, *79* (13), 3968-3972.
(17) Ghosh, A.; Bansal, M. A glossary of DNA structures from A to Z. *Acta Crystallographica Section D: Biological Crystallography* **2003**, *59* (4), 620-626.
(18) Blackburn, G. M.; Gait, M. J.; Williams, D. M.; Loakes, D. *Nucleic acids in chemistry and biology*; Royal Society of Chemistry, 2006.
(19) Weiss, S. B.; Nakamoto, T. Net synthesis of ribonucleic acid with a microbial enzyme requiring deoxyribonucleic acid and four ribonucleoside triphosphates. *Journal of Biological Chemistry* **1961**, *236* (3), PC18-PC20.
(20) Furuichi, Y.; Muthukrishnan, S.; Shatkin, A. 5'-Terminal m-7G (5') ppp (5') Gmp in vivo: identification in reovirus genome RNA. *Proceedings of the National Academy of Sciences* **1975**, *72* (2), 742-745.
(21) Philipson, L.; Wall, R.; Glickman, G.; Darnell, J. Addition of polyadenylate sequences to virus-specific RNA during adenovirus replication. *Proceedings of the National Academy of Sciences* **1971**, *68* (11), 2806-2809.
(22) Brody, E.; Abelson, J. The" Spliceosome": Yeast Pre-Messenger RNA Associates with a 40 S Complex in a Splicing-Dependent Reaction. *Science* **1985**, *228* (4702), 963-967.
(23) Palade, G. E. A small particulate component of the cytoplasm. *The Journal of biophysical and biochemical cytology* **1955**, *1* (1), 59.
(24) Nissen, P.; Hansen, J.; Ban, N.; Moore, P. B.; Steitz, T. A. The structural basis of ribosome activity in peptide bond synthesis. *Science* **2000**, *289* (5481), 920-930.
(25) Hoagland, M. B.; Stephenson, M. L.; Scott, J. F.; Hecht, L. I.; Zamecnik, P. C. A soluble ribonucleic acid intermediate in protein synthesis. *J. biol. Chem* **1958**, *231* (1), 241-257.
(26) Coffin, J. M.; Hughes, S. H.; Varmus, H. E. Retroviruses. **1997**.
(27) Zamecnik, P. C.; Stephenson, M. L. Inhibition of Rous sarcoma virus replication and cell transformation by a specific oligodeoxynucleotide. *Proceedings of the National Academy of Sciences* **1978**, *75* (1), 280-284.

(28) Deleavey, G. F.; Damha, M. J. Designing chemically modified oligonucleotides for targeted gene silencing. *Chemistry & biology* **2012**, *19* (8), 937-954.
(29) Watts, J. K.; Corey, D. R. Silencing disease genes in the laboratory and the clinic. *The Journal of pathology* **2012**, *226* (2), 365-379.
(30) Aartsma-Rus, A.; Straub, V.; Hemmings, R.; Haas, M.; Schlosser-Weber, G.; Stoyanova-Beninska, V.; Mercuri, E.; Muntoni, F.; Sepodes, B.; Vroom, E. Development of exon skipping therapies for Duchenne muscular dystrophy: a critical review and a perspective on the outstanding issues. *Nucleic acid therapeutics* **2017**, *27* (5), 251-259.
(31) Ward, A. J.; Norrbom, M.; Chun, S.; Bennett, C. F.; Rigo, F. Nonsense-mediated decay as a terminating mechanism for antisense oligonucleotides. *Nucleic acids research* **2014**, *42* (9), 5871-5879.
(32) Egli, M.; Manoharan, M. Chemistry, structure and function of approved oligonucleotide therapeutics. *Nucleic Acids Research* **2023**, gkad067.
(33) Bennett, C. F. Therapeutic antisense oligonucleotides are coming of age. *Annual review of medicine* **2019**, *70*, 307-321.
(34) Fire, A.; Xu, S.; Montgomery, M. K.; Kostas, S. A.; Driver, S. E.; Mello, C. C. Potent and specific genetic interference by double-stranded RNA in Caenorhabditis elegans. *nature* **1998**, *391* (6669), 806-811.
(35) Liu, J.; Carmell, M. A.; Rivas, F. V.; Marsden, C. G.; Thomson, J. M.; Song, J.-J.; Hammond, S. M.; Joshua-Tor, L.; Hannon, G. J. Argonaute2 is the catalytic engine of mammalian RNAi. *Science* **2004**, *305* (5689), 1437-1441.
(36) Hu, B.; Zhong, L.; Weng, Y.; Peng, L.; Huang, Y.; Zhao, Y.; Liang, X.-J. Therapeutic siRNA: state of the art. *Signal transduction and targeted therapy* **2020**, *5* (1), 1-25.
(37) Jinek, M.; Chylinski, K.; Fonfara, I.; Hauer, M.; Doudna, J. A.; Charpentier, E. A programmable dual-RNA–guided DNA endonuclease in adaptive bacterial immunity. *science* **2012**, *337* (6096), 816-821.
(38) Liu, G.; Lin, Q.; Jin, S.; Gao, C. The CRISPR-Cas toolbox and gene editing technologies. *Molecular Cell* **2021**.
(39) Barrangou, R.; Doudna, J. A. Applications of CRISPR technologies in research and beyond. *Nature biotechnology* **2016**, *34* (9), 933-941.

(40) BioSciences, S. CRISPR therapeutics push into human testing. *Nature Biotechnology* **2017**, *35* (1), 3.
(41) Anzalone, A. V.; Randolph, P. B.; Davis, J. R.; Sousa, A. A.; Koblan, L. W.; Levy, J. M.; Chen, P. J.; Wilson, C.; Newby, G. A.; Raguram, A. Search-and-replace genome editing without double-strand breaks or donor DNA. *Nature* **2019**, *576* (7785), 149-157.
(42) Khalil, A. M. The genome editing revolution. *Journal of genetic engineering and biotechnology* **2020**, *18* (1), 1-16.
(43) Zhu, G.; Chen, X. Aptamer-based targeted therapy. *Advanced drug delivery reviews* **2018**, *134*, 65-78.
(44) Lu, T. X.; Rothenberg, M. E. MicroRNA. *Journal of allergy and clinical immunology* **2018**, *141* (4), 1202-1207.
(45) Scheiermann, J.; Klinman, D. M. Clinical evaluation of CpG oligonucleotides as adjuvants for vaccines targeting infectious diseases and cancer. *Vaccine* **2014**, *32* (48), 6377-6389.
(46) Sullenger, B. A.; Nair, S. From the RNA world to the clinic. *Science* **2016**, *352* (6292), 1417-1420.
(47) Park, J. W.; Lagniton, P. N.; Liu, Y.; Xu, R.-H. mRNA vaccines for COVID-19: what, why and how. *International journal of biological sciences* **2021**, *17* (6), 1446.
(48) Pardi, N.; Hogan, M. J.; Porter, F. W.; Weissman, D. mRNA vaccines—a new era in vaccinology. *Nature reviews Drug discovery* **2018**, *17* (4), 261-279.
(49) Khvorova, A.; Watts, J. K. The chemical evolution of oligonucleotide therapies of clinical utility. *Nature biotechnology* **2017**, *35* (3), 238-248.
(50) Walters, W. P. Going further than Lipinski's rule in drug design. *Expert opinion on drug discovery* **2012**, *7* (2), 99-107.
(51) Geary, R. S. Antisense oligonucleotide pharmacokinetics and metabolism. *Expert opinion on drug metabolism & toxicology* **2009**, *5* (4), 381-391.
(52) Al Shaer, D.; Al Musaimi, O.; Albericio, F.; de la Torre, B. G. 2019 FDA TIDES (peptides and oligonucleotides) harvest. *Pharmaceuticals* **2020**, *13* (3), 40.
(53) Debacker, A. J.; Voutila, J.; Catley, M.; Blakey, D.; Habib, N. Delivery of oligonucleotides to the liver with GalNAc: from research to registered therapeutic drug. *Molecular Therapy* **2020**, *28* (8), 1759-1771.

(54) Pitsch, S.; Wendeborn, S.; Jaun, B.; Eschenmoser, A. Why Pentose-and Not Hexose-Nucleic Acids??. Part VII. Pyranosyl-RNA ('p-RNA'). Preliminary communication. *Helvetica chimica acta* **1993**, *76* (6), 2161-2183.
(55) Jana, S. K.; Harikrishna, S.; Sudhakar, S.; El-Khoury, R.; Pradeepkumar, P.; Damha, M. J. Nucleoside Analogues with a Seven-Membered Sugar Ring: Synthesis and Structural Compatibility in DNA–RNA Hybrids. *The Journal of Organic Chemistry* **2022**, *87* (5), 2367-2379.
(56) Eckstein, F. Nucleoside phosphorothioates. *Journal of the American Chemical Society* **1970**, *92* (15), 4718-4723.
(57) Vlaho, D. *Synthesis and biological properties of oligonucleotides containing phosphoramidate internucleotide linkages*; McGill University (Canada), 2017.
(58) Siddiquee, S.; Rovina, K.; Azriah, A. A review of peptide nucleic acid. *Advanced Techniques in Biology & Medicine* **2015**, 1-10.
(59) Saleh, A. F.; Arzumanov, A. A.; Gait, M. J. Overview of alternative oligonucleotide chemistries for exon skipping. *Exon Skipping: Methods and Protocols* **2012**, 365-378.
(60) McKenzie, L. K.; El-Khoury, R.; Thorpe, J. D.; Damha, M. J.; Hollenstein, M. Recent progress in non-native nucleic acid modifications. *Chemical Society Reviews* **2021**, *50* (8), 5126-5164.
(61) Reese, C. B. Oligo-and poly-nucleotides: 50 years of chemical synthesis. *Organic & biomolecular chemistry* **2005**, *3* (21), 3851-3868.
(62) Michelson, A.; Todd, A. R. Nucleotides part XXXII. Synthesis of a dithymidine dinucleotide containing a 3′: 5′-internucleotidic linkage. *Journal of the Chemical Society (Resumed)* **1955**, 2632-2638.
(63) Corby, N.; Kenner, G.; Todd, A. 704. Nucleotides. Part XVI. Ribonucleoside-5′ phosphites. A new method for the preparation of mixed secondary phosphites. *Journal of the Chemical Society (Resumed)* **1952**, 3669-3675.
(64) Khorana, H.; Razzell, W.; Gilham, P.; Tener, G.; Pol, E. Syntheses of dideoxyribonucleotides. *Journal of the American Chemical Society* **1957**, *79* (4), 1002-1003.
(65) Gilham, P. T.; Khorana, H. G. Studies on polynucleotides. I. A new and general method for the chemical synthesis of the C5 ″-C3 ″internucleotidic linkage. *Journal of the American Chemical Society* **1958**, *80* (23), 6212-6222.

(66) Schaller, H.; Weimann, G.; Lerch, B.; Khorana, H. Studies on Polynucleotides. XXIV.[1] The Stepwise Synthesis of Specific Deoxyribopolynucleotides (4).[2] Protected Derivatives of Deoxyribonucleosides and New Syntheses of Deoxyribonucleoside-3 ″Phosphates[3]. *Journal of the American Chemical Society* **1963**, *85* (23), 3821-3827.
(67) Agarwal, K.; Yamazaki, A.; Cashion, P.; Khorana, H. Chemical synthesis of polynucleotides. *Angewandte Chemie International Edition in English* **1972**, *11* (6), 451-459.
(68) Shampo, M. A.; Kyle, R. A. Har Gobind Khorana—Nobel Prize for Physiology or Medicine. In *Mayo Clinic Proceedings*, 2006; Elsevier: Vol. 81, p 284.
(69) Letsinger, R. L.; Mahadevan, V. Oligonucleotide synthesis on a polymer support[1, 2]. *Journal of the American Chemical Society* **1965**, *87* (15), 3526-3527.
(70) Tener, G. 2-Cyanoethyl Phosphate and its Use in the Synthesis of Phosphate Esters[1]. *Journal of the American Chemical Society* **1961**, *83* (1), 159-168.
(71) Letsinger, R. L.; Caruthers, M. H.; Jerina, D. M. Reactions of nucleosides on polymer supports. Synthesis of thymidylylthymidylylthymidine. *Biochemistry* **1967**, *6* (5), 1379-1388.
(72) Letsinger, R. L.; Mahadevan, V. Stepwise Synthesis of Oligodeoxyribonucleotides on an Insoluble Polymer Support[1, 2]. *Journal of the American Chemical Society* **1966**, *88* (22), 5319-5324.
(73) Letsinger, R. L.; Ogilvie, K. K. Convenient method for stepwise synthesis of oligothymidylate derivatives in large-scale quantities. *Journal of the American Chemical Society* **1967**, *89* (18), 4801-4803.
(74) Eckstein, F.; Rizk, I. Synthesis of oligonucleotides by use of phosphoric triesters. *Angewandte Chemie (International ed. in English)* **1967**, *6* (8), 695-697.
(75) Reese, C.; Saffhill, R. Oligonucleotide synthesis via phosphotriester intermediates: The phenyl-protecting group. *Chemical Communications (London)* **1968**, (13), 767-768.
(76) Reese, C. A systematic approach to oligonucleotide synthesis. In *Colloq. Int. CNRS*, 1970; Vol. 182, pp 319-328.
(77) Reese, C. B.; Zard, L. Some observations relating to the oximate ion promoted unblocking of oligonucleotide aryl esters. *Nucleic Acids Research* **1981**, *9* (18), 4611-4626.
(78) Letsinger, R. L.; Lunsford, W. B. Synthesis of thymidine oligonucleotides by phosphite triester intermediates. *Journal of the American Chemical Society* **1976**, *98* (12), 3655-3661.

(79) Alvarado-Urbina, G.; Sathe, G. M.; Liu, W.-C.; Gillen, M. F.; Duck, P. D.; Bender, R.; Ogilvie, K. K. Automated synthesis of gene fragments. *Science* **1981**, *214* (4518), 270-274.
(80) Beaucage, S.; Caruthers, M. Deoxynucleoside phosphoramidites—a new class of key intermediates for deoxypolynucleotide synthesis. *Tetrahedron letters* **1981**, *22* (20), 1859-1862.
(81) McBride, L.; Caruthers, M. An investigation of several deoxynucleoside phosphoramidites useful for synthesizing deoxyoligonucleotides. *Tetrahedron letters* **1983**, *24* (3), 245-248.
(82) Sinha, N.; Biernat, J.; Köster, H. β-Cyanoethyl N, N-dialkylamino/N-morpholinomonochloro phosphoamidites, new phosphitylating agents facilitating ease of deprotection and work-up of synthesized oligonucleotides. *Tetrahedron letters* **1983**, *24* (52), 5843-5846.
(83) Caruthers, M. DNA synthesis for nonchemists: the phosphoramidite method on silica supports. *Synthesis and Applications of DNA and RNA* **1987**, 47-94.
(84) Ogilvie, K. K.; Beaucage, S. L.; Schifman, A. L.; Theriault, N. Y.; Sadana, K. L. The synthesis of oligoribonucleotides. II. The use of silyl protecting groups in nucleoside and nucleotide chemistry. VII. *Canadian Journal of Chemistry* **1978**, *56* (21), 2768-2780.
(85) Van Boom, J.; Burgers, P. The application of levulinic acid as protective group to the synthesis of tetradecaribonucleotide U-A-U-A-U-A-U-A-U-A-U-A-U-A via the modified phosphotriester method. *Recueil des Travaux Chimiques des Pays-Bas* **1978**, *97* (3), 73-80.
(86) Lackey, J. G.; Mitra, D.; Somoza, M. M.; Cerrina, F.; Damha, M. J. Acetal levulinyl ester (ALE) groups for 2′-hydroxyl protection of ribonucleosides in the synthesis of oligoribonucleotides on glass and microarrays. *Journal of the American Chemical Society* **2009**, *131* (24), 8496-8502.
(87) Westheimer, F.; Huang, S.; Covitz, F. Rates and mechanisms of hydrolysis of esters of phosphorous acid. *Journal of the American Chemical Society* **1988**, *110* (1), 181-185.
(88) Stawinski, J.; Kraszewski, A. How to get the most out of two phosphorus chemistries. Studies on H-phosphonates. *Accounts of chemical research* **2002**, *35* (11), 952-960.
(89) Garegg, P. J.; Lindh, I.; Regberg, T.; Stawinski, J.; Strömberg, R.; Henrichson, C. Nucleoside H-phosphonates. III. Chemical synthesis of oligodeoxyribonucleotides by the hydrogenphosphonate approach. *Tetrahedron letters* **1986**, *27* (34), 4051-4054.

(90) Garegg, P. J.; Lindh, I.; Regberg, T.; Stawinski, J.; Strömberg, R.; Henrichson, C. Nucleoside H-phosphonates. IV. Automated solid phase synthesis of oligoribonucleotides by the hydrogenphosphonate approach. *Tetrahedron letters* **1986**, *27* (34), 4055-4058.
(91) Kraszewski, A.; Stawinski, J. H-Phosphonates: Versatile synthetic precursors to biologically active phosphorus compounds. *Pure and Applied Chemistry* **2007**, *79* (12), 2217-2227.
(92) Reese, C. B.; Yan, H. Solution phase synthesis of ISIS 2922 (Vitravene) by the modified H-phosphonate approach. *Journal of the Chemical Society, Perkin Transactions 1* **2002**, (23), 2619-2633.
(93) Meena; Lemaitre, M. M. Stereocontrolled oligonucleotides for nucleic acid therapeutics: a perspective. *nucleic acid therapeutics* **2021**, *31* (1), 1-6.
(94) Vargesson, N. Thalidomide-induced teratogenesis: History and mechanisms. *Birth Defects Research Part C: Embryo Today: Reviews* **2015**, *105* (2), 140-156.
(95) Boczkowska, M.; Guga, P.; Stec, W. J. Stereodefined phosphorothioate analogues of DNA: relative thermodynamic stability of the model PS-DNA/DNA and PS-DNA/RNA complexes. *Biochemistry* **2002**, *41* (41), 12483-12487.
(96) Koziolkiewicz, M.; Krakowiak, A.; Kwinkowski, M.; Boczkowska, M.; Stec, W. J. Stereodifferentiation—the effect of P chirality of oligo (nucleoside phosphorothioates) on the activity of bacterial RNase H. *Nucleic acids research* **1995**, *23* (24), 5000-5005.
(97) Krieg, A. M.; Guga, P.; Stec, W. P-chirality-dependent immune activation by phosphorothioate CpG oligodeoxynucleotides. *Oligonucleotides* **2003**, *13* (6), 491-499.
(98) Jahns, H.; Roos, M.; Imig, J.; Baumann, F.; Wang, Y.; Gilmour, R.; Hall, J. Stereochemical bias introduced during RNA synthesis modulates the activity of phosphorothioate siRNAs. *Nature communications* **2015**, *6* (1), 6317.
(99) Yu, D.; Kandimalla, E. R.; Roskey, A.; Zhao, Q.; Chen, L.; Chen, J.; Agrawal, S. Stereo-enriched phosphorothioate oligodeoxynucleotides: synthesis, biophysical and biological properties. *Bioorganic & medicinal chemistry* **2000**, *8* (1), 275-284.
(100) Okruszek, A.; Guga, P.; Stec, W. J. Direct transformation of ribonucleoside cyclic 3′, 5′-phosphorothioates into cyclic 2′, 3′-phosphates. *Journal of the Chemical Society, Chemical Communications* **1985**, (18), 1225-1226.
(101) Stec, W. J.; Wilk, A. Stereocontrolled synthesis of oligo (nucleoside phosphorothioate) s. *Angewandte Chemie International Edition in English* **1994**, *33* (7), 709-722.

(102) Stec, W. J.; Karwowski, B.; Boczkowska, M.; Guga, P.; Koziołkiewicz, M.; Sochacki, M.; Wieczorek, M. W.; Błaszczyk, J. Deoxyribonucleoside 3 '-O-(2-thio-and 2-oxo-"spiro"-4, 4-pentamethylene-1, 3, 2-oxathiaphospholane) s: monomers for stereocontrolled synthesis of oligo (deoxyribonucleoside phosphorothioate) s and chimeric PS/PO oligonucleotides. *Journal of the American Chemical Society* **1998**, *120* (29), 7156-7167.
(103) Almer, H.; Stawinski, J.; Strömberg, R. Synthesis of stereochemically homogeneous oligoribonucleoside all-RP-phosphorothioates by combining H-phosphonate chemistry and enzymatic digestion. *Journal of the Chemical Society, Chemical Communications* **1994**, (12), 1459-1460.
(104) Wang, J.-C.; Just, G. A stereoselective synthesis of dinucleotide phosphorothioate triesters through a chiral indol-oxazaphosphorine intermediate. *Tetrahedron Letters* **1997**, *38* (5), 705-708.
(105) Iyer, R. P.; Yu, D.; Ho, N.-H.; Tan, W.; Agrawal, S. A novel nucleoside phosphoramidite synthon derived from 1R, 2S-ephedrine. *Tetrahedron: Asymmetry* **1995**, *6* (5), 1051-1054.
(106) Beaucage, S. L.; Iyer, R. P. Advances in the synthesis of oligonucleotides by the phosphoramidite approach. *Tetrahedron* **1992**, *48* (12), 2223-2311.
(107) Iyer, R. P.; Guo, M.-J.; Yu, D.; Agrawal, S. Solid-phase stereoselective synthesis of oligonucleoside phosphorothioates: The nucleoside bicyclic oxazaphospholidines as novel synthons. *Tetrahedron Letters* **1998**, *39* (17), 2491-2494.
(108) Wilk, A.; Grajkowski, A.; Phillips, L. R.; Beaucage, S. L. Deoxyribonucleoside cyclic N-acylphosphoramidites as a new class of monomers for the stereocontrolled synthesis of oligothymidylyl-and oligodeoxycytidylyl-phosphorothioates. *Journal of the American Chemical Society* **2000**, *122* (10), 2149-2156.
(109) Stec, W. J.; Zon, G. Stereochemical studies of the formation of chiral internucleotide linkages by phosphoramidite coupling in the synthesis of oligodeoxyribonucleotides. *Tetrahedron letters* **1984**, *25* (46), 5279-5282.
(110) Iyer, R. P.; Egan, W.; Regan, J. B.; Beaucage, S. L. 3H-1, 2-Benzodithiole-3-one 1, 1-dioxide as an improved sulfurizing reagent in the solid-phase synthesis of oligodeoxyribonucleoside phosphorothioates. *Journal of the American Chemical Society* **1990**, *112* (3), 1253-1254.

(111) Oka, N.; Wada, T.; Saigo, K. Diastereocontrolled synthesis of dinucleoside phosphorothioates using a novel class of activators, dialkyl (cyanomethyl) ammonium tetrafluoroborates. *Journal of the American Chemical Society* **2002**, *124* (18), 4962-4963.
(112) Oka, N.; Wada, T.; Saigo, K. An oxazaphospholidine approach for the stereocontrolled synthesis of oligonucleoside phosphorothioates. *Journal of the American Chemical Society* **2003**, *125* (27), 8307-8317.
(113) Wada, T.; Maizuru, Y.; Shimizu, M.; Oka, N.; Saigo, K. Stereoselective synthesis of dinucleoside boranophosphates by an oxazaphospholidine method. *Bioorganic & medicinal chemistry letters* **2006**, *16* (12), 3111-3114.
(114) Iwamoto, N.; Oka, N.; Sato, T.; Wada, T. Stereocontrolled Solid-Phase Synthesis of Oligonucleoside H-Phosphonates by an Oxazaphospholidine Approach. *Angewandte Chemie International Edition* **2009**, *48* (3), 496-499.
(115) Vlaho, D.; Fakhoury, J. F.; Damha, M. J. Structural studies and gene silencing activity of siRNAs containing cationic phosphoramidate linkages. *nucleic acid therapeutics* **2018**, *28* (1), 34-43.
(116) Oka, N.; Yamamoto, M.; Sato, T.; Wada, T. Solid-phase synthesis of stereoregular oligodeoxyribonucleoside phosphorothioates using bicyclic oxazaphospholidine derivatives as monomer units. *Journal of the American Chemical Society* **2008**, *130* (47), 16031-16037.
(117) Oka, N.; Kondo, T.; Fujiwara, S.; Maizuru, Y.; Wada, T. Stereocontrolled synthesis of oligoribonucleoside phosphorothioates by an oxazaphospholidine approach. *Organic letters* **2009**, *11* (4), 967-970.
(118) Nukaga, Y.; Yamada, K.; Ogata, T.; Oka, N.; Wada, T. Stereocontrolled solid-phase synthesis of phosphorothioate oligoribonucleotides using 2′-O-(2-cyanoethoxymethyl)-nucleoside 3′-O-oxazaphospholidine monomers. *The Journal of organic chemistry* **2012**, *77* (18), 7913-7922.
(119) Oka, N.; Wada, T. Stereocontrolled synthesis of oligonucleotide analogs containing chiral internucleotidic phosphorus atoms. *Chemical Society Reviews* **2011**, *40* (12), 5829-5843.
(120) Iwamoto, N.; Butler, D. C.; Svrzikapa, N.; Mohapatra, S.; Zlatev, I.; Sah, D. W.; Standley, S. M.; Lu, G.; Apponi, L. H.; Frank-Kamenetsky, M. Control of phosphorothioate stereochemistry substantially increases the efficacy of antisense oligonucleotides. *Nature biotechnology* **2017**, *35* (9), 845-851.

(121) Nielsen, J.; Caruthers, M. H. Directed Arbuzov-type reactions of 2-cyano-1, 1-dimethylethyl deoxynucleoside phosphites. *Journal of the American Chemical Society* **1988**, *110* (18), 6275-6276.
(122) Crooke, S. T.; Geary, R. S. Clinical pharmacological properties of mipomersen (K ynamro), a second generation antisense inhibitor of apolipoprotein B. *British journal of clinical pharmacology* **2013**, *76* (2), 269-276.
(123) Østergaard, M. E.; De Hoyos, C. L.; Wan, W. B.; Shen, W.; Low, A.; Berdeja, A.; Vasquez, G.; Murray, S.; Migawa, M. T.; Liang, X.-h. Understanding the effect of controlling phosphorothioate chirality in the DNA gap on the potency and safety of gapmer antisense oligonucleotides. *Nucleic Acids Research* **2020**, *48* (4), 1691-1700.
(124) Li, M.; Lightfoot, H. L.; Halloy, F.; Malinowska, A. L.; Berk, C.; Behera, A.; Schümperli, D.; Hall, J. Synthesis and cellular activity of stereochemically-pure 2′-O-(2-methoxyethyl)-phosphorothioate oligonucleotides. *Chemical communications* **2017**, *53* (3), 541-544.
(125) Knouse, K. W.; deGruyter, J. N.; Schmidt, M. A.; Zheng, B.; Vantourout, J. C.; Kingston, C.; Mercer, S. E.; Mcdonald, I. M.; Olson, R. E.; Zhu, Y. Unlocking P (V): Reagents for chiral phosphorothioate synthesis. *Science* **2018**, *361* (6408), 1234-1238.
(126) Clivio, P.; Coantic-Castex, S.; Guillaume, D. (3′-5′)-Cyclic dinucleotides: Synthetic strategies and biological potential. *Chemical Reviews* **2013**, *113* (10), 7354-7401.
(127) Lioux, T.; Mauny, M.-A.; Lamoureux, A.; Bascoul, N.; Hays, M.; Vernejoul, F.; Baudru, A.-S.; Boularan, C.; Lopes-Vicente, J.; Qushair, G. Design, synthesis, and biological evaluation of novel cyclic adenosine–inosine monophosphate (cAIMP) analogs that activate stimulator of interferon genes (STING). *Journal of medicinal chemistry* **2016**, *59* (22), 10253-10267.
(128) Huang, Y.; Knouse, K. W.; Qiu, S.; Hao, W.; Padial, N. M.; Vantourout, J. C.; Zheng, B.; Mercer, S. E.; Lopez-Ogalla, J.; Narayan, R. AP (V) platform for oligonucleotide synthesis. *Science* **2021**, *373* (6560), 1265-1270.
(129) Okruszek, A.; Sierzcha-la, A.; Fearon, K. L.; Stec, W. J. Synthesis of oligo (deoxyribonucleoside phosphorodithioate) s by the dithiaphospholane approach. *The Journal of Organic Chemistry* **1995**, *60* (21), 6998-7005.
(130) Wiesler, W. T.; Caruthers, M. H. Synthesis of Phosphorodithioate DNA via Sulfur-Linked, Base-Labile Protecting Groups1. *The Journal of Organic Chemistry* **1996**, *61* (13), 4272-4281.

(131) de Koning, M. C.; Ghisaidoobe, A. B.; Duynstee, H. I.; Ten Kortenaar, P. B.; Filippov, D. V.; van der Marel, G. A. Simple and efficient solution-phase synthesis of oligonucleotides using extractive work-up. *Organic process research & development* **2006**, *10* (6), 1238-1245.
(132) Jahns, H.; Taneja, N.; Willoughby, J. L.; Akabane-Nakata, M.; Brown, C. R.; Nguyen, T.; Bisbe, A.; Matsuda, S.; Hettinger, M.; Manoharan, R. M. Chirality matters: stereo-defined phosphorothioate linkages at the termini of small interfering RNAs improve pharmacology in vivo. *Nucleic acids research* **2022**, *50* (3), 1221-1240.
(133) Featherston, A. L.; Kwon, Y.; Pompeo, M. M.; Engl, O. D.; Leahy, D. K.; Miller, S. J. Catalytic asymmetric and stereodivergent oligonucleotide synthesis. *Science* **2021**, *371* (6530), 702-707.
(134) Xu, D.; Rivas-Bascón, N.; Padial, N. M.; Knouse, K. W.; Zheng, B.; Vantourout, J. C.; Schmidt, M. A.; Eastgate, M. D.; Baran, P. S. Enantiodivergent formation of C–P bonds: Synthesis of P-chiral phosphines and methylphosphonate oligonucleotides. *Journal of the American Chemical Society* **2020**, *142* (12), 5785-5792.
(135) Andrews, B. I.; Antia, F. D.; Brueggemeier, S. B.; Diorazio, L. J.; Koenig, S. G.; Kopach, M. E.; Lee, H.; Olbrich, M.; Watson, A. L. Sustainability challenges and opportunities in oligonucleotide manufacturing. *The Journal of Organic Chemistry* **2020**, *86* (1), 49-61.
(136) Cedillo, I.; Jarvis, B.; Pavone, T. Designing Commercial-Scale Oligonucleotide Synthesis. *Rookie of the year* **2020**, 25.
(137) Sanghvi, Y. S. Large-scale automated synthesis of therapeutic oligonucleotides: A status update. *Advances in Nucleic Acid Therapeutics* **2019**, *68*, 453.
(138) Hayatsu, H.; Khorana, H. G. Polynucleotides. LXXII. Deoxyribooligonucleotide synthesis on a polymer support. *Journal of the American Chemical Society* **1967**, *89* (15), 3880-3887.
(139) Schott, H.; Brandstetter, F.; Bayer, E. Liquid-phase-synthese von oligothymidylphosphaten. *Die Makromolekulare Chemie: Macromolecular Chemistry and Physics* **1973**, *173* (1), 247-251.
(140) Bonora, G. M.; Biancotto, G.; Maffini, M.; Scremin, C. L. Large scale, liquid phase synthesis of oligonucleotides by the phosphoramidite approach. *Nucleic acids research* **1993**, *21* (5), 1213-1217.

(141) Donga, R. A.; Khaliq-Uz-Zaman, S. M.; Chan, T.-H.; Damha, M. J. A novel approach to oligonucleotide synthesis using an imidazolium ion tag as a soluble support. *The Journal of organic chemistry* **2006**, *71* (20), 7907-7910.
(142) Hassler, M. Advancements in the synthesis of oligoribonucleotides on solid support and in solution: Ionic soluble supports, blockmer ribonucleotide amidites, and orthogonal linkers. **2013**. McGill University e-thesis.
(143) Molina, A. G.; Sanghvi, Y. S. Liquid-Phase Oligonucleotide Synthesis: Past, Present, and Future Predictions. *Current protocols in nucleic acid chemistry* **2019**, *77* (1), e82.
(144) Katayama, S.; Hirai, K. Liquid-phase synthesis of oligonucleotides. *Synthesis of therapeutic oligonucleotides* **2018**, 83-95.
(145) Lönnberg, H. Synthesis of oligonucleotides on a soluble support. *Beilstein Journal of Organic Chemistry* **2017**, *13* (1), 1368-1387.
(146) Gaffney, P. R.; Kim, J. F.; Valtcheva, I. B.; Williams, G. D.; Anson, M. S.; Buswell, A. M.; Livingston, A. G. Liquid-Phase Synthesis of 2′-Methyl-RNA on a Homostar Support through Organic-Solvent Nanofiltration. *Chemistry–A European Journal* **2015**, *21* (26), 9535-9543.
(147) Vandezande, P.; Gevers, L. E.; Vankelecom, I. F. Solvent resistant nanofiltration: separating on a molecular level. *Chemical Society Reviews* **2008**, *37* (2), 365-405.
(148) Kim, J. F.; Gaffney, P. R.; Valtcheva, I. B.; Williams, G.; Buswell, A. M.; Anson, M. S.; Livingston, A. G. Organic solvent nanofiltration (OSN): a new technology platform for liquid-phase oligonucleotide synthesis (LPOS). *Organic Process Research & Development* **2016**, *20* (8), 1439-1452.
(149) Creusen, G.; Akintayo, C. O.; Schumann, K.; Walther, A. Scalable one-pot-liquid-phase oligonucleotide synthesis for model network hydrogels. *Journal of the American Chemical Society* **2020**, *142* (39), 16610-16621.
(150) Kahn, J. S.; Hu, Y.; Willner, I. Stimuli-responsive DNA-based hydrogels: from basic principles to applications. *Accounts of chemical research* **2017**, *50* (4), 680-690.
(151) Tanaka, S.; Wakabayashi, K.; Fukushima, K.; Yukami, S.; Maezawa, R.; Takeda, Y.; Tatsumi, K.; Ohya, Y.; Kuzuya, A. Intelligent, Biodegradable, and Self-Healing Hydrogels Utilizing DNA Quadruplexes. *Chemistry–An Asian Journal* **2017**, *12* (18), 2388-2392.

(152) Tanaka, S.; Yukami, S.; Fukushima, K.; Wakabayashi, K.; Ohya, Y.; Kuzuya, A. Bulk pH-Responsive DNA Quadruplex Hydrogels Prepared by Liquid-Phase, Large-Scale DNA Synthesis. *ACS Macro Letters* **2018**, *7* (3), 295-299.
(153) Zhou, X.; Kiesman, W. F.; Yan, W.; Jiang, H.; Antia, F. D.; Yang, J.; Fillon, Y. A.; Xiao, L.; Shi, X. Development of kilogram-scale convergent liquid-phase synthesis of oligonucleotides. *The Journal of Organic Chemistry* **2021**, *87* (4), 2087-2110.
(154) Takahashi, D.; Inomata, T.; Fukui, T. AJIPHASE®: A Highly Efficient Synthetic Method for One-Pot Peptide Elongation in the Solution Phase by an Fmoc Strategy. *Angewandte Chemie* **2017**, *129* (27), 7911-7915.
(155) Van Giesen, K. J.; Thompson, M. J.; Meng, Q.; Lovelock, S. L. Biocatalytic Synthesis of Antiviral Nucleosides, Cyclic Dinucleotides, and Oligonucleotide Therapies. *JACS Au* **2022**, *3* (1), 13-24.
(156) Kestemont, D.; Herdewijn, P.; Renders, M. Enzymatic Synthesis of Backbone-Modified Oligonucleotides Using T4 DNA Ligase. *Current Protocols in Chemical Biology* **2019**, *11* (2), e62.
(157) Crameri, A.; Hill, M. L.; Tew, D. G. Novel processes for the production of oligonucleotides. Google Patents: 2020.
(158) Jensen, M. A.; Davis, R. W. Template-independent enzymatic oligonucleotide synthesis (TiEOS): its history, prospects, and challenges. *Biochemistry* **2018**, *57* (12), 1821-1832.

Chapter 2:

Mechanochemical coupling of nucleotides

"When the mind is allowed to relax, inspiration often follows."

- Phil Jackson

2.1: Introduction

The use of mechanical forces such as impact, shearing, and friction to drive chemical reactions is known as mechanochemistry[1]. Although the use of mechanochemistry has been known for thousands of years[2], a renewed interest in recent years has shown mechanochemistry to be a powerful avenue for chemical synthesis[3], cocrystal formation[4], materials processing[5], and has rapidly emerged as one of the pillars of Green Chemistry[6]. In traditional solution-phase reactions, bulk solvent is often an afterthought, but can play an important role in reaction rates, yields, and selectivities[7]. In contrast, mechanochemistry often foregoes the use of solvents completely which can lead to modulation of the reaction outcome while simultaneously reducing the environmental footprint of the process. Alternatively, small amounts of solvent can be added to mechanochemical reactions known as liquid-assisted grinding (LAG) [8] which can enhance reactivity or control selectivity[9]. LAG is defined by the ratio of liquid volume to reactant weight and has been defined by η and is substantially less (LAG, $\eta < 2$ μL mg^{-1}) than a solution-phase reaction ($\eta > 12$ μL mg^{-1}) [10]. The most common mechanochemical instrument at the laboratory scale is undoubtedly the vibration ball mill (VBM), but others exist which operate at different scales and impart different types of forces (**Figure 2.1**) [11].

Figure 2.1 *Different mechanochemical instruments, their forces, and scales.* ***A****: Vibration ball mill, impact, multi-gram.* ***B****: Planetary ball mill, shearing and friction, hundreds of grams.* ***C****: Twin-screw extruder, friction, continuous kilogram.*

The use of mechanochemistry for organic synthesis has been adopted for many classic chemical reactions[12] and has been well-reviewed[13]. Despite being recently reviewed[14], the use of mechanochemistry for transformations involving nucleic acids remains relatively underdeveloped, with few research groups working on this. There have been some examples of protection of nucleosides by mechanochemistry (DMTr[15], silyl[16], Boc[17]), but they did not lead to dramatically improved yields or selectivity over solution-phase methods. More interestingly, Migaud reported the use of ionic liquids combined with VBM to facilitate phosphitylation of

nucleosides in 30 minutes to yield a wide range of phosphoramidites (70-90%)[18]. Although the Vyle group also reported the use of VBM to synthesize novel pyrophosphate[19] and pyrophosphorothioate[20] linked dinucleotide, there have been no reports of the synthesis of naturally linked nucleotides of any length.

As covered briefly in the introduction (**1.5.6**), the environmental impact of oligonucleotide synthesis cannot be overstated. A recent analysis of the sustainability challenges of large-scale oligonucleotide manufacturing identified six of twelve principles of Green Chemistry[21] in dire need of improvement with the process. This study identified prevention of waste as the most glaring issue with solid-phase oligonucleotide synthesis (SPOS). In addition, it closely examined eight different oligonucleotides in different phases of clinical development and calculated their process mass intensity (PMI, **Figure 2.2A**). The PMI is defined as the quantity of raw materials inputted into the process (kg) divided by the quantity of active pharmaceutical ingredient (API) obtained at the end of the process (kg). It represents a global sum of all reagents, including water and other solvents, used in the manufacturing process. The study presented an average PMI for the eight oligonucleotide drug candidates to be approximately 4 300, or approximately 200 on a per nucleotide basis (**Figure 2.2B**). The PMI values were divided into material type, and synthesis stage or step with orange representing organic materials and blue aqueous (**Figure 2.3B**). Forty three percent the total PMI comes solely from organic solvents such as DCM, pyridine, ACN, and toluene. This represents on average 86kg of organic solvents, per nucleotide, to generate 1kg of an oligonucleotide. Another analysis estimated that a process plant run by Ionis Pharmaceuticals generated 4 416L of waste per kilogram of API manufactured[22]. This represents a huge amount of waste generated during oligonucleotide manufacturing and must be a focus of the industry moving forward.

$$\text{Process mass intensity} = \frac{\text{quantity of raw materials in (kg)}}{\text{quantity of API out (kg)}}$$

compd	phase of development	no. of nucleotides	PMI	PMI per nucleotide
A	1	20	4841	242
B	1	20	3369	168
C	2	21	4134	197
D	2	40	7023	176
E	2	19	3385	178
F	2	16	3581	224
G	3	20	3035	152
H	3	20	5028	251

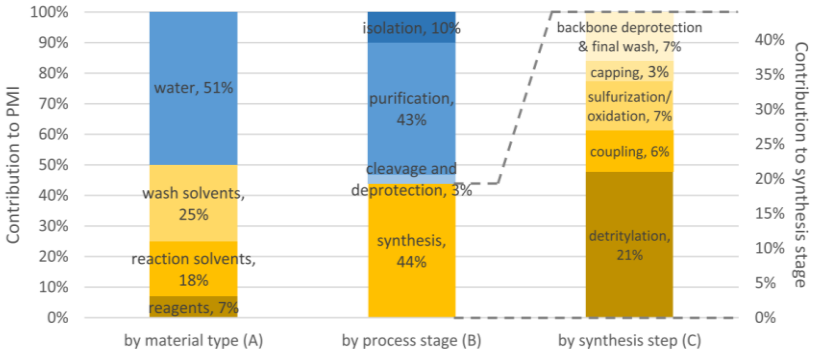

Figure 2.2: *Analysis of sustainability of oligonucleotide manufacturing, figures adapted from reference[21]. **A:** Equation for calculation of PMI. **B:** PMI analysis of eight oligonucleotides in clinical development. **C:** Subdivision of PMI into material type, process stage, and synthesis step.*

Given the rapid rise in the demand for therapeutic oligonucleotides and the huge solvent footprint of solid-phase oligonucleotide synthesis (SPOS) [21], we determined that mechanochemistry may be a viable strategy to improve the sustainability of oligonucleotide synthesis. In this chapter we will highlight our work on optimizing the reaction conditions for recreating the oligonucleotide synthesis cycle using VBM and H-phosphonate chemistry.

2.2: Results and discussion

2.2.1: H-phosphonate coupling in solution

In order to synthesize oligonucleotides by VBM, we would need to optimize three distinct reactions of the synthesis cycle: coupling, oxidation, and detritylation. Before attempting mechanochemical reactions, we set out to perform the H-phosphonate coupling in solution to establish a baseline and characterize the products. Thus H-phosphonate monoester **1a** (**Scheme 2.1**, cation is triethyl ammonium unless otherwise stated) was condensed with 3′-O-levulinyl protected nucleoside **2** in the presence of pivaloyl chloride (PvCl) in pyridine[23]. The reaction was complete by TLC analysis after 15 minutes when using equimolar amounts of **1a** and **2** and five equivalents of PvCl. The crude mixture was precipitated from cold hexanes:Et_2O (1:1, v/v)

yielding the desired H-phosphonate diester **3a** in 88% yield. No further purification was carried out. Analysis of the product by ^{31}P NMR shows a set of two peaks around 7-9 ppm as expected for the two P-diastereomers isolated (**Figure 2.3B**). These are distinct from H-phosphonate monoester **1a**, which shows a single peak around 3ppm (**Figure 2.3A**) [24]. Thus, we anticipated analysis by ^{31}P NMR of crude reactions during our optimization of the mechanochemical process would be a quick and efficient way to monitor the reactions for formation of the diester intermediate **3a**.

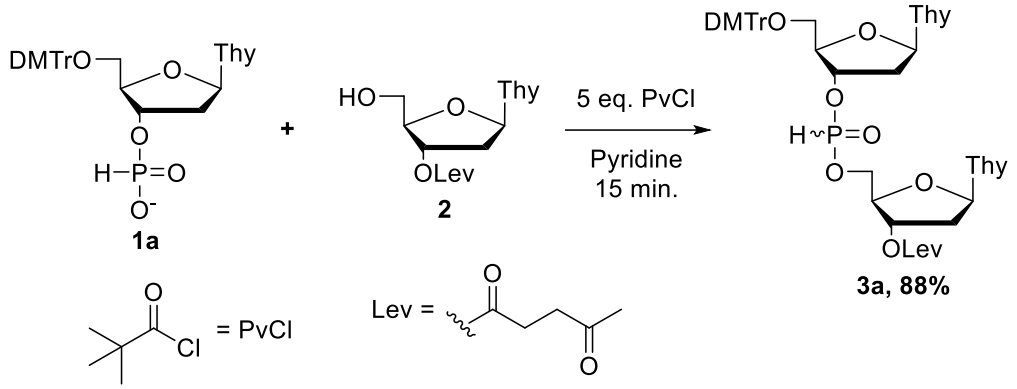

Scheme 2.1 *Solution-phase H-phosphonate coupling.*

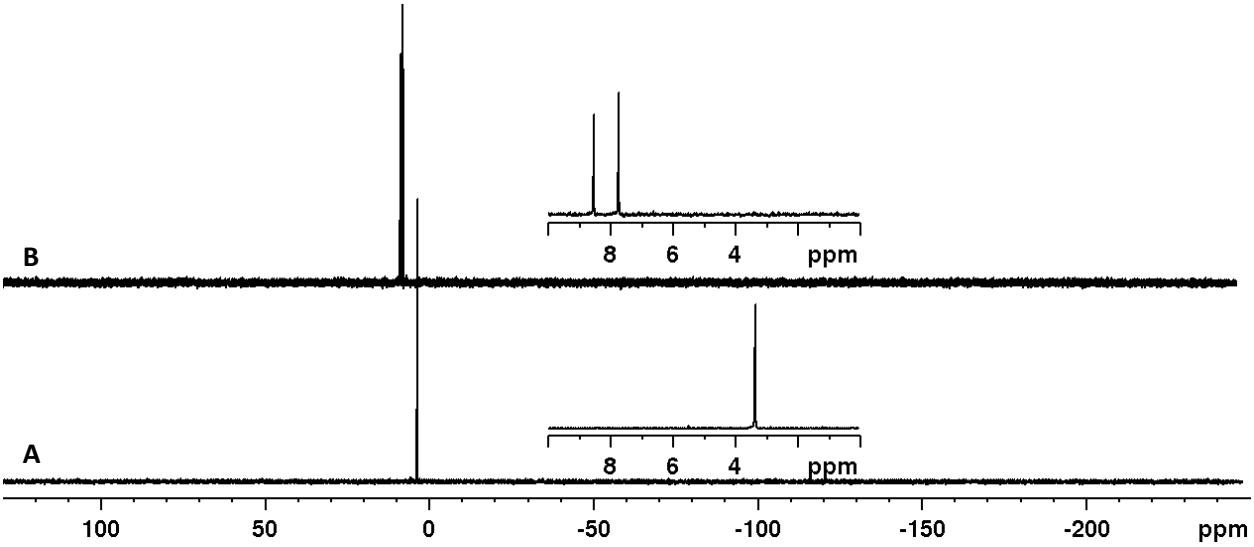

Figure 2.3: *^{31}P NMR of H-phosphonate monoester **1a** (A) and diester **3a** (B).*

2.2.2 H-phosphonate coupling by vibration ball milling

Having established a system to monitor the reaction, we set out to couple **1a** with **2** using VBM (**Scheme 2.2**). It should be noted that in **Scheme 2.2** we use the now widely accepted symbol for mechanochemistry[25]. Conditions to be screened included: activator choice, activator equivalents, base, reaction time, and reaction frequency (**Table 2.1**). Initial efforts were attempted using a 1:1 ratio of **1a** to **2.** We began by using the solid adamantane carbonyl chloride (AdaCl) instead of liquid PvCl as we first wanted to test if the reaction could be done "neat" (η = 0) and AdaCl has been shown to be an effective activator for H-phosphonates as well[26]. Typical H-phosphonate couplings are carried out in pyridine as a base is required since HCl is liberated during the reaction when activated with an acyl chloride or a phosphoryl chloride, but efforts to use only solids were attempted at first.

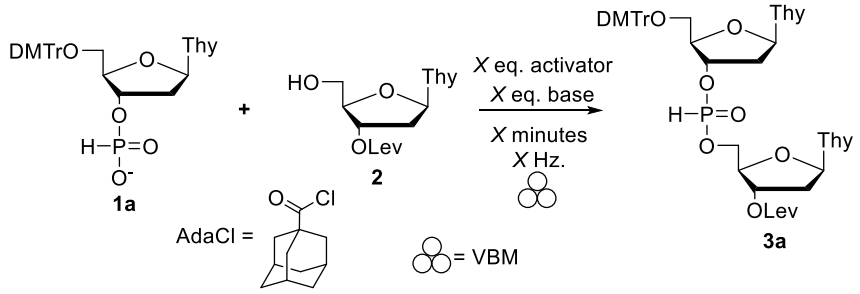

Scheme 2.2: *Mechanochemical H-phosphonate coupling.*

Initial efforts with solid bases (**Table 2.1**, entries 1-2) were unsuccessful and produced only starting material. An orange color characteristic of the DMTr cation was also observed, indicating to us detritylation was occurring despite the presence of base. When switching to pyridine (entry 3), detritylation was no longer occurring, but only **1a** was detected. Increasing the reaction time (entry 4) had no effect. However, increasing the equivalents of activator from 2-10 (entries 5-8, **Figure 2.4A-D**) showed progressively more formation of **3a** until complete consumption of **1a** was observed when reacting with 5 equivalents of AdaCl (entry 7, **Figure 2.4D**). However, using 5 or 10 equivalents of the activator did produce some side products (~-2.5 ppm) and using 10 equivalents produced messier reactions (entry 8). Changing the reaction frequency from 30 Hz to 25 Hz (entry 9) yielded a cleaner reaction (**Figure 2.4E**), but reducing the time back down to 5 minutes showed an incomplete reaction (entry 10). Having switched to pyridine as the base and moved to a LAG strategy, we also attempted the reaction with PvCl and

observed no reaction when using 1 equivalent (entry 11) and full consumption of **1a** when using 5 equivalents (entry 12, **Figure 2.4F**), but some side products were also detected.

Entry	*Activator (eq.)*	*Base (eq.)*	*Time (min)*	*Frequency (Hz)*	*^{31}P NMR (ppm)*
1	AdaCl (1)	Imidazole (1)	5	30	3.00
2	AdaCl (1)	DMAP (1)	5	30	3.01
3	AdaCl (1)	Pyridine (1)	5	30	2.98
4	AdaCl (1)	Pyridine (1)	15	30	2.97
5	AdaCl (2)	Pyridine (2)	15	30	2.39. 7.81, 8.62
6	AdaCl (3)	Pyridine (3)	15	30	4.29, 7.89. 8.63
7	AdaCl (5)	Pyridine (5)	15	30	7.10, 7.18, 7.22, 7.25, 7.30, 8.51, 8.62
8	AdaCl (10)	Pyridine (10)	15	30	-2.99, -2.76 7.05. 7.79, 7.91, 7.93, 7.95, 8.02, 8.10, 8.62, 8.67, 8.76, 9.37
9	AdaCl (5)	Pyridine (5)	15	25	-2.35, 7.18, 8.52
10	AdaCl (5)	Pyridine (5)	5	25	2.44, 7.66, 8.58
11	PvCl (1)	Pyridine (1)	15	25	4.20
12	PvCl (5)	Pyridine (5)	15	25	-2.82, -2.66, 7.12, 8.68

Table 2.1 *Optimization of H-phosphonate coupling by VBM. All reactions carried out with 0.2mmol of **2** and the stoichiometry of all reagents are in relation to this.*

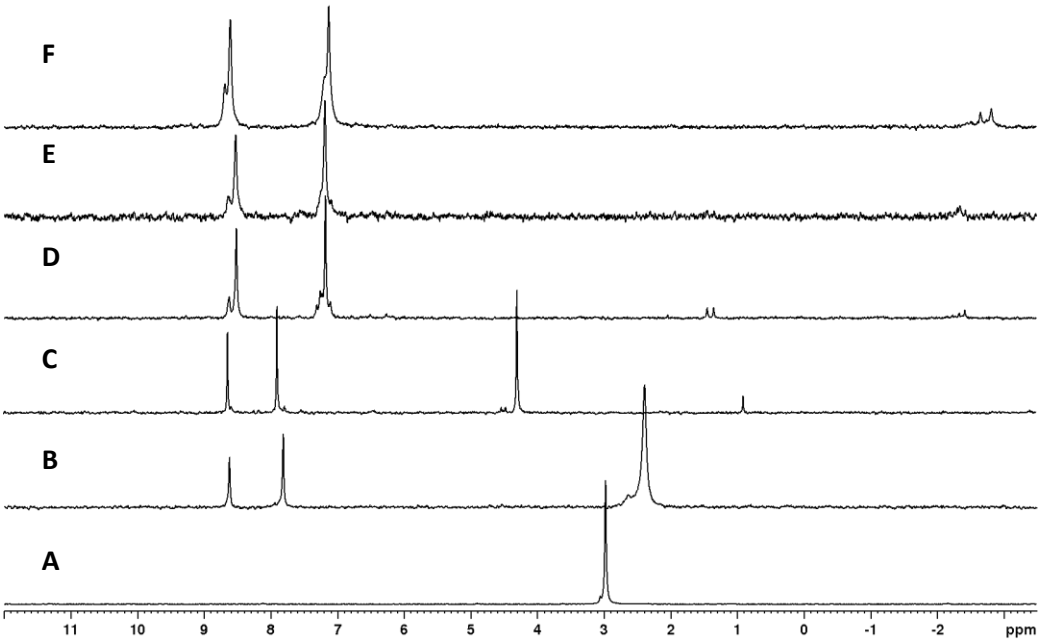

Figure 2.4 *Crude ^{31}P NMR spectra of select reactions from* ***Table 2.1****.* ***A:*** *Entry 4.* ***B:*** *Entry 5.* ***C:*** *Entry 5.* ***D:*** *Entry 7.* ***E:*** *Entry 9.* ***F:*** *Entry 12.*

Investigating the nature of these small impurities around -2.5ppm led us to perform an exclusion experiment to explore the mechanism of the reaction. The mechanism of H-phosphonate activation with acid chlorides was closely studied by Stawinski in solution[24], and we referred to this study to aid in determination of products. Reaction of **1a** with 5 equivalents of AdaCl and 5 equivalents of pyridine, but in the absence of **2** (**Scheme 2.3**) led to the formation of a major product at 126.32 ppm in the ^{31}P NMR spectrum and a set of two peaks centered at 1.38 ppm (**Figure 2.5**). The singlet at 126.32 ppm is consistent with formation of acyl phosphite triester **4** due to the chemical shift and single peak indicating an achiral phosphorous species which can be formed from the tautomer of **1a**. Based on the chemical shift and closely spaced peaks, we expect the peaks at 1.38 ppm to correspond to mixed anhydride **5** formed from direct nucleophilic attack of **1a** to AdaCl. This species was also observed in the coupling experiment (**Figure 2.4D**). Repeating the same reaction without pyridine produced a messy reaction with most peaks unidentified by Stawinski, and clear detritylation consistent with the orange color of the mixture. The identification of the peaks at -2.5 ppm (**Figure 2.4F**) was then most likely pyrophosphonate **6**, consistent with the formation of two peaks at this chemical shift[24]. Although **6** is not reactive to further activation with acid chlorides, its formation as a small side product led us to increase the equivalents of **1a** to 1.1 to ensure complete conversion of **2** even if a small amount of **6** was formed. Additionally, we observed a slight orange color during the reaction

with pyridine (**Scheme 2.3**) and decided to increase the equivalents of pyridine from 5 to 10 to be certain no detritylation would occur.

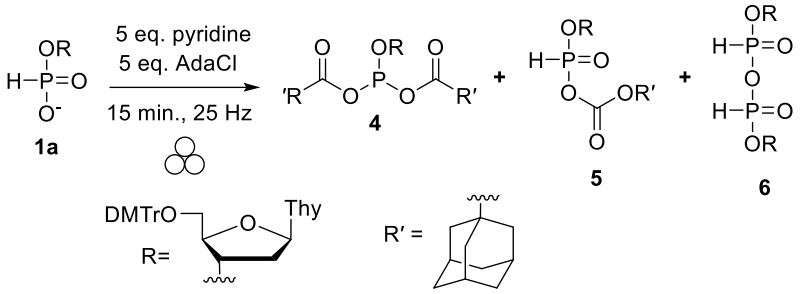

Scheme 2.3 *H-phosphonate activation by VBM in the absence of* ***2****.*

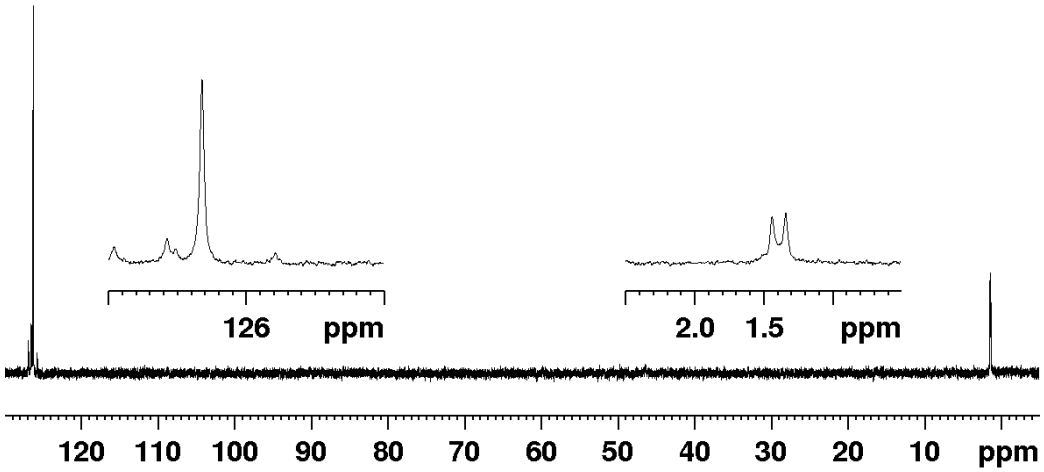

Figure 2.5*: Crude* ^{31}*P NMR spectrum of the reaction carried out in* ***Scheme 2.3****.*

Having optimized conditions using AdaCl (entry 9) and PvCl (entry 12) we set out to purify the reactions and assess the yield and recovery. The synthesis of longer oligonucleotides requires removal of reagents and any remaining H-phosphonates as their presence could lead to the formation of n+1 impurities. While precipitation was used for our control reaction, we had to ensure a higher standard of purity when moving forward with the synthesis.

2.2.3: Instability of H-phosphonate diesters

Purification of **3a** proved challenging as we consistently observed decomposition when attempting to work up the reaction mixture or purify it by column chromatography. Specifically, we observed degradation of **3a** back to **1a** and **2** after a workup with 5% sodium bicarbonate solution (**Figure 2.6**). After combing through the literature we found evidence for the instability of H-phosphonate diesters[27]. The authors studied the rates of alkaline hydrolysis of a range of phosphorous species. They assigned a relative rate of one to the degradation of phosphite triester **7** (**Scheme 2.4A**) to basic aqueous conditions. Comparatively, methyl phosphonate **8** degraded

10 times faster and H-phosphonate **9** degraded at a rate 10^5 faster than **7**. A proposed general mechanism for the degradation of H-phosphonate diesters is shown in **Scheme 2.4B**. The pK_a of the hydrogen of **9** is often ignored, but has been estimated to be around 14.6[28] and must explain the rapid rate of hydrolysis of **9**. Therefore, even under weakly basic conditions **9** should be slightly ionized and can form phosphite anion **10**. Acidic activation of **10** (kinetically equivalent to basic activation of the neutral species) liberates methanol to form the highly reactive metaphosphite **11** which then rapidly reacts with water to produce H-phosphonate monoester **12**. Other studies have also observed the degradation of H-phosphonate diesters in basic aqueous conditions, but have observed their stability in organic basic conditions reinforcing the role of H_2O in the proposed mechanism in **Scheme 2.4**[29]. While H-phosphonate chemistry is amenable to solid-phase synthesis where conditions are typically highly controlled and dry, an important study showed that H-phosphonate oligonucleotides degrade within 4 hours when left to stand in a pyridine/ACN solution containing 1% water or even in ACN without pyridine[30]. Having a better understanding of the stability of H-phosphonate diesters, we had to adjust our strategy.

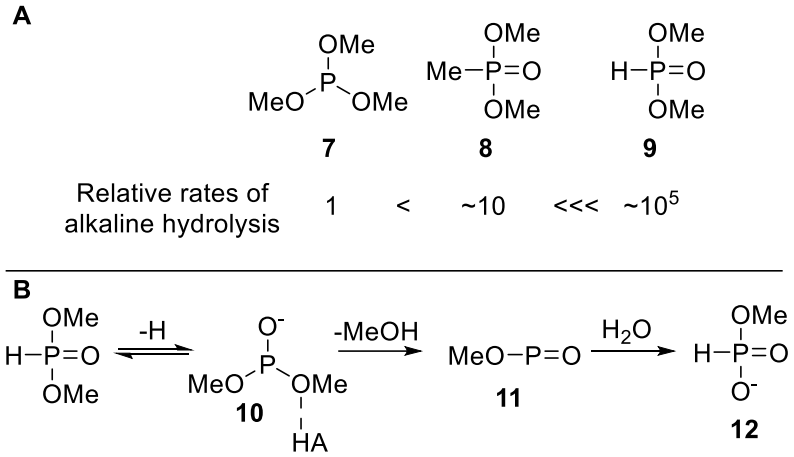

Scheme 2.4 *Relative rates (**A**) and mechanism (**B**) of the alkaline hydrolysis of different phosphorous esters.*

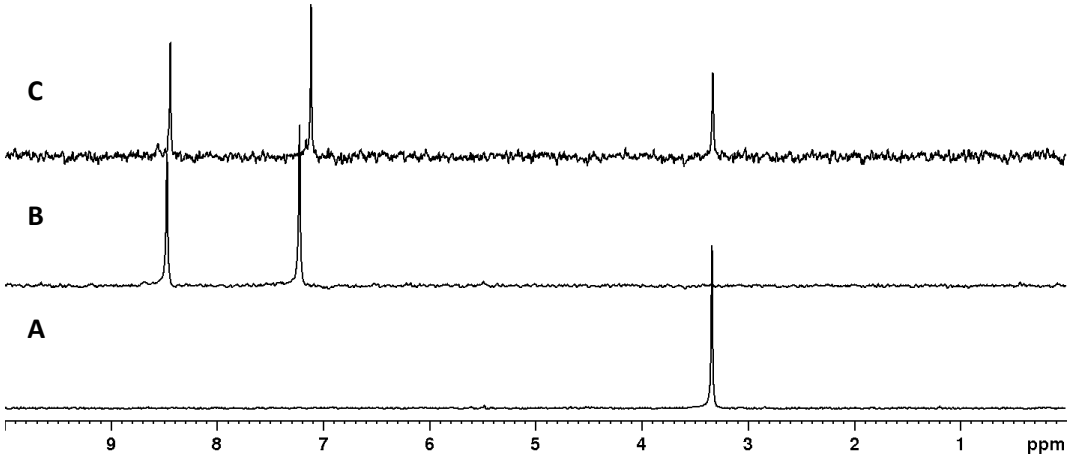

Figure 2.6 *^{31}P NMR spectra showing degradation of H-phosphonate diester* ***3a*** *observed after basic work up.* ***A****:* ***1a****.* ***B: 3a*** *after precipitation.* ***C****:* ***3a*** *synthesized by VBM after basic workup.*

2.2.4: The modified H-phosphonate approach

Probably the most successful strategy for the synthesis of oligonucleotides by H-phosphonate chemistry has been pioneered by Colin Reese and he has coined it as the modified H-phosphonate approach[31]. Although similar to the phosphotriester approach[32], rather than reacting a phosphodiester and maintaining a phosphotriester throughout the synthesis, Reese formed H-phosphonate diesters and directly reacted them with sulfur transfer reagents such as *N*-phenylthiophthalimide (PTP, **Scheme 2.5**) to form phosphorothioate triesters, which were easily isolable and stable[33]. These phosphorothioate triesters can be selectively deprotected using oximate ions[34] to yield phosphodiester bonds. This is due to the increased leaving group ability (pK_a) of the thiophenoxide as compared to the alkoxides derived from either the 5′- or 3′-nucleosides. Reese has used this approach for the synthesis of 21-mer oligonucleotides in solution on a multi-gram scale and modification of the sulfur transfer reagent from PTP to (2-cyanoethyl)thiophthalimide[35] (CTP) allowed for synthesis of oligomers with PS backbones after β-elimination of the cyanoethyl group[31].

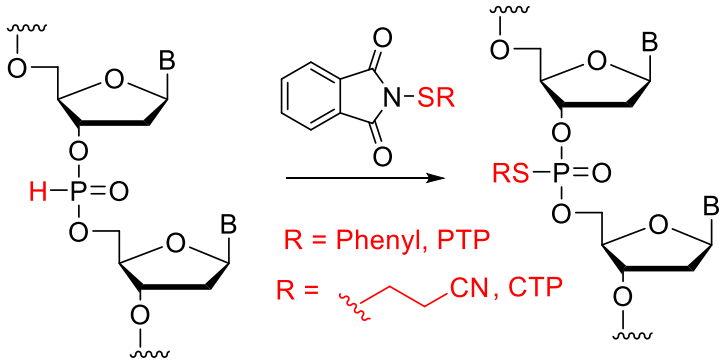

Scheme 2.5 *Reese's modified H-phosphonate approach for the synthesis of phosphorothioate triesters.*

Instead of isolating H-phosphonate diester **3a**, we adopted Reese's strategy in hopes of synthesizing isolable dimers. Fortunately, this reaction did not require much optimization, but some of the experiments are highlighted in **Table 2.2**. Using the optimized conditions from **Scheme 2.2**, we added PTP directly to the crude reaction mixtures with different bases. Given the previous experiments showing the effectiveness of the reaction at 25 Hz for 15 minutes, we also carried forward with those conditions for the sulfur transfer step (**Scheme 2.6**). Similarly monitoring the reactions by ^{31}P NMR proved to be an effective method for determining the extent of the reaction. Initial efforts with 1 eq. of PTP and 3 eq. DIPEA showed excellent conversion from **3a** to **13a** (~24 ppm in ^{31}P NMR) when analyzing the crude ^{31}P NMR, although some small impurities were present (entry 1). Increasing the equivalents of base from 3 to 5 (entry 2) reduced the presence of some impurities. Increasing the equivalents of PTP from 1 to 1.5 further reduced the presence of impurities (entry 3). To keep the reaction more homogeneous, we switched the base in the second step back to pyridine and observed similar effects when adding an additional 5 equivalents of pyridine (entry 4). Removing the base added in the second step completely showed the formation of more impurities, but still showed some conversion to **13a** (entry 5). Thus, we settled on using pyridine for the second step of the reaction as well. Finally, we attempted to reduce the equivalents of PTP from 1.5 down to 1.1 which also reduced impurity formation during the reaction and produced clean ^{31}P NMR spectra (entry 6, **Figure 2.7A**).

Entry	*Eq. PTP*	*Base (eq.)*	*^{31}P NMR (ppm)*
1	1	DIPEA (3)	1.87, 12.16, 23.44, 23.96
2	1	DIPEA (5)	1.78, 23.40, 24.00
3	1.5	DIPEA (5)	23.46, 23.97
4	1.5	Pyridine (5)	24.05, 24.23
5	1.5	0	2.31, 12.91, 13.21, 23.53, 23.73
6	1.1	Pyridine (5)	24.00, 24.20

Table 2.2*: Optimization of sulfur transfer step converting H-phosphonate diester **3** to phosphorothioate triester **13**.*

Having optimized the reaction for H-phosphonate coupling (**Scheme 2.2**) followed by conversion of the H-phosphonate diester **3a** to **13a**, we set out to purify the reactions and collect pure products. Fortunately, we found **13a** was much more stable than **3a** and we were able to purify it in 73% yield over two steps (**Figure 2.7B**). We expanded the strategy from thymidine H-phosphonate **1a** to H-phosphonates of the other nucleobases (**1b-d, Figure 2.7C-E**) and were able to isolate their corresponding phosphorothioate triesters in 70-77% yield (84-88% per step). Although we carried out the coupling reactions in **Scheme 2.6** using AdaCl, similar results were also obtained when using PvCl. The identity of compounds **13a-d** was also confirmed by HRMS after purification. Although initial optimization experiments were carried out on 0.1 mmol scale, we were able to scale up the reactions to 0.45 mmol with no change in yield.

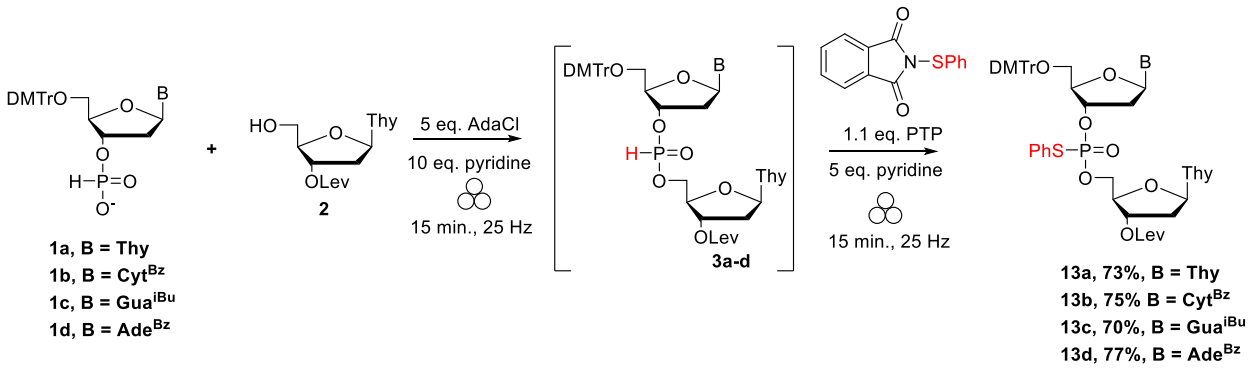

Scheme 2.6: *Optimized mechanochemical adoption of the modified H-phosphonate approach for dimer nucleotide synthesis.*

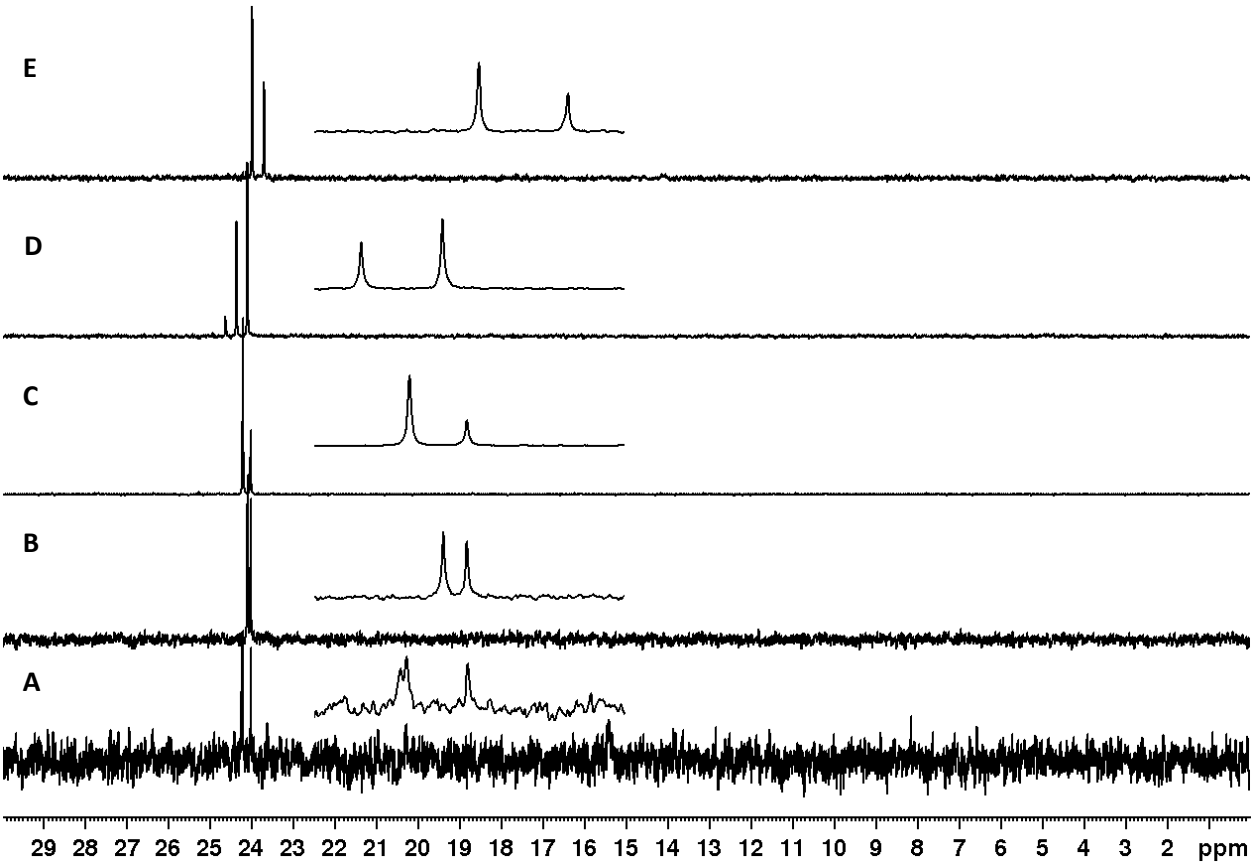

Figure 2.7: *^{31}P NMR spectra of reactions carried out in **Scheme 2.6**. **A:** Crude reaction with **1a** showing complete conversion of **3a** to **13a**. **B**: Purified **13a**. **C**: Purified **13b**. **D**: Purified **13c**. **E**: Purified **13d**.*

Although Reese and co-workers used PvCl for the synthesis of H-phosphonate monoesters **1**[33], he relied on a different activating reagent for the coupling reactions. They found that activation with diphenyl phosphoryl chloride (DPC) was rapid and efficient. He also found that concomitant addition of the sulfur transfer reagent with the activator to the reaction mixture was an effective strategy to rapidly transform H-phosphonate monoesters to phosphorothioate triesters[31]. We also set out to study if this kind of approach was possible by VBM and investigated the use of DPC as an activator (**Scheme 2.7**). We used the optimized conditions from the previous reactions (5 eq. activator, 1.1 eq. PTP, 25Hz), but increased the reaction time to 30 minutes to account for both reactions taking place. Monitoring reactions by ^{31}P NMR was made more difficult due to large signals from DPC (and diphenyl phosphate, formed after activation) dwarfing the signal from **13a**. Interestingly, in screening reaction conditions, we found that reducing equivalents of pyridine from 10 (15 total for both steps) down to 5 allowed us to observe *in situ* detritylation of phosphorothioate triester **13a** yielding **14a** in one reaction.

This led us to believe that the rate of reaction between the hydroxyl of **2** is much faster with activated **1a** (presumably mixed anhydride **5**) than the rate of detritylation of either **1a** or **13a**. In the complete absence of pyridine complete detritylation was observed, but the presence of a small amount of pyridine slowed the reaction down enough for coupling to occur followed by detritylation. Thus, we developed an efficient three-step protocol for H-phosphonate coupling, conversion to phosphorothioate triester and, serendipitously, detritylation in one-pot by VBM (**Scheme 2.7**). Similarly to previous experiments, we conducted this reaction with all four H-phosphonates (**1a-d**) and were able to synthesize 5′-deprotected dimers **14a-d** in 60-69% isolated yields over three steps (84-89% per step). Analysis by ^{31}P NMR showed a slight downfield shift of the signals after detritylation (**Figure 2.8**). The same conditions were repeated with AdaCl or PvCl, but the detritylation was not observed which is consistent with previous observations that DPC is a more reactive activator than the acid chlorides[33]. The identity of compounds **14a-d** was also confirmed by HRMS after purification.

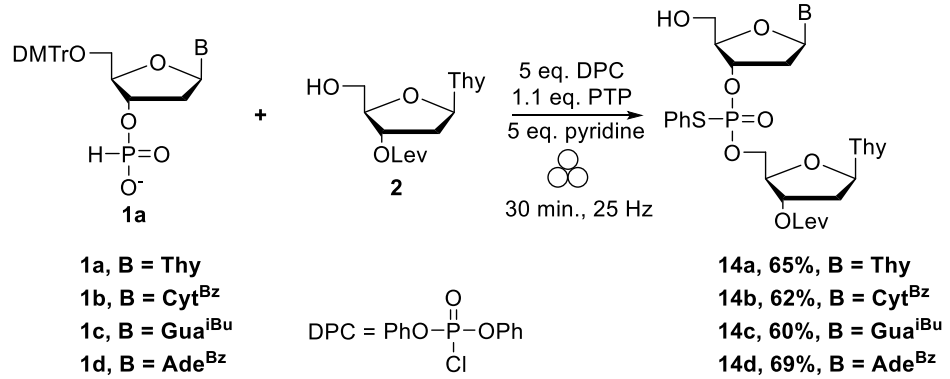

Scheme 2.7: *Optimized mechanochemical adoption of the modified H-phosphonate approach using DPC as an activator leading to in situ detritylation.*

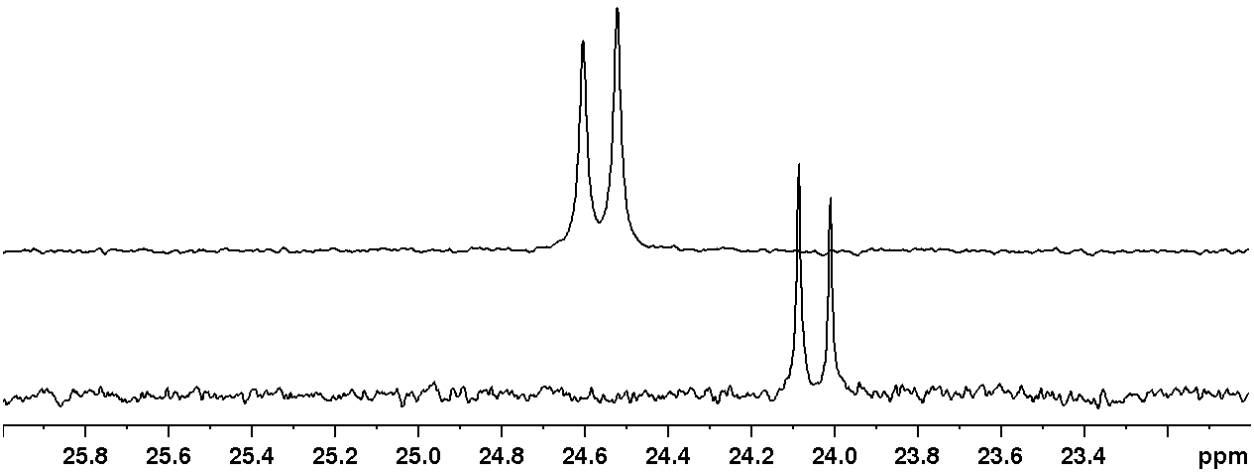

Figure 2.8: *^{31}P NMR spectrum of pure **13a** (bottom) and pure **14a** (top) after reaction in **Scheme 2.7**.*

Having established two separate procedures for the synthesis of full protected nucleotide dimers (**Scheme 2.6,** DMTr-ON) or 5′-hydroxyl nucleotide dimers (**Scheme 2.7,** DMTr-OFF) rapidly by VBM, we set out to repeat the synthesis cycle. Dimers **14a-d** were ready for coupling of another nucleotide after a single reaction. Using **14c** and **1d**, we applied the DMTr-ON procedure from **Scheme 2.6** to synthesize trimer **15** using AdaCl (**Scheme 2.8A**). Gratifyingly, using the exact same coupling conditions as previously we were able to isolate **15** in 72% yield. We were excited to see no drop off in yield when advancing from the dimer to the trimer as often seen by solution phase[36], indicating that the cycle could be repeated without loss of efficiency. Analysis of trimer **15** by ^{31}P NMR after purification produced the expected spectrum containing eight signals around 24 ppm (**Figure 2.9A**). The eight signals arise from the four possible diastereomers (two chiral phosphorus centers) each of which have two phosphorus signals. We also used the DMTr-OFF strategy using DPC as the activator with PTP in one-pot on dimer **14a** to synthesize 5′-hydroxyl trimer **16.** Similarly to the synthesis of **15**, trimer **16** was synthesized using the exact same conditions as synthesis of dimers and was isolated in 64% yield (**Scheme 2.9B**), consistent with the results obtained in **Scheme 2.7**. We also observed a clean ^{31}P NMR spectrum for **16** with eight signals in the expected region (**Figure 2.9B**) and both **15** and **16** were confirmed by HRMS. These experiments both the DMTr-ON and DMTr-OFF strategy were compatible with longer sequences without a drop in yield as well as with different nucleobases[37].

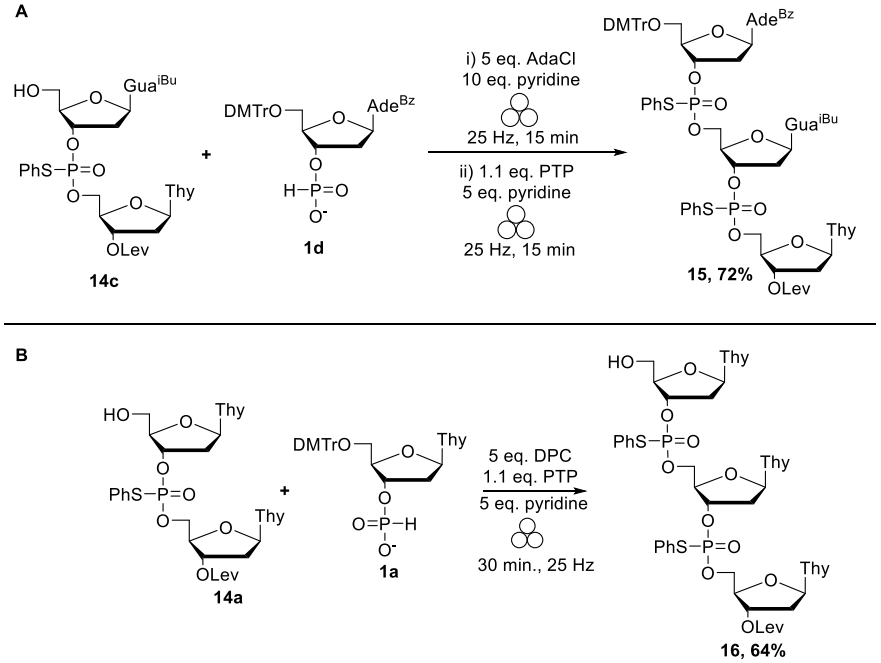

Scheme 2.7*: Synthesis of DNA trimers by VBM.* ***A:*** *DMTr-ON approach for trimer synthesis.* ***B:*** *DMTr-OFF approach for trimer synthesis.*

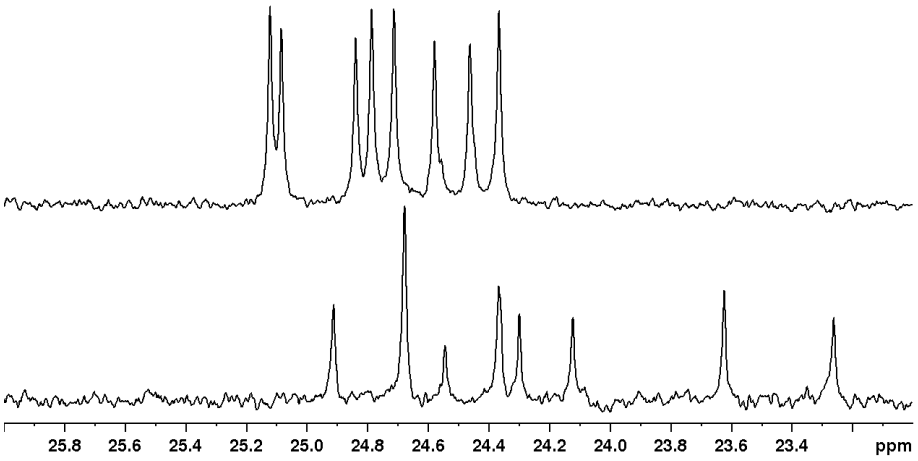

Figure 2.9: *^{31}P NMR spectra of trimers **15** (bottom) and **16** (top) after purification.*

To demonstrate how the SPh protecting group of the backbone can be deprotected we fully deprotected a dimer. As mentioned earlier, similar to the phosphotriester approach, the SPh group can be converted to a phosphodiester backbone by oximate promoted deprotection[34] (mechanism **Scheme 2.8**). After significant investigations in the past, researchers have identified 2-nitrobenzaldoxime (NBO) as an ideal deblocking reagent in the presence of a base, usually *N,N,N′,N′*-tetramethylguanidine (TMG) [38]. The reaction is driven by the good thiophenoxide leaving group and the formation of the stable 2-nitrobenzonitrile after the β-elimination leading to the desired phosphodiester product.

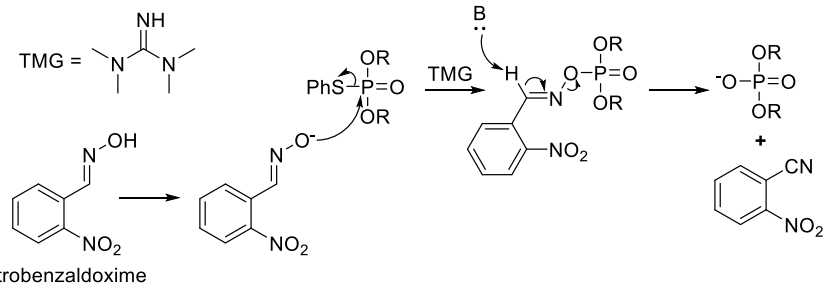

Scheme 2.8: *Mechanism of the deprotection of SPh protecting groups by oximate treatment leading to phosphodiesters.*

Therefore, we treated detritylated dimer **14c** first with a solution containing 5% by volume TMG and 5% by weight NBO overnight. Following concentration of the reaction we then treated it with concentrated ammonium hydroxide overnight to remove any nucleobase protecting groups (iBu, amide in this case) and the 3′-levulinyl protecting group. Concentrating the reaction mixture followed by washing with ether yielded the desired fully deprotected dimer **17** in quantitative yield (**Scheme 2.9**). ^{31}P NMR showed conversion of the peaks at ~24 ppm to a

single peak at -0.94 ppm, consistent with the formation of a phosphodiester (**Figure 2.10**, achiral phosphorus so only one single). HRMS also confirmed the formation of **17**.

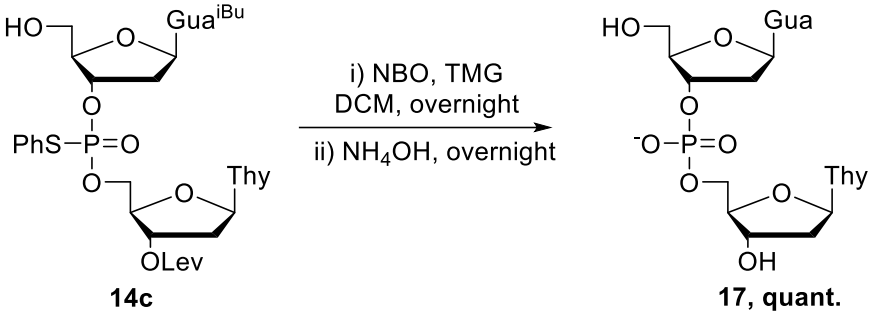

14c **17, quant.**

Scheme 2.9: *Full deprotection of nucleotide dimer yielding natural DNA phosphodiester.*

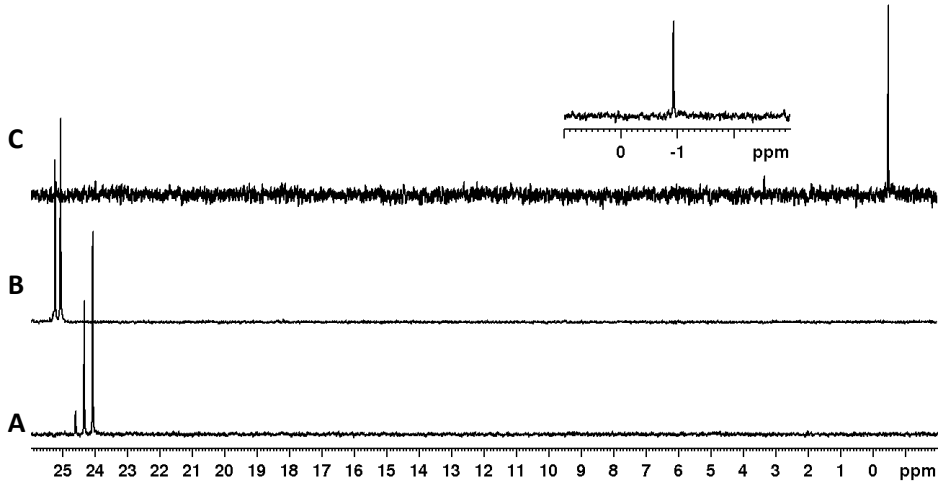

Figure 2.10: *^{31}P NMR spectrum showing different variations of a dGT dimer.* ***A:*** *Compound* ***13c*** *(DMTr ON).* ***B:*** *Compound* ***14C*** *(DMTr OFF).* ***C:*** *Compound* ***17****.*

2.3: Conclusions and outlook

We demonstrated the first use of mechanochemistry for the synthesis of protected DNA dimers and trimers which serve as precursors to natural DNA. We estimate that this approach, using stoichiometric amounts of solvent, uses up to 90% less solvent during reactions than comparable solution-phase methods and an even higher reduction when compared to solid-phase methods. We investigated the coupling of H-phosphonates by VBM, with some light investigation into the mechanism which we hypothesize to be similar to that in solution. Adoption of the modified H-phosphonate approach to protect fragile H-phosphonate diesters as phosphorothioate triesters proved amenable to VBM. Using mechanochemistry we discovered two possible protocols for coupling, conversion to phosphorothioate triesters, and detritylation if desired. The first, DMTr-ON method, used an acid chloride activator (AdaCl or PvCl) followed by addition of the sulfur transfer reagent (PTP) yielded fully protected dimers and a trimer in

good yields. The second, DMTr-OFF method, used a phosphoryl chloride activator (DPC) at the same time as the sulfur transfer reagent with reduced equivalents of pyridine yielding detritylated dimers and a trimer also in good yields. We also demonstrated the effective deprotection of a dimer, which we expand to longer sequences in the next chapter.

While reducing solvent use during coupling reactions, we still required chromatography to purify the compounds which uses significant amounts of solvent. It is estimated that up to 18% of the total mass of reagents used during SPOS is organic solvents consumed during reactions[21] and therefore any reduction of solvent in this phase is still significant. Future work using soluble supports[39] to reduce solvent consumption during purification would make this strategy more attractive from a Green Chemistry perspective. Additionally, while the yields reported are good for dimer and trimer synthesis, it should be noted that synthesis of longer oligonucleotides (>10 mer) would be extremely challenging with this strategy as the loss of material at each step would be too high, resulting in very low overall yields for longer sequences. Finally, the current strategy focused solely on DNA, but RNA and modified nucleic acids are extremely important[40] for therapeutic applications and adopting the strategy to these, as well as the synthesis of longer sequences will be discussed in the following chapter.

2.4: Experimental

2.4.1: General information

Solvents such as pyridine, dichloromethane (DCM), and methanol were purchased from Fisher Scientific. Nucleosides, nucleotides, and activating reagents (adamantane carbonyl chloride) were purchased from ChemGenes Corporation. All other chemicals were purchased from Sigma-Aldrich, Fisher Scientific, or TCI. Pyridine used for mechanochemical reactions was dried using 5Å molecular sieves and stored under an argon atmosphere. Mechanochemical reactions were performed on a FTS-1000 Shaker Mill and were performed using SmartSnapTM Grinding Jars, all purchased from FormTech Scientific. Reactions were performed in 30mL stainless steel SmartSnap^{TM} Grinding Jars with one 10mm ball of the same material. Solution-phase reactions that were air or moisture sensitive were carried out in oven dried glassware under an argon atmosphere. Thin-layer chromatography (TLC) was performed on 0.15-0.2 mm precoated silica gel (10-40 μm) plates using UV light and heat as visualizing agents. Column chromatography was performed using silica gel 60 (40-63 μm) purchased from Silicycle. Yields refer to chromatographically and spectroscopically (^{1}H NMR) homogeneous samples. NMR spectra were recorded on Bruker-500 spectrometers and were calibrated using residual undeuterated solvent as an internal reference ($CDCl_3$ ^{1}H NMR δ = 7.26 ppm) and ^{31}P NMR spectra were measured from 85% H_3PO_4 as an external standard. High-resolution mass spectra (HRMS) were recorded on a mass spectrometer under electron spray ionization (ESI) conditions.

2.4.2: Synthetic procedures

General procedure **A** (DMTr-ON method)**:**

To a 30 mL stainless steel milling jar was added **1** (1.1 eq.), **2** (or detritylated dimer **14**, 1 eq.), and an acid chloride activator (AdaCl or PvCl, 5 eq.). Immediately prior to beginning the reaction, pyridine (10 eq.) was added to the milling jar and the mixture was allowed to react on a vibration ball mill at 25 Hz for 15 minutes. The jar was opened and PTP (1.1 eq.) and pyridine (5 eq.) were added sequentially to the jar and the mixture was allowed to react for another period of 15 minutes at 25 Hz. After the reaction was complete, the white slurry was taken up in DCM and concentrated. The resulting crude residue was purified on a short silica gel column neutralized with triethylamine using DCM-MeOH as the eluent (gradient: 100:0-97:3, v/v). The appropriate

fractions were combined and concentrated under reduced pressure to yield fully protected phosphorothioate triester **13** as a white foam.

General procedure **B** (DMTr-OFF method)**:**

To a 30 mL stainless steel milling jar was added **1** (1.1 eq.), **2** (or detritylated dimer **14**, 1 eq.), PTP (1.1 eq.), pyridine (5 eq.), and DPC (5 eq.). It was important to add pyridine prior to addition of DPC, otherwise detritylation could occur. The mixture was allowed to react on a vibration ball mill for 30 minutes at 25Hz. After the reaction was complete, the white slurry was taken up in DCM and concentrated. The resulting crude residue was purified on a short silica gel column using DCM-MeOH as the eluent (gradient: 99:1-95:5, v/v). The appropriate fractions were combined and concentrated under reduced pressure to yield detritylated phosphorothioate triester **14** as a white foam.

5′DMTrO-T*p*(H)T-OLev **3a**

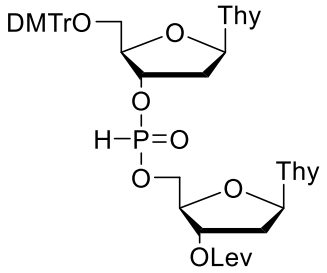

3a

1a (71 mg, 0.1 mmol) and **2** (34 mg, 0.1 mmol) were coevaporated twice with anhydrous pyridine. The gummy residue was dissolved in dry pyridine (5 mL) and PvCl (37 µL, 0.3 mmol) was added in one portion while stirring. Once the reaction was complete by TLC (DCM-MeOH, 95:5, v/v) after approximately 15 minutes the reaction mixture was concentrated under reduced pressure. The residue was dissolved in a minimal amount of DCM and precipitated into a stirring mixture of Et_2O:hexanes (1:1, v/v) at 0°C. The solution was filtered yielding **3a** as a fine white solid (88%, 91 mg). ^{31}P-NMR δP ($CDCl_3$) 7.72, 8.52.

5′DMTrO-T*p*(SPh)T-OLev **13a**

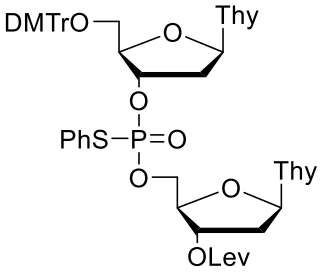

13a

This compound was prepared following general procedure **A** using **1a** (351 mg, 0.495 mmol), **2** (153 mg, 0.45 mmol), AdaCl (447 mg, 2.25 mmol), and pyridine (0.36 mL, 4.5 mmol). The sulfur transfer step was carried out with PTP (126 mg, 0.495 mmol) and pyridine (0.18 mL, 2.25 mmol) The title compound was purified on a short silica gel column neutralized with triethylamine using DCM-MeOH as the eluent (gradient: 100:0 – 97:3 v/v). The appropriate fractions were combined and concentrated under reduced pressure to yield **13a** as a white foam (341 mg, 73%). HRMS calc. [M+Na] = 1061.3014. HRMS found [M+Na] = 1061.3052. ^{31}P-NMR δP ($CDCl_3$) 24.01, 24.08.

5′DMTrO-C*p*(SPh)T-OLev **13b**

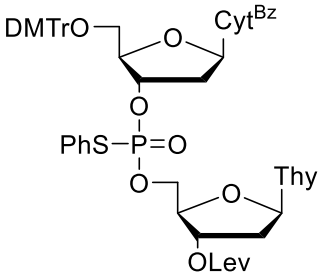

13b

This compound was prepared following general procedure **A** using **1b** (395 mg, 0.495 mmol), **2** (153 mg, 0.45 mmol), AdaCl (447 mg, 2.25 mmol), and pyridine (0.36 mL, 4.5 mmol). The sulfur transfer step was carried out with PTP (126 mg, 0.495 mmol) and pyridine (0.18 mL, 2.25 mmol) The title compound was purified on a short silica gel column neutralized with triethylamine using DCM-MeOH as the eluent (gradient: 100:0 – 97:3 v/v). The appropriate fractions were combined and concentrated under reduced pressure to yield **13b** as a white foam (381 mg, 75%). HRMS calc. [M+Na] = 1150.3280. HRMS found [M+Na] = 1150.3258. ^{31}P-NMR δP ($CDCl_3$) 24.01, 24.19.

5′DMTrO-G*p*(SPh)T-OLev **13c**

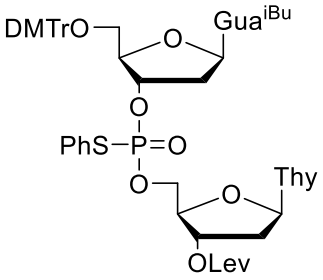

13c

This compound was prepared following general procedure **A** using **1c** (398 mg, 0.495 mmol), **2** (153 mg, 0.45 mmol), AdaCl (447 mg, 2.25 mmol), and pyridine (0.36 mL, 4.5 mmol). The sulfur transfer step was carried out with PTP (126 mg, 0.495 mmol) and pyridine (0.18 mL, 2.25 mmol) The title compound was purified on a short silica gel column neutralized with triethylamine using DCM-MeOH as the eluent (gradient: 100:0 – 97:3 v/v). The appropriate fractions were combined and concentrated under reduced pressure to yield **13c** as a white foam (357 mg, 70%). HRMS calc. [M+Na] = 1156.3498. HRMS found [M+Na] = 1156.3483. ^{31}P-NMR δP ($CDCl_3$) 24.09, 24.35.

5′DMTrO-A*p*(SPh)T-OLev **13d**

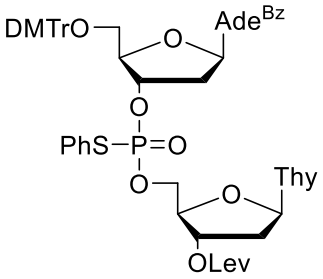

13d

This compound was prepared following general procedure **A** using **1d** (407 mg, 0.495 mmol), **2** (153 mg, 0.45 mmol), AdaCl (447 mg, 2.25 mmol), and pyridine (0.36 mL, 4.5 mmol). The sulfur transfer step was carried out with PTP (126 mg, 0.495 mmol) and pyridine (0.18 mL, 2.25 mmol) The title compound was purified on a short silica gel column neutralized with triethylamine using DCM-MeOH as the eluent (gradient: 100:0 – 97:3 v/v). The appropriate fractions were combined and concentrated under reduced pressure to yield **13d** as a white foam (391 mg, 77%). HRMS calc. [M+H] = 1152.3573. HRMS found [M+H] = 1152.3571. ^{31}P-NMR δP ($CDCl_3$) 23.68, 23.97.

5′HO-T*p*(SPh)T-OLev **14a**

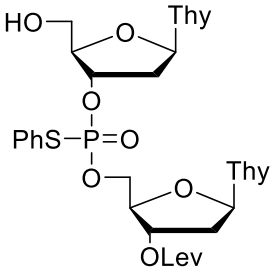

14a

This compound was prepared following general procedure **B** using **1a** (351 mg, 0.495 mmol), **2** (153 mg, 0.45 mmol), DPC (0.467 mL, 2.25 mmol), PTP (126 mg, 0.495 mmol), and pyridine (0.18 mL, 2.25 mmol). The title compound was purified on a short silica gel column using DCM-MeOH as the eluent (gradient: 99:1 – 95:5 v/v). The appropriate fractions were combined and concentrated under reduced pressure to yield **14a** as a white foam (215 mg, 65%). HRMS calc. [M+Na] = 759.1708. HRMS found [M+Na] = 759.1723. ^{31}P-NMR δP ($CDCl_3$) 24.52, 24.60.

5′HO-C*p*(SPh)T-OLev **14b**

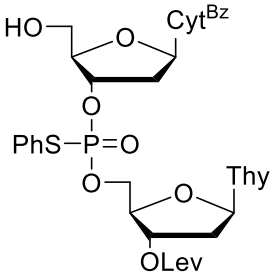

14b

This compound was prepared following general procedure **B** using **1b** (395 mg, 0.495 mmol), **2** (153 mg, 0.45 mmol), DPC (0.467 mL, 2.25 mmol), PTP (126 mg, 0.495 mmol), and pyridine (0.18 mL, 2.25 mmol). The title compound was purified on a short silica gel column using DCM-MeOH as the eluent (gradient: 99:1 – 95:5 v/v). The appropriate fractions were combined and concentrated under reduced pressure to yield **14b** as a white foam (230 mg, 62%). HRMS calc. [M+Na] = 848.1973. HRMS found [M+Na] = 848.1955. ^{31}P-NMR δP ($CDCl_3$) 24.80, 24.87.

5′HO-G*p*(SPh)T-OLev **14c**

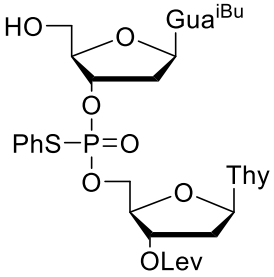

14c

This compound was prepared following general procedure **B** using **1c** (398 mg, 0.495 mmol), **2** (153 mg, 0.45 mmol), DPC (0.467 mL, 2.25 mmol), PTP (126 mg, 0.495 mmol), and pyridine (0.18 mL, 2.25 mmol). The title compound was purified on a short silica gel column using DCM-MeOH as the eluent (gradient: 99:1 – 95:5 v/v). The appropriate fractions were combined and concentrated under reduced pressure to yield **14c** as a white foam (224 mg, 60%). HRMS calc. [M+Na] = 854.2191. HRMS found [M+Na] = 854.2193. ^{31}P-NMR δP ($CDCl_3$) 23.61, 23.77.

5′HO-A*p*(SPh)T-OLev **14d**

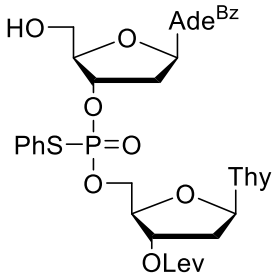

14d

This compound was prepared following general procedure **B** using **1d** (407 mg, 0.495 mmol), **2** (153 mg, 0.45 mmol), DPC (0.467 mL, 2.25 mmol), PTP (126 mg, 0.495 mmol), and pyridine (0.18 mL, 2.25 mmol). The title compound was purified on a short silica gel column using DCM-MeOH as the eluent (gradient: 99:1 – 95:5 v/v). The appropriate fractions were combined and concentrated under reduced pressure to yield **14d** as a white foam (267 mg, 69%). HRMS calc. [M+Na] = 872.2085. HRMS found [M+Na] 872.2078. ^{31}P-NMR δP ($CDCl_3$) 23.70, 24.06.

5′DMTrO-A*p*(SPh)G*p*(SPh)T-OLev **15**

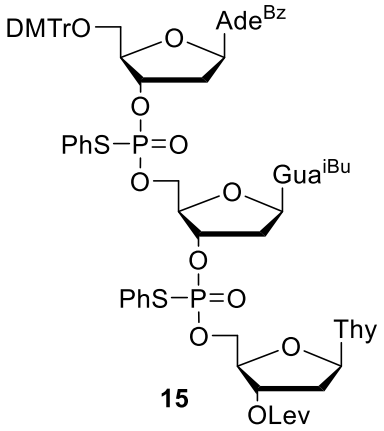

15

This compound was prepared following general procedure **A** using **1d** (245 mg, 0.3 mmol), **14c** (225mg, 0.27 mmol), AdaCl (268 mg, 1.35 mmol), and pyridine (0.22 mL, 2.7 mmol). The sulfur transfer step was carried out with PTP (77 mg, 0.3 mmol) and pyridine (0.11 mL, 1.35 mmol) The title compound was purified on a short silica gel column neutralized with triethylamine using DCM-MeOH as the eluent (gradient: 100:0 – 97:3 v/v). The appropriate fractions were combined and concentrated under reduced pressure to yield **15** as a white foam (283 mg, 64%). HRMS calc. [M+Na+H] = 1666.4493. HRMS found [M+Na+H] = 1666.4480. ^{31}P-NMR δP ($CDCl_3$) 23.26, 23.62, 24.12, 24.30, 24.36, 24.54, 24.68, 24.91.

5′HO-T*p*(SPh)T*p*(SPh)T-OLev **16**

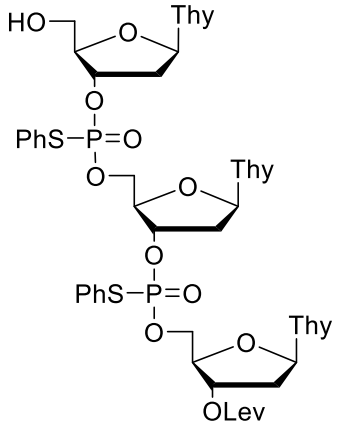

16

This compound was prepared following general procedure **B** using **1a** (89 mg, 0.125 mmol), **14a** (84 mg, 0.114 mmol), DPC (0.12 mL, 0.572 mmol), PTP (32 mg, 0.125 mmol), and pyridine (45 µL, 0.572 mmol). The title compound was purified on a short silica gel column using DCM-MeOH as the eluent (gradient: 99:1 – 95:5 v/v). The appropriate fractions were combined and

concentrated under reduced pressure to yield **16** as a white foam (83 mg, 64%). HRMS calc. [M+Na] = 1155.2253. HRMS found [M+Na] = 1155.2250. ^{31}P-NMR δP ($CDCl_3$) 24.36, 24.46, 24.58, 24.71, 24.78, 24.84, 25.08, 25.12.

5′HO-G*p*T-OH **17**

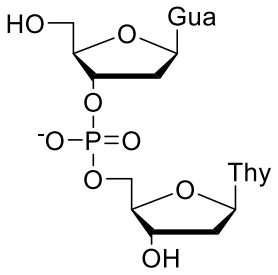

17

Compound **14c** (10 mg, 12 μmol) was dissolved in 1 mL of DCM containing 5% by volume TMG and 5% by weight NBO. The mixture was allowed to stir at room temperature overnight for 16 hours. Once the reaction was complete, the mixture was concentrated under reduced pressure. The residue was dissolved in 1mL of concentrated NH_4OH and allowed to stir at room temperature overnight for 16 hours. Once the reaction was complete, the mixture was concentrated under reduced pressure. The residue was redissolved in 5mL of H_2O and washed with Et_2O (3x5mL). The aqueous layer was concentrated yielding **17** in quantitative yield (7 mg). HRMS calc. [M-H] = 570.1355. HRMS found [M-H] = 570.1357. ^{31}P-NMR δP ($CDCl_3$) -0.98.

2.5: References

(1) James, S. L.; Friščić, T. Mechanochemistry. *Chemical Society Reviews* **2013**, *42* (18), 7494-7496.

(2) Takacs, L. The historical development of mechanochemistry. *Chemical Society Reviews* **2013**, *42* (18), 7649-7659.

(3) Friščić, T.; Mottillo, C.; Titi, H. M. Mechanochemistry for synthesis. *Angewandte Chemie* **2020**, *132* (3), 1030-1041.

(4) Hasa, D.; Schneider Rauber, G.; Voinovich, D.; Jones, W. Cocrystal Formation through Mechanochemistry: from Neat and Liquid-Assisted Grinding to Polymer-Assisted Grinding. *Angewandte Chemie* **2015**, *127* (25), 7479-7483.

(5) Baláž, P.; Baláž, P. *Mechanochemistry in minerals engineering*; Springer, 2008.

(6) Anastas, P. T.; Warner, J. C. Principles of green chemistry. *Green chemistry: Theory and practice* **1998**, *29*.

(7) Dyson, P. J.; Jessop, P. G. Solvent effects in catalysis: rational improvements of catalysts via manipulation of solvent interactions. *Catalysis Science & Technology* **2016**, *6* (10), 3302-3316.

(8) Ying, P.; Yu, J.; Su, W. Liquid-Assisted Grinding Mechanochemistry in the Synthesis of Pharmaceuticals. *Advanced Synthesis & Catalysis* **2021**, *363* (5), 1246-1271.

(9) Chierotti, M. R.; Ferrero, L.; Garino, N.; Gobetto, R.; Pellegrino, L.; Braga, D.; Grepioni, F.; Maini, L. The Richest Collection of Tautomeric Polymorphs: The Case of 2-Thiobarbituric Acid. *Chemistry–A European Journal* **2010**, *16* (14), 4347-4358. Trask, A. V.; Shan, N.; Motherwell, W. S.; Jones, W.; Feng, S.; Tan, R. B.; Carpenter, K. J. Selective polymorph transformation via solvent-drop grinding. *Chemical communications* **2005**, (7), 880-882.

(10) Friščić, T.; Childs, S. L.; Rizvi, S. A.; Jones, W. The role of solvent in mechanochemical and sonochemical cocrystal formation: a solubility-based approach for predicting cocrystallisation outcome. *CrystEngComm* **2009**, *11* (3), 418-426.

(11) Liu, X.; Li, Y.; Zeng, L.; Li, X.; Chen, N.; Bai, S.; He, H.; Wang, Q.; Zhang, C. A review on mechanochemistry: Approaching advanced energy materials with greener force. *Advanced Materials* **2022**, *34* (46), 2108327.

(12) Tan, D.; Friščić, T. Mechanochemistry for organic chemists: an update. *European Journal of Organic Chemistry* **2018**, *2018* (1), 18-33.

(13) Do, J.-L.; Friščić, T. Mechanochemistry: a force of synthesis. *ACS central science* **2017**, *3* (1), 13-19.
(14) Eguaogie, O.; Vyle, J. S.; Conlon, P. F.; Gîlea, M. A.; Liang, Y. Mechanochemistry of nucleosides, nucleotides and related materials. *Beilstein journal of organic chemistry* **2018**, *14* (1), 955-970.
(15) Patil, P. R.; Ravindranathan Kartha, K. Application of ball milling technology to carbohydrate reactions: I. Regioselective primary hydroxyl protection of hexosides and nucleoside by planetary ball milling. *Journal of Carbohydrate Chemistry* **2008**, *27* (5), 279-293.
(16) Giri, N.; Bowen, C.; Vyle, J. S.; James, S. L. Fast, quantitative nucleoside protection under solvent-free conditions. *Green Chemistry* **2008**, *10* (6), 627-628.
(17) Sikchi, S. A.; Hultin, P. G. Solventless protocol for efficient bis-N-boc protection of adenosine, cytidine, and guanosine derivatives. *The Journal of organic chemistry* **2006**, *71* (16), 5888-5891.
(18) Crossey, K.; Hardacre, C.; Migaud, M. E. Nucleoside phosphitylation using ionic liquid stabilised phosphorodiamidites and mechanochemistry. *Chemical Communications* **2012**, *48* (98), 11969-11971. Hardacre, C.; Huang, H.; James, S. L.; Migaud, M. E.; Norman, S. E.; Pitner, W. R. Overcoming hydrolytic sensitivity and low solubility of phosphitylation reagents by combining ionic liquids with mechanochemistry. *Chemical Communications* **2011**, *47* (20), 5846-5848.
(19) Eguaogie, O.; Vyle, J. S. Vibration Ball Milling for the Synthesis of 5′-Thioadenosine 5′-Pyrophosphate (P′→ 5′) Adenosine (dASppA). *Current protocols in nucleic acid chemistry* **2017**, *70* (1), 1.41. 41-41.41. 12.
(20) Eguaogie, O.; Cooke, L. A.; Martin, P. M.; Ravalico, F.; Conway, L. P.; Hodgson, D. R.; Law, C. J.; Vyle, J. S. Synthesis of novel pyrophosphorothiolate-linked dinucleoside cap analogues in a ball mill. *Organic & biomolecular chemistry* **2016**, *14* (4), 1201-1205.
(21) Andrews, B. I.; Antia, F. D.; Brueggemeier, S. B.; Diorazio, L. J.; Koenig, S. G.; Kopach, M. E.; Lee, H.; Olbrich, M.; Watson, A. L. Sustainability challenges and opportunities in oligonucleotide manufacturing. *The Journal of Organic Chemistry* **2020**, *86* (1), 49-61.
(22) Cedillo, I.; Jarvis, B.; Pavone, T. Designing Commercial-Scale Oligonucleotide Synthesis. *Rookie of the year* **2020**, 25.
(23) J. Stawinski, R. S. *Oligonucleotide Synthesis*; Humana Press, 2005.

(24) Garegg, P. J.; Regberg, T.; Stawinski, J.; Strömberg, R. Nucleoside H-phosphonates. V. The mechanism of hydrogenphosphonate diester formation using acyl chlorides as coupling agents in oligonucleotide synthesis by the hydrogenphosphonate approach. *Nucleosides & nucleotides* **1987**, *6* (3), 655-662.
(25) Rightmire, N. R.; Hanusa, T. P. Advances in organometallic synthesis with mechanochemical methods. *Dalton Transactions* **2016**, *45* (6), 2352-2362.
(26) Vlaho, D.; Damha, M. J. Synthesis of Chimeric Oligonucleotides Having Modified Internucleotide Linkages via an Automated H-Phosphonate/Phosphoramidite Approach. *Current protocols in nucleic acid chemistry* **2018**, *73* (1), e53.
(27) Westheimer, F.; Huang, S.; Covitz, F. Rates and mechanisms of hydrolysis of esters of phosphorous acid. *Journal of the American Chemical Society* **1988**, *110* (1), 181-185.
(28) Lewis, E. S.; Spears Jr, L. G. Ionization of the phosphorus-hydrogen bond in diethyl phosphonate. *Journal of the American Chemical Society* **1985**, *107* (13), 3918-3921.
(29) Kume, A.; Fujii, M.; Sekine, M.; Hata, T. Acylphosphonates. 4. Synthesis of dithymidine phosphonate. A new method for generation of phosphonate function via aroylphosphonate intermediates. *The Journal of Organic Chemistry* **1984**, *49* (12), 2139-2143.
(30) Froehler, B. C.; Ng, P. G.; Matteucci, M. D. Synthesis of DNA via deoxynucleoside H-phosphonate intermediates. *Nucleic Acids Research* **1986**, *14* (13), 5399-5407.
(31) Reese, C. B.; Yan, H. Solution phase synthesis of ISIS 2922 (Vitravene) by the modified H-phosphonate approach. *Journal of the Chemical Society, Perkin Transactions 1* **2002**, (23), 2619-2633.
(32) Reese, C.; Saffhill, R. Oligonucleotide synthesis via phosphotriester intermediates: The phenyl-protecting group. *Chemical Communications (London)* **1968**, (13), 767-768. Letsinger, R. L.; Mahadevan, V. Oligonucleotide synthesis on a polymer support1, 2. *Journal of the American Chemical Society* **1965**, *87* (15), 3526-3527.
(33) Reese, C. The H-phosphonate approach to the synthesis of oligonucleotides and their phosphorothioate analogues in solution. *Journal of the Chemical Society, Perkin Transactions 1* **1999**, (11), 1477-1486.
(34) Reese, C. B.; Zard, L. Some observations relating to the oximate ion promoted unblocking of oligonucleotide aryl esters. *Nucleic Acids Research* **1981**, *9* (18), 4611-4626.

(35) Klose, J.; Reese, C. B.; Song, Q. Preparation of 2-(2-cyanoethyl) sulfanyl-1H-isoindole-1, 3-(2H)-dione and related sulfur-transfer agents. *Tetrahedron* **1997**, *53* (42), 14411-14416.
(36) Damha, M. J. Developments in the chemical synthesis of nucleic acids and their analogues. **1987**. McGill University e-thesis.
(37) Thorpe, J. D.; O'Reilly, D.; Friščić, T.; Damha, M. J. Mechanochemical synthesis of short DNA fragments. *Chemistry–A European Journal* **2020**, *26* (41), 8857-8861.
(38) Reese, C. B. Oligo-and poly-nucleotides: 50 years of chemical synthesis. *Organic & biomolecular chemistry* **2005**, *3* (21), 3851-3868.
(39) Molina, A. G.; Sanghvi, Y. S. Liquid-Phase Oligonucleotide Synthesis: Past, Present, and Future Predictions. *Current protocols in nucleic acid chemistry* **2019**, *77* (1), e82.
(40) McKenzie, L. K.; El-Khoury, R.; Thorpe, J. D.; Damha, M. J.; Hollenstein, M. Recent progress in non-native nucleic acid modifications. *Chemical Society Reviews* **2021**, *50* (8), 5126-5164.

Chapter 3:

Mechanochemical synthesis of short oligonucleotides

"I've failed over and over and over again in my life. And that is why I succeed."

- Michael Jordan

3.1: Introduction

Despite the many advantages of solid-phase synthesis such as high yields and ease of purification, there are some disadvantages with the method[1]. One of the main issues, as mentioned previously, is the huge volumes of solvent consumed during large scale syntheses due to the frequent washing with organic solvents (ACN) in between steps of the synthesis cycle[2]. Besides the environmental issues this poses, this also adds unnecessary cost to an already very expensive process. Large excess of incoming nucleotides (phosphoramidites) used during coupling reactions ensures high yields, but wastes material which is unrecoverable. Finally, while crude purities of oligonucleotides synthesis on solid-phase are generally very high, separation of the final sequence from short-mers (n-1, n-2 etc.) is challenging, especially for longer sequences.

To improve the final separation, one popular strategy has been the so-called "block coupling" approach[3]. Rather than coupling of monomers, coupling of dimer, trimer, or longer blocks offers some key advantages. First, coupling of blocks reduces the total number of synthesis cycles carried out which can improve final yield, assuming block coupling yields are similar to monomer coupling yields. Perhaps more importantly, coupling of blocks improves the separation during the final purification. Even carrying out the final coupling with a dimer or trimer block has been a worthwhile strategy, preventing any n-1 sequence from forming where n-2 or n-3 sequences are much easier to separate from the desired oligonucleotide. Indeed, block coupling has been applied to oligonucleotide synthesis in a number of settings, in solution (phosphotriester, phosphoramidite[4] and H-phosphonate[5]) as well as by solid-phase synthesis (DNA[6] and RNA[7]).

Given our success in synthesizing DNA dimers and trimers using H-phosphonate chemistry and vibration ball milling, we sought to develop a strategy that would enable us to synthesize longer, more therapeutically relevant sequences. While DNA synthesis is important, all therapeutic oligonucleotides contain some chemical modifications, with the most common being the PS backbone, 2′OMe, and 2′F nucleosides as well as others[8]. To that end, we further elaborated the mechanochemical strategy outlined in **Chapter 2**, by applying the chemistry developed to the synthesis of H-phosphonate blocks. We also expand the strategy to RNA, modified nucleosides, and adopt a strategy for PS backbone synthesis.

3.2: Results and discussion

3.2.1: H-phosphonate block synthesis

Having previously established an efficient protocol for the synthesis of fully protected dimers by VBM (**Scheme 2.6**), we set out to synthesize dimers with 3′-H-phosphonates. The 3′-levulinyl protecting group of dimers **1a-d** (**Scheme 3.1**) was selectively removed by treatment with hydrazine hydrate in pyridine-AcOH (3:2, v/v) yielding dimers **2a-d** in quantitative yield as judged by TLC analysis. Given the high purity of **2a-d** by TLC, subsequent phosphonylation was carried out without any further purification using diphenyl hydrogen phosphite (DPHP) [9] in pyridine resulting in dimer blocks **3a-d** over two steps in generally good yields (62-73%). While nucleotide H-phosphonate monomers prepared in this manner are often purified by column chromatography (DCM-MeOH, 0-10%), we found the purification of dimers **3a-d** to be challenging by chromatography due to their high polarity (baseline by TLC analysis using DCM-MeOH, 90:10, v/v). While purification was possible by increasing the polarity of the eluent up to 20-25% methanol in DCM, this could result in dissolution of small amounts of silica eluting with the product. In general, we found precipitation of crude **3a-d** from a stirring mixture of hexanes:Et_2O (1:1, v/v) at 0°C resulted in isolation of highly pure products and was much simpler. Analysis of the dimer blocks by ^{31}P NMR (**Figure 3.1**) showed the expected peaks for the H-phosphonate monoester (~2 ppm) and the phosphorothioate triester (~24 ppm). As expected, both regions in the ^{31}P NMR spectrum display two peaks, as H-phosphonate dimers **3a-d** are each isolated as a pair of diastereomers due to the chiral internucleotide linkage. Analysis by HRMS also confirmed the identity of the products.

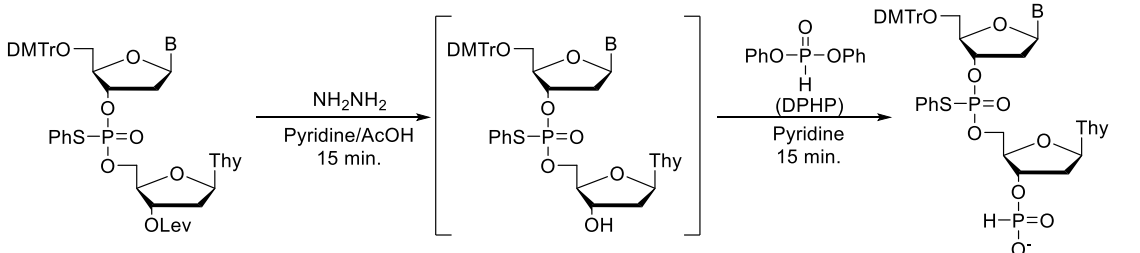

Scheme 3.1: *Synthesis of dimer blocks containing 3′-H-phosphonates.*

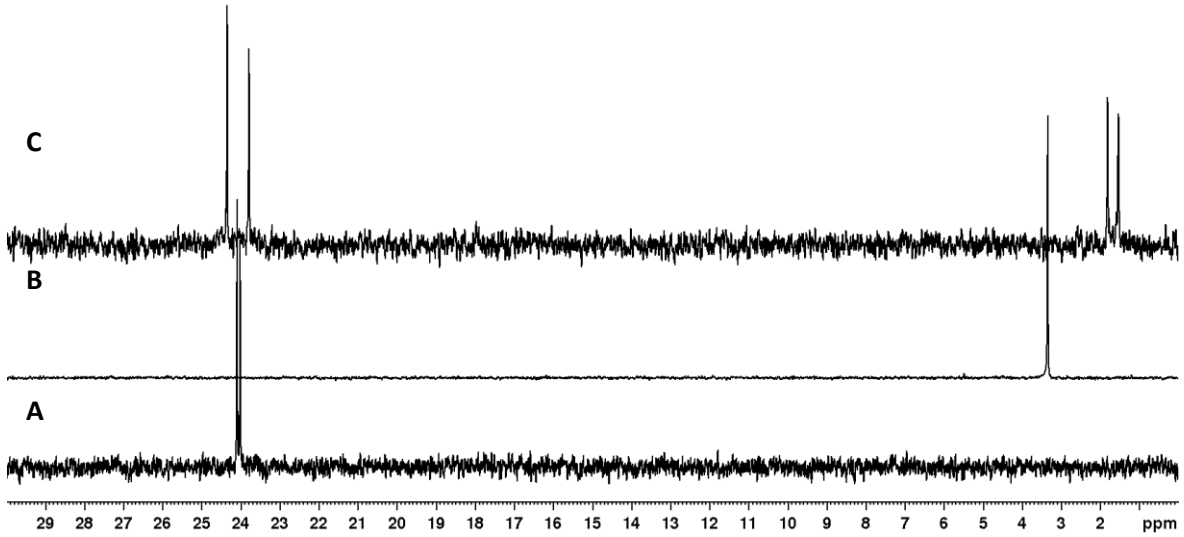

Figure 3.1: *^{31}P NMR showing differences between **A:** Dimer **1a**. **B:** dT H-phosphonate monoester. **C:** Dimer block **3a**.*

3.2.2: Phosphoramidite block synthesis

In an alternate strategy to that presented previously, we also synthesized dimer phosphoramidite blocks in an analogous strategy. Although we previously published work using phosphoramidite chemistry to couple nucleotides with VBM[10], we have also encountered difficulties with this strategy due to the highly reactive nature of the phosphoramidites, which are easily hydrolyzed. Rather than using these phosphoramidite blocks for further coupling by VBM, we envisioned using these dimer blocks in conjunction with solid-phase synthesis. This would reduce synthesis cycles during the assembly of an oligonucleotide, and if we could prepare dimer phosphoramidites on a larger scale while simultaneously reducing solvent use, this could be an effective strategy to reduce the PMI.

Therefore, from dimers **1a-d** as prepared in **Scheme 3.1**, we delevulinated then directly phosphitylated the 3′-OH using (*N*,*N*-diisopropylamino)cyanoethyl phosphonamidic-Cl (DPCP) and diisoproylethylamine (DIPEA) in DCM to yield dimer phosphoramidites **4a-d** (**Scheme 3.2**). Dimers **4a-d** were also purified by column chromatography and isolated in good yields (66-74%) over two steps. Analysis of the ^{31}P NMR displayed the expected signals corresponding to the phosphoramidite (~149 ppm) and the phosphorothioate triester (~24 ppm) (**Figure 3.2**). In contrast to compounds **3a-d**, phosphoramidite dimers **4a-d** each constituted a mixture of four diastereoisomers and displayed four peaks in each region of the ^{31}P NMR spectrum. Analysis by HRMS also confirmed the identity of the products.

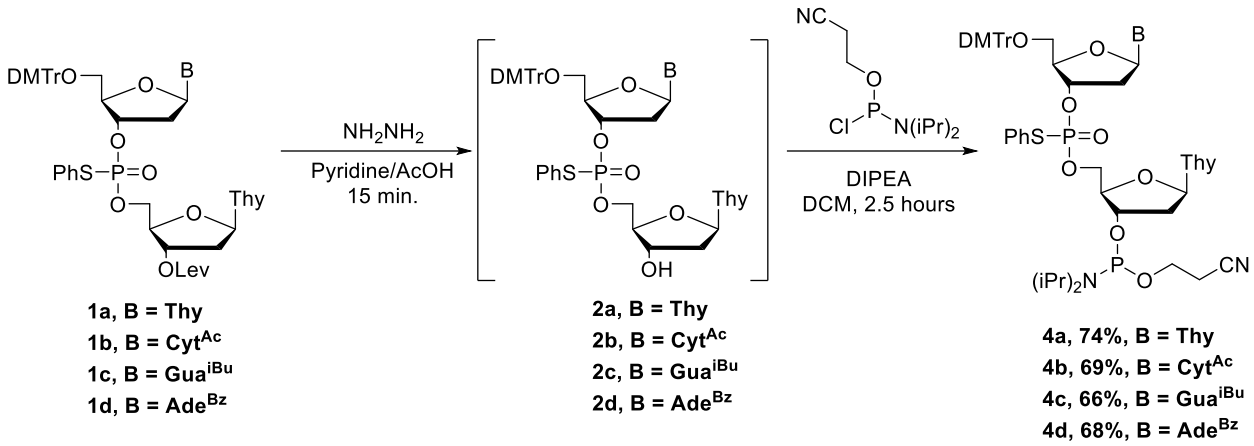

1a, B = Thy
1b, B = Cyt^{Ac}
1c, B = Gua^{iBu}
1d, B = Ade^{Bz}

2a, B = Thy
2b, B = Cyt^{Ac}
2c, B = Gua^{iBu}
2d, B = Ade^{Bz}

4a, 74%, B = Thy
4b, 69%, B = Cyt^{Ac}
4c, 66%, B = Gua^{iBu}
4d, 68%, B = Ade^{Bz}

Scheme 3.2: *Synthesis of dimer blocks containing 3′-phosphoramidites.*

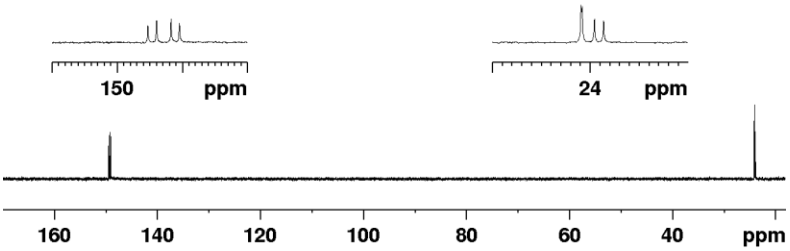

Figure 3.2: *^{31}P NMR spectrum of compound **4d**.*

3.2.3: Mechanochemical block coupling of H-phosphonate dimers

Having synthesized dimer H-phosphonates **3a-d,** we set out to establish a protocol for dimer + dimer (2+2) block coupling by VBM. Using dimer **5** (see section **2.2.4**) and dimer H-phosphonate **3a** we attempted the coupling by mechanochemistry using the previously optimized conditions. The reaction conditions also proved amenable to the block coupling approach without any modifications of equivalents, time, or frequency of the reaction. From this reaction we were able to synthesize tetramer **6** and isolate it in excellent yield (83%). We used AdaCl for coupling since using DPC would result *in situ* detritylation, making purification of the crude tetramer more difficult. To that end, we then detritylated **6** in solution using trifluoroacetic acid (TFA) in DCM/MeOH yielding 5′-OH trimer **7** in high yield after purification (86%). The yields obtained from using the AdaCl maintaining the DMTr group approach followed by detritylation in solution were similar to the yields obtained if the DMTr group was cleaved *in situ* during

coupling using DPC. The relief of some of the challenges encountered during the strategy using DPC as the activator resulting in *in situ* detritylation rendered this strategy just as effective and more straightforward. Analysis of **6** and **7** by ^{31}P NMR proved more difficult than previous analyses of dimers and trimers. Both compounds now contain three chiral phosphorous centers leading to a total of eight diastereomers each of which contain three signals and we would therefore expect 24 signals total. Although we observed signals in the characteristic range for the phosphorothioate triesters as previously observed (~24 ppm), the large number of signals and significant overlapping of them meant the NMR spectra were less diagnostic of the products than previously, but still supported their structures. TLC analysis of the reaction mixtures proved an important qualitative factor for formation of the products, as acid spraying or heating of TLC plates will cause any products containing DMTr functionalities to turn orange. Thus, formation of new, faster migrating spots as compared to **5** (no orange color on heating) that turned orange upon heating confirmed formation of a new product. The only other spot that turned orange of the reaction mixture was **3a**, which remains baseline even when using highly polar solvent systems (DCM-MeOH, 90:10, v/v). However, we relied more on the HRMS which confirmed the formation of the desired tetramers **6** and **7** after isolation.

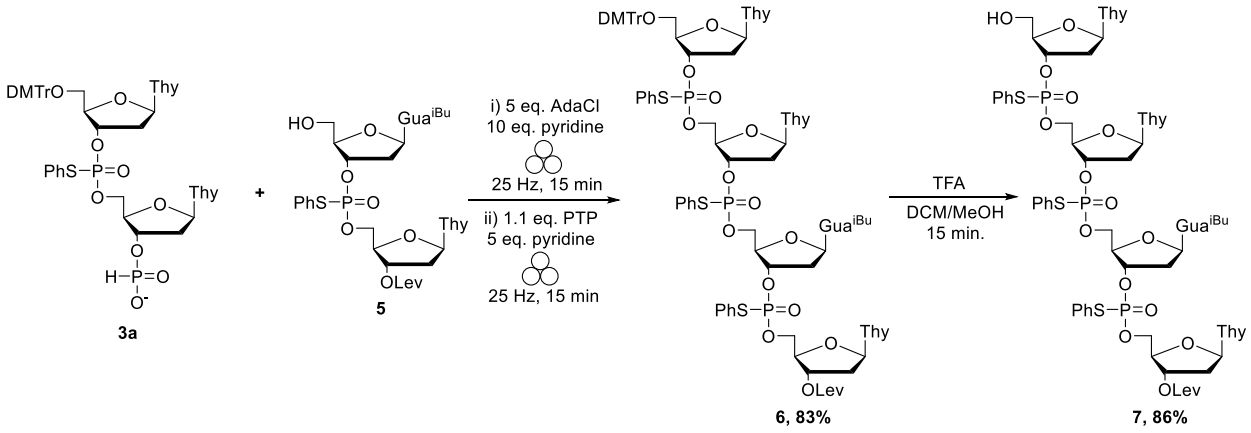

Scheme 3.3: *Mechanochemical coupling of dimer H-phosphonates.*

Having established the success of the block coupling strategy for the synthesis of a tetramer followed by successful detritylation, we set out to repeat the block coupling approach for the synthesis of a hexamer. Therefore, we coupled **7** (**Scheme 3.4**) with another equivalent of **3a** under the exact same conditions using VBM and were able to synthesize hexamer **8** in very good yield (74%). Following the same logic as above for analysis of the tetramers, the ^{31}P NMR

spectrum of **8** grew exponentially more complicated (total of 32 diastereomers with five signals each = 160 expected peaks), but we still observed signals in the expected range (~24 ppm, **Figure 3.4**). Analysis of the TLC of the reaction mixture revealed a faster migrating spot which turned orange upon treatment of the TLC with acid, indicating formation of the product. This is because the presence of the DMTr group and numerous thiophenyl groups on the backbone rendered both the tetramers and hexamer to be relatively non-polar and isolation by column chromatography was straightforward. HRMS analysis confirmed the formation of the hexamer **8**.

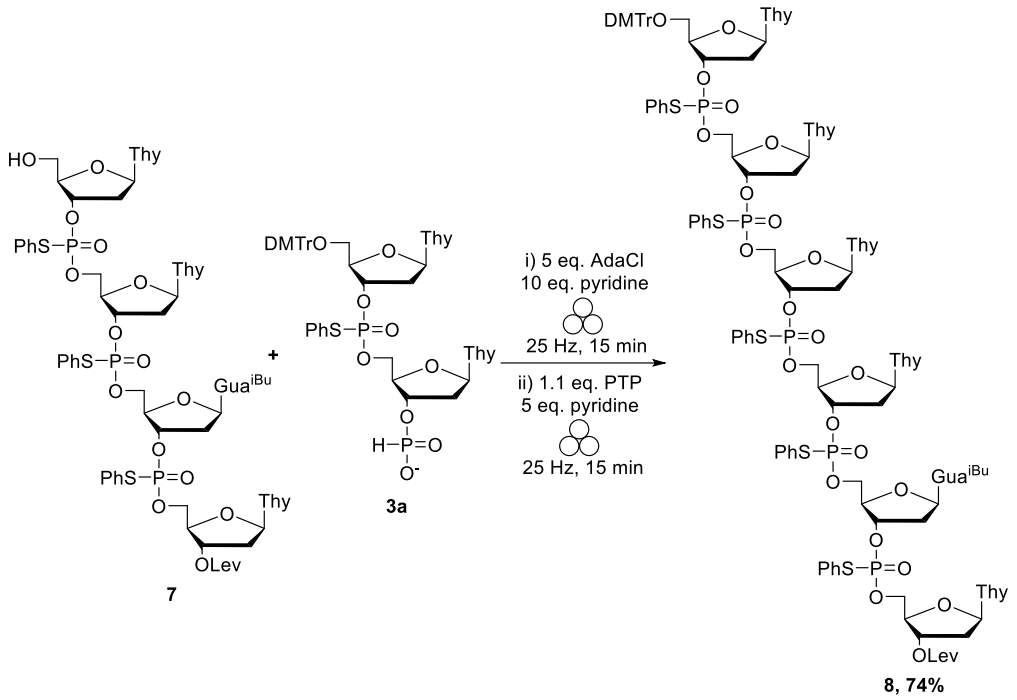

Scheme 3.4: *Mechanochemical block coupling of dimer H-phosphonate with a tetramer.*

3.2.4: Mechanochemical coupling of modified nucleosides and RNA

We further adopted the mechanochemical strategy to the application of nucleosides other than DNA, which have tremendous importance in therapeutic applications[11]. To that end, we adopted the strategy to 2′F nucleosides and 2′OMe nucleosides. Although DNA H-phosphonates are commercially available, we had to synthesize the H-phosphonates of the modified nucleosides. The phosphonylation of nucleosides was carried out under the same conditions we used to prepare dimer H-phosphonates **3a-d**, using DPHP in pyridine. Thus, we synthesized nucleoside H-phosphonates **10a** and **10b** (**Scheme 3.5**), in excellent yields (80-95%) from commercially available 5′DMTr and nucleobase protected nucleosides **9a** and **9b**. The dimer H-phosphonates were difficult to purify by column chromatography, however, H-phosphonate

monomers could be purified by column chromatography or by precipitation with good purity. We also applied the strategy to the synthesis of RNA H-phosphonates using a 2′-*tert*-butyldimethyl silyl (TBDMS) protecting group and were able to isolate **10c** in good yield (88%).

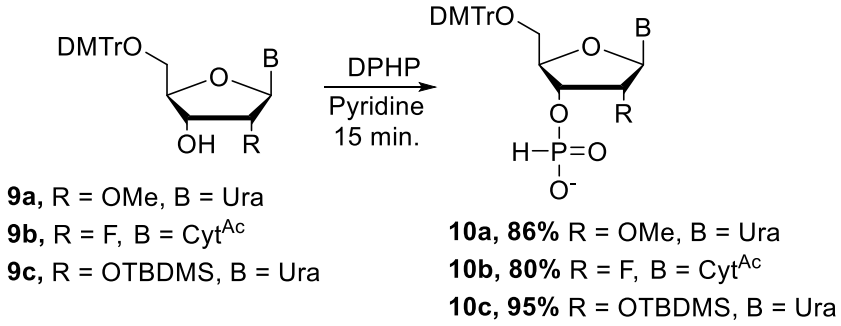

Scheme 3.5: *Synthesis of modified nucleoside and RNA H-phosphonates.*

Having some modified and RNA H-phosphonates in hand, we set out to determine if the mechanochemical coupling conditions developed in **Chapter 2** would be amenable to nucleotides other than DNA. It was important to optimize these conditions separately as in solid-phase synthesis and in solution-phase reactions, nucleotides with 2′-substituents (particularly OMe and RNA) have been shown in our lab in unpublished data to couple significantly slower than DNA monomers. We first attempted coupling modified H-phosphonates with the same 3′-levulinyl DNA monomer used in **Chapter 2**, following the previously optimized conditions. Fortunately, coupling of the H-phosphonates using the same conditions previously optimized provided satisfactory results and the modified and RNA H-phosphonates (**Scheme 3.6**) were coupled to **11** to yield dimers **12a-c** which were isolated in good yields (67-73%).

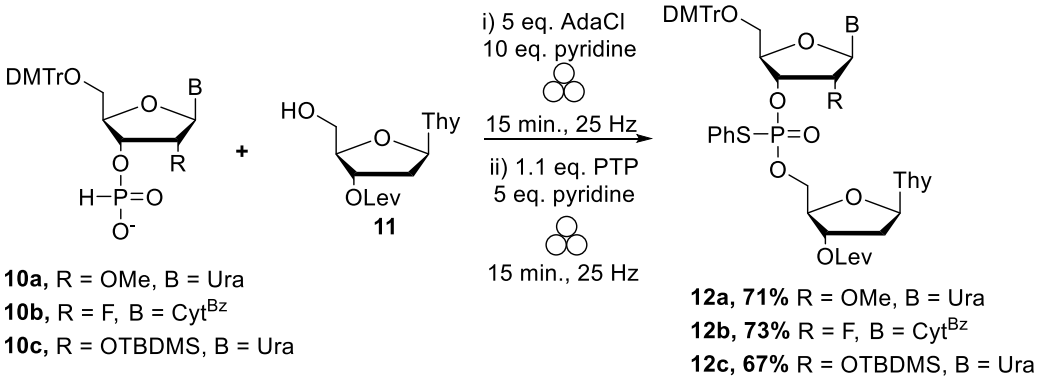

Scheme 3.6: *Mechanochemical coupling of modified and RNA H-phosphonates.*

Having confirmed the efficiency of conditions previously developed for nucleosides other than DNA, we also set out to synthesize dimers modified at the 3′-nucleoside as well. To that

end, we synthesized 3′-levulinyl 2′-OMe nucleoside **13a** as well as 3′-levulinyl 2′-triisopropyl silyl (TIPS) nucleoside **13b** in excellent yield. The synthesis of these compounds is detailed in the experimental section (**3.4.2**). The use of the TIPS protecting group was necessary at this position if we were to apply this strategy to the synthesis of dimer blocks. Previous work in our lab on the synthesis of RNA block amidites has shown that under the conditions used to deprotect the 3′-levulinyl ester group, a 2′-OTBDMS group can migrate to the 3′-position, but the more sterically hindered TIPS group at the same position does not[7]. Therefore, TBDMS groups can be tolerated at positions internal to a dimer or trimer block, but not at the 3′-end and the TIPS group must be used. Having now both modified H-phosphonates and suitably protected modified nucleosides, we synthesized modified dimers and RNA dimers by coupling H-phosphonates **10a** and **10c** with protected nucleoside **13a-b** (**Scheme 3.7**). The same conditions from the previous conditions also proved effective in synthesizing the modified dimers **14a-b** in good yields (67-72%).

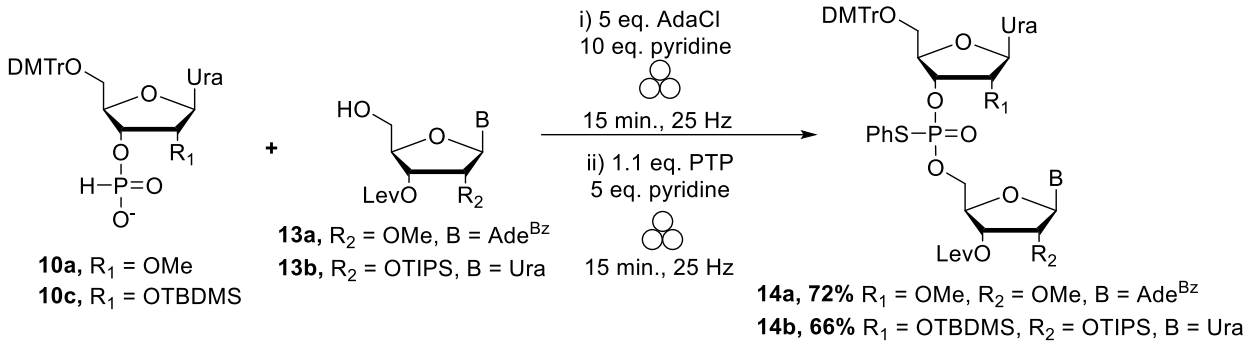

Scheme 3.7: *Mechanochemical synthesis of non-DNA dimers.*

3.2.5: Mechanochemistry to synthesize PS backbone dimers

Having established our conditions were generally applicable for the mechanochemical coupling of modified and RNA H-phosphonates with both DNA and other nucleosides, we sought to develop a strategy for the synthesis of dimers which can be deprotected to a PS backbone rather than the PO backbone derived from the SPh protecting group (**Figures 2.8 and 2.9**). Reese used a modified reagent from the sulfur transfer reagent we used (PTP), (2-cyanoethyl)thiophthalimide (CTP), which when deprotected would yield the desired PS backbone[5]. Unfortunately, CTP was not commercially available and had to be synthesized as shown in **Scheme 3.8**[12]. Despite many efforts, in our hands we were unable to recreate Reese's synthesis of CTP effectively, which he reported in 90% yield. His conditions required conducting

the reaction at 0°C for approximately three hours, but we still observed incomplete reaction after allowing the reaction to continue overnight at room temperature. Crystallization of the products also resulted in crystallization of excess phthalimide used in the reaction. Increasing equivalents of bromine and 3,3′-dithiobis(propionitrile) did not improve the reaction much. We also attempted the reaction using *N*-bromophthalimide instead of phthalimide and bromine, which Reese reported as also a possible strategy, and observed similar results. Despite these challenges, we were able to synthesize CTP in low yield and decent purity (24% and ~50%, respectively, assessed by ^{1}H NMR) and attempted VBM coupling using it as a sulfur-transfer reagent (**Scheme 3.9**). Using a large excess of crude CTP (2.5 eq.), we were only able to isolate *S*-cyanoethyl dimer **16** in moderate yield (38%) after coupling **15** with **11.** Analysis of the ^{31}P NMR spectrum showed a shift from ~24 ppm to ~27 ppm (**Figure 3.3**), but we observed some small impurities around 8 ppm, likely due to incomplete conversion from the H-phosphonate diester to **16**. The identity of the product was confirmed by HRMS. Although in principle, further purification of CTP or use of a higher excess to offset any impurities could result in higher yields, we determined this to be an inefficient strategy moving forward due to the challenges encountered with the synthesis of CTP.

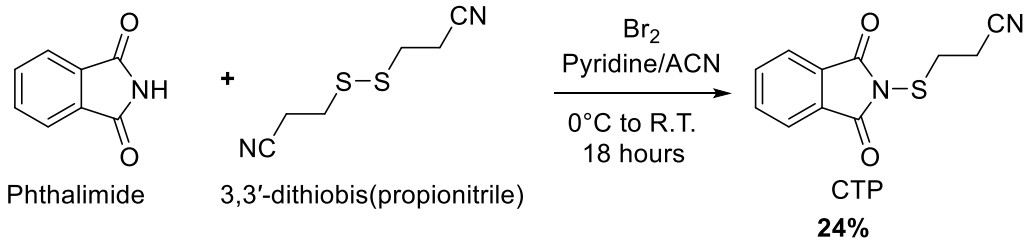

Scheme 3.8: *Attempted synthesis of sulfur-transfer reagent CTP.*

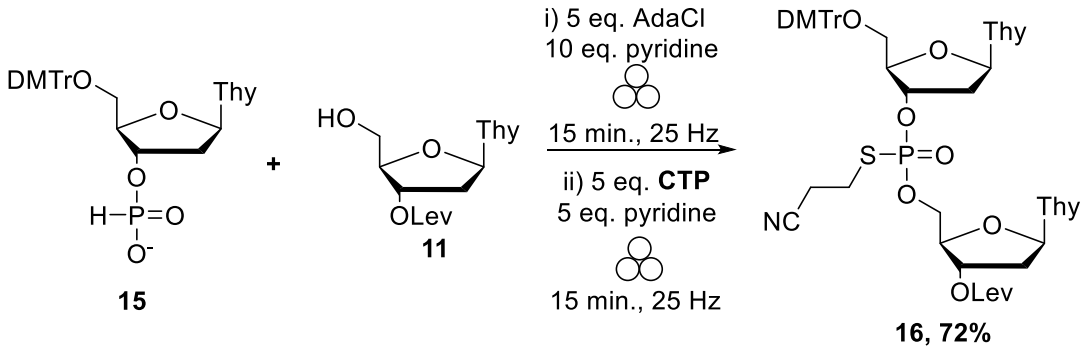

Scheme 3.9: *Use of impure CTP for mechanochemical coupling.*

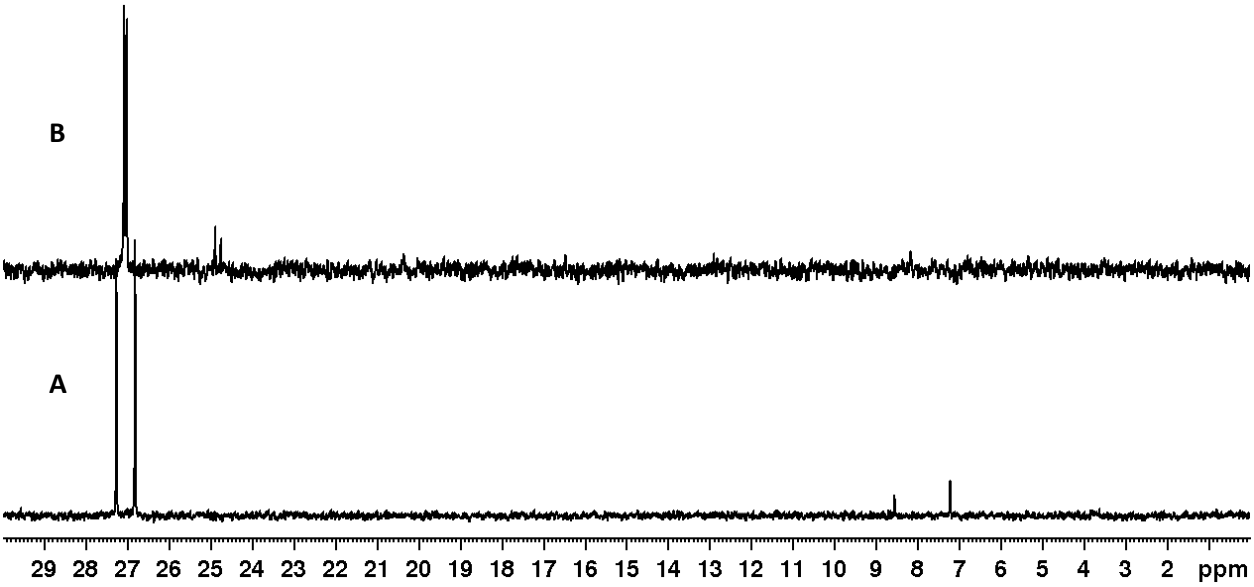

Figure 3.3: *^{31}P NMR of S-cyanoethyl dimer **16**. **A: 16** synthesized using CTP in **Scheme 3.9**. **B: 16** synthesized using **20** in **Scheme 3.10.***

Despite moderate success with CTP, we decided to attempt using a different sulfur-transfer reagent that would give better results. Additionally, the 3,3′-dithiobis(propionitrile) used in the reaction is an expensive reagent (~$60 CAD/g) and we wanted to adopt a more economically friendly strategy. After looking through the literature we identified **17** (**Scheme 3.10, top**) as a possible sulfur-transfer reagent with a straightforward synthesis that had been used by Wave Life Sciences as an electrophilic sulfurization reagent[13]. We expected that the mechanism of sulfurization with **17** should be similar to that of PTP, with the lone pair of the tautomer of an H-phosphonate diester attacking the sulfur atom with a good leaving group (Me-$S(O_2)^-$). However, the methyl derivative of **17** was synthesized from sodium methane thiosulfonate, which is also quite expensive (~$100 CAD/g). We identified the toluene derivative **20**, could likely be prepared analogously from potassium *p*-toluene thiosulfonate **16** (~$6 CAD/g). We also suspected that **20** would be crystalline (**17** is an oil) and should be cheaper to synthesize. Thus, we synthesized **20** from **18** and 3-bromopropionitrile **19** in DMF at 50°C for 18 hours. Compound **20** was isolated in modest yield (55%) by column chromatography, but with further optimization we expect this can be improved.

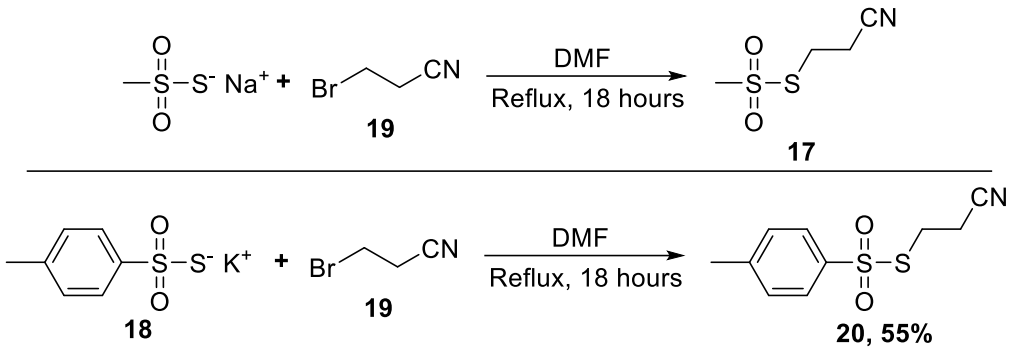

Scheme 3.10: *Synthesis of alternative thiosulfonate-based sulfur transfer reagent.*

Having a new sulfur-transfer reagent in hand in good purity, we set out to evaluate whether it would be amenable to our mechanochemical conditions. Thus, we repeated the reaction carried out in **Scheme 3.11** using **20** as the sulfur transfer reagent. Unfortunately, despite our hopes that **20** would be crystalline, it turned out to be an oil which made it difficult to weigh out precise amounts for VBM reactions. We instead premixed the pyridine and **20** used in the sulfur transfer step such that 1.1 eq. of **20** and 5 eq. of pyridine were added at once. Gratifyingly, we obtained dimer **16** in good yield (62%; after column chromatography) when **15** was coupled to **11**. Analysis of the ^{31}P NMR showed **16** synthesized from **20** to be identical when synthesized from CTP (**Figure 3.3**), although there was a small impurity around ~24 ppm.

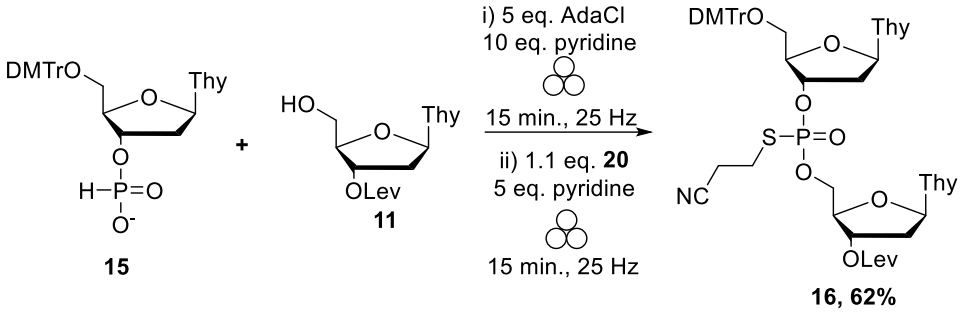

Scheme 3.11: *Mechanochemical coupling of nucleosides using **18** as a sulfur-transfer reagent as a strategy for PS backbones following deprotection.*

3.3: Conclusions and outlook

In this chapter, we expanded the mechanochemical strategy developed in **Chapter 2** to syntheses of DNA and RNA fragments. The conditions developed allowed for the block coupling synthesis of a DNA hexamer. Modification of the sulfur transfer reagent from PTP allowed for synthesis of dimers which after deprotection would yield PS backbones. The work in this chapter demonstrates the versatility of the mechanochemical synthesis of short

oligonucleotides by VBM with a wide range of substrates. Of course a non-exhaustive list of sugar modifications have been described in the literature[11], but some of the most widely used (2'F, 2'OMe) were compatible with the VBM strategy we developed. The H-phosphonate chemistry used here should provide a versatile synthetic handle for accessing a wide range of backbones[14]. The successful synthesis of dimer 3'-phosphoramidites by VBM could be applied to SPOS thus representing another potential path forward for this approach. We envision scaling up of dimer or trimer synthesis under mechanochemical conditions would allow for the synthesis of blocks on large scales with minimal use of solvents. Combined with SPOS, the potential to reduce couplings during synthesis cycles by half or more represents a huge reduction in waste generated.

3.4: Experimental

3.4.1: General information

Solvents such as pyridine, dichloromethane (DCM), dimethyl formamide (DMF), and methanol were purchased from Fisher Scientific. Nucleosides, nucleotides, and activating reagents (adamantane carbonyl chloride) were purchased from ChemGenes Corporation. All other chemicals were purchased from Sigma-Aldrich, Fisher Scientific, or TCI. Pyridine used for mechanochemical reactions was dried using 5Å molecular sieves and stored under an argon atmosphere. Mechanochemical reactions were performed on a FTS-1000 Shaker Mill and were performed using SmartSnap^{TM} Grinding Jars, all purchased from FormTech Scientific. Reactions were performed in 30mL stainless steel SmartSnapTM Grinding Jars with one 10mm ball of the same material. Solution-phase reactions that were air or moisture sensitive were carried out in oven dried glassware under an argon atmosphere. Thin-layer chromatography (TLC) was performed on 0.15-0.2 mm precoated silica gel (10-40µm) plates using UV light and heat as visualizing agents. Column chromatography was performed using silica gel 60 (40-63 µm) purchased from Silicycle. Yields refer to chromatographically and spectroscopically (^{1}H NMR) homogeneous samples. NMR spectra were recorded on Bruker-500 spectrometers and were calibrated using residual undeuterated solvent as an internal reference ($CDCl_3$ ^{1}H NMR δ = 7.26 ppm) and ^{31}P NMR spectra were measured from 85% H_3PO_4 as an external standard. High-resolution mass spectra (HRMS) were recorded on a mass spectrometer under electron spray ionization (ESI) conditions.

3.4.2: Synthetic procedures

General procedure **A** for phosphonylation of nucleosides:

5′DMTr-3′OH nucleoside (1 eq.) was dissolved in dry pyridine. While stirring at room temperature, diphenyl hydrogen phosphite (10 eq.) was added in one portion. Once the reaction was complete by TLC analysis with DCM-MeOH as the eluent (90:10, v/v) after approximately 15 minutes, first 2 mL of triethylamine then 2 mL of water were added and the mixture was allowed to stir at room temperature. After 10 minutes, the mixture was diluted with DCM and washed twice with a saturated sodium bicarbonate solution. The aqueous layers were back-extracted with DCM and the combined organic layers were dried over sodium sulfate and

concentrated under reduced pressure. The crude mixture was purified by column chromatography with silica neutralized by triethylamine with DCM-MeOH as the eluent (gradient depending on monomer or dimer) or precipitated into a stirring mixture of Et_2O:hexanes (1:1, v/v) at 0°C yielding the desired product as a white precipitate.

General procedure **B** for delevulination followed by phosphonylation of dimers:

5′DMTr-3′Levulinyl dimer (1 eq.) was dissolved in a minimal amount of DCM. Separately, a 0.5M solution of hydrazine hydrate (10 eq.) in pyridine/acetic acid (3:2, v/v) was prepared. The hydrazine solution was added to the stirring dimer in one portion. Once the reaction was complete by TLC analysis with DCM-MeOH as the eluent (95:5, v/v) after approximately 15 minutes, 2,4-pentanedione (10 eq.) was added and the mixture turned yellow. After 10 minutes of stirring, the mixture was carefully poured into a saturated sodium bicarbonate solution and allowed to separate. The mixture was washed once more with saturated sodium bicarbonate. The aqueous layers were back-extracted with DCM and the combined organic layers were dried over sodium sulfate and concentrated under reduced pressure. The crude residue was subjected to general procedure **B** for phosphonylation. The crude mixture was purified by column chromatography with silica neutralized by triethylamine with DCM-MeOH as the eluent (gradient 95:5-80:20, v/v) or precipitated into a stirring mixture of Et_2O:hexanes (1:1, v/v) at 0°C yielding the desired product as a white precipitate.

General procedure **C** for delevulination followed by phosphitylation of dimers:

5′DMTr-3′Levulinyl dimer (1 eq.) was dissolved in a minimal amount of DCM. Separately, a 0.5M solution of hydrazine hydrate (10 eq.) in pyridine/acetic acid (3:2, v/v) was prepared. The hydrazine solution was added to the stirring dimer in one portion. Once the reaction was complete by TLC analysis with DCM-MeOH as the eluent (95:5, v/v) after approximately 15 minutes, 2,4-pentanedione (10 eq.) was added and the mixture turned yellow. After 10 minutes of stirring, the mixture was carefully poured into a saturated sodium bicarbonate solution and allowed to separate. The mixture was washed once more with saturated sodium bicarbonate. The aqueous layers were back-extracted with DCM and the combined organic layers were dried over sodium sulfate and concentrated under reduced pressure. The crude residue was rendered anhydrous by coevaporation with pyridine (2x5 mL). The residue was dissolved in dry DCM under argon and cooled to 0°C. While stirring, DIPEA (5 eq.) was added to the solution. After 10

minutes, DPCP (4 eq.) was added and the solution was allowed to warm to room temperature and stirred for a further period of 2.5 hours. Once the reaction was complete by TLC analysis, the reaction mixture was directly purified by column chromatography with silica neutralized by triethylamine with DCM-MeOH as the eluent (gradient 100:0-95:5, v/v).

5′DMTrO-T*p*(SPh)T-O-PO_2H **3a**

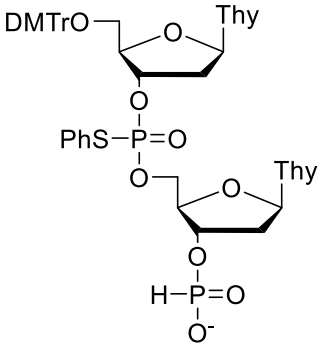

3a

This compound was prepared according to general procedure **B** using **1a** (0.9604 g, 0.924 mmol), hydrazine hydrate (0.45 mL, 9.24 mmol), pyridine (11.1 mL), acetic acid (7.4 mL), and 2,4-pentanedione (0.94 mL, 9.24 mmol) for the delevulination. The phosphonylation was carried out using DPHP (1.77 mL, 9.24 mmol) in pyridine (15 mL). The crude residue after workup was precipitated to yield **3a** as a finely divided white precipitate (0.65 g, 64%). HRMS calc. [M+2Na] = 1049.2180. HRMS found [M+2Na] = 1049.2182. ^{31}P-NMR δP ($CDCl_3$) 1.53, 1.80, 23.80, 24.34.

5′DMTrO-C*p*(SPh)T-O-PO_2H **3b**

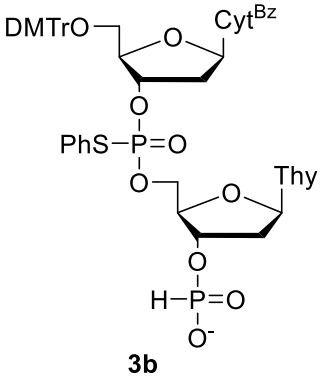

3b

This compound was prepared according to general procedure **B** using **1b** (0.6569 g, 0.582 mmol), hydrazine hydrate (0.28 mL, 5.82 mmol), pyridine (7 mL), acetic acid (4.5 mL), and 2,4-

pentanedione (0.60 mL, 5.82 mmol) for the delevulination. The phosphonylation was carried out using DPHP (1.14 mL, 5.82 mmol) in pyridine (10 mL). The crude residue after workup was precipitated to yield **3b** as a finely divided white precipitate (0.48 g, 69%). HRMS calc. [M-H] = 1092.2661. HRMS found [M-H] = 1092.2673. ^{31}P-NMR δP ($CDCl_3$) 3.38, 3.45, 23.84, 24.18.

5′DMTrO-G*p*(SPh)T-O-PO_2H **3c**

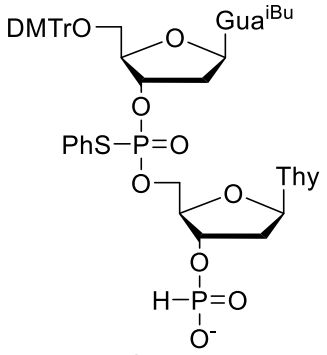

3c

This compound was prepared according to general procedure **B** using **1c** (0.331 g, 0.292 mmol), hydrazine hydrate (0.14 mL, 2.92 mmol), pyridine (3.5 mL), acetic acid (2.3 mL), and 2,4-pentanedione (0.30 mL, 2.92 mmol) for the delevulination. The phosphonylation was carried out using DPHP (0.56 mL, 2.92 mmol) in pyridine (10 mL). The crude residue after workup was precipitated to yield **3c** as a finely divided white precipitate (0.22 g, 62%). HRMS calc. [M+2Na] = 1144.2664. HRMS found [M+2Na] = 1144.2653. ^{31}P-NMR δP ($CDCl_3$) 2.64, 3.41, 21.73, 24.62.

5′DMTrO-A*p*(SPh)T-O-PO_2H **3d**

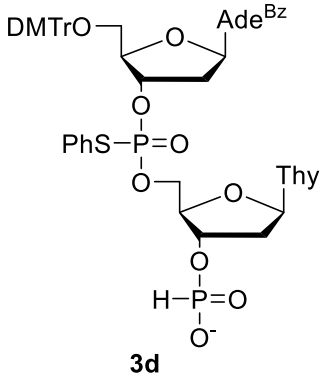

3d

This compound was prepared according to general procedure **B** using **1d** (0.411 g, 0.357 mmol), hydrazine hydrate (0.17 mL, 3.57 mmol), pyridine (4.3 mL), acetic acid (2.8 mL), and 2,4-pentanedione (0.36 mL, 3.57 mmol) for the delevulination. The phosphonylation was carried out

using DPHP (0.68 mL, 3.57 mmol) in pyridine (10 mL). The crude residue after workup was precipitated to yield **3d** as a finely divided white precipitate (0.32 g, 73%). HRMS calc. [M+2Na] = 1162.2558. HRMS found [M+2Na] = 1162.2558. ^{31}P-NMR δP ($CDCl_3$) 3.18, 23.46, 24.06.

5′DMTrO-T*p*(SPh)T-O-PN(iPr_2)OCE **4a**

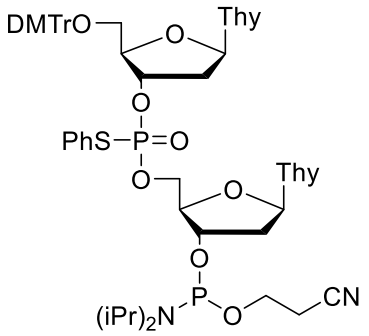

4a

This compound was prepared according to general procedure **C** using **1a** (1.46 g, 1.41 mmol), hydrazine hydrate (0.62 mL, 14.1 mmol), pyridine (15 mL), acetic acid (10 mL), and 2,4-pentanedione (1.30 mL, 9.24 mmol) for the delevulination. The phosphitylation was carried out using DIPEA (1.23 mL, 7.05 mmol) and DPCP (1.26 mL, 6.64 mmol) in DCM (50 mL). The title compound was purified on a short silica gel column neutralized with triethylamine using DCM-MeOH as the eluent (gradient: 100:0 – 95:5 v/v). The appropriate fractions were combined and concentrated under reduced pressure to yield **4a** as a white foam (1.193 g, 74%). HRMS calc. [M+Na] = 1163.3725. HRMS found [M+Na] = 1163.3693. ^{31}P-NMR δP ($CDCl_3$) 23.93, 24.05, 24.15, 149.05, 149.17, 149.43, 149.52.

5′DMTrO-C*p*(SPh)T-O-PN(iPr$_2$)OCE **4b**

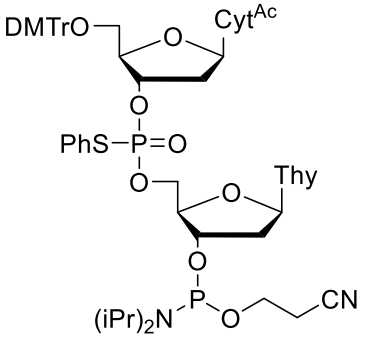

4b

This compound was prepared according to general procedure **C** using **1b** (0.322 g, 0.286 mmol), hydrazine hydrate (0.14 mL, 2.86 mmol), pyridine (3.4 mL), acetic acid (2.2 mL), and 2,4-pentanedione (0.30 mL, 2.86 mmol) for the delevulination. The phosphitylation was carried out using DIPEA (0.25 mL, 1.43 mmol) and DPCP (0.26 mL, 1.14 mmol) in DCM (20 mL). The title compound was purified on a short silica gel column neutralized with triethylamine using DCM-MeOH as the eluent (gradient: 100:0 – 95:5 v/v). The appropriate fractions were combined and concentrated under reduced pressure to yield **4b** as a white foam (0.251 g, 69%). HRMS calc. [M+Na] = 1252.3991. HRMS found [M+Na] = 1252.4030. ^{31}P-NMR δP ($CDCl_3$) 23.92, 24.03, 24.37, 24.42, 149.09, 149.34, 149.43, 149.55.

5′DMTrO-G*p*(SPh)T-O-PN(iPr$_2$)OCE **4c**

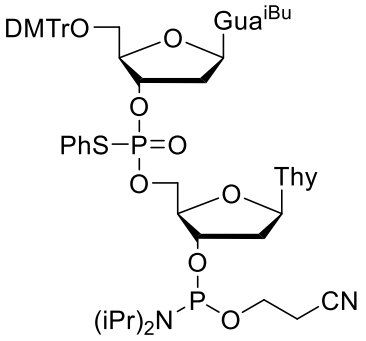

4c

This compound was prepared according to general procedure **C** using **1c** (0.748 g, 0.931 mmol), hydrazine hydrate (0.41 mL, 9.31 mmol), pyridine (10 mL), acetic acid (6.6 mL), and 2,4-pentanedione (0.86 mL, 9.31 mmol) for the delevulination. The phosphitylation was carried out using DIPEA (0.81 mL, 4.66 mmol) and DPCP (0.83 mL, 3.72 mmol) in DCM (40 mL). The title compound was purified on a short silica gel column neutralized with triethylamine using DCM-MeOH as the eluent (gradient: 100:0 – 95:5 v/v). The appropriate fractions were combined and

concentrated under reduced pressure to yield **4c** as a white foam (0.760 g, 66%). HRMS calc. [M+Na] = 1258.4209. HRMS found [M+Na] = 1258.4217. ^{31}P-NMR δP ($CDCl_3$) 24.14, 24.26, 24.31, 24.35, 149.16, 149.23, 149.28, 149.50.

5′DMTrO-A*p*(SPh)T-O-PN(iPr_2)OCE **4d**

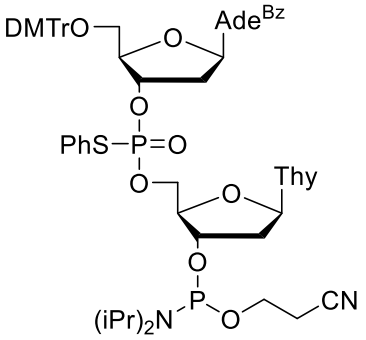

4d

This compound was prepared according to general procedure **C** using **1d** (0.748 g, 0.931 mmol), hydrazine hydrate (0.41 mL, 9.31 mmol), pyridine (10 mL), acetic acid (6.6 mL), and 2,4-pentanedione (0.86 mL, 9.31 mmol) for the delevulination. The phosphitylation was carried out using DIPEA (0.81 mL, 4.66 mmol) and DPCP (0.83 mL, 3.72 mmol) in DCM (40 mL). The title compound was purified on a short silica gel column neutralized with triethylamine using DCM-MeOH as the eluent (gradient: 100:0 – 95:5 v/v). The appropriate fractions were combined and concentrated under reduced pressure to yield **4d** as a white foam (0.760 g, 66%). HRMS calc. [M+Na] = 1276.4103. HRMS found [M+Na] = 1276.4086. ^{31}P-NMR δP ($CDCl_3$) 23.86, 23.95, 24.08, 24.09. 149.04, 149.17, 149.40, 149.53.

5′HO-G*p*(SPh)T-OLev **5**

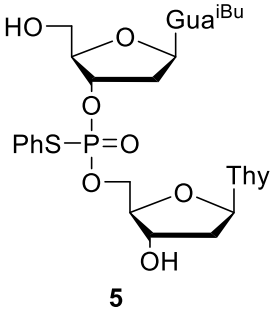

5

This compound was prepared by dissolving **1c** (g, mmol) in DCM (50 mL) followed by addition of TFA (mL, mmol) while stirring at room temperature. The solution turned dark orange and methanol was added until the solution was a clear light orange color. Once the

reaction was complete by TLC (DCM-MeOH, 95:5, v/v) after approximately 15 minutes, the solution was carefully poured into a saturated aqueous $NaHCO_3$ solution (50 mL). The organic layer was washed once more with saturated aqueous $NaHCO_3$ (50 mL) and the aqueous layers were back-extracted with DCM. The combined organic layers were dried over Na_2SO_4 and concentrated under reduced pressure. The resulting residue was taken up in DCM and purified on a short silica gel column using DCM-MeOH as the eluent (gradient: 99:1 – 95:5, v/v). The appropriate fractions were combined and concentrated under reduced pressure to yield **5** as a white foam (). HRMS calc. [M+Na] = . HRMS found [M+Na] = . ^{31}P-NMR δP ($CDCl_3$) .

5′DMTrO-T*p*(SPh)T*p*(SPh)G*p*(SPh)T-OLev **6**

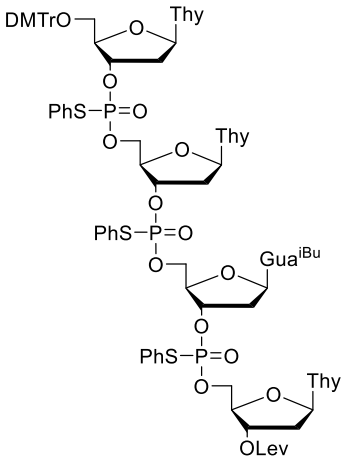

6

This compound was prepared following general procedure **A from Chapter 2** (DMTr-ON method) using **3a** (0.413 g, 0.374 mmol), **5** (0.283 g, 0.340 mmol), AdaCl (0.338 g, 1.70 mmol), and pyridine (0.270 mL, 3.40 mmol). The sulfur transfer step was carried out with PTP (95 mg, 0.374 mmol) and pyridine (0.135 mL, 1.70 mmol) The title compound was purified on a short silica gel column neutralized with triethylamine using DCM-MeOH as the eluent (gradient: 100:0 – 95:5 v/v). The appropriate fractions were combined and concentrated under reduced pressure to yield **6** as a white foam (0.544 g, 83%). HRMS calc. [M+Na] = 1948.4589. HRMS found [M+Na] = 1948.4640. ^{31}P-NMR δP ($CDCl_3$) 23.53, 23.66, 23.94, 24.06, 24.08, 24.11, 24.19, 24.29, 24.39, 24.42, 24.48, 24.58, 24.81.

5′HO-T*p*(SPh)T*p*(SPh)G*p*(SPh)T-OLev **7**

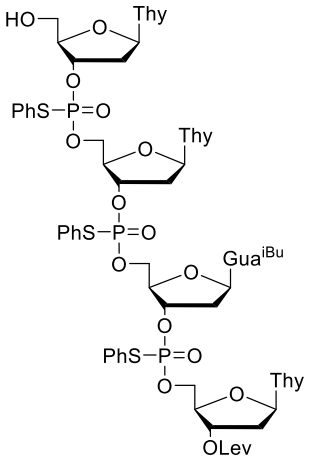

7

This compound was prepared by dissolving **6** (0.316 g,0.164 mmol) in DCM (10 mL) followed by addition of TFA (0.25 mL, 3.28 mmol) while stirring at room temperature. The solution turned dark orange and methanol was added until the solution was a clear light orange color. Once the reaction was complete by TLC (DCM-MeOH, 95:5, v/v) after approximately 15 minutes, the solution was carefully poured into a saturated aqueous $NaHCO_3$ solution (50 mL). The organic layer was washed once more with saturated aqueous $NaHCO_3$ (50 mL) and the aqueous layers were back-extracted with DCM. The combined organic layers were dried over Na_2SO_4 and concentrated under reduced pressure. The resulting residue was taken up in DCM and purified on a short silica gel column using DCM-MeOH as the eluent (gradient: 99:1 – 95:5, v/v). The appropriate fractions were combined and concentrated under reduced pressure to yield **7** as a white foam (0.229g, 86%). HRMS calc. [M+Na] = 1646.3281. HRMS found [M+Na] = 1646.3266. ^{31}P-NMR δP ($CDCl_3$) 23.43, 23.92, 24.03, 24.23, 24.29, 24.32, 24.38, 24.46, 24.55, 24.61, 24.73, 24.78, 24.98, 25.17, 25.31.

5′DMTrO- T*p*(SPh)T*p*(SPh)T*p*(SPh)T*p*(SPh)G*p*(SPh)T-OLev **8**

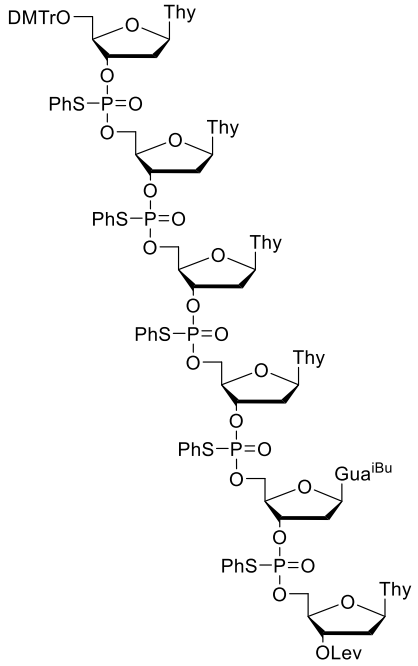

8

This compound was prepared following general procedure **A from Chapter 2** (DMTr-ON method) using **3a** (0.103 g, 0.093 mmol), **7** (0.137 g, 0.084 mmol), AdaCl (84 mg, 0.421 mmol), and pyridine (70 µL, 0.842 mmol). The sulfur transfer step was carried out with PTP (24 mg, 0.093 mmol) and pyridine (35 µL, 0.421 mmol) The title compound was purified on a short silica gel column neutralized with triethylamine using DCM-MeOH as the eluent (gradient: 100:0 – 95:5 v/v). The appropriate fractions were combined and concentrated under reduced pressure to yield **8** as a white foam (0.170 g, 74%). HRMS calc. [M-H] = 2716.5713. HRMS found [M-H] = 2716.5825. ^{31}P-NMR spectra (below) showed many overlapping peaks and individual peaks were not useful in analyzing the product, but showed up in the expected range (~24ppm).

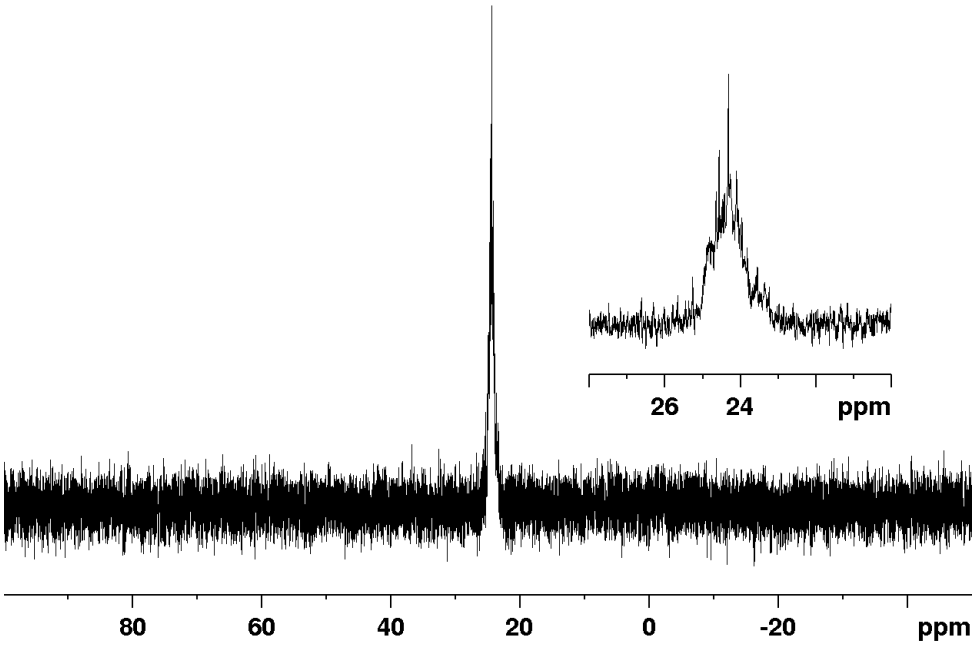

Figure 3.4: *^{31}P NMR spectrum of hexamer **8**.*

5′DMTrO-Um-O-PO_2H **10a**

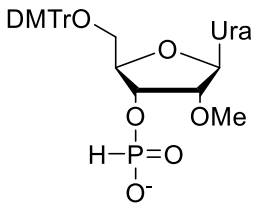

10a

This compound was prepared according to general procedure **A** from **9a** (5.00g, 8.92 mmol) and DPHP (16.4mL, 89.2 mmol) in pyridine (90mL). The mixture was purified on a short silica gel column using DCM-MeOH as the eluent (gradient 98:2-90:10, v/v) to yield **10a** as an off-white foam (5.59g, 86%). HRMS calc: [M-H] 623.1800. HRMS found: ESI-[M-H]+: 623.1804. ^{1}H-NMR δH (500 MHz, $CDCl_3$) 3.53 (dd, 1H, J=2.6Hz, 11.2Hz, H5′), 3.58 (dd, 1H, J=2.5Hz, 11.2Hz, H5′), 3.61 (s, 3H, 2′OMe), 3.81 (s, 3H, DMTr-OMe), 3.82 (s, 3H, DMTr-OMe), 4.08 (m, 1H, H2′), 4.33 (m, 1H, H4′), 4.94 (m, 1H, H3′), 5.19 (d, 1H, J=8.6Hz, H5) 5.78 (d, 1H, J=3.0Hz, H1′), 6.86 (m, 4H, DMTr H) 7.19-7.35 (m, 7H, DMTr H overlapped with $CDCl_3$) 7.40 (m, 2H, DMTr H) 7.95 (d, 1H, J=8.2Hz, H6). ^{31}P-NMR δP (500 MHz, $CDCl_3$) 3.10 (s).

5′DMTrO-Cf-O-PO_2H **10b**

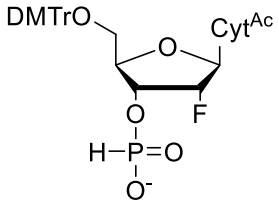

10b

This compound was prepared according to general procedure **B** from **9b** (5.00g, 8.48 mmol) and DPHP (16.2mL, 84.8 mmol) in pyridine (90mL). The mixture was purified on a short silica gel column using DCM-MeOH as the eluent (gradient 98:2-90:10, v/v) to yield **10b** as an off-white foam (5.12g, 80%). HRMS calc: [M-H] 652.1866. HRMS found: ESI-[M-H]+: 652.1867. ^{1}H-NMR δH (500 MHz, $CDCl_3$) 2.04 (s, 3H, Ac), 3.50 (dd, 1H, J=1.3Hz, 11.4Hz, H5′), 3.69 (dd, 1H, J=1.8Hz, 11.5Hz, H5′), 3.85 (s, 3H, DMTr-OMe), 3.86 (s, 3H, DMTr-OMe), 4.28 (d, 1H, J=9.9Hz, H3′), 5.23 (m, 1H, H4′), 5.93 (dd, 1H, J=2.9Hz, 51.3Hz, H2′), 6.16 (d, 1H, J=16.3Hz, H5) 5.78 (d, 1H, J=3.0Hz, H1′), 6.90 (m, 4H, DMTr H) 7.23-7.30 (m, 2H, DMTr H), 7.32-7.41 (m, 5H, DMTr H) 7.46-4.49 (m, 2H, DMTr H) 8.63 (d, 1H, J=8.6Hz, H6). ^{31}P-NMR δP (500 MHz, $CDCl_3$) 1.80 (s).

5′DMTrO-rU-O-PO_2H **10c**

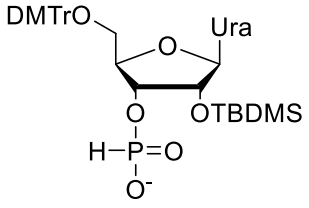

10c

This compound was prepared according to general procedure **B** from **9c** (0.500g, 0.757 mmol) and DPHP (1.44 mL, 7.57 mmol) in pyridine (10 mL). The mixture was purified on a short silica gel column using DCM-MeOH as the eluent (gradient 98:2-90:10, v/v) to yield **10c** as an off-white foam (0.596g, 96%). HRMS calc: [M-H] 723.2508. HRMS found: ESI-[M-H]+: 723.2503. ^{1}H-NMR δH (500 MHz, $CDCl_3$) 0.16 (s, 3H, Si-Me), 0.20 (s, 3H, Si-Me), 0.93 (s, 9H, S-tBu), 3.56 (m, 2H, H5′), 3.81 (s, 3H, DMTr-OMe), 3.82 (s, 3H, DMTr-OMe), 4.41 (m, 1H, H3′), 4.48 (t, 1H, J=4.3Hz, H2′), 4.81 (quintet, 1H, J=4.8Hz, H4′), 5.16 (d, 1H, J=7.8Hz, H5), 5.96 (d, 1H, J=4.2Hz, H1′), 6.85 (m, 4H, DMTr H7.24-7.33 (m, 7H, DMTr H), 7.40 (m, 2H, DMTr H), 7.97 (d, 1H, J=8.2Hz, H6). ^{31}P-NMR δP (500 MHz, $CDCl_3$) 3.47 (s).

5′DMTrO-Um*p*(SPh)T-OLev **12a**

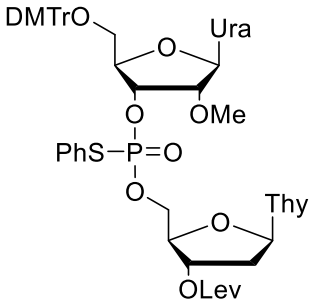

12a

This compound was prepared following general procedure **A from Chapter 2** using **10a** (0.359 g, 0.495 mmol), **11** (0.153 g, 0.45 mmol), AdaCl (0.447 g, 2.25 mmol), and pyridine (0.36 mL, 4.5 mmol). The sulfur transfer step was carried out with PTP (126 mg, 0.495 mmol) and pyridine (0.18 mL, 2.25 mmol) The title compound was purified on a short silica gel column neutralized with triethylamine using DCM-MeOH as the eluent (gradient: 100:0 – 97:3 v/v). The appropriate fractions were combined and concentrated under reduced pressure to yield **12a** as a white foam (0.337 g, 71%). HRMS calc. [M+Na] = 1077.2964. HRMS found [M+Na] = 1077.2981. ^{31}P-NMR δP ($CDCl_3$) 24.34, 24.93.

5′DMTrO-Cf*p*(SPh)T-OLev **12b**

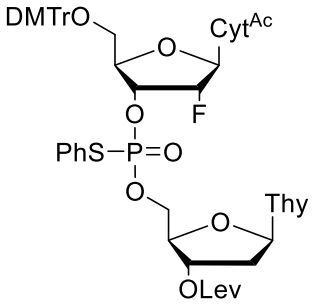

12b

This compound was prepared following general procedure **A from Chapter 2** using **10b** (0.376 g, 0.495 mmol), **11** (0.153 g, 0.45 mmol), AdaCl (0.447 g, 2.25 mmol), and pyridine (0.36 mL, 4.5 mmol). The sulfur transfer step was carried out with PTP (126 mg, 0.495 mmol) and pyridine (0.18 mL, 2.25 mmol) The title compound was purified on a short silica gel column neutralized with triethylamine using DCM-MeOH as the eluent (gradient: 100:0 – 97:3 v/v). The appropriate fractions were combined and concentrated under reduced pressure to yield **12b** as a white foam (0.356 g, 73%). HRMS calc. [M+Na] = 1106.3029. HRMS found [M+Na] = 1106.3025. ^{31}P-NMR δP ($CDCl_3$) 25.08, 25.32.

5′DMTrO-rU*p*(SPh)T-OLev **12c**

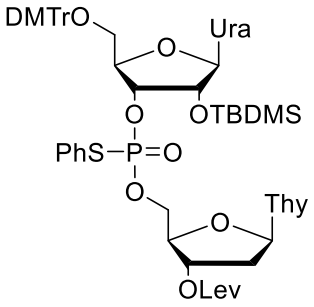

12c

This compound was prepared following general procedure **A from Chapter 2** using **10c** (0.409 g, 0.495 mmol), **11** (0.153 g, 0.45 mmol), AdaCl (0.447 g, 2.25 mmol), and pyridine (0.36 mL, 4.5 mmol). The sulfur transfer step was carried out with PTP (126 mg, 0.495 mmol) and pyridine (0.18 mL, 2.25 mmol) The title compound was purified on a short silica gel column neutralized with triethylamine using DCM-MeOH as the eluent (gradient: 100:0 – 97:3 v/v). The appropriate fractions were combined and concentrated under reduced pressure to yield **12c** as a white foam (0.346 g, 67%). HRMS calc. [M+Na] = 1177.3672. HRMS found [M+Na] = 1177.3667. ^{31}P-NMR δP ($CDCl_3$) 23.30, 24.73.

5′HO-Am-OLev-3′ **13a**

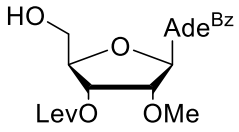

13a

5′DMTr-3′OH-2′OMe adenosine (N-Bz) (5.00g, 7.27 mmol) was dissolved in THF (60mL). Separately, levulinic acid (2.53g, 21.8 mmol), DCC (4.50g, 21.8 mmol), and DMAP (0.444g, 3.64 mmol) were dissolved in THF (40mL) and the mixture was stirred at room temperature for 30 minutes. Any precipitated DCU was filtered off, and the levulinic anhydride solution was added to the solution containing the nucleoside and the mixture was allowed to stir overnight for 16 hours. Once the reaction was complete by TLC analysis with DCM-MeOH as the eluent (95:5, v/v) any remaining DCU was filtered off and the solution was concentrated under reduced pressure. The residue was redissolved in DCM (50mL) and washed with a saturated sodium bicarbonate solution (2x50mL). The aqueous layers were back-extracted with DCM and the combined organic layers were dried over sodium sulfate and concentrated under reduced pressure. The crude residue was dissolved in DCM (100mL) and while stirring, trifluoroacetic

acid (11.1mL, 0.145 mol) was added. The mixture was diluted with MeOH until most of the dark orange color from the trityl cation disappeared, leaving a light orange clear solution. Once the reaction was complete after approximately 30 minutes, the mixture was carefully poured into a saturated sodium bicarbonate solution (100mL) and allowed to separate. The mixture was washed once more with saturated sodium bicarbonate (100mL). The aqueous layers were back-extracted with DCM and the combined organic layers were dried over sodium sulfate and concentrated under reduced pressure. The crude mixture was purified on a short silica gel column using DCM-MeOH as the eluent (gradient 99:1-95:5, v/v) to yield **13a** as a white foam (3.12g, 88%). HRMS calc: [M+H] 484.1827. HRMS found: ESI+[M+H]+: 484.1841. ^{1}H-NMR δH (500 MHz, $CDCl_3$) 2.25 (s, 3H, Lev-Me), 2.74 (m, 2H, Lev-CH_2), 2.85 (m, 2H, Lev-CH_2), 3.30 (s, 3H, 2′OMe), 3.86 (m, 1H, H5′), 4.01 (m, 1H, H5′), 4.80 (m, 1H, H2′), 5.67 (d, 1H, J=5.0Hz, H4′), 5.93 (d, 1H, J=7.9 Hz, H3′), 6.20 (dd, 1H, J=2.5Hz, 12.0 Hz, H1′), 7.56 (t, 2H, J=7.8 Hz, Bz), 7.65 (t, 1H, J=7.6 Hz, Bz), 8.05 (m, 2H, Bz), 8.09 (s, 1H, H2), 8.82 (s, 1H, H8), 9.03 (s, 1H, NH).

5′HO-rU-OLev-3′ **13b**

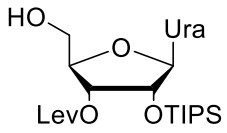

13b

5′DMTr-3′OH-2′OTIPS uracil[7] (2.51g, 3.57 mmol) was dissolved in THF (50mL). Separately, levulinc acid (0.912g, 7.86 mmol), DCC (1.47g, 7.14 mmol), and DMAP (0.218g, 1.79 mmol) were dissolved in THF (25mL) and the mixture was stirred at room temperature for 30 minutes. Any precipitated DCU was filtered off, and the levulinic anhydride solution was added to the solution containing the nucleoside and the mixture was allowed to stir overnight for 16 hours. Once the reaction was complete by TLC analysis with DCM-MeOH as the eluent (95:5, v/v) any remaining DCU was filtered off and the solution was concentrated under reduced pressure. The residue was redissolved in DCM (30mL) and washed with a saturated sodium bicarbonate solution (2x30mL). The aqueous layers were back-extracted with DCM and the combined organic layers were dried over sodium sulfate and concentrated under reduced pressure. The crude residue was dissolved in DCM (70mL) and while stirring, trifluoroacetic acid (5.5 mL, 71.4 mmol) was added. The mixture was diluted with MeOH until most of the dark orange color from the trityl cation disappeared, leaving a light orange clear solution. Once the reaction was

complete after approximately 30 minutes, the mixture was carefully poured into a saturated sodium bicarbonate solution (70mL) and allowed to separate. The mixture was washed once more with saturated sodium bicarbonate (70mL). The aqueous layers were back-extracted with DCM and the combined organic layers were dried over sodium sulfate and concentrated under reduced pressure. The crude mixture was purified on a short silica gel column using DCM-MeOH as the eluent (gradient 99:1-95:5, v/v) to yield **13b** as a white foam (1.22g, 69%). HRMS calc: [M+Na] 521.2290. HRMS found: ESI+[M+Na] 521.2286. ^{1}H-NMR δH (500 MHz, $CDCl_3$) 1.05 (m, 18H, iPr-Me), 2.23 (s, 3H, Lev-CH_3), 2.57-2.89 (m, 7H, iPr-H and CH_2 of Lev), 3.82 (dd, 1H, J=1.9, 12.5Hz, H5′), 3.94 (dd, 1H, J=1.9, 12.4Hz, H5′), 4.21 (m, 1H, H4′), 4.85 (t, 1H, J=5.4Hz, H3′), 5.20 (dd, 1H, J=3.5, 5.0Hz, H2′), 5.72 (d, 1H, J=5.8Hz, H1′), 5.78 (d, 1H, J=8.2Hz, H5), 7.73 (d, 1H, J=8.2Hz, H6).

5′DMTrO-Um*p*(SPh)Am-OLev **14a**

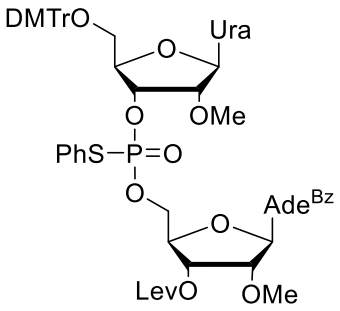

14a

This compound was prepared following general procedure **A from Chapter 2** using **10a** (0.359 g, 0.495 mmol), **13a** (0.218 g, 0.45 mmol), AdaCl (0.447 g, 2.25 mmol), and pyridine (0.36 mL, 4.5 mmol). The sulfur transfer step was carried out with PTP (126 mg, 0.495 mmol) and pyridine (0.18 mL, 2.25 mmol) The title compound was purified on a short silica gel column neutralized with triethylamine using DCM-MeOH as the eluent (gradient: 100:0 – 97:3 v/v). The appropriate fractions were combined and concentrated under reduced pressure to yield **13a** as a white foam (0.388 g, 72%). HRMS calc. [M+Na] = 1220.3447. HRMS found [M+Na] = 1220.3405. ^{31}P-NMR δP ($CDCl_3$) 24.21, 25.31.

5′DMTrO-Um*p*(SPh)rU-OLev **14b**

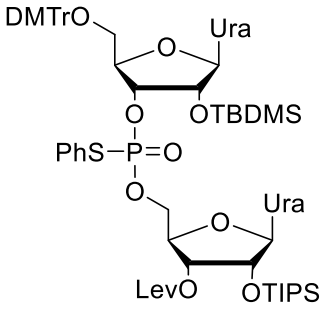

14b

This compound was prepared following general procedure **A from Chapter 2** using **10c** (0.409 g, 0.495 mmol), **13b** (0.224 g, 0.45 mmol), AdaCl (0.447 g, 2.25 mmol), and pyridine (0.36 mL, 4.5 mmol). The sulfur transfer step was carried out with PTP (126 mg, 0.495 mmol) and pyridine (0.18 mL, 2.25 mmol) The title compound was purified on a short silica gel column neutralized with triethylamine using DCM-MeOH as the eluent (gradient: 100:0 – 97:3 v/v). The appropriate fractions were combined and concentrated under reduced pressure to yield **14b** as a white foam (0.393 g, 66%). HRMS calc. [M+Na] = 1335.4799 HRMS found [M+Na] = 1335.4834. ^{31}P-NMR δP ($CDCl_3$) 23.43, 24.64.

Synthesis of CTP:

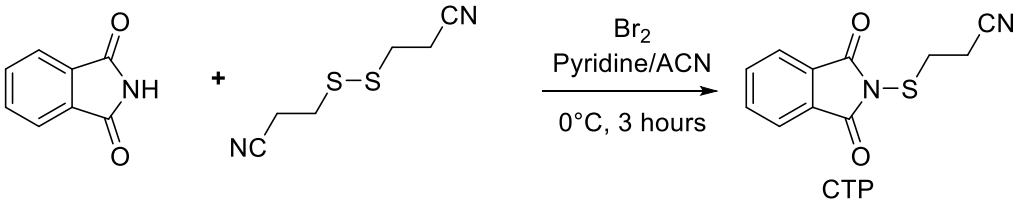

Phthalimide (6.28g, 33.9 mmol) and 3,3′-dithiobis(propionitrile) (3.08g, 17.4 mmol) were dissolved in pyridine (10 mL) and ACN (15 mL) and heated at 60°C with stirring until fully dissolved. Separately, bromine (1.03mL, 20.0 mmol) was dissolved in ACN (20 mL). Once both reagents were fully dissolved in the pyridine-ACN solution, the mixture was cooled to 0°C. The bromine solution was added dropwise over the course of 30 minutes while stirring. Water (60 mL) was added dropwise over the course of 30 minutes and the mixture was allowed to stir for a further 2 hours at 0°C[12]. The reaction was not complete and was allowed to warm to room temperature and stirred overnight for 18 hours. After this period, the solution was filtered and the precipitate was collected then recrystallized from ethanol to yield CTP (1.89g, 24%) as colorless needles[12]. HRMS calc: [M+Na] 255.0199. HRMS found: ESI+[M+Na] 255.0189. ^{1}H-NMR δH

(500 MHz, $CDCl_3$) 2.81 (t, 2H, J=7.5Hz, CH_2), 3.14 (t, 2H, J=7.3Hz), 7.84 (dd, 2H, J=2.3, 5.5Hz, Ar-H), 7.98 (dd, 2H, J=2.3, 5.5Hz, Ar-H). Major peaks remained at 7.79 (dd, 2H, J=2.4, 5.4Hz, Ar-H) and 7.90 (dd, 2H, J=2.3, 5.3Hz, Ar-H) for phthalimide in a ~1:1 ratio of other peaks, indicating approximately 50% purity.

Attempted synthesis of 16 with impure CTP:

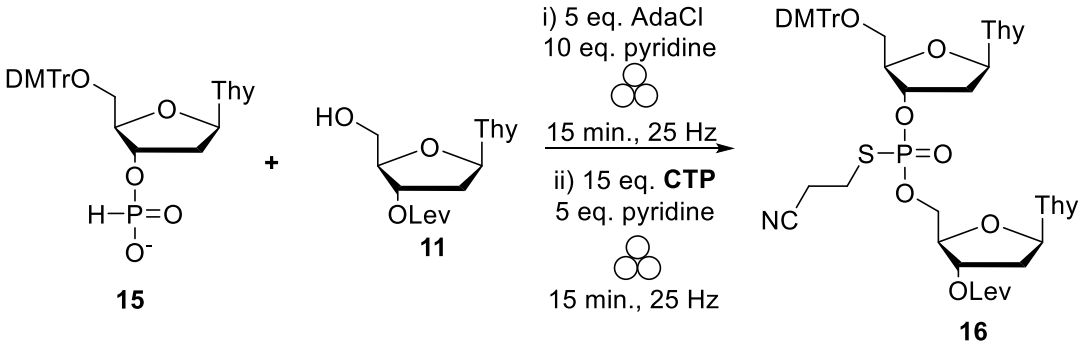

This compound was prepared following general procedure **A from Chapter 2** using **15** (0.351 g, 0.495 mmol), **11** (0.153 g, 0.45 mmol), AdaCl (0.447 g, 2.25 mmol), and pyridine (0.36 mL, 4.5 mmol). The sulfur transfer step was carried out with **CTP** (0.261 g, 1.125 mmol) and pyridine (0.18 mL, 2.25 mmol) The title compound was purified on a short silica gel column neutralized with triethylamine using DCM-MeOH as the eluent (gradient: 100:0 – 97:3 v/v). The appropriate fractions were combined and concentrated under reduced pressure to yield **16** as a white foam (0.174 g, 38%). HRMS calc. [M+Na] = 1038.2967 HRMS found [M+Na] = 1038.2978. ^{31}P-NMR δP ($CDCl_3$) 7.21, 8.55, 26.82, 27.26.

S-cyanoethyl 4-methylbenzenelthiosulfonate 20:

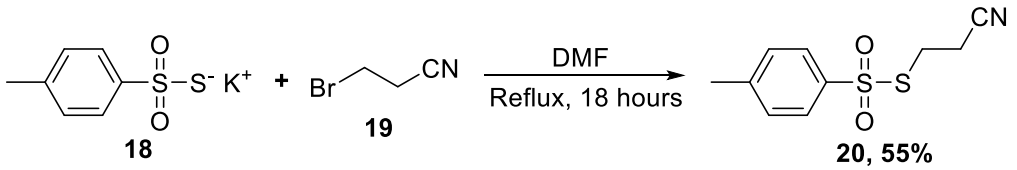

Compound **18** (2.00g, 4.42 mmol) was dissolved in dry DMF (10 mL) with stirring. Once fully dissolved, **19** (0.74 mL, 4.42 mmol) was added and the reaction was allowed to stir over night for 18 hours at 50°C. Once complete by TLC analysis (EtOAc-hexanes, 50:50, v/v), the mixture was cooled to room temperature and diluted with EtOAc (50 mL) and partitioned with H_2O (50 mL). The organic layer was washed with H_2O (4x50mL), dried over sodium sulfate, and concentrated under reduced pressure. The crude residue was purified on a short silica gel column using EtOAc-hexanes as the eluent (gradient: 20:80 – 60:40 v/v). The appropriate fractions were

combined and concentrated under reduced pressure to yield **20** as a colorless oil (1.178 g, 55%) which was identical to literature. HRMS calc. [M+Na] = 264.0123 HRMS found [M+Na] = 264.0116. ^{1}H-NMR δH (500 MHz, $CDCl_3$) 2.50 (s, 3H, CH_3), 2.84, (t, 2H, J=7.0Hz, CH_2), 3.22 (t, 2H, J=7.1Hz), 7.41 (d, 2H, J=8.1Hz, Ar-H), 7.85 (d, 2H, J=8.3Hz, Ar-H). ^{13}C-NMR δC (500 MHz, $CDCl_3$) 18.65, 21.74, 30.91, 117.10, 127.17, 130.22, 141.12, 145.72.

Synthesis of 16 with 20:

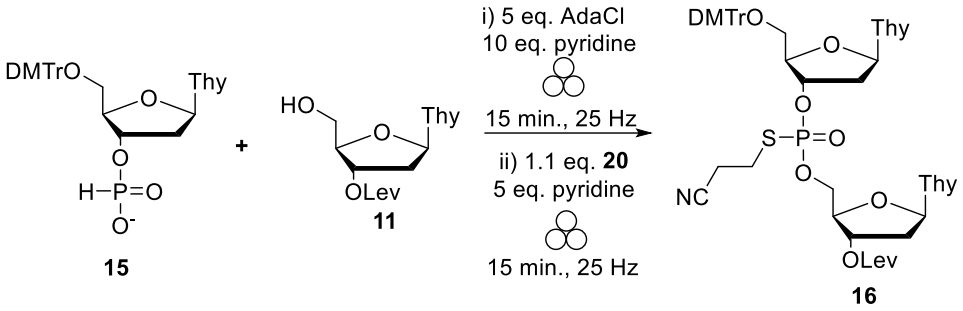

This compound was prepared following general procedure **A from Chapter 2** using **15** (0.351 g, 0.495 mmol), **11** (0.153 g, 0.45 mmol), AdaCl (0.447 g, 2.25 mmol), and pyridine (0.36 mL, 4.5 mmol). The sulfur transfer step was carried out by premixing **20** (0.119 g, 0.495 mmol) with pyridine (0.18 mL, 2.25 mmol) then adding it to the reaction vessel. The title compound was purified on a short silica gel column neutralized with triethylamine using DCM-MeOH as the eluent (gradient: 100:0 – 97:3 v/v). The appropriate fractions were combined and concentrated under reduced pressure to yield **16** as a white foam (0.283g, 62%). HRMS calc. [M+Na] = 1038.2967 HRMS found [M+Na] = 1038.3003. ^{31}P-NMR δP ($CDCl_3$) 26.57, 26.63.

3.5: References:

(1) Reese, C. B. Oligo-and poly-nucleotides: 50 years of chemical synthesis. *Organic & biomolecular chemistry* **2005**, *3* (21), 3851-3868.

(2) Andrews, B. I.; Antia, F. D.; Brueggemeier, S. B.; Diorazio, L. J.; Koenig, S. G.; Kopach, M. E.; Lee, H.; Olbrich, M.; Watson, A. L. Sustainability challenges and opportunities in oligonucleotide manufacturing. *The Journal of Organic Chemistry* **2020**, *86* (1), 49-61.

(3) Ohtsuka, E.; Khorana, H. Studies on Polynucleotides. LXVI. 1 The Synthesis of Deoxyribopolynucleotides Containing Repeating Tetranucleotide Sequences (3). A Further Study of the Synthetic Approach Involving Condensation of Preformed Oligonucleotide Blocks2. *Journal of the American Chemical Society* **1967**, *89* (9), 2195-2202.

(4) Zhou, X.; Kiesman, W. F.; Yan, W.; Jiang, H.; Antia, F. D.; Yang, J.; Fillon, Y. A.; Xiao, L.; Shi, X. Development of kilogram-scale convergent liquid-phase synthesis of oligonucleotides. *The Journal of Organic Chemistry* **2021**, *87* (4), 2087-2110.

(5) Reese, C. B.; Yan, H. Solution phase synthesis of ISIS 2922 (Vitravene) by the modified H-phosphonate approach. *Journal of the Chemical Society, Perkin Transactions 1* **2002**, (23), 2619-2633.

(6) Ono, A.; Matsuda, A.; Zhao, J.; Santi, D. V. The synthesis of blocked triplet-phosphoramidites and their use in mutagenesis. *Nucleic acids research* **1995**, *23* (22), 4677-4682.

(7) Hassler, M.; Wu, Y. Q.; Reddy, N. M.; Chan, T. H.; Damha, M. J. RNA synthesis via dimer and trimer phosphoramidite block coupling. *Tetrahedron letters* **2011**, *52* (20), 2575-2578.

(8) Khvorova, A.; Watts, J. K. The chemical evolution of oligonucleotide therapies of clinical utility. *Nature biotechnology* **2017**, *35* (3), 238-248.

(9) J. Stawinski, R. S. *Oligonucleotide Synthesis*; Humana Press, 2005.

(10) Thorpe, J. D.; O'Reilly, D.; Friščić, T.; Damha, M. J. Mechanochemical synthesis of short DNA fragments. *Chemistry–A European Journal* **2020**, *26* (41), 8857-8861.

(11) McKenzie, L. K.; El-Khoury, R.; Thorpe, J. D.; Damha, M. J.; Hollenstein, M. Recent progress in non-native nucleic acid modifications. *Chemical Society Reviews* **2021**, *50* (8), 5126-5164.

(12) Klose, J.; Reese, C. B.; Song, Q. Preparation of 2-(2-cyanoethyl) sulfanyl-1H-isoindole-1, 3-(2H)-dione and related sulfur-transfer agents. *Tetrahedron* **1997**, *53* (42), 14411-14416.

(13) Iwamoto, N.; Butler, D. C.; Svrzikapa, N.; Mohapatra, S.; Zlatev, I.; Sah, D. W.; Standley, S. M.; Lu, G.; Apponi, L. H.; Frank-Kamenetsky, M. Control of phosphorothioate stereochemistry substantially increases the efficacy of antisense oligonucleotides. *Nature biotechnology* **2017**, *35* (9), 845-851.
(14) Kraszewski, A.; Stawinski, J. H-Phosphonates: Versatile synthetic precursors to biologically active phosphorus compounds. *Pure and Applied Chemistry* **2007**, *79* (12), 2217-2227.

Chapter 4:

Next-generation oligonucleotide synthesis

"Dedication sees dreams come true."

- Kobe Bryant

4.1: Introduction

In recent years, researchers have turned to more novel technologies for oligonucleotide synthesis (see sections **1.5.5** and **1.5.6**). While SPOS has undoubtedly remained the most effective strategy for oligonucleotide synthesis, the adoption of soluble supports[1] for LPOS[2] has emerged as the next most popular strategy. However, the emergence of enzymes[3] for biocatalytic synthesis and other novel technologies such as organic solvent nanofiltration[4] for oligonucleotide synthesis have started to disrupt the industry. In this chapter, we will introduce two novel and distinct techniques for oligonucleotide synthesis. The first is the use of resonant acoustic mixing (RAM), a highly efficient mixing process, for oligonucleotide synthesis. The second is the development of a new process for synthesizing oligonucleotides on a polyethylene glycol (PEG) support using thermal control for carrying out and purifying reactions.

4.2: Resonant acoustic mixing

Resonant acoustic mixing (RAM) (**Figure 4.1A**) is a relatively new materials processing method that has mostly been used for high efficiency mixing, but has recently found some applications for co-crystal formation[5] and chemical synthesis[6]. Resonant acoustic mixers operate at the resonant frequency (58-62 Hz) of the entire system by constantly adjusting the frequency to specifically stay at the resonant condition. This unique approach allows for modification of the force imparted upon the mixture, usually measured in units of *g* (acceleration on Earth due to gravity), up to 100*g*. Additionally, this allows the system to maximize the amplitude while simultaneously minimizing the power consumption. Compared to other mixing technologies such as ultrasonic, paint shaker, or vibration ball mills (**Figures 4.1B-D**), RAM operates at an intermediate frequency, but with relatively large displacements and low power usage[7]. The unique conditions occurring at the resonant frequency of the system allow for highly efficient mixing by generating intense mixing zones with diameters of approximately 50 μm[8]. In contrast to VBM strategies, RAM mixing does not use any milling media (such as the balls used in VBM) and instead relies on the intense mixing zones. In principle, this allows for simpler scale up of

RAM processes than other mechanochemical processes and should have lower maintenance costs due to less wear-and-tear on the instruments[9].

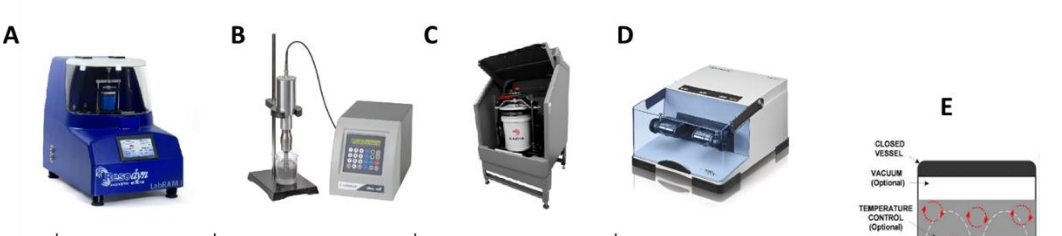

Instrument	*RAM*	*Ultrasonic*	*Paint Mixer*	*VBM*
Displacement (cm)	1.4	<<1	5-10 or more	1-2
Frequency (Hz)	58-62	25 000	10-15	15-30

Figure 4.1: *Different mixing instruments, parameters, and representation of mixing by RAM.* ***A:*** *RAM instrument.* ***B:*** *Ultrasonic mixer.* ***C:*** *Paint shaker.* ***D:*** *Vibrational ball mill.* ***E:*** *Representation of mixing zones generated during RAM*[8].

RAM has only recently been applied to conducting chemical reactions by the Friščić group starting with their use of liquid-assisted RAM (LA-RAM, analogous to LAG from of VBM) to synthesize metal-organic frameworks in 2020[10]. More recently, they applied RAM to metal-catalyzed organic reactions[9], polymorph control[11], redox reactions[6], and click reactions catalyzed by a copper spring[12]. To date, the Friščić group has been essentially the only one using RAM for chemical synthesis, with only one other publication to prepare lipid-based liquid-crystal nanoparticles[13]. As far as nucleic acid chemistry, there have been no reports using RAM for any kind of reactions. Given our previous success with VBM in **Chapters 2-3**, we set out to see if similar results could be produced using resonant acoustic mixing.

4.2.1: Optimization of reaction conditions

Having already optimized the reaction conditions once using VBM and determined the instability of H-phosphonate diesters already (**2.2.3**), we had a strong foundation for optimizing the conditions using RAM. To that end, we decided to test the reaction using similar conditions optimized for VBM. Rather than testing different frequencies as we did with VBM, we could vary the acceleration, *g*, but typical reactions are carried out at 60*g*. We also decided to try carrying out the coupling and sulfur-transfer reactions out in one step and later as a two-step process. Thus, we screened conditions for the coupling of **1a** with **2** to produce **3a** (**Scheme 4.1**) in the presence of different activators and equivalents, equivalents of pyridine, equivalents of

PTP, times, and accelerations (**Table 4.1**). As before, we monitored the reactions by analyzing the ^{31}P NMR spectra of crude products before any isolation (**Figure 4.3**).

We carried out the reactions using a commercially available LabRAM I instrument from Resodyn corporation (**Figure 4.2A**). This instrument is typically used with a large mixing vessel as shown with a capacity of up to 500 grams. Obviously, for our purposes this was much too large of a scale, and we had a custom-designed sample holder built that could hold up to 33 plastic or glass vials (**Figure 4.2B**). This allowed us to conduct smaller scale reactions and screen a wide range of conditions simultaneously.

Figure 4.2: *RAM instrumentation.* ***A:*** *Resodyn's LabRAM I instrument.* ***B:*** *Our custom-built sample holder compatible with the LabRAM I.*

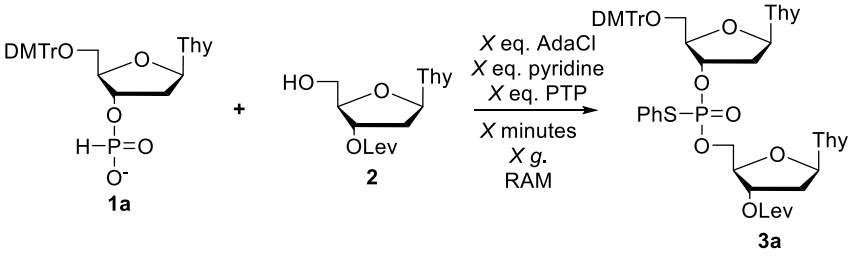

Scheme 4.1: *Optimization of H-phosphonate coupling and sulfur-transfer by RAM.*

Beginning with similar conditions optimized for VBM (**Chapter 2**), but attempting the sulfur-transfer step simultaneously to the coupling, we started with 5 eq. of AdaCl, 1.1 eq. of PTP, and 10 eq. of pyridine at 60*g* for 60 minutes (entry 1). The crude ^{31}P NMR displayed formation of the product (**Figure 4.3A**) around 24 ppm, but also formation of numerous side products. Reducing the equivalents of pyridine down from 10 to 5 (entry 2) resulted in less conversion to the desired product and 0 equivalents of pyridine led to almost no product formation (entry 3). Reducing the equivalents of AdaCl from 5 to 3 (entry 4, **Figure 4.3B**) while

maintaining 10 equivalents of pyridine led to a cleaner reaction. Five equivalents of pyridine led to a messier reaction (entry 5). Satisfied with the equivalents of the activator, we continued to optimize the equivalents of pyridine and PTP while also examining the effect of increasing *g*. Increasing *g* to 90 (entry 6) led to an almost identical spectrum as at 60*g* (entry 4), but we continued to test some conditions here. Increasing the equivalents of pyridine to 15 (entry 7) led to a much cleaner reaction. Increasing equivalents of PTP from 1.1 to 1.5 with 10 or 15 equivalents of pyridine (entries 8-9) led to formation of more side-products. Repeating the reaction with 1.1 eq. of PTP and 15 eq. of pyridine at 60*g* (entry 10, **Figure 4.3C**) resulted in an almost identical reaction as at 90*g* (entry 7), with minor impurities around -2 ppm and a larger impurity at 15 ppm. Satisfied now with the equivalents of all reagents, we set out to determine if the formation of side-products could be controlled by reaction time. At this point we decided to split up the coupling and sulfur-transfer steps as described in **Chapter 2**. Performing coupling and sulfur-transfer for 30 minutes each (entry 11) reduced the formation of the impurity at 15 ppm, but not completely. Reducing the reaction times to 15 minutes each completely suppressed the formation of this side-product, with only minor impurities around -2 ppm (entry 12, **Figure 4.3D**). Reducing the reaction times further to 5 minutes each led to incomplete sulfur-transfer, evidenced by peaks around 7-9 ppm for H-phosphonate diester (entry 13). Finally, we also wanted to try PvCl as another coupling reagent and to determine when the minor impurities around -2 and -6 ppm were forming. We conducted the coupling step with PvCl for 15 minutes (entry 14) and took a sample of the reaction mixture and analyzed the ^{31}P NMR (**Figure 4.3E**) which showed two minor peaks around -2.5 ppm and H-phosphonate diester at 7-9 ppm. We then performed the sulfur-transfer step with PTP for 5 minutes and analyzed the ^{31}P NMR again (**Figure 4.3F**). The H-phosphonate diester peaks were completely gone and the peaks for phosphorothioate triester **3a** were the major product at 24 ppm. However, the peaks at -2 ppm remained and some new minor peaks emerged at -7 ppm. Nonetheless, the crude reaction product was relatively clean and we were satisfied with the optimized conditions.

Entry	*Eq. AdaCl*	*Eq. PTP*	*Eq. pyr.*	*Time (min)*	*g*	*^{31}P NMR shift (ppm)*
1	5	1.1	10	60	60	-6.42, -5.82, -2.77, -2.58, -2.44, 6.72, 7.17, 8.61, 14.99, 15.10, 18.77, 19.09, **23.64, 23.86, 23.91, 23.94, 23.96, 24.05**
2	5	1.1	5	60	60	-6.26, -5.70, -1.49, -2.08, 7.16, 7.46, 8.57, 8.67, 15.32, 18.97, 19.34, **23.83, 24.00, 24.14, 24.20**
3	5	1.1	0	60	60	1.89, 2.50, 6.31, 6.60, 6.78, 7.59, 7.73, 8.37, 8.82, 22.31, 22.74, 28.43, 28.89
4	3	1.1	10	60	60	-2.75, -2.54, 3.85, 6.73, 7.20, 8.63, 14.92, 15.04, 23.11, **23.71, 23.88, 24.00, 24.06, 24.35**
5	3	1.1	5	60	60	-6.28, -5.72, 7.12, 8.63, 15.34, 18.93, 19.03, 19.11, 19.28, 19.35, 19.41, 19.52, **23.71, 23.76, 23.95, 24.09, 24.15, 24.22**
6	3	1.1	10	60	90	-2.41, -2.37, -1.07, 6.71, 7.10, 8.60, 15.23, 15.36, 15.45, **23.90, 23.97**
7	3	1.1	15	60	90	-2.76, -2.55, -2.40, 14.87, 22.59, 22.75, 23.07, 23.09, **23.97, 24.02, 24.30**
8	3	1.5	10	60	90	-2.66, -2.41, 2.38, 15.34, 15.90, 18.99, 19.33, 22.82, 23.28, **23.82, 24.00, 24.12, 24.19, 24.31**
9	3	1.5	15	60	90	-2.75, -2.53, -2.40, 14.77, 14.90, 15.20, 18.76, 19.09, 22.61, 22.76, 23.08, 23.11, **23.72, 23.85**
10	3	1.1	15	60	60	-2.84, -2.64, -2.45, -1.57, 14.64, **23.56, 23.72**
11	3	1.1	15	30/30	60	-2.39, -1.38, 14.95, **23.78, 23.88**
12	3	1.1	15	15/15	60	-2.37, -1.25, **23.83, 23.91**
13	3	1.1	15	5/5	60	-2.37, -1.22, 7.15, 8.60, **23.85, 23.93**
14	3 (PvCl)	1.1	15	15/5	60	Before sulfur transfer: -2.73, -2.50, 7.07, 8.62 After sulfur transfer: -6.99, -6.59, -3.06, -2.91, **23.32, 23.52**

Table 4.1: *Optimization of H-phosphonate coupling and sulfur-transfer by RAM. All reactions carried out with 0.2mmol of **2** and the stoichiometry of all reagents are in relation to this. Peaks corresponding to the typical range of **3a** are in bold. Some very minor peaks not reported.*

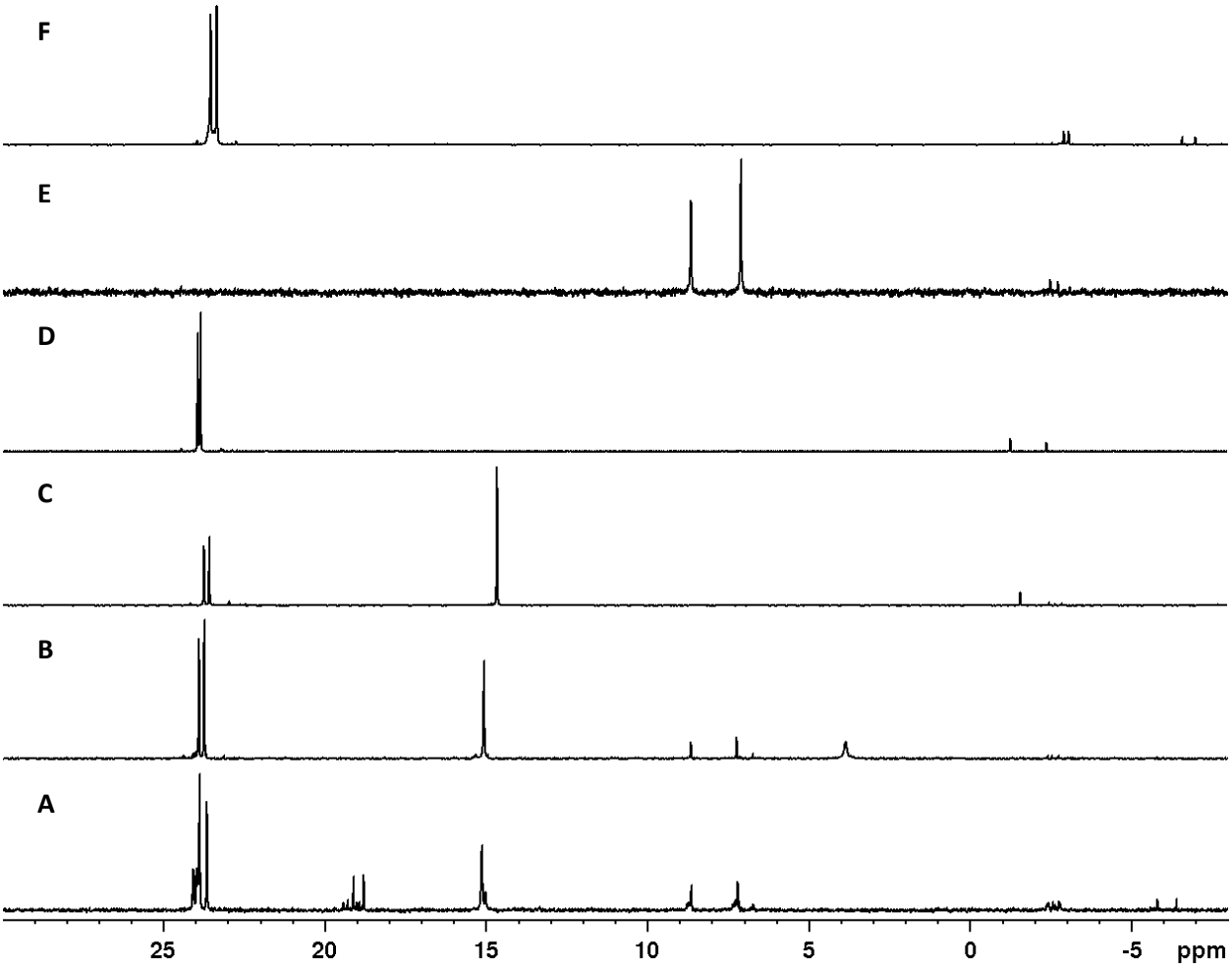

Figure 4.3: *^{31}P NMR spectra of select experiments from* ***Table 4.1****.* ***A:*** *Entry 1.* ***B:*** *Entry 4.* ***C:*** *Entry 10.* ***D:*** *Entry 12.* ***E:*** *Entry 14, before sulfur transfer.* ***F:*** *Entry 14, after sulfur transfer.*

4.2.2: Synthesis of dimers and trimers

Having established optimal conditions for coupling and sulfur-transfer of H-phosphonates by RAM, we set out to expand the strategy to other nucleobases and purify the products to assess the yield. Thus, we repeated the reaction with H-phosphonates **1a-d** and **2** to yield dimers **3a-d** in excellent yield (81-90%, **Scheme 4.2**). These yields corresponded to an average yield of over 90% per step for coupling followed by sulfur transfer which represents an improvement over VBM while using the same stoichiometry of pyridine and even reducing the equivalents of activator. Although AdaCl was effective as an activator as well, PvCl seemed to be more efficient, likely due to improved mixing when using a liquid under these conditions. The

products were analyzed by ^{31}P NMR (**Figure 4.4**) and HRMS and were identical to dimers previously prepared by VBM.

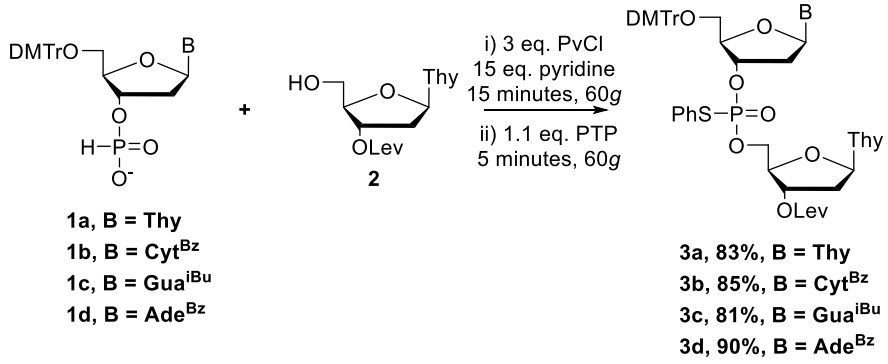

Scheme 4.2: *Optimized RAM conditions for H-phosphonate coupling and sulfur-transfer.*

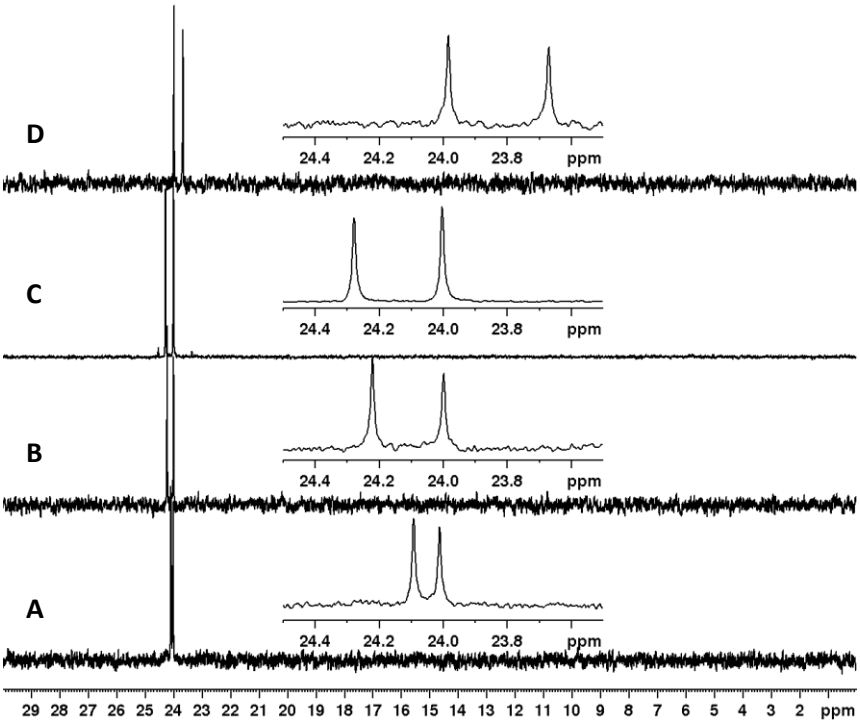

Figure 4.4: *^{31}P NMR ($CDCl_3$) spectra of dimers **3a-d** synthesized by RAM. **A: 3a. B: 3b. C: 3c. D: 3d.***

Although the reactions carried out above were limited by the size of the vials used in the same holder, we wanted to see if scaling up the reaction was possible. Although the mixing vessel provided with the LabRAM I was much too large for our purposes and likely would require upwards of 50 g of total material to be even partially full, we came up with a different way of using it (**Figure 4.5**). Additionally, the plastic jars provided were not chemically compatible with pyridine and other solvents used to take up the product before isolation. While not the most elegant design, when we scaled up the reaction from 0.2 mmol to 1 mmol using the

system shown in **Figure 4.5**, we found it be similarly efficient and dimer **3a** was isolated in 74% yield (**Scheme 4.3**). Even under these conditions, the vial used for the reaction was not close to full and we set out to further scale up the reaction. We doubled the scale of the reaction from 1 mmol to 2 mmol and synthesized dimer **3d** from **1d** and **2**. While the crude ^{31}P NMR spectra of the scaled-up reactions of **3a** and **3d** were extremely clean (**Figure 4.6**), the isolated yield was still slightly lower than the 0.2 mmol scale reactions. We did notice using the setup in **Figure 4.5** generated quite a bit of heat during the reaction, likely due to friction from the vibrating material inside the jar. While this did not seem to affect the reaction outcome much, it may explain the slightly lower yields observed.

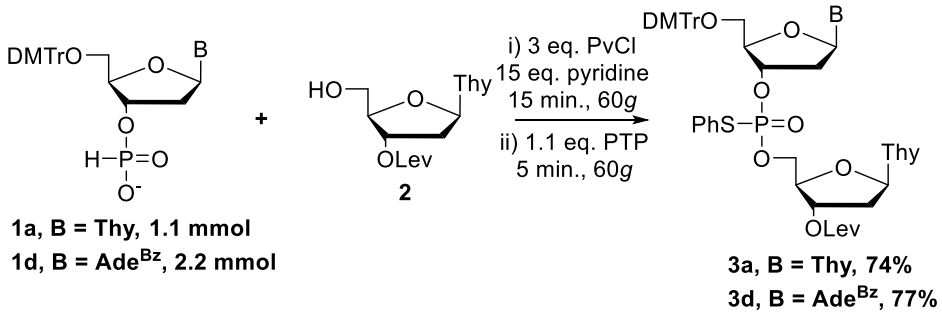

Scheme 4.3: *Scaling up of H-phosphonate coupling and sulfur-transfer by RAM.*

Figure 4.5: *Improvised set-up for scaling up RAM reactions from sub-mmol to mmol scales.* ***Left****: Reaction vial with* ***1a*** *and* ***2*** *on a 1 mmol scale:* ***Right****: Vial wrapped in packing material and placed in Resodyn jar.*

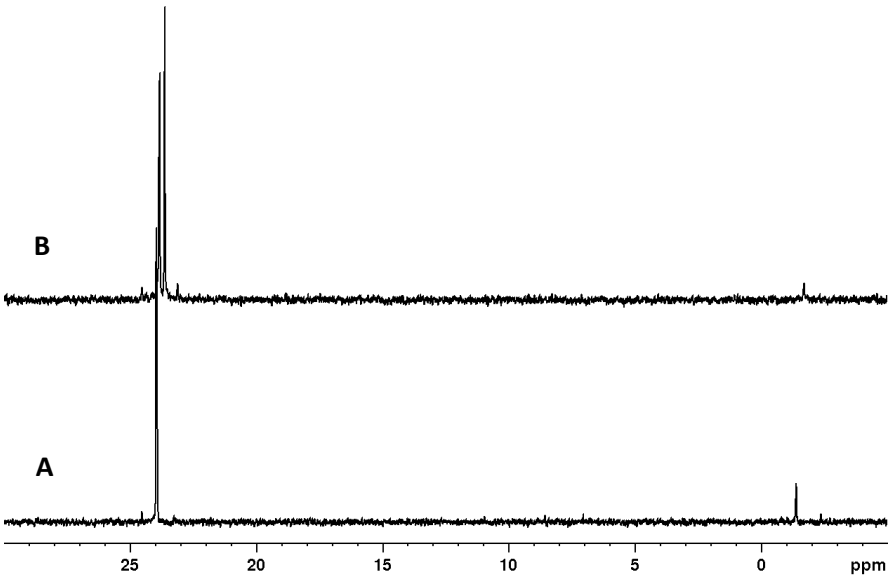

Figure 4.6: *Crude ^{31}P NMR spectra of scaled up RAM reactions.* ***A: 3a. B: 3d.***

Having scaled up the reaction successfully, we also set out to synthesize longer sequences. Dimer **3d** was detritylated with a solution of TFA in DCM to yield **4** in 87% yield (**Scheme 4.4**). Subsequent coupling of **4** with **1b** by RAM yielded mixed-base trimer **5** in good yield (79%). Analysis of the ^{31}P NMR spectrum of **5** (**Figure 4.7**) is consistent with the diastereomeric mixture expected for this compound. HRMS analysis confirmed the identity of **5**.

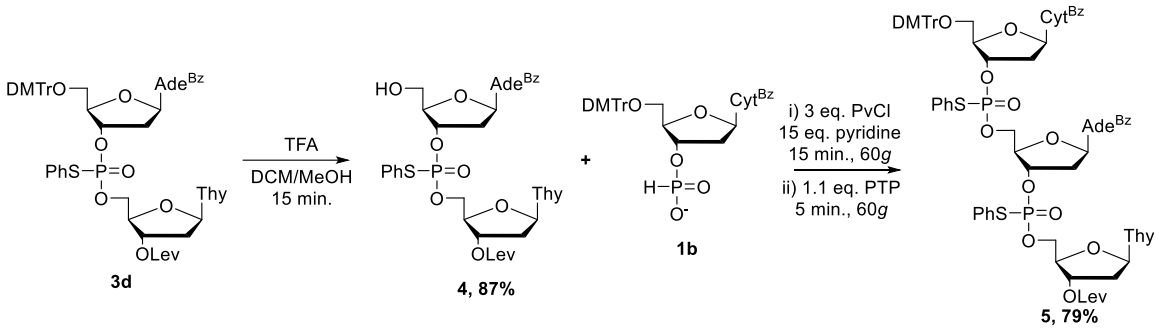

Scheme 4.4: *Synthesis of a nucleotide trimer by RAM.*

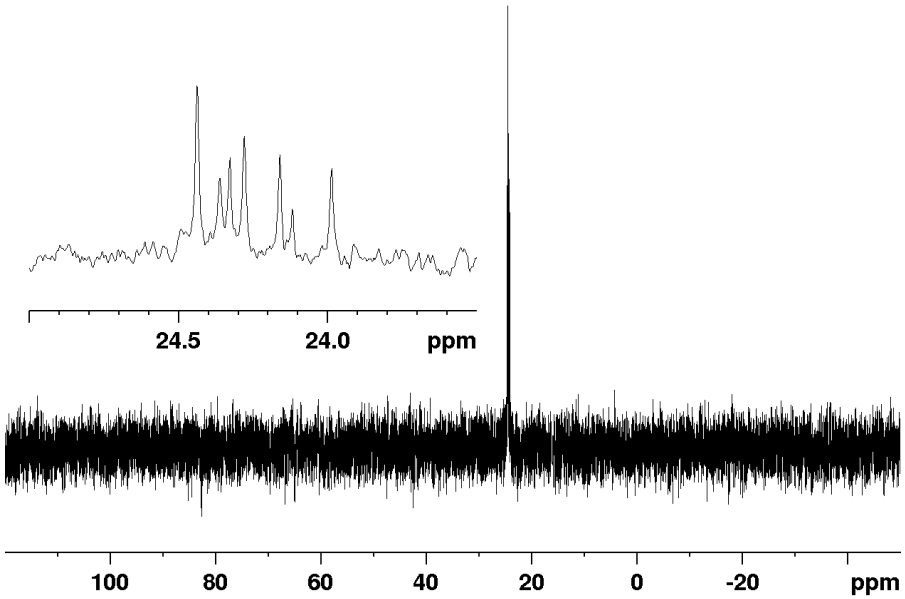

Figure 4.7: *^{31}P NMR of trimer **5** synthesized by RAM.*

4.3: Thermally controlled oligonucleotide synthesis (TCOS)

While our previous work using VBM and RAM significantly reduced solvent usage during reactions, we still had the issue of consuming large volumes of solvent during time-consuming purifications by column chromatography. Previous work both from our lab[14] and other researchers[1] have relied on soluble supports that typically allow for selective precipitation, extraction, crystallization, or filtration[4] of growing oligonucleotide chains[2]. However, there have been few accounts of feasible large-scale LPOS strategies often due to the large number of operational steps (usually at least two precipitations, extractions, or recrystallizations per step, see **1.5.6** for more details) which require manual labor and consume large volumes of solvent. Solubility of high MW oligonucleotides also becomes an issue and reaction concentration must be lowered which negatively affects the rate of reaction. Bearing these challenges in mind, we sought to develop a strategy for oligonucleotide that could be readily scaled up but avoided the two main issues of LPOS: the large number of operational steps and the large volume of solvent consumed during these steps. A schematic representation of our strategy is outlined in **Figure 4.8**, which we have termed thermally controlled oligonucleotide synthesis (TCOS). Using TCOS we envisioned taking advantage of the physical properties of a polymer, namely by conjugating a nucleoside to a polymer which could be then melted to establish a liquid-phase reaction. Addition of the next incoming nucleotide and any reagents required (activators, oxidizers etc.) in

a small amount of solvent comprises the chain extension phase. After the reaction is complete, the mixture can be simply cooled resulting in precipitation of the oligonucleotide-polymer, leaving any reagents in solution allowing the oligonucleotide to be purified by filtration. We identified a few key areas that would require special attention for this strategy to be viable: polymer choice, effects of an oligonucleotide on the melting temperature of the polymer, stability of the construct to repeated cycles of heating and cooling, and solvent choice such that the oligonucleotide-polymer construct remains insoluble at low temperatures.

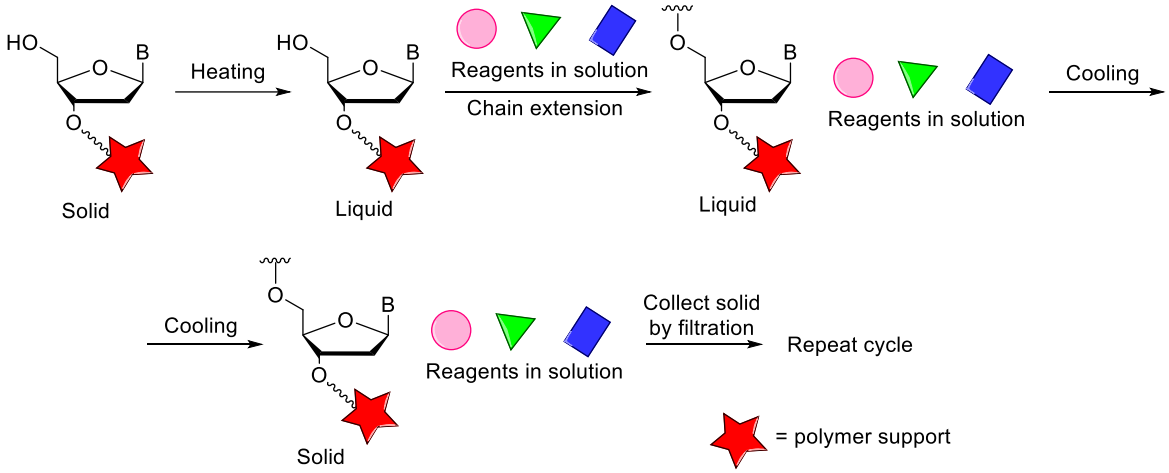

Figure 4.8: *Schematic representation of TCOS strategy.*

4.3.1: Synthesis and characterization of PEG monomer

We rapidly identified polyethylene glycol (PEG) as a potential candidate for our TCOS strategy for several reasons: PEG is non-toxic, cheap, well-studied, available in various MWs, compatible with oligonucleotide synthesis[15], and has a melting point that remains more or less constant once a certain MW has been reached (65-70°C). We eventually settled on methyl-capped PEG 5 000 (**7**, **Scheme 4.5**) as a starting point due to the previous work by Bonora and co-workers who used it in LPOS strategies[16]. Thus, **7** was functionalized with 5′-DMTr 3′-succinyl thymidine **6** (see **4.5.2** for synthesis of **6**) to yield PEG-nucleoside **8**, with a capping step to protect any free hydroxyl groups of **7**. We then evaluated the melting temperature of **8** and found it be very similar to that of unconjugated PEG **7**, with **8** being fully liquid at 75°C (**Figure 4.9**). We evaluated the yield of the coupling reaction and the loading by integration of the DMTr (ortho to OMe groups, ~6.8 ppm) peaks in the solvent-suppressed ^{1}H NMR spectrum as compared with the PEG OMe peak, where in a 100% reaction the ratio would be 4:3 (**Figure 4.10A**). We confirmed average yield of the reaction to be 92% which corresponds to a loading of

163 µM/g which is consistent with previous work (see **Figure 4.13** in section **4.5.2** for spectrum and calculations) [16]. Additionally, we set out to determine the stability of **8**, particularly the DMTr group, to multiple rounds of heating and cooling. After four successive rounds of heating to 75°C followed by cooling to 0°C we observed no evidence of degradation when examining the ^{1}H NMR spectrum of **8** (**Figure 4.11**). We attempted to analyze both **7** and **8** by MS and found that the envelope patterns observed from PEG made it difficult to determine extent of the reaction and thus NMR was used as the main tool for assessing reactions.

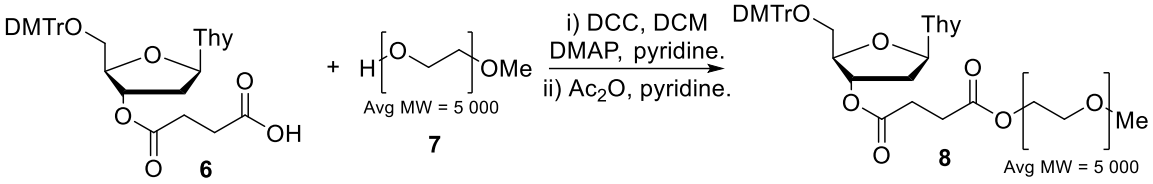

Scheme 4.5: *Functionalization of PEG with a 5'-DMTr-3'-succinyl nucleoside.*

Figure 4.9: *Compound **8** at room temperature (left) and 75°C (right).*

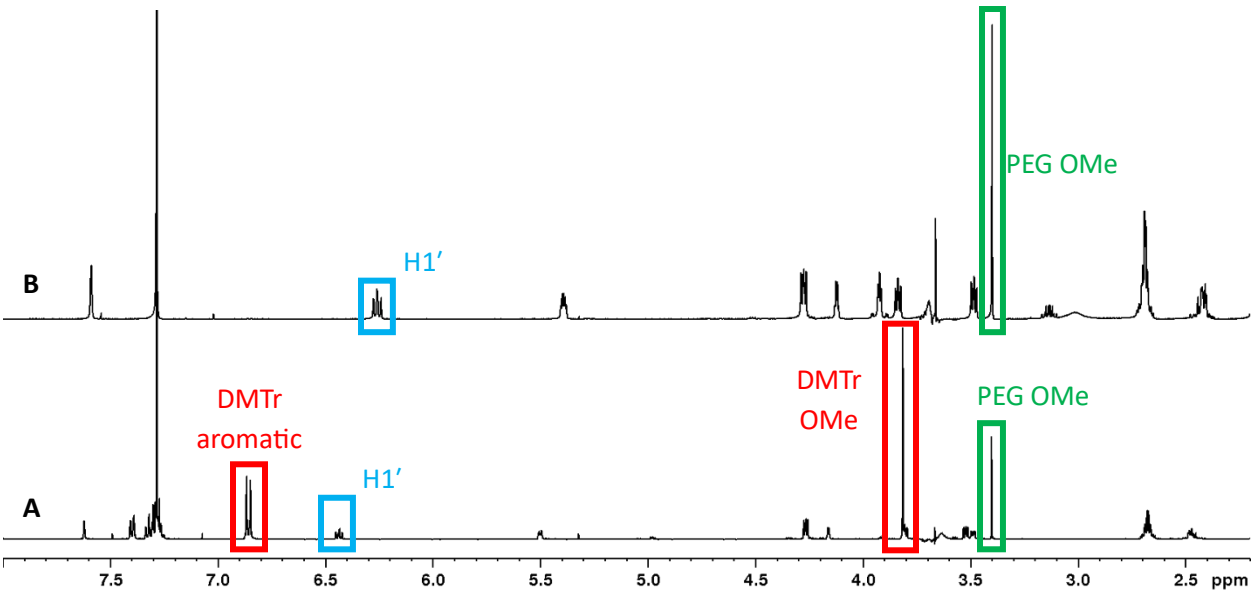

Figure 4.10: *Solvent suppressed ^{1}H NMR spectra of **A: 8**. **B**: **9** after thermally controlled detritylation of **8**.*

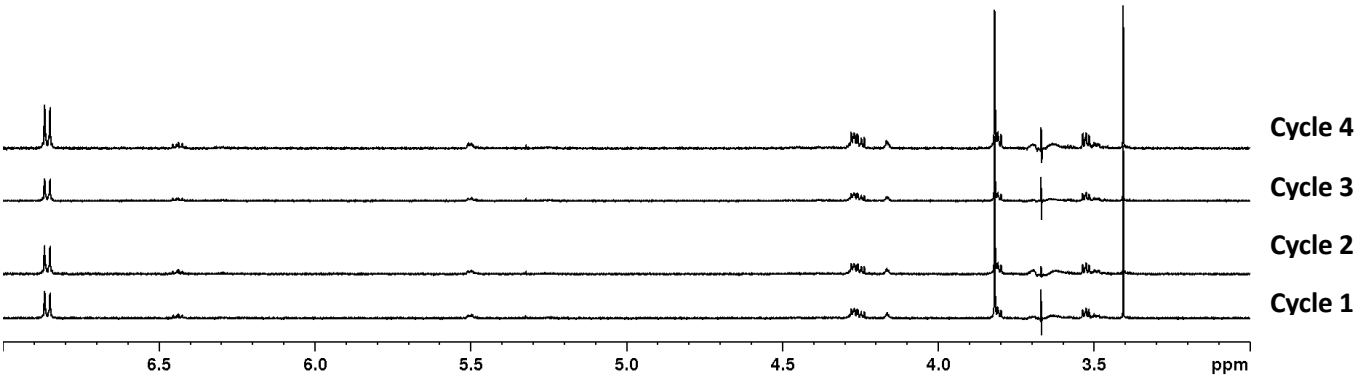

Figure 4.11: *^{1}H NMR spectra of **8** after multiple cycles of heating to 75°C followed by cooling to 0°C.*

4.3.2: Detritylation

Having established some baseline information on **8**, we set out to evaluate whether the first step of the synthesis cycle, detritylation, could be reproduced by TCOS. When melting **8**, we noted that while the compound was liquid, it was very viscous, and mixing was inefficient necessitating the addition of small amounts of solvent. After careful consideration, we settled on ethanol as the solvent of choice for the detritylation for two main reasons: 1) Bonora recrystallized PEG-oligonucleotides from ethanol and therefore at low temperatures **8** should be insoluble[16] and 2) the use of a scavenger for the trityl cation is necessary during LPOS and we anticipated ethanol could also fulfil this role[17]. Thus, **8** (**Scheme 4.6**) was melted at 75°C and a small amount of ethanol (~2 mL/g of **8**) was added to facilitate mixing. Once the mixture was

adequately mixed, 10 equivalents of trifluoroacetic acid (TFA) was added. The reaction was complete after 10 minutes by TLC (DCM-MeOH, 90:10, v/v, baseline **8** displayed no orange color after heating) and the mixture was removed from the heat and cooled to 0°C. Addition of another few milliliters of ethanol facilitated recrystallization. The solution was filtered and washed with cold ethanol and the solid was analyzed. Analysis of the ^{1}H NMR spectrum showed complete detritylation (**Figure 4.10B**, complete disappearance of DMTr OMe and aromatic peaks in red) and formation of **9**. Although previous reports required the use of additional DMTr cation scavengers (dodecanethiol[18], triethyl silane[17]), we found the excess ethanol was sufficient to push the reaction to completion. The average recovery after this step was 98% and analysis of wash and recrystallization solvents after filtration showed no evidence of **9**.

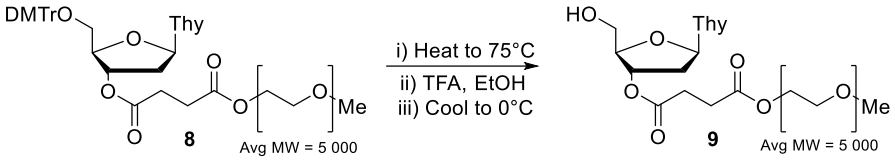

Scheme 4.6: *Detritylation and purification of **8** by thermal control.*

4.3.3: Coupling

Having a good understanding of H-phosphonate chemistry, we set out to use this chemistry to continue the synthesis cycle using TCOS. Although we showed in this chapter (**Table 4.1**, entry 3) and in previous chapters the necessity for pyridine during H-phosphonate coupling and sulfur-transfer, we found **9** to be soluble in pyridine even at low temperatures and would therefore be incompatible with TCOS. After studying the solubility of **9** further, we identified ethyl acetate and toluene as possible solvent additives for the coupling reaction. Initial efforts using ethyl acetate gave inconsistent results and we moved forward with toluene as the solvent of choice. Initial efforts using 4-dimethylamino-pyridine (DMAP) still resulted in detritylation which was due to incomplete dissolution of the base during the reaction. We settled on using a stoichiometric amount of pyridine during the reaction, which we expected would not be sufficient to solubilize **9** at low temperatures. Thus, we optimized the conditions for the H-phosphonate coupling by TCOS (**Scheme 4.7**) using 1.1 eq. of the incoming H-phosphonate **1a**, 3 eq. of pivaloyl chloride (PvCl), 5 eq. of pyridine, and a small amount of toluene (~2 mL/g of **9**) at 75°C. The same general procedure as **Scheme 4.6** was followed where **9** was fully melted at 75°C followed by addition of all other reagents (see experimental for details). After stirring for five minutes, 1.1 eq. of PTP was added and the mixture was stirred for five more minutes.

Addition of a small amount of ethanol to quench the reaction and facilitate recrystallization resulted in collection of solid **10** after cooling at 0°C, filtration, and washing with cold EtOH. ^{31}P NMR showed exclusive formation of the desired product (**Figure 4.12A**) and the yield was estimated to be 98% from ^{1}H NMR (see **Figure 4.15** in section **4.5.2** for spectrum and calculation) [16]. We also found this reaction proceeded efficiently in a flask exposed to air with no coevaporation required for drying as is often the case in other LPOS strategies.

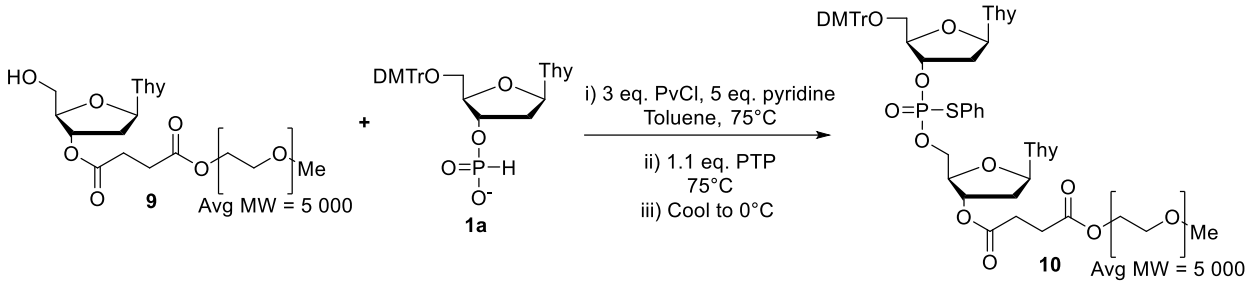

Scheme 4.7: *Nucleoside H-phosphonate coupling, sulfur-transfer, and purification by thermal control.*

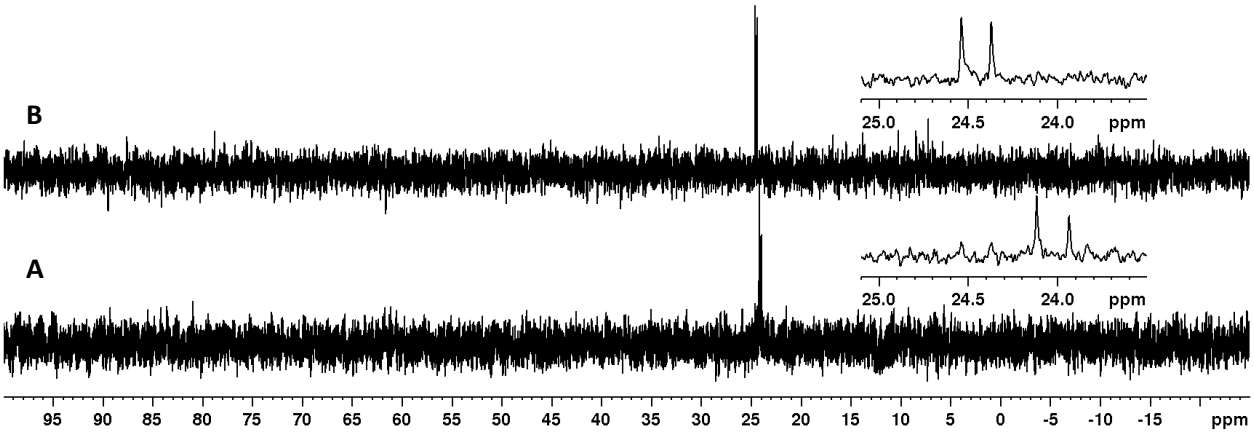

Figure 4.12: *^{31}P NMR spectra of 5'-DMTr dimer **10** (**A**) and 5'-OH dimer **11** (**B**).*

4.3.4: Cycle repetition

Detritylation of **10** was achieved in the same way as detritylation of monomer **8** to yield dimer **11**. Similarly, examination of the ^{1}H NMR (**Figure 4.14** in section **4.5.2**) indicated complete detritylation and a slight shift of the peaks in the ^{31}P NMR (**Figure 4.12B**) which was consistent with previous observations[19]. Detritylated dimer **11** was then subjected to the same coupling conditions as in **Scheme 4.7** to yield trimer **12** (**Scheme 4.8**). The coupling to yield **12** was estimated to be 91% by ^{1}H NMR (**Figure 4.16** in section **4.5.2**) and the ^{31}P NMR showed a complex splitting pattern consistent with formation of protected trimer diastereomers (**Figure 4.17** in section **4.5.2**). Although we did not observe the clean eight peaks expected for **12** as we

did with trimers previously (**Chapter 2** and compound **5** in section **4.2.2**), we were confident based on the ^{1}H NMR integrations and ^{31}P NMR that the trimer was formed.

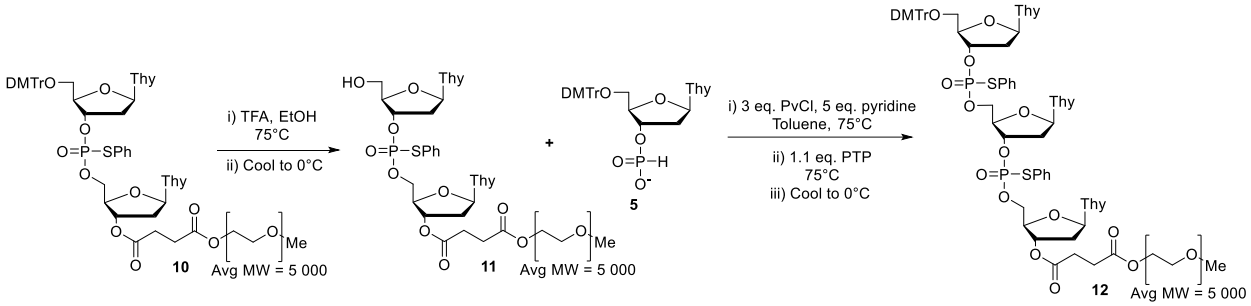

Scheme 4.8: *General synthesis cycle of TCOS consisting of detritylation and coupling used to synthesize trimer **12**.*

4.4: Conclusions and outlook

In this chapter, we demonstrated two novel "next-generation" methods for oligonucleotide synthesis. Our use of RAM to prepare short DNA fragments is the first for nucleic acid chemistry. We have demonstrated the use of RAM for synthesizing DNA dimers and trimers while reducing solvent use by up to 90% during reactions and have shown scalability up to the multi-gram scale. Scaling up was successful up to 10x the original scale with no immediate issues detected, besides heat generation which we have addressed. Further scaling of the RAM experiments seems to be straightforward with the proper equipment. We believe that RNA and modified RNA fragments will be compatible with RAM given our experience with VBM.

We have also developed TCOS - a new method for the synthesis and purification of short oligonucleotides on a PEG support by simple heating and cooling. As compared with other LPOS strategies, TCOS uses a minimal amount of solvent during the reaction itself since the melted oligonucleotide acts as a cosolvent and requires only small amount of solvents to achieve uniform mixing. Additionally, our method requires only a single cooling/recrystallization step with minimal amount of solvent used, and thus compares favorably to other LPOS strategies[2]. By our estimation, when directly comparing with Bonora's[15] PEG synthesis, we observe a reduction in solvent usage by up to 95% (**Chapter 5**) taking into account both carrying out the reaction and purification. While it is unclear how the melting temperature of PEG-oligonucleotides will be affected as the MW of the oligonucleotide becomes higher, we hypothesize that with additional optimization the strategy developed here can be applied to PEG of different MWs and potentially

other polymers or supports[1]. Additionally, given that the relatively low MW soluble supports used by Biogen[18] and Ajiphase[20] can control the solubility profile of oligonucleotide conjugates, it is reasonable to assume that the melting temperature of PEG-oligonucleotides may remain consistent even when the oligonucleotide grows longer. We envision TCOS will be amenable to traditional large scale batch reactors, or even twin-screw extruders where temperature at each point along the extruder can be precisely controlled[21].

4.5: Experimental

4.5.1: General information

Solvents such as pyridine, dichloromethane (DCM), ethanol (EtOH), methanol (MeOH), ethyl acetate (EtOAc) and toluene were purchased from Fisher Scientific or Sigma-Aldrich. Nucleosides and nucleotides were purchased from ChemGenes Corporation. All other chemicals (PEG, pivaloyl chloride, PTP, DCC, DBU, succinic anhydride, TFA, DMAP etc.) were purchased from Sigma-Aldrich, Fisher Scientific, or TCI. Pyridine used for reactions was dried using 5Å molecular sieves. Reactions that required heating were heated in an oil bath. RAM reactions were performed on a LabRAM I instrument from Resodyn. The custom-designed sample holder was made from Delrin Acetal Resin and RAM reactions were performed in 2.5mL polypropylene vials or 4mL clear glass vials. Both vials had dimensions of 15 mm x 45 mm x 8 mm (outer diameter, height, inner diameter, respectively). Thin-layer chromatography (TLC) was performed on 0.15-0.2 mm pre-coated silica gel (10-40 µm) plates using UV light and heat as visualizing agents. NMR spectra were recorded on a Bruker-500 MHz spectrometer and were calibrated using residual undeuterated solvent as an internal reference ($CDCl_3$ ^1H NMR δ = 7.26 ppm) and ^{31}P NMR spectra were measured from 85% H_3PO_4 as an external standard.

4.5.2: Experimental procedures

General procedure **A** for H-phosphonate coupling and sulfur-transfer using RAM:

To a plastic or glass vial was added **1** (1.1 eq.), **2** (1 eq.), pyridine (15 eq.) and PvCl (3 eq.) in that order. The vial was closed and allowed to react for 15 minutes at 60*g* on a RAM instrument. After the 15 minutes were up, the vial was opened and PTP (1.1 eq.) was added and the mixture was allowed to react by RAM for another 5 minutes at 60*g*. After the reaction was complete, the white slurry was taken up in DCM and concentrated. The resulting crude residue was purified on a short silica gel column neutralized with triethylamine using DCM-MeOH as the eluent (gradient: 100:0-97:3, v/v). The appropriate fractions were combined and concentrated under reduced pressure to yield fully protected phosphorothioate triester **3** as a white foam.

5′DMTrO-T*p*(SPh)T-OLev **3a**

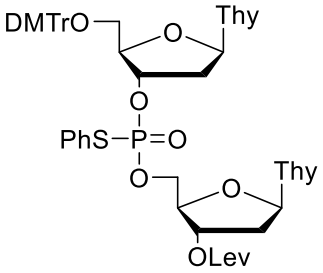

3a

This compound was prepared following general procedure **A** using **1a** (156 mg, 0.22 mmol), **2** (68 mg, 0.2 mmol), PvCl (74 µL, 0.6 mmol), and pyridine (0.24 mL, 3 mmol). The sulfur transfer step was carried out with PTP (56 mg, 0.22 mmol). The title compound was purified on a short silica gel column neutralized with triethylamine using DCM-MeOH as the eluent (gradient: 100:0 – 97:3 v/v). The appropriate fractions were combined and concentrated under reduced pressure to yield **3a** as a white foam (172 mg, 83%). HRMS calc. [M+Na] = 1061.3014. HRMS found [M+Na] = 1061.3044. ^{31}P-NMR δP ($CDCl_3$) 24.01, 24.09.

5′DMTrO-C*p*(SPh)T-OLev **3b**

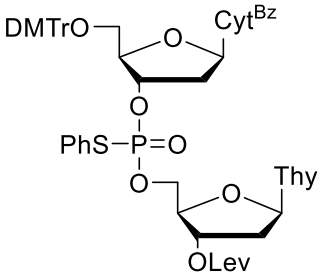

3b

This compound was prepared following general procedure **A** using **1b** (176 mg, 0.22 mmol), **2** (68 mg, 0.2 mmol), PvCl (74 µL, 0.6 mmol), and pyridine (0.24 mL, 3 mmol). The sulfur transfer step was carried out with PTP (56 mg, 0.22 mmol). The title compound was purified on a short silica gel column neutralized with triethylamine using DCM-MeOH as the eluent (gradient: 100:0 – 97:3 v/v). The appropriate fractions were combined and concentrated under reduced pressure to yield **3b** as a white foam (192 mg, 85%). HRMS calc. [M+Na] = 1150.3280. HRMS found [M+Na] = 1150.3301. ^{31}P-NMR δP ($CDCl_3$) 24.00, 24.22.

5′DMTrO-G*p*(SPh)T-OLev **3c**

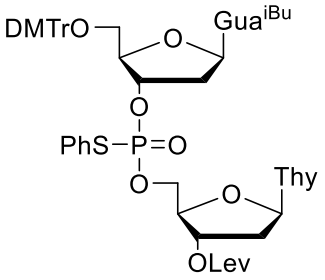

3c

This compound was prepared following general procedure **A** using **1c** (177 mg, 0.22 mmol), **2** (68 mg, 0.2 mmol), PvCl (74 µL, 0.6 mmol), and pyridine (0.24 mL, 3 mmol). The sulfur transfer step was carried out with PTP (56 mg, 0.22 mmol). The title compound was purified on a short silica gel column neutralized with triethylamine using DCM-MeOH as the eluent (gradient: 100:0 – 97:3 v/v). The appropriate fractions were combined and concentrated under reduced pressure to yield **3c** as a white foam (184 mg, 81%). HRMS calc. [M+Na] = 1156.3498. HRMS found [M+Na] = 1156.3542. ^{31}P-NMR δP ($CDCl_3$) 24.00, 24.28.

5′DMTrO-A*p*(SPh)T-OLev **3d**

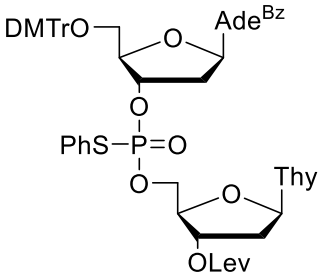

3d

This compound was prepared following general procedure **A** using **1d** (181 mg, 0.22 mmol), **2** (68 mg, 0.2 mmol), PvCl (74 µL, 0.6 mmol), and pyridine (0.24 mL, 3 mmol). The sulfur transfer step was carried out with PTP (56 mg, 0.22 mmol). The title compound was purified on a short silica gel column neutralized with triethylamine using DCM-MeOH as the eluent (gradient: 100:0 – 97:3 v/v). The appropriate fractions were combined and concentrated under reduced pressure to yield **3d** as a white foam (207 mg, 90%). HRMS calc. [M+Na] = 1174.3392. HRMS found [M+Na] = 1174.3418. ^{31}P-NMR δP ($CDCl_3$) 23.68, 23.93.

Scale up to 1 mmol of dimer synthesis of 3a by RAM

This compound was prepared following general procedure **A** except using a large glass vial as in **Figure 4.5** using **1a** (0.78 g, 1.1 mmol), **2** (0.34 g, 1 mmol), PvCl (0.37 mL, 3 mmol), and

pyridine (1.2 mL, 15 mmol). The sulfur transfer step was carried out with PTP (0.28 g, 1.1 mmol). The title compound was purified on a short silica gel column neutralized with triethylamine using DCM-MeOH as the eluent (gradient: 100:0 – 97:3 v/v). The appropriate fractions were combined and concentrated under reduced pressure to yield **3a** as a white foam (0.77 g, 74%). ^{31}P-NMR δP ($CDCl_3$) 24.02, 24.07. This product was not analyzed by HRMS, but was identical as previous samples of **3a** by ^{31}P NMR and by TLC analysis (DCM-MeOH, 95:5).

Scale up to 2 mmol of dimer synthesis of 3d by RAM

This compound was prepared following general procedure **A** except using a large glass vial as in **Figure 4.5** using **1a** (1.81 g, 2.2 mmol), **2** (0.68 g, 2 mmol), PvCl (0.74 mL, 6 mmol), and pyridine (2.4 mL, 30 mmol). The sulfur transfer step was carried out with PTP (0.56 g, 2.2 mmol). The title compound was purified on a short silica gel column neutralized with triethylamine using DCM-MeOH as the eluent (gradient: 100:0 – 97:3 v/v). The appropriate fractions were combined and concentrated under reduced pressure to yield **3d** as a white foam (1.75g, 76%). ^{31}P-NMR δP ($CDCl_3$) 23.67, 23.97. This product was not analyzed by HRMS, but was identical as previous samples of **3d** by ^{31}P NMR and by TLC analysis (DCM-MeOH, 95:5, v/v).

Detritylation of dimer 3d to synthesize 4:

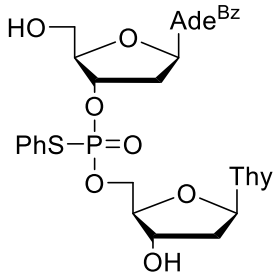

4

This compound (**4**) was prepared by dissolving **3d** (1.75 g, 1.52 mmol) in DCM (50 mL) followed by addition of TFA (2.3 mL, 30.4 mmol) while stirring at room temperature. The solution turned dark orange and methanol was added until the solution was a clear light orange color. Once the reaction was complete by TLC (DCM-MeOH, 95:5, v/v) after approximately 15 minutes, the solution was carefully poured into a saturated aqueous $NaHCO_3$ solution (50 mL). The organic layer was washed once more with saturated aqueous $NaHCO_3$ (50 mL) and the aqueous layers were back-extracted with DCM. The combined organic layers were dried over

Na_2SO_4 and concentrated under reduced pressure. The resulting residue was taken up in DCM and purified on a short silica gel column using DCM-MeOH as the eluent (gradient: 99:1 – 95:5, v/v). The appropriate fractions were combined and concentrated under reduced pressure to yield **5** as a white foam (1.12 g, 87%). HRMS calc. [M+H] = 850.2266. HRMS found [M+H] = 850.2250. ^{31}P-NMR δP ($CDCl_3$) 23.61, 24.1.

Synthesis of trimer 5 by RAM:

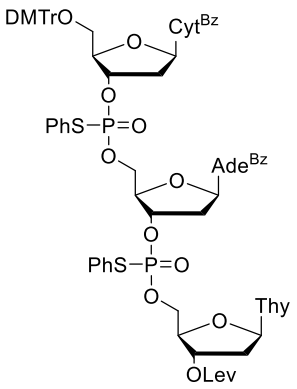

5

This compound was prepared following general procedure **A** using **4** (0.170 mg, 0.2 mmol), **1a** (176 mg, 0.22 mmol), PvCl (74 µL, 0.6 mmol), and pyridine (0.24 mL, 3 mmol). The sulfur transfer step was carried out with PTP (56 mg, 0.22 mmol). The title compound was purified on a short silica gel column neutralized with triethylamine using DCM-MeOH as the eluent (gradient: 100:0 – 97:3 v/v). The appropriate fractions were combined and concentrated under reduced pressure to yield **5** as a white foam (259 mg, 79%). HRMS calc. [M+Na] = 1659.4203. HRMS found [M+Na] = 1659.4222. ^{31}P-NMR δP ($CDCl_3$) 23.99, 24.12, 24.16, 24.28, 24.33, 24.36, 24.44.

Synthesis of 5′DMTr-3′succinyl thymidine 6

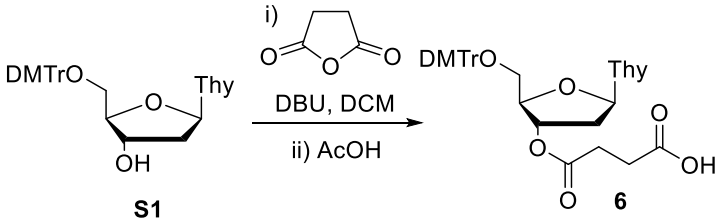

S1 **6**

5′DMTr thymidine **S1** (5.00g, 9.18mmol) and succinic anhydride (1.38g, 13.8 mmol) were dissolved in 100mL of DCM. While stirring at room temperature, 1,8-diazabicyclo[5.4.0]undec-7-ene (DBU, 1.37 mL, 9.18 mmol) was added in one portion and the mixture was allowed to react for 2 hours. Once the reaction was complete by TLC (DCM-MeOH, 95:5 v/v), acetic acid

(1.05mL, 18.36 mmol) was added and the mixture was stirred for 10 minutes. The reaction mixture was washed with water (3x50 mL) and the organic layers were dried over sodium sulfate and concentrated under reduced pressure to yield **6** as a white foam (5.84g, 99%). The compound was used without any further purification. ^{1}H-NMR δ_H ($CDCl_3$) 1.39 (s, 3H, thymidine methyl), 2.42 (m, 1H, H2′), 2.51 (m, 1H, H2′), 2.68 (m, 4H, succinyl methylene), 3.81 (s, 6H, DMTr-OMe), 4.19 (m, 1H, H3′), 5.48 (m, 1H, H4′), 6.42 (dd, 1H, H1′), 6.86 (m, 4H, DMTr H), 7.18-7.34 (m, 9H, DMTr-H), 7.64 (s, 1H, H6).

Conjugation of PEG to 6

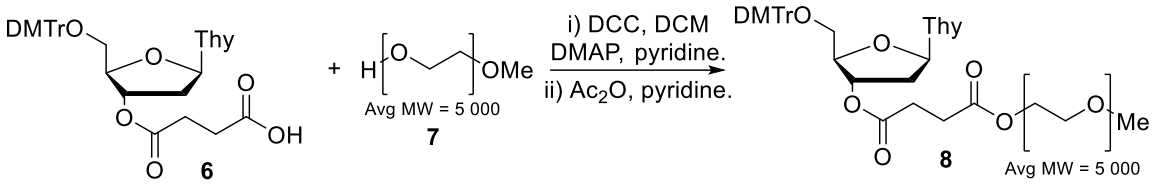

6 (5.84g, 9.06 mmol) and DCC (1.87g, 9.06 mmol) were dissolved in 100mL of DCM containing 0.5% pyridine at 0°C. The mixture was stirred for 15 minutes then any precipitated DCU was filtered off. The mixture containing the nucleoside anhydride was added to a solution of PEG **7** (15.1g, 3.02 mmol) in 100mL of DCM and DMAP (1.11g, 9.06 mmol) was added. The reaction volume was concentrated under reduced pressure to approximately 1/3 of the original volume then the mixture was allowed to stir for three days at room temperature. Once the reaction was complete, any further DCU was filtered off and the reaction mixture was concentrated under reduced pressure. The residue was dissolved in 150mL of pyridine containing 10% by volume acetic anhydride (1mL of Ac_2O/g of PEG) and allowed to react for 1 hour in order to cap any unreacted hydroxyl groups of PEG. Once complete, the reaction mixture was concentrated under reduced pressure and the crude residue was dissolved in a minimal amount of DCM and cooled to 0°C. While stirring, diethyl ether was added (~500mL) and the mixture was filtered and the solid was collected. The white solid was then recrystallized from ethanol to yield **8** as an amorphous white solid (16.18g, 95% recovery).

$$\%\ \text{loading} = \frac{\text{Integration of DMTr H}}{(\text{Integration of PEG OMe}) * \frac{4}{3}} * 100\% = \frac{4.00 * 3}{3.26 * 4} * 100\% = 92\% = 163\mu\text{M/g}$$

The loading was converted to µM/g by taking into account the increased average molecular weight of **8** as compared with **7**, resulting in a lower loading in µM/g corresponding to a 100% yield[16]. The integrations used are below.

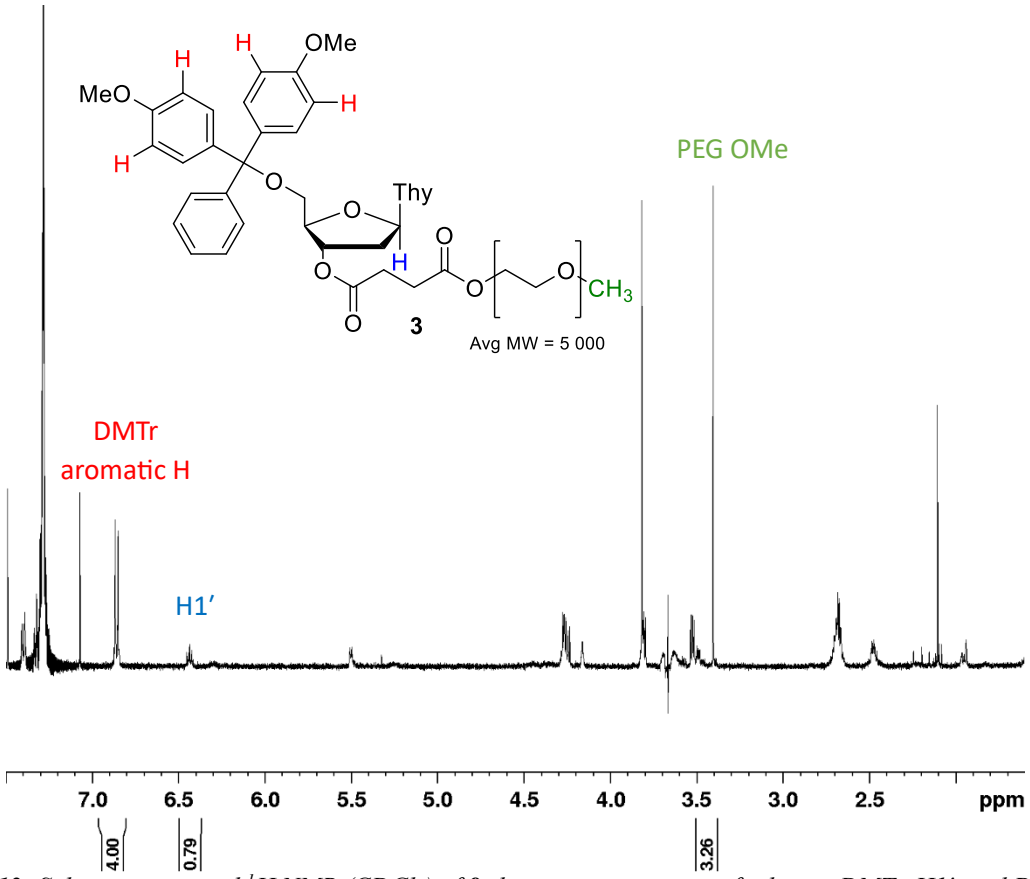

***Figure 4.13**: Solvent suppressed ^1H NMR ($CDCl_3$) of **8** showing integrations of relevant DMTr, H1', and PEG OMe peaks. Calculation for loading above.*

Thermal detritylation of 8

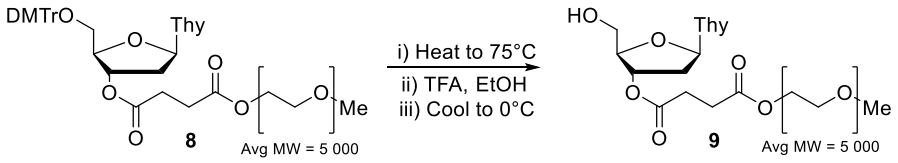

8 (1.0g, 0.177 mmol) was heated to 75°C until fully melted. Approximately 2mL of ethanol was added to the viscous **8** and allowed to heat until the mixture was homogeneous and mixing consistently. TFA (0.14mL, 1.77 mmol) was added and the mixture turned bright orange and allowed to stir for 10 minutes. Another portion of 3mL of ethanol was added to the reaction mixture which reduced the orange color and it was removed from the heat and cooled to 0°C. After 15 minutes, the mixture was filtered and washed with 10mL of cold ethanol yielding 8 as a

white solid (0.94g, 98% recovery). It should be noted that occasionally **9** maintained a faint orange color after the reaction, but complete detritylation was still observed. Previous work has indicated that the orange color may persist even after full detritylation has occured[17].

Thermal coupling of 9 with 1a

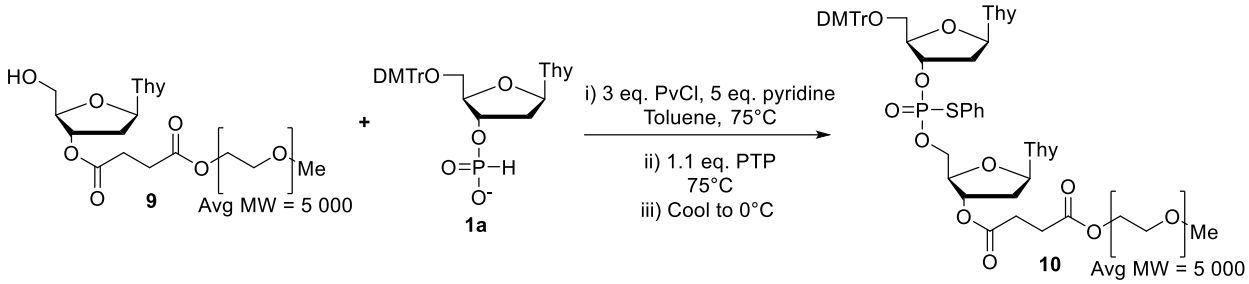

9 (1.0g, 0.188 mmol) was heated to 75°C until fully melted. Approximately 2mL of toluene was added to the viscous **9** and allowed to heat until the mixture was homogeneous and mixing consistently. Pyridine (75µL, 0.939 mmol) and **1a** (0.147g, 0.207 mmol) were added to the mixture followed by addition of pivaloyl chloride (70µL, 0.563 mmol). The reaction was stirred for 5 minutes at which point *N*-phenylthiophthalimide (PTP, 53mg, 0.207 mmol) was added and the reaction was stirred for another period of 5 minutes. Approximately 3mL of ethanol was added to the reaction mixture and it was removed from the heat and cooled to 0°C. After 15 minutes, the mixture was filtered and washed with 10mL of cold ethanol yielding **10** as a white solid (1.06g, 92% recovery).

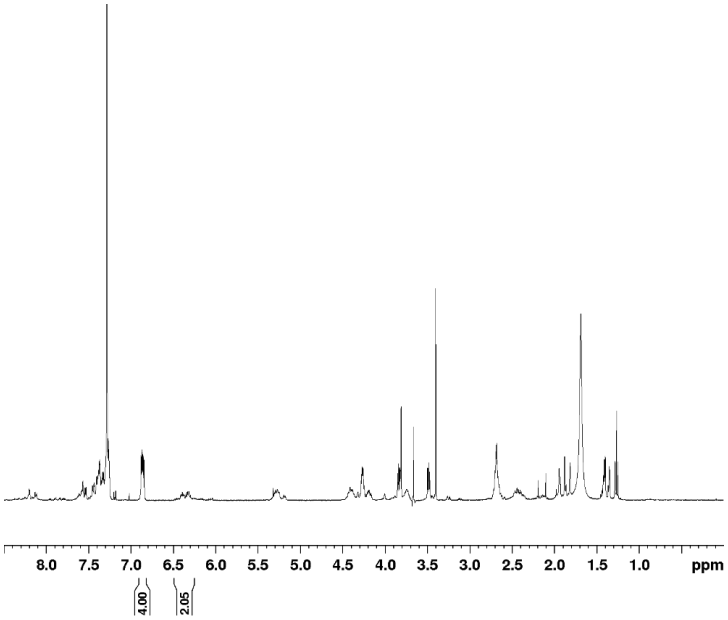

Figure 4.14: *^{1}H NMR spectrum ($CDCl_3$) of dimer **10**. Integrals of DMTr and H1' protons are shown. Coupling yield is assessed by comparing the ratios of these peaks where the ratio is 4:n where n is the number of nucleosides[16]. Calculation is shown below.*

$$\% \text{ yield} = \frac{\text{Integration of DMTr H}}{\text{Integration of H1}'*2} * 100\% = \frac{4.00}{2.05*2} * 100\% = 98\%$$

Thermal detritylation of 10

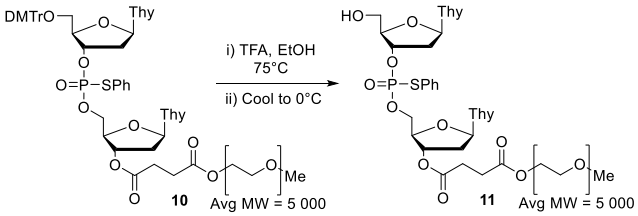

10 (1.0g, 0.163 mmol) was heated to 75°C until fully melted. Approximately 2mL of ethanol was added to the viscous **10** and allowed to heat until the mixture was homogeneous and mixing consistently. TFA (0.125 mL, 1.63 mmol) was added and the mixture turned bright orange and allowed to stir for 10 minutes. Another portion of 3mL of ethanol was added to the reaction mixture and it was removed from the heat and cooled to 0°C. After 15 minutes, the mixture was filtered and washed with 10mL of cold ethanol yielding **11** as a white solid (0.89g, 93% recovery). It should be noted that occasionally **11** maintained a faint orange color after the reaction, but complete detritylation was still observed. Previous work has indicated that the orange color may persist even after full detritylation has occured[17].

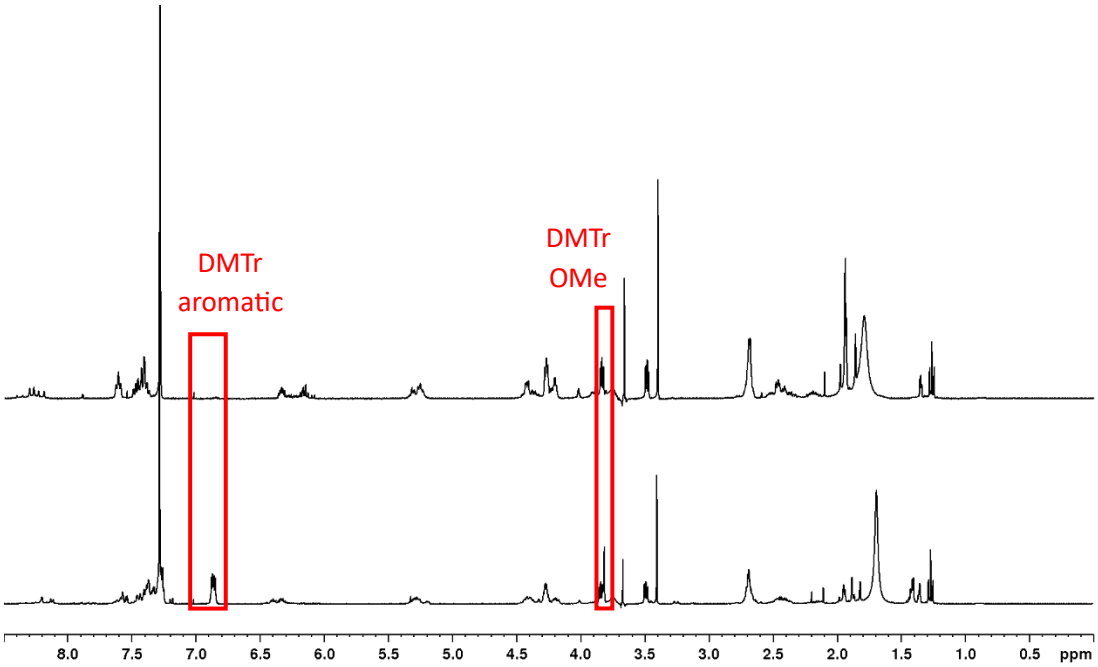

Figure 4.15: *^{1}H NMR spectra ($CDCl_3$) of dimers **10** (bottom) and **11** (top) showing complete removal of the DMTr protecting group. Relevant peaks are highlighted.*

Thermal coupling of 11 with 1a

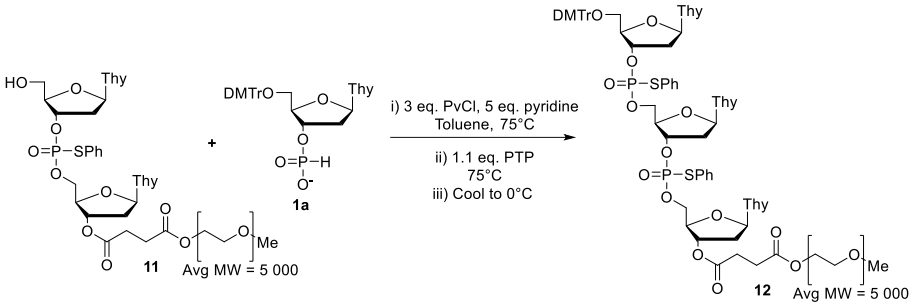

11 (1.0g, 0.171 mmol) was heated to 75°C until fully melted. Approximately 2mL of toluene was added to the viscous **11** and allowed to heat until the mixture was homogeneous and mixing consistently. Pyridine (68µL, 0.856 mmol) and **1a** (0.133g, 0.188 mmol) were added to the mixture followed by addition of pivaloyl chloride (63µL, 0.5s14 mmol). The reaction was stirred for 5 minutes at which point *N*-phenylthiophthalimide (PTP, 48mg, 0.188 mmol) was added and the reaction was stirred for another period of 5 minutes. Approximately 3mL of ethanol was added to the reaction mixture and it was removed from the heat and cooled to 0°C. After 15 minutes, the mixture was filtered and washed with 10mL of cold ethanol yielding **12** as a white solid (1.07g, 94% recovery).

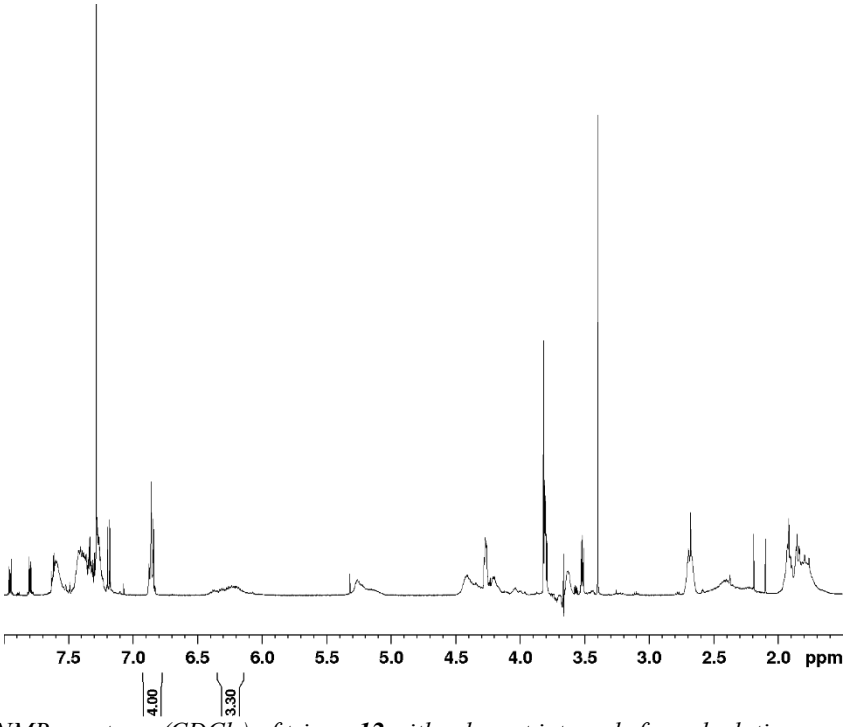

Figure 4.16: *^{1}H NMR spectrum ($CDCl_3$) of trimer **12** with relevant integrals for calculating coupling yield. The yield was calculated in the same as in previously, but the ratio of DMTr to H1' peaks is now 4:3 in a 100% yield reaction.*

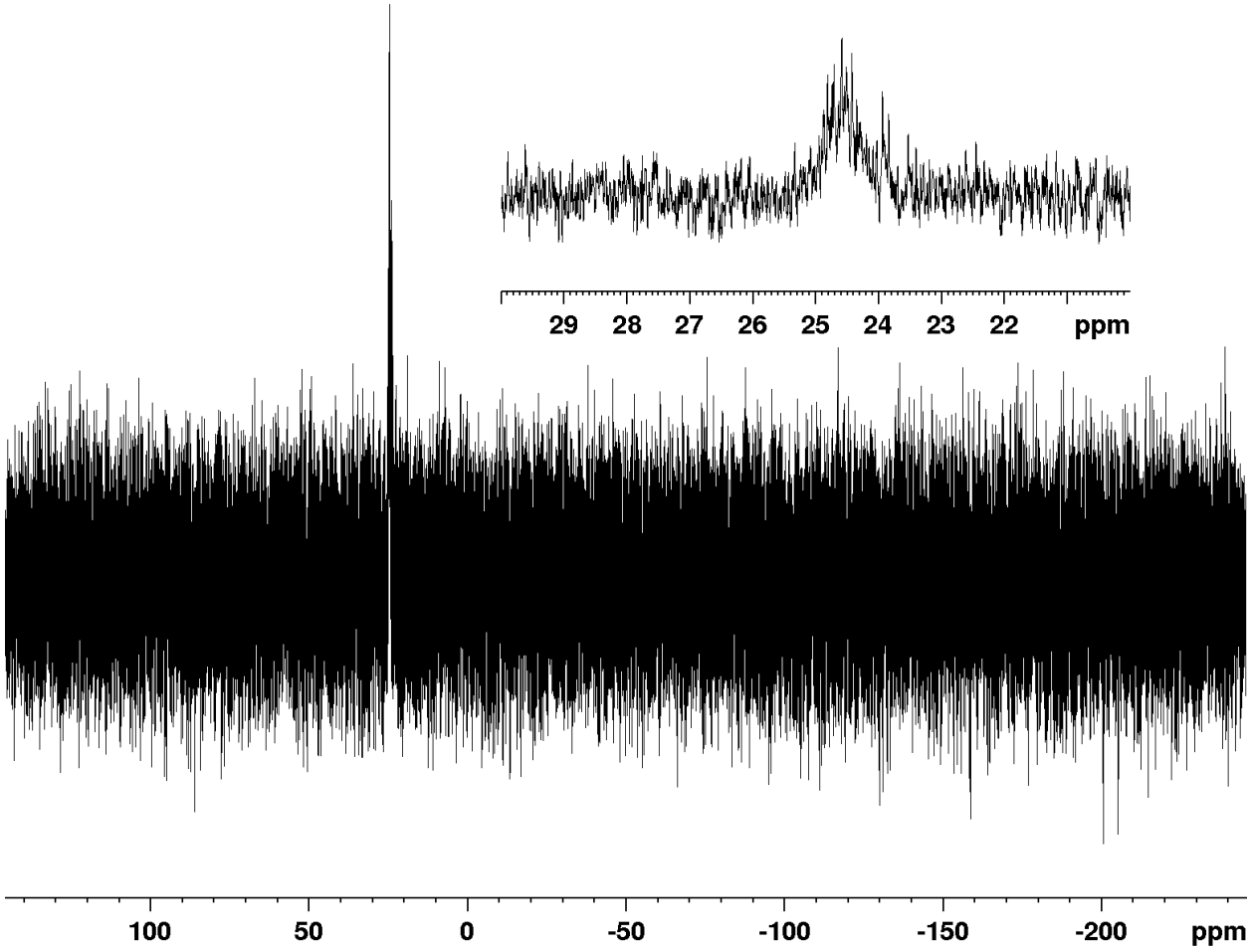

Figure 4.17: *^{31}P NMR spectrum ($CDCl_3$) of trimer **12** after thermal coupling.*

4.6: References

(1) Lönnberg, H. Synthesis of oligonucleotides on a soluble support. *Beilstein Journal of Organic Chemistry* **2017**, *13* (1), 1368-1387.

(2) Molina, A. G.; Sanghvi, Y. S. Liquid-Phase Oligonucleotide Synthesis: Past, Present, and Future Predictions. *Current protocols in nucleic acid chemistry* **2019**, *77* (1), e82.

(3) Van Giesen, K. J.; Thompson, M. J.; Meng, Q.; Lovelock, S. L. Biocatalytic Synthesis of Antiviral Nucleosides, Cyclic Dinucleotides, and Oligonucleotide Therapies. *JACS Au* **2022**, *3* (1), 13-24.

(4) Kim, J. F.; Gaffney, P. R.; Valtcheva, I. B.; Williams, G.; Buswell, A. M.; Anson, M. S.; Livingston, A. G. Organic solvent nanofiltration (OSN): a new technology platform for liquid-phase oligonucleotide synthesis (LPOS). *Organic Process Research & Development* **2016**, *20* (8), 1439-1452.

(5) Nagapudi, K.; Umanzor, E. Y.; Masui, C. High-throughput screening and scale-up of cocrystals using resonant acoustic mixing. *International Journal of Pharmaceutics* **2017**, *521* (1-2), 337-345.

(6) Effaty, F.; Gonnet, L.; Koenig, S. G.; Nagapudi, K.; Ottenwaelder, X.; Friščić, T. Resonant acoustic mixing (RAM) for efficient mechanoredox catalysis without grinding or impact media. *Chemical Communications* **2023**.

(7) *How RAM Mixes, Resodyn Acoustic Mixers*. https://resodynmixers.com/how-ram-mixes/ (accessed March 20th, 2023).

(8) Hope, K. S.; Lloyd, H. J.; Ward, D.; Michalchuk, A. A.; Pulham, C. R. Resonant acoustic mixing and its applications to energetic materials. *New Trends in Research of Energetic Materials* **2015**, 134-143.

(9) Gonnet, L.; Lennox, C. B.; Do, J. L.; Malvestiti, I.; Koenig, S. G.; Nagapudi, K.; Friščić, T. Metal-Catalyzed Organic Reactions by Resonant Acoustic Mixing. *Angewandte Chemie* **2022**, *134* (13), e202115030.

(10) Titi, H. M.; Do, J.-L.; Howarth, A. J.; Nagapudi, K.; Friščić, T. Simple, scalable mechanosynthesis of metal–organic frameworks using liquid-assisted resonant acoustic mixing (LA-RAM). *Chemical Science* **2020**, *11* (29), 7578-7584.

(11) Gonnet, L.; Borchers, T. H.; Lennox, C. B.; Vainauskas, J.; Teoh, Y.; Titi, H. M.; Barrett, C. J.; Koenig, S. G.; Nagapudi, K.; Friščić, T. The "η-sweet-spot"(η max) in liquid-assisted

mechanochemistry: polymorph control and the role of a liquid additive as either a catalyst or an inhibitor in resonant acoustic mixing (RAM). *Faraday Discussions* **2023**.
(12) Lennox, C.; Borchers, T.; Gonnet, L.; Barrett, C.; Koenig, S.; Nagapudi, K.; Friscic, T. Direct mechanocatalysis using Resonant Acoustic Mixing (RAM). **2023**.
(13) Yalcin, D.; Rajesh, S.; White, J.; Howard, S. C.; Pigram, P. J.; Tran, N.; Muir, B. W. Resonant acoustic mixing method to produce lipid-based liquid-crystal nanoparticles. *The Journal of Physical Chemistry C* **2021**, *125* (19), 10653-10664.
(14) Donga, R. A.; Khaliq-Uz-Zaman, S. M.; Chan, T.-H.; Damha, M. J. A novel approach to oligonucleotide synthesis using an imidazolium ion tag as a soluble support. *The Journal of organic chemistry* **2006**, *71* (20), 7907-7910.
(15) Bonora, G. M.; Biancotto, G.; Maffini, M.; Scremin, C. L. Large scale, liquid phase synthesis of oligonucleotides by the phosphoramidite approach. *Nucleic acids research* **1993**, *21* (5), 1213-1217.
(16) Bonora, G. M.; Scremin, C. L.; Colonna, F. P.; Garbesi, A. HELP (High Efficiency Liquid Phase) new oligonucleotide synthesis on soluble polymeric support. *Nucleic acids research* **1990**, *18* (11), 3155-3159.
(17) Creusen, G.; Akintayo, C. O.; Schumann, K.; Walther, A. Scalable one-pot-liquid-phase oligonucleotide synthesis for model network hydrogels. *Journal of the American Chemical Society* **2020**, *142* (39), 16610-16621.
(18) Zhou, X.; Kiesman, W. F.; Yan, W.; Jiang, H.; Antia, F. D.; Yang, J.; Fillon, Y. A.; Xiao, L.; Shi, X. Development of kilogram-scale convergent liquid-phase synthesis of oligonucleotides. *The Journal of Organic Chemistry* **2021**, *87* (4), 2087-2110.
(19) Thorpe, J. D.; O'Reilly, D.; Friščić, T.; Damha, M. J. Mechanochemical synthesis of short DNA fragments. *Chemistry–A European Journal* **2020**, *26* (41), 8857-8861.
(20) Takahashi, D.; Inomata, T.; Fukui, T. AJIPHASE®: A Highly Efficient Synthetic Method for One-Pot Peptide Elongation in the Solution Phase by an Fmoc Strategy. *Angewandte Chemie* **2017**, *129* (27), 7911-7915.
(21) Martin, C. Twin screw extruders as continuous mixers for thermal processing: a technical and historical perspective. *AAPS PharmSciTech* **2016**, *17* (1), 3-19.

Chapter 5:

Assessment of oligonucleotide synthesis methods

"I've got a theory that if you give 100% all of the time, somehow things will work out in the end."

- Larry Bird

5.1: Introduction

The field of green chemistry has rapidly grown in the past few decades as our understanding of hazardous chemicals (for both humans and the environment) has also grown[1]. Unmitigated climate change has galvanized the chemical community to design more efficient, safer, and less wasteful synthetic pathways to produce the materials and drugs that we rely on. Indeed, the pharmaceutical industry is one of the worst offenders when it comes to waste generation in drug production. A popular metric for assessing the sustainability of a process is known as the *E* factor[2]. Introduced in 1992, the *E* factor is a catch-all number that considers atom economy, yield, waste production, and energy use and is generally calculated by the total mass of waste produced divided by the mass of the product. It differs slightly from PMI introduced in **Chapter 2** in that it also considers CO_2 emissions and other similar waste generated from energy use, but for the pharmaceutical industry it is often difficult to calculate this. However, despite producing the lowest total mass of other chemical industries, the pharmaceutical industry has the highest *E* factor, estimated to be at least 25 and possibly over 100, depending on the process[3]. While it is understandable that many pharmaceutical compounds are extremely complex and have lengthy synthetic routes, the problem remains.

The production of oligonucleotide therapeutics may in fact be one of the most wasteful sectors within the pharmaceutical industry. Highlighted in **Chapter 2**, it is worth mentioning that the average PMI calculated per nucleotide to produce 1 kg of an oligonucleotide is on the order of 200, significantly higher than other pharmaceutical processes, without taking into the mass of CO_2 produced from energy consumption[4]. Given that most therapeutic oligonucleotides are at least 18 nucleotides long, the *E* factor is undoubtedly enormous. The huge *E* factor, or PMI, for oligonucleotide synthesis arises mainly from the use of organic solvents for reactions and washing, and from the use of large volumes of water for purification by chromatography. Atom economy (36% for DNA phosphoramidite[4]) is also a major issue for oligonucleotide synthesis due to the numerous and often high MW protecting groups (particularly DMTr). However, this is another issue entirely and not the focus of the work contained within this thesis, but improving protecting group strategies should also be a focus of the industry moving forward. Use of stoichiometric amounts of non-catalytic reagents is also an issue and the adoption of catalysts[5] should be an important focus of the industry as well.

The past three chapters of this thesis have focused on the use of different technologies (VBM, RAM) or the development of new strategies (TCOS) for oligonucleotide synthesis to improve the sustainability of the process. Particularly, we have focused on reducing the solvent consumption during reactions (VBM and RAM) as well as during purification (TCOS). This chapter will focus on assessing these strategies against one another, against solution-phase methodologies, and against solid-phase data available for industrial manufacturing.

5.2: Results and discussion

5.2.1: Solution-phase benchmark

Before beginning our assessment of the strategies developed in this thesis, we had to have a benchmark for a basic reaction in solution. Thus, we repeated the most basic reaction from all three strategies, a simple coupling of **1a** with **2a** in the presence of PvCl using PTP as the sulfur transfer reagent to synthesize **3** (**Scheme 5.1**). We performed the reaction in an analogous way and at a similar scale (0.45 mmol) to the previous strategies, but in solution. Compounds **1a** and **2a** were dissolved in pyridine (5 mL) and PvCl was added. The reaction was stirred for 15 minutes and then PTP was added, and the reaction was stirred for a further period of 15 minutes. We performed this reaction in two ways, the first involved concentration of the reaction mixture followed by purification by column chromatography, as we did with the other strategies (VBM and RAM). However, Reese's strategy using similar chemistry in solution performed a basic workup after the reaction and we attempted the reaction this way as well, by washing the reaction mixture with a saturated aqueous sodium bicarbonate solution[6]. The isolated yields of **3** were almost identical (73 vs 75%) following both strategies, and TLC analysis of both reactions prior to purification by column chromatography were also identical. It should be noted that monitoring of the reaction by TLC showed complete consumption of **2a** after 15 minutes using 1.1 equivalents of **1a** and in general we found the workup unnecessary. However, to recreate a full synthesis cycle, detritylation must also be carried out. Given the clean TLC after the reaction to produce **3**, we found detritylation could be carried out on the crude material by concentrating the reaction mixture and redissolving it in DCM followed by the addition of TFA. After 15 minutes the reaction was complete (TLC analysis), and methanol was added to the reaction mixture to quench the trityl cation that had formed. Similarly to above, we found the workup unnecessary after detritylation and we were able to isolate **4** in good yield (72%) over two steps.

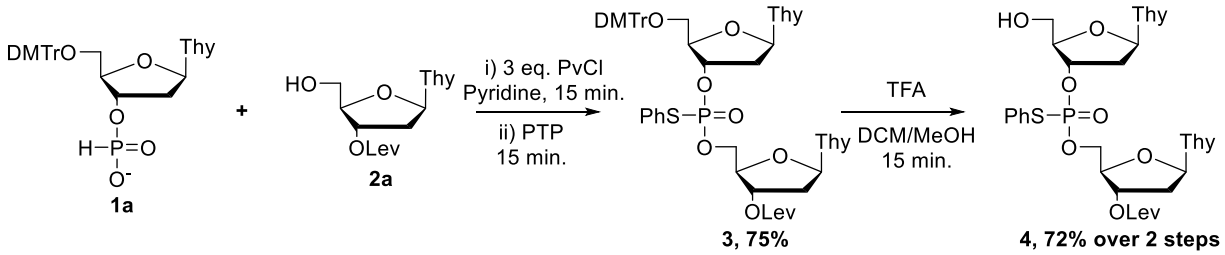

Scheme 5.1: *Solution-phase H-phosphonate coupling and sulfur-transfer.*

While the yields we obtained for this reaction were generally good, they were significantly lower than the yields reported by Reese using similar chemistry (**Scheme 5.2**)[7]. Reese reported the coupling of H-phosphonate **1** with **2** using di-(2-chlorophenyl) phosphorochloridate (DCPP, derivative of DCP from **Chapter 2**) followed by oxidation to the phosphorothioate triester using *N*-[(4-Chlorophenyl)sulfanyl]phthalimide (CPTP), essentially the same as PTP that we used except with a chlorine at the *para* position. Under his conditions, he reported isolation of the fully protected dimer in 99% isolated yield, purified by column chromatography[7]. He additionally reported that coupling, oxidation, and detritylation could be carried out sequentially without purification between steps and dimer **5** could be isolated by column chromatography in 98% yield over three steps[8].

However, in our hands we were never able to recreate these results in solution. Although in **Scheme 5.1** we used PvCl instead of DCPP, we did attempt the same reactions in solution using DCP as in **Chapter 2**, but similarly found the purification more challenging when using DCP as the activator. While DCP may be slightly less active than DCPP, Reese did eventually adopt his strategy to using DCP at room temperature instead of DCPP at -40°C[6]. Similarly, we used PTP instead of CPTP, but this should not affect the reaction much, and should have a greater effect on the rate of deprotection, which should remain relatively high with PTP. For our solution-phase reaction in **Scheme 5.1** we also sought to keep the reactions as close as possible to those used in the other methods, thus we performed no coevaporations or drying of nucleosides before conducting the reaction. The pyridine used was dried, but other than that there were no precautionary drying steps carried out. Ultimately, we were unable to recreate much of Reese's work, including his synthesis of CTP[9] and the closely related succinimide derivative *N*-[(2-cyanoethyl)sulfanyl]succinimide (CTS, **Scheme 5.3**), which he used to synthesize Vitravene, a 21-mer PS antisense oligonucleotide using this approach in solution[6]. Based on this, we will assess the methods developed in this thesis against our own solution-phase experiments using

PvCl as an activator as a more direct comparison, but we will also compare with Reese's work due to his success using similar chemistry. Perhaps the lack of drying in **Scheme 5.1**, the change of activator (despite reported success using PvCl[10]), and the lack of additional protecting groups (Thy^{Ph}, **Scheme 5.3**) contributed to the lower yields obtained than those reported by Reese.

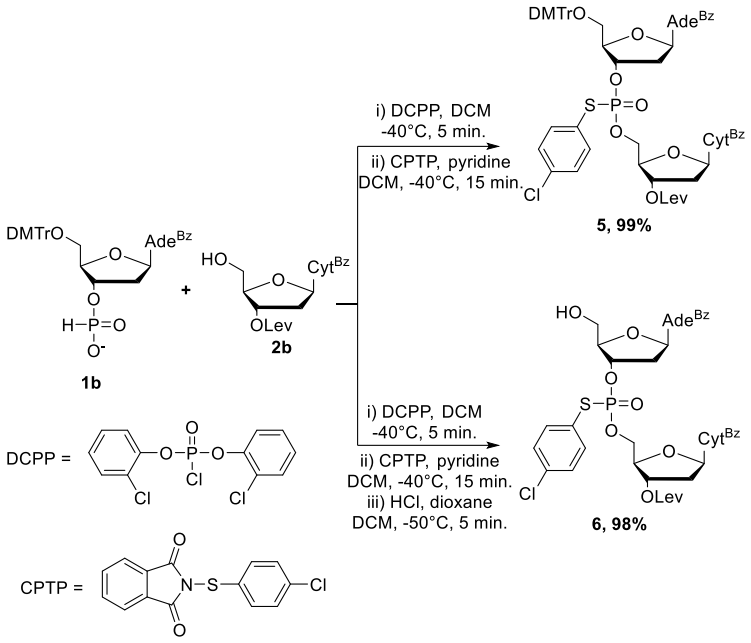

Scheme 5.2: *Reese's approach for H-phosphonate coupling followed by sulfur-transfer (top) and detritylation (bottom).*

5.2.2: Calculation of *E* factor/PMI for literature procedures

To begin our assessment, we closely examined the procedures used in the literature for oligonucleotide synthesis in solution. As explained above, we have selected Reese's work as a good comparison for solution-phase synthesis using the modified H-phosphonate approach. We will also examine Bonora's PEG-supported approach using phosphoramidite chemistry[11] as a comparison for the TCOS strategy outlined in **Chapter 4**. While it would be impossible to accurately calculate the *E* factor for procedures reported in the literature (we cannot determine the waste generated due to energy consumption), we can do our best to estimate the amount of waste generated from reagents and solvents. Thus, PMI is perhaps a better metric for this assessment. Additionally, we will standardize the values obtained to a per kilogram scale as most of the strategies described operated on vastly different scales.

Beginning with Reese's approach, we closely examined his optimized reaction conditions for the coupling, sulfur transfer, and detritylation (**Scheme 5.2**, bottom) [6]. As stated above, his

optimized conditions operated at room temperature, used DCP as the activator, used CSP as the sulfur-transfer reagent, and performed both the coupling and sulfur-transfer in one step (**Scheme 5.3**). Additionally, under these conditions he carried out the detritylation on the crude dimer with purification only occurring after liberation of the 5′-hydroxyl. He never published using the room temperature conditions for the synthesis of oligonucleotides of any length containing PO backbones, thus the comparison is not the same. However, we will continue to analyze these conditions as they are the best he reported and based on his previous results there is no reason to believe he could not have optimized the chemistry for PO backbones just as well. We anticipate the PMI for such a strategy would be similar to the one outlined in **Scheme 5.3**. It should also be noted that Reese used additional nucleobase protecting groups such as the phenyl group for the O4 of T and a 2,5-dichlorophenyl group for the O6 of G, but once again to keep conditions like those used in previous chapters, we opted to not use these extra protecting groups.

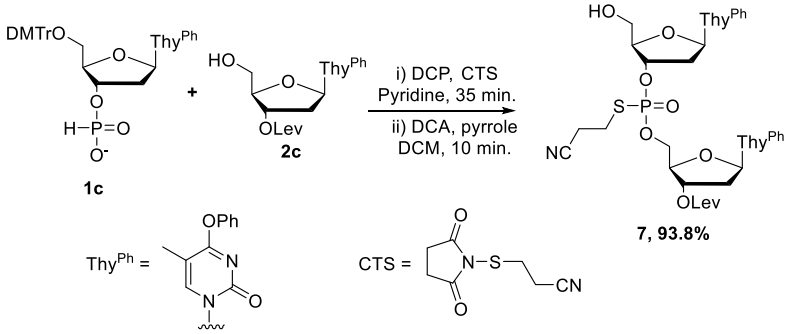

Scheme 5.3: *Reese's optimized strategy for the synthesis of PS oligonucleotide in solution.*

Reese's strategy began with coevaporation of 7.08 g (9.01 mmol) of **1c** and 3.126g (7.51 mmol) of **2c** with 15 mL of pyridine followed by dissolution of the residue in 30 mL of dry pyridine. Both DCP and CTS (2 equivalents of each) were dissolved in 40 mL of dry pyridine and added to the mixture of **1c** and **2c** over the course of 10 minutes**.** After a further period of 10 minutes, 5 mL of water was added to the reaction, and it was stirred for 15 more minutes. The reaction mixture was partitioned between 250 mL of DCM and 250 mL of a saturated $NaHCO_3$ solution, and the aqueous layer was back extracted twice with 20 mL of DCM. After drying and concentration, the crude residue was coevaporated three times with 50 mL of toluene, then dissolved in 80 mL of DCM. The solution was cooled to 0°C and 4.16 mL (10 eq.) of pyrrole was added (as a DMTr scavenger[12]) followed by addition of 4.95 mL of DCA (10 eq.) in 40 mL of DCM. After 10 minutes, the reaction mixture was poured into 250 mL of a saturated $NaHCO_3$ solution and the organic layer was washed a second time with 250 mL of a saturated $NaHCO_3$

solution, then dried and concentrated. The crude residue was then purified by column chromatography using a mixture of DCM-MeOH (97:3, v/v). It is difficult to estimate how much solvent was required for the purification step here but given the relatively large scale of the reaction (6.10g of **7** isolated, over 10 g of reagents total), it can reasonably be assumed that at least 3-4L of solvent were required, most of which was DCM. For this analysis, we will estimate a rough total of 3 L required for purification by column chromatography.

The total solvent consumption is tallied in **Figure 5.1** divided by solvent type and process stage, in a similar manner to Andrews *et al.* in their analysis of oligonucleotide manufacturing[4]. We have ignored the masses and volumes of reagents and nucleic acids used as they make up less than 1% of the total masses of all compounds used and are similar across all methods. Based on this analysis, we see a total of 4 400 mL of solvents used for Reese's method and when converting to mass this translates to 5.527 kg of solvents required to synthesize 6.10g of **7**. Thus, on a per kg basis of **7**, if scaling up linearly we can calculate a PMI of approximately 906 for a single synthesis cycle of Reese's strategy consisting of coupling, sulfur-transfer, and detritylation. It should be noted that the scaling up is most likely not linear and should this process be scaled up, the PMI would likely drop from the large value calculated. Nonetheless, it is apparent from **Figure 5.1** that the major contributors to solvent usage are during purification, either extractions or column chromatography, but it should be noted as well that most of the solvent used during extractions is water. Finally, the yield of **7** was 93.8%, but the average yield obtained during Reese's approach for similar reactions (with different bases) was 95.4%, which would further reduce the average PMI of his strategy. However, the use of extra protecting groups on the nucleobases would reduce the yield of the final deprotected oligonucleotide, thus

increasing the PMI. On average, both facts taken together would likely mostly cancel each other out or have a negligible effect on the PMI.

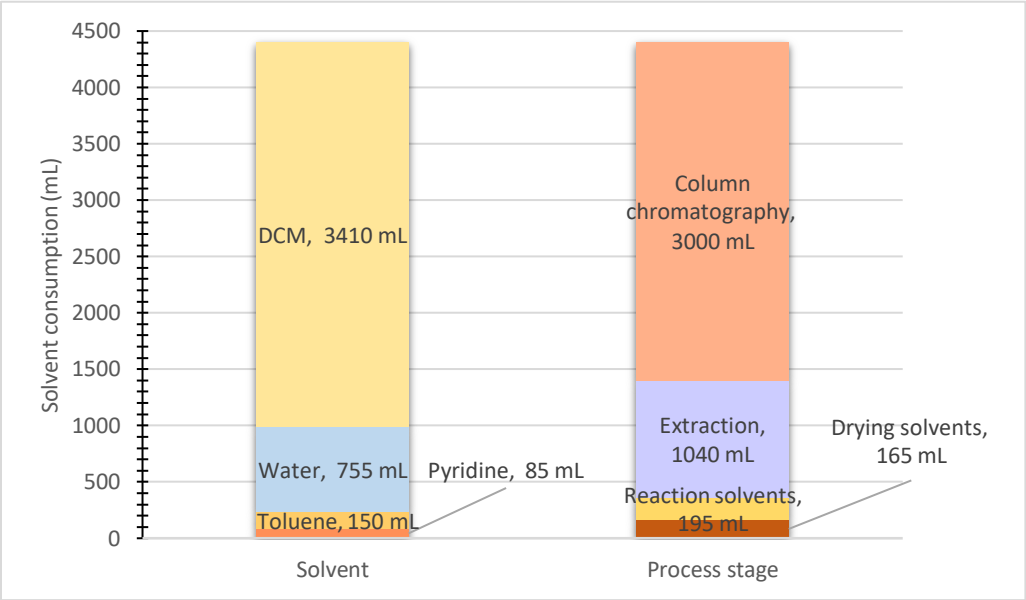

Figure 5.1: *Analysis of solvent use during the reaction and purification performed by Reese in* ***Scheme 5.3.***

We continued by analyzing the solvent consumption during Bonora's PEG supported strategy (**Scheme 5.4**) [11]. Bonora first published the use of PEG as a soluble support for oligonucleotide synthesis using a phosphotriester approach[13], but we analyzed the subsequent publication using phosphoramidite chemistry as the phosphotriester approach is generally not used currently and the phosphoramidite approach was much higher yielding. While Bonora's synthesis strategy began with detritylation of PEG nucleoside to yield **8,** we analyzed the strategy with detritylation occurring at the end of the cycle. This ensures that all compounds analyzed have no DMTr group, which is a large protecting group that would inflate the yield of the product leading to discrepancies in PMI calculated. Other standard protecting groups were left as part of the analysis as they are more less ubiquitous across strategy. Thus, prior to coupling, they coevaporated 1.0 g of **8** three times with a few mL of ACN; we estimate a total of approximately 10 mL of solvent for this step. Coupling was carried out by first adding 1 mL of ACN to **8**, followed by addition of 2.5 equivalents of phosphoramidite **9** in 0.1M solution of ACN then addition of 10 equivalents of tetrazole in a 0.5M solution ACN. Based on the loading value of 180 µM/g of **8** they reported, we calculated the use of 4.5 mL of ACN required to deliver 2.5 equivalents of **9** and 3.6 mL of ACN required to deliver 10 equivalents of tetrazole at the given concentrations. However, we should note that for the detritylation to yield **7** they used

1.0 g of the PEG nucleoside, but they also used 1.0 g of **8** for the coupling reaction. Given the lower MW of **7** compared to before detritylation, assuming 100% detritylation, this corresponds to more than 180 μM/g and thus slightly more **9** and tetrazole were required. Based on this, we estimate the total solvent use to be approximately 15 mL of ACN for the coupling step. The phosphite triester **10** was precipitated using 10 volumes (150 mL) of diethyl ether, followed by recrystallization from ACN and diethyl ether which based on our earlier estimate likely only required approximately 5 mL. They also performed a capping step after coupling, but we will ignore it for now to provide a more accurate comparison to our TCOS approach, which may require a capping step as well for the synthesis of longer oligonucleotides. Oxidation of **10** to phosphate triester **11** was carried out by dissolving **10** in 20 mL of ACN using 1.2mL of *tert*-butylhydroperoxide (TBHP) in di-*tert*-butylperoxide, but we will treat this as a reagent for the PMI calculations of solvent use. Compound **11** was precipitated using 10 volumes of diethyl ether (200 mL) followed by recrystallization from ACN and diethyl ether, using another 5 mL of solvent. Following oxidation, detritylation of **11** was carried out using 10 mL of a 6% solution of trichloroacetic acid (TCA) in 1,2-dichloroethane (DCE). They then precipitated the product using diethyl ether, although a specific volume was not mentioned, based on other steps using 10 volumes of either, we can assume they used at least 100 mL of diethyl ether for this step. Following the precipitation, they then recrystallized the detritylated product **12** from DCE/ethanol, but a specific volume was not mentioned, and we conservatively estimate they would require approximately 5 mL of solvent for this step. For recrystallizations, we assumed a 1:1 (v/v) mixture of the solvents stated.

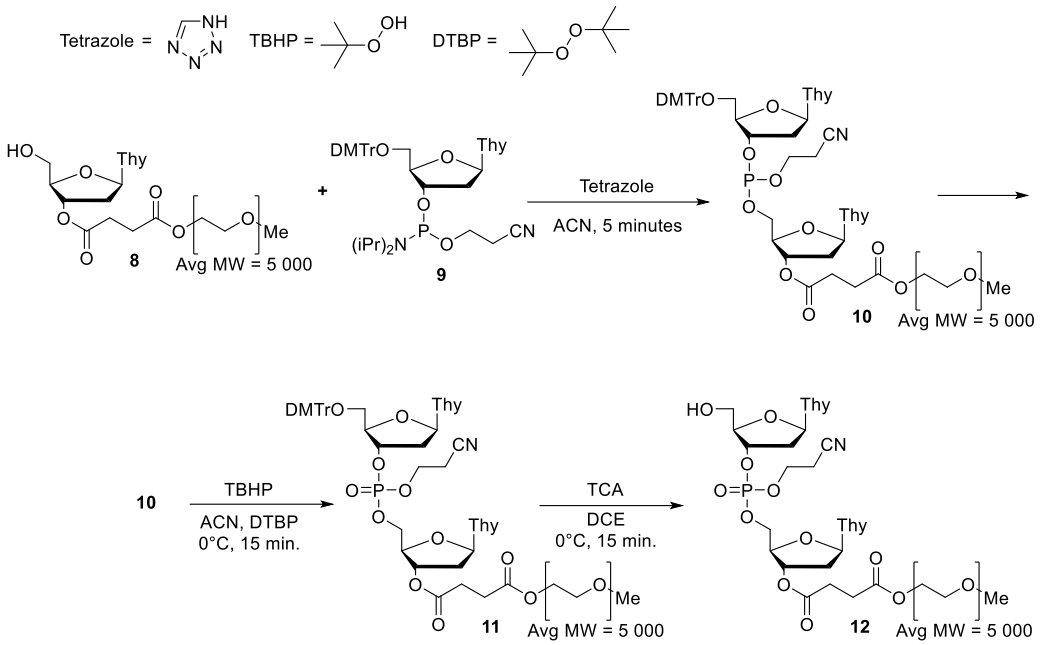

Scheme 5.4: *Bonora's phosphoramidite synthesis cycle.*

The total solvent consumption is outlined in **Figure 5.2** for one full synthesis cycle. Similarly, to Reese's approach, most of the solvent use comes from diethyl ether required during purification by precipitation. Bonora used this strategy to synthesize an octamer in >95% crude purity and in 93% overall yield, corresponding to a 99% average yield per synthesis cycle, but they also noticed an approximate loss of less than 1% of the total material after each step. Based on the loading of 180 μM/g of **8**, taking into account the loss of material (assumed 1%), after one synthesis cycle, they should have approximately 176 μM of the TT dimer. Ignoring the MW of the PEG (but including the succinyl linker), this corresponds to 123 mg of product after one synthesis cycle. Converting the volume of solvent (520 mL) to mass equals 0.378 kg per 123 mg of product synthesized. Scaling this up to 1 kg, we calculated the PMI to be approximately 3073. The large value obtained for Bonora's method is reflective of the low loading capacity and low MW of the dimer compared to PEG, thus requiring large volumes of solvent to precipitate the growing oligonucleotide chain. While the relative weight of the oligonucleotide increases as more cycles are repeated, this still represents a huge amount of solvent required for the synthesis of a small amount of an oligonucleotide.

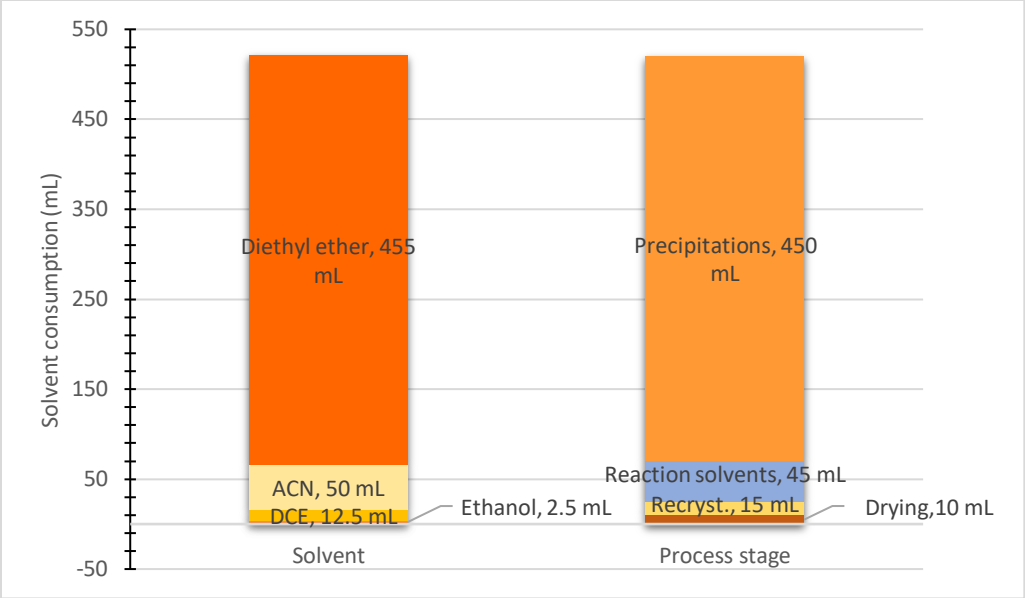

Figure 5.2: *Analysis of solvent use during the reaction and purification performed by Bonora in* ***Scheme 5.4.***

5.2.3: Calculation of PMI for VBM, RAM, and solution-phase syntheses

Having established at least a rough estimate of the PMI of both Reese's and Bonora's strategies for oligonucleotide synthesis, we set out to repeat the analysis with the methods developed in this thesis, starting with the VBM strategy outlined in **Chapters 2** and **3**. In **Chapter 2**, we developed a method to synthesize DNA dimers with 5′-DMTr groups (DMTr-ON) or without (DMTr-OFF) depending on the specific conditions used. While the DMTr-OFF method successfully completes a full synthesis cycle, similarly to Reese's two-step approach in **Scheme 5.3**, in general we relied more on the DMTr-ON strategy, followed by detritylation in solution of the crude material (**Scheme 5.5**) in a very similar manner to **Scheme 5.1**. For this reaction, we used PvCl to closely mirror the conditions we used in solution, even though Reese used DCP for his reactions. We were able to synthesize **4** in this manner in good yield (68%) over two steps.

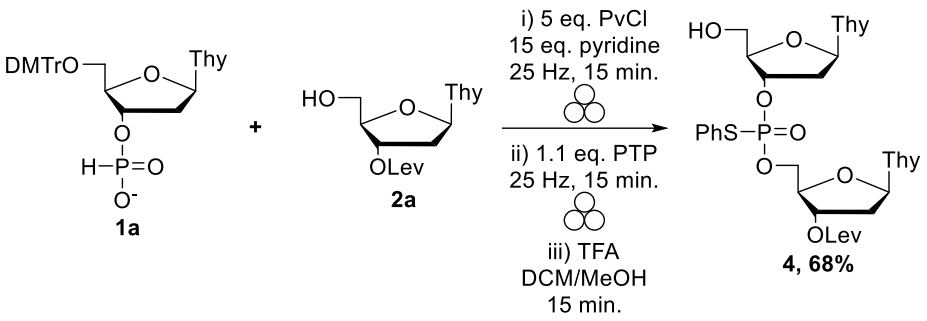

Scheme 5.5: *Two-step procedure for synthesis of 5'OH dimers by VBM.*

Following the procedure we used, the reaction required a total of 15 equivalents of pyridine during ball milling, which corresponded to 0.54 mL. After the reaction was complete, approximately 10 mL of DCM was required to dissolve the resulting crude reaction mixture before adding the solution to a round-bottomed flask. The TFA was added for the detritylation, followed by the addition of approximately 10 mL of MeOH to quench the trityl cation. The reaction mixture was concentrated and directly purified by column chromatography. Given our estimate of 3 L of solvent used for Reese's approach on a 7.51 mmol scale of **2c** and our scale of 0.45 mmol of **2a**, we estimated the use of approximately 750 mL required for the purification of **4** by column chromatography. As noted previously, the use of solvent for purification by column chromatography likely does not scale linearly and therefore the solvent consumption for larger scale columns is likely relatively lower. The gradient used for the column was the same as used in previous chapters for dimers with free 5′-hydroxyls (DCM-MeOH, 99:1-95:5, v/v). Using methanol at a maximum of 5% of the eluent of the column meant that the maximum amount used was 37.5 mL, but we estimate it to be closer to 25 mL. The amount of pyridine was so small relative to the total solvents used (<0.01%) that it was ignored in the analysis summarized in **Figure 5.3.** The total solvent used for the isolation of 0.225 g of **4** was 770 mL following our strategy using vibrational ball milling. This 770 mL corresponds to 1.013 kg of solvents used. Scaling this up to a kilogram scale corresponds to a PMI of 4502.

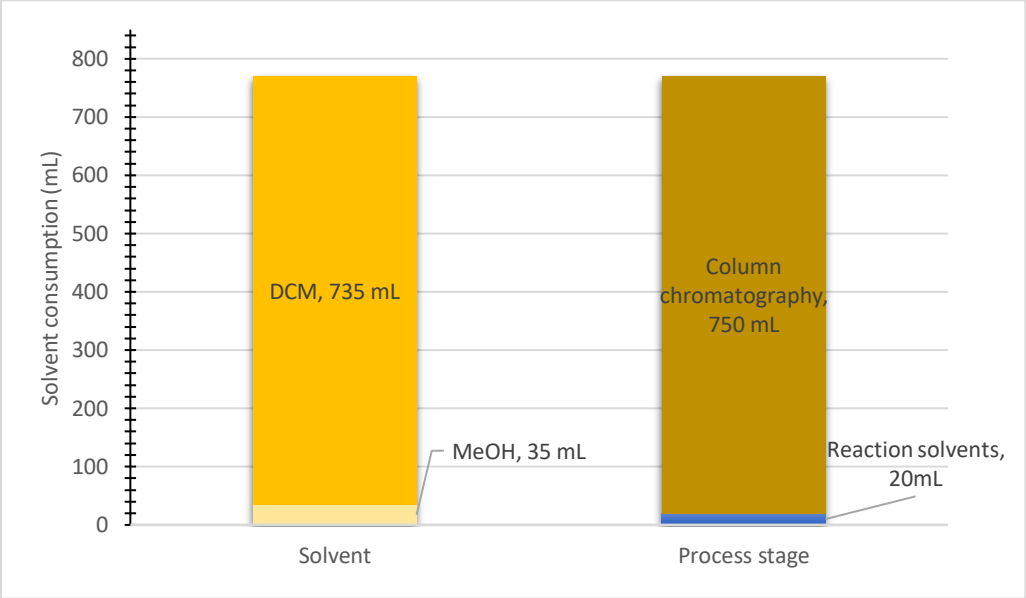

Figure 5.3: *Analysis of solvent use during the reaction and purification in* ***Scheme 5.5*** *by VBM and* ***Scheme 5.6*** *by RAM.*

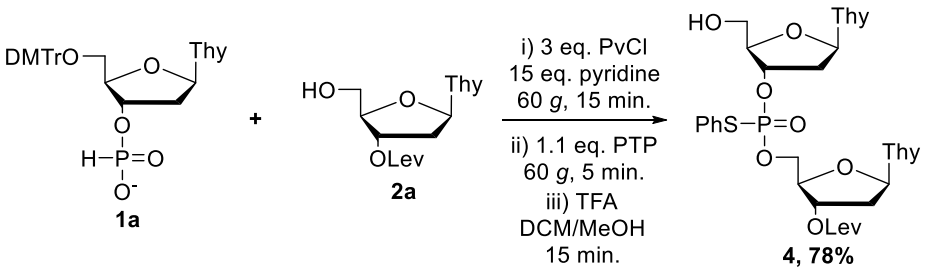

Scheme 5.6: *Two-step procedure for synthesis of 5'OH dimers by RAM.*

The same two-step process used for VBM above was also carried out by using RAM (**Scheme 5.6**). In **Chapter 4** we synthesized a 5′-DMTr dimer on a 2 mmol scale, followed by detritylation in solution. We reduced the scale from 2 mmol to the same 0.45 mmol scale used in **Scheme 5.1** and **Scheme 5.5** and carried out the detritylation on the crude material to compare our strategies more accurately. Following this approach, we were able to synthesize **4** in good yield (78%) over two steps. The PMI analysis for the RAM strategy is essentially identical as the equivalents of pyridine used were the same (15 eq.) and the detritylation was carried out in the same way. Thus, the solvent usage for RAM and VBM was identical using the same conditions for the column, with the only variable changing in the PMI calculation being the yield obtained by RAM being slightly higher than by VBM. From this, we calculated the PMI to be 3911 when using our RAM approach. From both VBM and RAM, the vast majority (>95%) of the solvent use comes during purification by column chromatography. The omission of drying steps, extractions, and reaction solvents certainly reduces the solvent usage as compared with Reese's

approach but may reduce the yield compared to Reese's approach. Scaling up these methods would reduce the PMI further by reducing the relative amounts of solvent used during purification by column chromatography.

Similarly, the solution-phase approach of **Scheme 5.1** used essentially the same volumes of solvent as the VBM and RAM strategies. The only difference between the solution-phase reaction we performed and the VBM and RAM approaches was the use of 10 mL pyridine during the coupling and sulfur transfer reactions. After this step, the reactions were detritylated in the same way and purified the same way. Based on the yield of **4** in solution, we calculated the PMI to be 4280, only marginally different than by VBM or RAM, and less than the PMI calculated for VBM.

5.2.4: Calculation of PMI for TCOS synthesis

We finally set out to analyze the solvent use during the TCOS method developed in **Chapter 4**. Starting with 1.0 g of the same detritylated PEG nucleoside **8** (**Scheme 5.7**) as used by Bonora, we melted the compound at 75°C. It should be noted that the loading of **8** (163 μM/g) in our hands was slightly lower than Bonora's approach which would result in a lower overall yield. Continuing with the strategy for coupling, we added approximately 2 mL of toluene and 75 μL of pyridine to facilitate mixing. The amount of pyridine is so insignificant at this stage that we also ignored it during our analysis. H-phosphonate **1a** was added, followed by PvCl, then PTP after 5 minutes. Once the reaction was complete, approximately 3 mL of ethanol was added, and the mixture was cooled to 0°C. Once the product precipitated, we filtered the solid and washed it with 10 mL of cold ethanol. The PEG dimer **13** was collected and once again melted at 75°C, followed by the addition of 2 mL of ethanol to facilitate mixing and scavenge trityl cations. TFA was added and once the reaction was complete, 3 mL more of ethanol was added and the mixture was cooled to 0 °C Once the product precipitated and was filtered, another 10 mL of cold ethanol was used to wash the detritylated dimer **14**. Average recovery over these two

steps was 98%, the coupling yield was estimated to be 98% from ^{1}H NMR analysis of **13** and detritylation was estimated to be quantitative from ^{1}H NMR and TLC analysis of **14**.

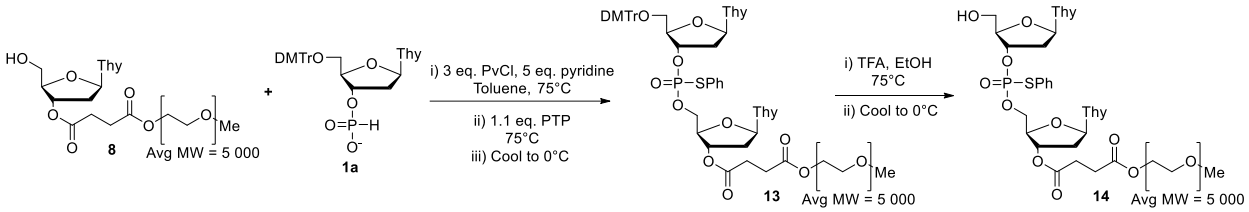

Scheme 5.7: *Synthesis cycle using TCOS.*

Based on the loading of **8**, recovery, and yield over these steps, we estimate that after one full synthesis cycle, we had approximately 156 µM of the dimer. As above, discounting the MW of PEG and including the succinyl linker, this corresponds to approximately 109 mg of product. The total solvent use during the TCOS synthesis cycle is outlined in **Figure 5.4**. Based on the total solvent use of approximately 30 mL for one synthesis cycle, this corresponds to 0.024 kg of solvent. Scaling up the yield to 1kg gives an approximate PMI of 220. The significant reduction in solvent use both during reactions and purification made up for the slightly lower yield of our TCOS strategy as compared with Bonora's synthesis.

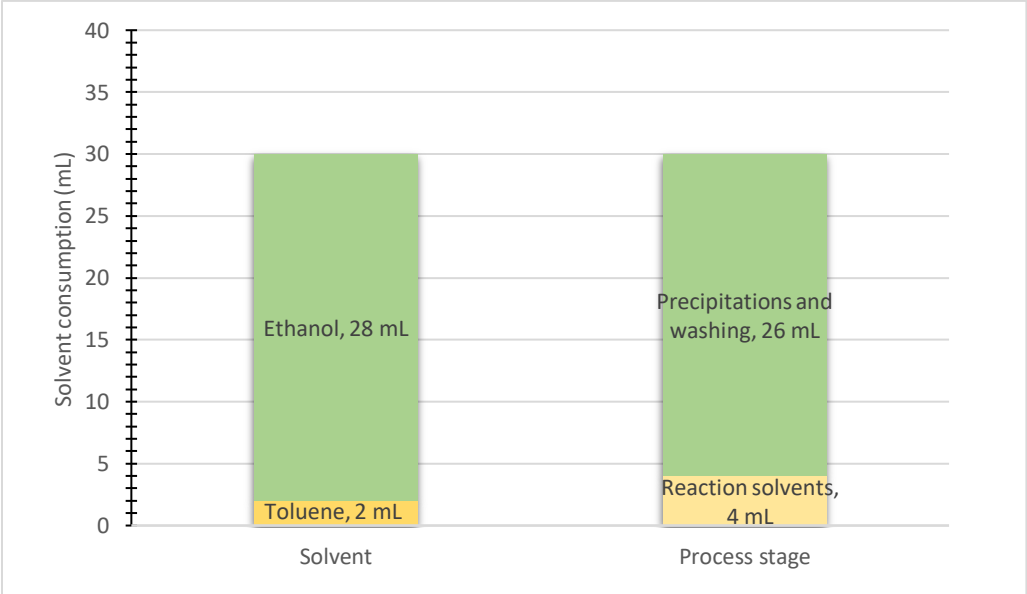

Figure 5.4: *Analysis of solvent use during the reaction and purification in* ***Scheme 5.7*** *by TCOS.*

5.2.5: Comparison of PMI of different oligonucleotide synthesis strategies

Based on the analyses from the previous sections, we have compiled the PMI values calculated for each method in **Figure 5.5**. Perhaps most surprisingly, Bonora's strategy had by far the highest PMI at over 3 000. On the surface, Bonora's strategy seemed to be one of the most effective, delivering oligonucleotides in high yields, excellent crude purity, and applicable to oligonucleotides at least up to 20 bases in length[11]. The low molar scale, but high molecular weight of the PEG compounds led to the use of large volumes of solvent required to precipitate up to 1.0 g of material. The pivot to lower MW soluble supports, such as Ajiphase[14] or Biogen's[15], or support with higher loading capacities would be necessary to offset the solvent use during precipitations. Although we had difficulties using phosphoramidite chemistry with TCOS due to the high temperatures, we found the modified H-phosphonate approach to be effective. Despite beginning with a lower loading capacity of **8**, and generally reporting lower yields than Bonora, our strategy still reduced the PMI by over 90%. By increasing the use of di-hydroxyl PEG instead of methyl-capped at one end, we could double the loading capacity and further reduce the PMI. Investigation of other polymers with even higher loading capacities could improve the strategy as well. However, the yield of our strategy did drop slightly when moving from the dimer to the trimer and some further optimization would be necessary for TCOS to be viable for longer oligonucleotides.

Comparing our solution-phase method with VBM, RAM, and Reese's methods does not reveal a clear process that is most efficient. The use of column chromatography for all strategies makes them generally unsuitable for scaling up. Although Reese's strategy did demonstrate high yields and the synthesis of a PS-backbone 21-mer, it did ultimately require column chromatography for each coupling step (20 total) [6]. It is clear that any viable large-scale process would have to avoid this and some sort of support is needed. In the end, VBM, RAM, and our solution-phase method did not ultimately reduce the PMI as compared to Reese's strategy, despite removing drying and extraction steps, although maybe those steps are what enabled Reese to achieve such high yields. Nonetheless, comparing our own three approaches yielded a very small difference between RAM and VBM, except for differences in yield, and a similarly small change in PMI when moving to solution-phase. The use of a few mL of solvent in the solution-phase reactions was very small relative to the total solvent required during the

purification and thus did not affect the PMI to a large degree. In fact, the PMI by VBM was higher than the solution-phase reaction we carried out due to the lower yield by VBM.

Ultimately, the average PMI from Andrews analysis of sustainability of oligonucleotide manufacturing by SPOS was the lowest of all strategies[4], although only slightly lower than TCOS. However, this analysis was the only one performed on a well-optimized industrial process. We assume that the PMI does not scale linearly when moving from multi-gram to the kilogram scale and there are ways of reducing the PMI as you scale up.

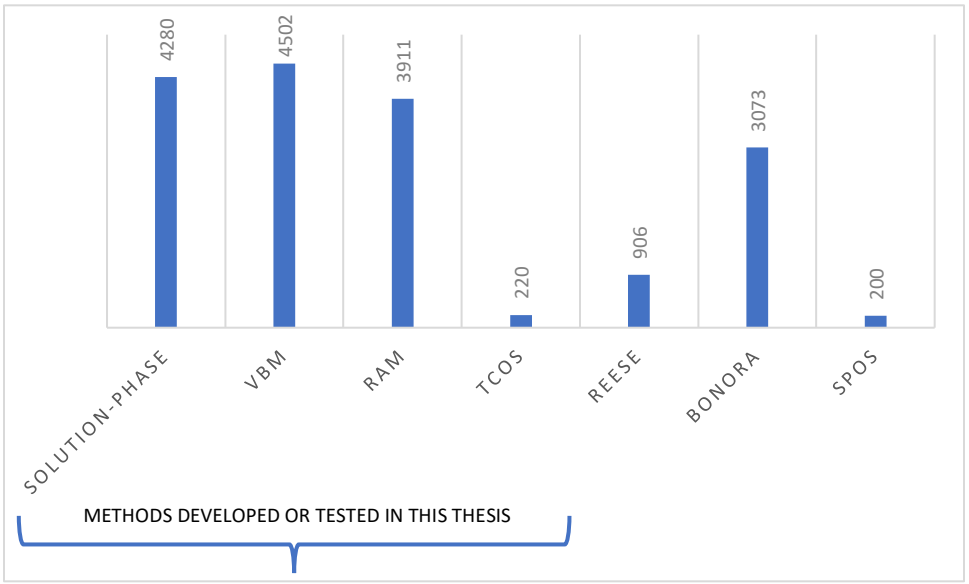

Figure 5.5: *Calculated PMI for different methods of oligonucleotide synthesis.*

However, the comparison between our solution-phase method, VBM, RAM, and Reese's strategy is misleading. Indeed, we calculated a much higher PMI for our methods than Reese's method and it is clear that this is due to the use of column chromatography for purification. The different scales used in the methods and the non-linear scaling of solvents used for column chromatography makes this analysis inaccurate. Thus, we recalculated the PMI for those strategies while ignoring the solvent used for column chromatography, with the data outlined in **Figure 5.6**. From this analysis, we see a more accurate comparison of how VBM and RAM reduce solvent consumption. We also see a significant reduction in PMI by forgoing the use of drying solvents and extractions in all strategies as compared to Reese's approach. When comparing between our solution-phase reaction, VBM, and RAM, we see a reduction of the PMI of 30-40%, but could be higher if the detritylation reaction carried out in solution was also carried out using VBM or RAM. Additionally, it is abundantly clear the use of column

chromatography for purification makes these strategies unsuitable for scaling up, but the use of soluble supports, such as the imidazolium[16] or phosphonium[17] tags developed in our lab, could reduce the PMI further by allowing for purification by simple precipitation.

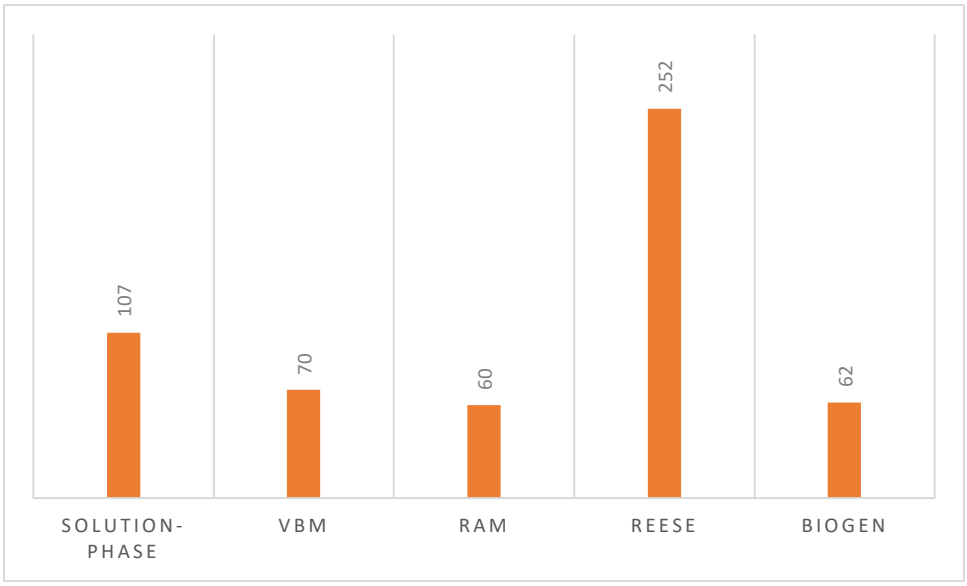

Figure 5.6: *Calculated PMI for our solution-phase approach, VBM, RAM, Reese's, and Biogen's approach ignoring solvent use for chromatography.*

Further analyzing Biogen's large-scale phosphoramidite synthesis of oligonucleotides[15], we calculated a PMI of 62 for one synthesis cycle of coupling, sulfurization, and detritylation without any purification by column chromatography. This further underscores the issues with comparing processes across scales. For example, calculating the PMI (not shown) of the imidazolium-supported approach developed in our lab[16], yielded a PMI of 1781, but the reactions were performed on a sub-milimolar scale. This is like Bonora's approach on a very small scale but resulted in a large PMI. On the other hand, Biogen's approach, on a scale of hundreds of grams, yielded a PMI of 62 and the solid-phase methods on industrial scales analyzed by Andrews[4] yielded a PMI of 200, despite the known sustainability challenges with SPOS. Thus, we expect that as methods are scaled up the PMI would further be reduced and the high PMI values calculated for VBM and RAM could be significantly reduced should they be scaled up and incorporate soluble supports.

Besides just analyzing the total amount of solvent used during the processes, we also analyzed the nature of solvents used. Certain solvents are regarded as more environmentally friendly for numerous possible reasons such as production from renewable feedstocks[18], energy demand from production, and safety[19]. The net cumulative energy demand (CED), which

considers the energy to produce a solvent and the energy that could be recovered by either incinerating or distilling it is a useful metric for assessing solvents. For example, the production of diethyl ether from naphtha mixtures actually results in a negative CED, while the production of toluene from pyrolysis of gasoline increased the CED by ~50%[20]. However, diethyl ether is generally one of the most avoided solvents by most solvent guides for industrial use due to high explosive risk and other potential safety hazards[21]. Thus, energy considerations and safety must both be considered when selecting solvents.

The worst offending solvent used in any of the above methods was diethyl ether, and almost every solvent guide recommends completely avoiding it[21]. The other solvents that had significant issues were DCM and pyridine. This places issue with Reese's approach, and our solution-phase, VBM, and RAM approaches which all rely on DCM as reaction solvents and for purification by column chromatography. While different reaction solvents could likely be determined, the use of purification by column chromatography still prevents these techniques from being easily scaled up. The use of pyridine is also generally recommended against, which similarly places issues on the four methods mentioned above. H-phosphonate couplings are usually carried out in pyridine, but likely could be carried out in other solvents should a base be present. The use of very small amounts of pyridine for VBM and RAM is still undesirable, but since it is such a small amount it could likely be dealt with on a larger scale.

The use of large volumes of diethyl ether for precipitation in Bonora's strategy almost certainly prevents the strategy from being directly scaled up. Changing the solvent used for precipitation from diethyl ether to methyl *tert*-butyl ether (MTBE) could help the process, but also poses challenges. Although only a small amount of it was used in Bonora's strategy, DCE is also regarded has a highly problematic solvent to work with[21]. The use of ACN as the reaction solvent is generally regarded as problematic, but it is already used on large scales in oligonucleotide synthesis and should not be an issue. Examining the solvents used in TCOS, the majority of solvent use is ethanol, which is highly recommended and can be produced from renewable feedstocks[22]. While regarded as problematic, the small amount of toluene used is likely acceptable as it has been classified with a similar risk as ACN[21]. Of all the strategies analyzed, TCOS is the only one that did not employ any solvents that are regarded as highly hazardous and to be avoided at all costs in industrial settings.

5.3: Conclusions and outlook

In this chapter we closely examined the sustainability of the methods developed in this thesis and benchmarked them against literature and industry reports. Our analysis showed the high PMI of some important strategies from the literature (Reese[6] and Bonora[11]) for synthesizing oligonucleotides in solution. Our own solution phase experiments showed much higher PMI to other solution-phase reactions that did not use any sort of support (Reese) likely due to the lower scale we used and lower yields we obtained. Unfortunately, the use of column chromatography in our synthesis by VBM or RAM also resulted in very high PMI values, despite reducing the solvent use during the reaction by 90% or more. For these strategies to be viable for the large-scale synthesis of longer oligonucleotides there would need to be two major improvements: 1) the yield would need to be much higher and 2) the use column chromatography for purification must be abandoned. The use of soluble supports in conjunction with these techniques for selective precipitation may be a strategy moving forward[23] and we expect that scaling up could further reduce the PMI. Large volumes of pyridine used for reactions by Reese and column chromatography also make this strategy difficult to scale up.

However, soluble supports also had their own issues. Particularly, Bonora's strategy using a PEG support resulted in a large PMI value due to the low loading capacity of the PEG used. The large volumes required to precipitate large amounts of PEG with micromolar amounts of oligonucleotide conjugated to it made this strategy untenable. Additionally, without reducing or eliminating the use of highly hazardous diethyl ether for precipitations, this strategy would have great difficulty in further scaling up. Our modification of the PEG-supported strategy for oligonucleotide synthesis by using temperature to facilitate reactions and purification reduced the PMI by over 90%. Furthermore, with careful solvent selection we were able to use mostly ethanol, a safe and green solvent, for the process, with a small amount of toluene. From our analysis, in their current forms, without significant process optimization, TCOS appears to be the only strategy analyzed that could be viable on a larger scale while also improving the sustainability of oligonucleotide synthesis.

5.4: Experimental

5.3.1: General information:

Solvents such as pyridine, dichloromethane (DCM), and methanol were purchased from Fisher Scientific. Nucleosides, nucleotides, and activating reagents (PEG, pivaloyl chloride, PTP, DCC, DBU, succinic anhydride, TFA, DMAP etc) were purchased from ChemGenes Corporation. All other chemicals were purchased from Sigma-Aldrich, Fisher Scientific, or TCI. Pyridine used for reactions was dried using 5Å molecular sieves. Reactions that required heating were heated in an oil bath. Mechanochemical reactions were performed on a FTS-1000 Shaker Mill and were performed using SmartSnapTM Grinding Jars, all purchased from FormTech Scientific. Reactions were performed in 30mL stainless steel SmartSnapTM Grinding Jars with one 10mm ball of the same material. RAM reactions were performed on a LabRAM I instrument from Resodyn. The custom-designed sample holder was made from Delrin Acetal Resin and RAM reactions were performed in 2.5mL polypropylene vials or 4mL clear glass vials. Both vials had dimensions of 15 mm x 45 mm x 8 mm (outer diameter, height, inner diameter, respectively). Solution-phase reactions that were air or moisture sensitive were carried out in oven dried glassware under an argon atmosphere. Thin-layer chromatography (TLC) was performed on 0.15-0.2 mm precoated silica gel (10-40µm) plates using UV light and heat as visualizing agents. Column chromatography was performed using silica gel 60 (40-63 µm) purchased from Silicycle. Yields refer to chromatographically and spectroscopically (^{1}H NMR) homogeneous samples. NMR spectra were recorded on Bruker-500 spectrometers and were calibrated using residual undeuterated solvent as an internal reference ($CDCl_3$ 1H NMR δ = 7.26 ppm) and ^{31}P NMR spectra were measured from 85% H_3PO_4 as an external standard. High-resolution mass spectra (HRMS) were recorded on a mass spectrometer under electron spray ionization (ESI) conditions.

5.3.2: Synthetic procedures

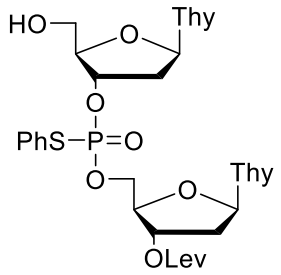

4

Solution-phase synthesis of 4:

1a (351 mg, 0.495 mmol) and **2a** (153 mg, 0.45 mmol) were dissolved in 10 mL of dry pyridine. While stirring, PvCl (0.28 mL, 2.25 mmol) was added in one portion. Once the reaction was complete by TLC analysis with DCM-MeOH as the eluent (95:5, v/v), PTP (126 mg, 0.495 mmol) was added and the mixture was allowed to stir for a further 15 minutes. Once the reaction was complete by TLC analysis with DCM-MeOH as the eluent (95:5, v/v), the reaction mixture was concentrated under reduced pressure and the crude residue was dissolved in 10 mL of DCM. While stirring, TFA (0.69 mL, 9 mmol) was added and the mixture turned dark orange. Approximately 10 mL of methanol was added with stirring until the solution was a clear, light orange color. After stirring for another 10 minutes and the reaction was complete by TLC analysis with DCM-MeOH as the eluent (95:5, v/v), the reaction mixture was concentrated under reduced pressure. The crude mixture was purified on a short silica gel column using DCM-MeOH as the eluent (gradient: 99:1 – 95:5 v/v). The appropriate fractions were combined and concentrated under reduced pressure to yield **4** as a white foam (239 mg, 72%). ^{31}P-NMR δP ($CDCl_3$) 24.45, 24.58. This product was not analyzed by HRMS, but was identical as previous samples of **4** by ^{31}P NMR and by TLC analysis (DCM-MeOH, 95:5).

VBM synthesis of 4:

The VBM coupling and sulfur-transfer was carried out exactly the same as in **Chapter 2** following general procedure **A** from that chapter using **1a** (351 mg, 0.495 mmol), **2a** (153 mg, 0.45 mmol), PvCl (0.28 mL, 2.25 mmol), and pyridine (0.36 mL, 4.5 mmol). The sulfur transfer step was carried out with PTP (126 mg, 0.495 mmol) and pyridine (0.18 mL, 2.25 mmol). After collecting the residue from the VBM jar, detritylation was carried out in the same way as above for the synthesis of **4** in solution. The crude mixture was purified on a short silica gel column

using DCM-MeOH as the eluent (gradient: 99:1 – 95:5 v/v). The appropriate fractions were combined and concentrated under reduced pressure to yield **4** as a white foam (225 mg, 68%). ^{31}P-NMR δP ($CDCl_3$) 24.49, 24.60. This product was not analyzed by HRMS, but was identical as previous samples of **4** by ^{31}P NMR and by TLC analysis (DCM-MeOH, 95:5).

RAM synthesis of 4:

The RAM coupling and sulfur transfer was carried out exactly the same as in **Chapter 2** following general procedure **A** from that chapter using **1a** (351 mg, 0.495 mmol), **2a** (153 mg, 0.45 mmol), PvCl (0.17 mL, 1.35 mmol), and pyridine (0.54 mL, 13.5 mmol). The sulfur transfer step was carried out with PTP (126 mg, 0.495 mmol). After collecting the residue from the VBM jar, detritylation was carried out in the same way as above for the synthesis of **4** in solution. The crude mixture was purified on a short silica gel column using DCM-MeOH as the eluent (gradient: 99:1 – 95:5 v/v). The appropriate fractions were combined and concentrated under reduced pressure to yield **4** as a white foam (259 mg, 78%). ^{31}P-NMR δP ($CDCl_3$) 24.26, 24.53. This product was not analyzed by HRMS, but was identical as previous samples of **4** by ^{31}P NMR and by TLC analysis (DCM-MeOH, 95:5).

TCOS synthesis of 14:

The synthesis of **14** was carried out the exact same way as described in **Chapter 4**.

5.4: References:

(1) Török, B.; Dransfield, T. Green chemistry: historical perspectives and basic concepts. In *Green Chemistry*, Elsevier, 2018; pp 3-16.

(2) Sheldon, R. A. Organic synthesis-past, present and future. *Chemistry and Industry* **1992**, (23), 903-906.

(3) Sheldon, R. A. The E factor 25 years on: the rise of green chemistry and sustainability. *Green Chemistry* **2017**, *19* (1), 18-43.

(4) Andrews, B. I.; Antia, F. D.; Brueggemeier, S. B.; Diorazio, L. J.; Koenig, S. G.; Kopach, M. E.; Lee, H.; Olbrich, M.; Watson, A. L. Sustainability challenges and opportunities in oligonucleotide manufacturing. *The Journal of Organic Chemistry* **2020**, *86* (1), 49-61.

(5) Featherston, A. L.; Kwon, Y.; Pompeo, M. M.; Engl, O. D.; Leahy, D. K.; Miller, S. J. Catalytic asymmetric and stereodivergent oligonucleotide synthesis. *Science* **2021**, *371* (6530), 702-707.

(6) Reese, C. B.; Yan, H. Solution phase synthesis of ISIS 2922 (Vitravene) by the modified H-phosphonate approach. *Journal of the Chemical Society, Perkin Transactions 1* **2002**, (23), 2619-2633.

(7) Reese, C. B.; Song, Q. A new approach to the synthesis of oligonucleotides and their phosphorothioate analogues in solution. *Bioorganic & Medicinal Chemistry Letters* **1997**, *7* (21), 2787-2792.

(8) Reese, C. The H-phosphonate approach to the synthesis of oligonucleotides and their phosphorothioate analogues in solution. *Journal of the Chemical Society, Perkin Transactions 1* **1999**, (11), 1477-1486.

(9) Klose, J.; Reese, C. B.; Song, Q. Preparation of 2-(2-cyanoethyl) sulfanyl-1H-isoindole-1, 3-(2H)-dione and related sulfur-transfer agents. *Tetrahedron* **1997**, *53* (42), 14411-14416.

(10) Garegg, P. J.; Lindh, I.; Regberg, T.; Stawinski, J.; Strömberg, R.; Henrichson, C. Nucleoside H-phosphonates. III. Chemical synthesis of oligodeoxyribonucleotides by the hydrogenphosphonate approach. *Tetrahedron letters* **1986**, *27* (34), 4051-4054.

(11) Bonora, G. M.; Biancotto, G.; Maffini, M.; Scremin, C. L. Large scale, liquid phase synthesis of oligonucleotides by the phosphoramidite approach. *Nucleic acids research* **1993**, *21* (5), 1213-1217.

(12) Reese, C. B.; Serafinowska, H. T.; Zappia, G. An acetal group suitable for the protection of 2′-hydroxy functions in rapid oligoribonucleotide synthesis. *Tetrahedron letters* **1986**, *27* (20), 2291-2294.
(13) Bonora, G. M.; Scremin, C. L.; Colonna, F. P.; Garbesi, A. HELP (High Efficiency Liquid Phase) new oligonucleotide synthesis on soluble polymeric support. *Nucleic acids research* **1990**, *18* (11), 3155-3159.
(14) Takahashi, D.; Inomata, T.; Fukui, T. AJIPHASE®: A Highly Efficient Synthetic Method for One-Pot Peptide Elongation in the Solution Phase by an Fmoc Strategy. *Angewandte Chemie* **2017**, *129* (27), 7911-7915.
(15) Zhou, X.; Kiesman, W. F.; Yan, W.; Jiang, H.; Antia, F. D.; Yang, J.; Fillon, Y. A.; Xiao, L.; Shi, X. Development of kilogram-scale convergent liquid-phase synthesis of oligonucleotides. *The Journal of Organic Chemistry* **2021**, *87* (4), 2087-2110.
(16) Donga, R. A.; Khaliq-Uz-Zaman, S. M.; Chan, T.-H.; Damha, M. J. A novel approach to oligonucleotide synthesis using an imidazolium ion tag as a soluble support. *The Journal of organic chemistry* **2006**, *71* (20), 7907-7910.
(17) Hassler, M. Advancements in the synthesis of oligoribonucleotides on solid support and in solution: Ionic soluble supports, blockmer ribonucleotide amidites, and orthogonal linkers. **2013**.
(18) Lomba, L.; Zuriaga, E.; Giner, B. Solvents derived from biomass and their potential as green solvents. *Current Opinion in Green and Sustainable Chemistry* **2019**, *18*, 51-56.
(19) Byrne, F. P.; Jin, S.; Paggiola, G.; Petchey, T. H.; Clark, J. H.; Farmer, T. J.; Hunt, A. J.; Robert McElroy, C.; Sherwood, J. Tools and techniques for solvent selection: green solvent selection guides. *Sustainable Chemical Processes* **2016**, *4*, 1-24.
(20) Capello, C.; Wernet, G.; Sutter, J.; Hellweg, S.; Hungerbühler, K. A comprehensive environmental assessment of petrochemical solvent production. *The International Journal of Life Cycle Assessment* **2009**, *14*, 467-479.
(21) Prat, D.; Hayler, J.; Wells, A. A survey of solvent selection guides. *Green Chemistry* **2014**, *16* (10), 4546-4551.
(22) Wyman, C. E. What is (and is not) vital to advancing cellulosic ethanol. *TRENDS in Biotechnology* **2007**, *25* (4), 153-157.
(23) Lönnberg, H. Synthesis of oligonucleotides on a soluble support. *Beilstein Journal of Organic Chemistry* **2017**, *13* (1), 1368-1387.

Chapter 6:

Contributions to knowledge

"It's about damn time."

- LeBron James

6.1: Contributions to knowledge and outlook

6.1.1: Development of an approach for DNA H-phosphonate coupling using vibration ball milling (Chapter 2)

In this chapter we developed a strategy for the coupling of DNA H-phosphonates using vibration ball milling (VBM). Initial efforts after optimization were successful in coupling H-phosphonates with nucleosides with free 5′-hydroxyl groups. However, we found the resulting H-phosphonate diester to be relatively unstable, particularly to basic aqueous conditions, and we were unable to isolate the products. The instability of H-phosphonate diesters is well-documented in the literature and we pivoted our strategy to avoid them. Thus, we adopted the modified H-phosphonate approach, developed by Colin Reese, and were able to oxidize the H-phosphonate diester to a phosphorothioate triester using a sulfur-transfer reagent, *N*-phenylthiophthalimide (PTP). Our optimized conditions, using AdaCl or PvCl as the activator and 10 equivalents of pyridine milling at 25 Hz for 15 minutes, followed by addition of 1.1 equivalents of PTP and 5 equivalents of pyridine and milling for another 15 minutes at 25 Hz allowed us to isolate fully protected DNA dimers in 70-80% yield over two steps. We also found in our screening of activators and conditions the use of a different activator, DPC, and reduced equivalents of pyridine allowed us to perform detritylation *in situ* and we were able to isolate 5′-hydroxyl DNA dimers in 60-70% yield over three steps.

We expanded this strategy to synthesize mixed-base trimers using the AdaCl activator resulting in the synthesis of the desired fully protected trimer in 72% yield. We also used the DPC activator to synthesize a 5′-hydroxyl trimer in 64% yield. In both cases we saw no drop off in yields as the sequence grew longer. We also showed how the thiophenyl protecting group on the backbone could be deprotected yielding a DNA dimer with a natural phosphodiester backbone in quantitative yield.

The work in this chapter represents the first use of mechanochemistry of any kind, to synthesize nucleic acids. The yields obtained were generally good over multiple steps and the solvent was reduced during the reactions by up to 90% by using stoichiometric amounts of pyridine, instead of bulk solvent.

6.1.2: Expansion of the vibration ball milling strategy to other nucleosides and chemical modifications (Chapter 3)

The work in this chapter expanded the general strategy developed in the previous chapter to a wider range of substrates and the synthesis of longer sequences. We were first able to deprotect the 3′-levulinyl protecting group of the fully protected dimers synthesized in the previous chapter and phosphonylate them using DPHP to yield DNA dimer H-phosphonates in 60-70% yield over two steps. Using these dimers were able to use the same conditions developed for vibration ball milling and synthesize a tetramer by a block coupling (dimer + dimer, or 2+2) approach in good yield (83%) followed by the synthesis of a hexamer by the same approach also in good yield (74%). We also used the same approach to synthesize DNA dimer phosphoramidites, which we envision combining with solid-phase synthesis methods to synthesize longer oligonucleotides with greater ease.

We then expanded the strategy to include common chemical modifications of nucleosides that used in therapeutic oligonucleotides. We were able to synthesize dimers containing 2′OMe and 2′F residues at different positions. We also expanded the strategy to RNA and found with the chemically modified nucleosides and RNA the yields to be in a similar range (66-73%) to the DNA couplings performed in the previous chapter. Finally, we continued to adapt Reese's approach and changed the sulfur transfer reagent such that the final product after deprotection would be a phosphorothioate backbone instead of the natural phosphodiester backbone. While we had difficulties in synthesizing the specific reagent used by Reese, we were able to synthesize a different reagent that provided the desired backbone and the fully protected dimer was isolated in good yield (62%).

The work in this chapter built upon the vibration ball milling strategy developed in the previous chapter, but expanded it to a much wider range of substrates. In particular, the expansion to 2′OMe, 2′F, and PS backbones, which are all commonly used in therapeutic oligonucleotides, demonstrates the versatility of the strategy. The use of the block-coupling approach to synthesize a hexamer also highlights the ability of the strategy to be applied for longer sequences. While the approach developed in these two chapters reduced solvent consumption by up to 90% during reactions, the use of column chromatography for purifications still resulted in large volumes of solvent being required. Further methods for scaling up,

improving the yield, and improving the purification process are still required. Nonetheless, these methods represent the first use of mechanochemistry for the synthesis of nucleic acids and represent an important step forward towards addressing the sustainability challenges of oligonucleotide synthesis.

6.1.3: Development of an approach for DNA H-phosphonate coupling using resonant acoustic mixing (Chapter 4)

In this chapter, we continued to develop novel methods for the synthesis of oligonucleotides. The first part of the chapter focused on our development of a strategy for the synthesis of oligonucleotides using resonant acoustic mixing, a highly efficient mixing process which has only recently been applied to bond-forming reactions. Using the same chemistry developed in **Chapter 2**, we optimized the conditions for using resonant acoustic mixing for the synthesis of DNA dimers and trimers. By reacting DNA H-phosphonates with protected nucleosides in the presence of AdaCl and PvCl and 15 equivalents of pyridine at 60*g* for 15 minutes, followed by addition of 1.1 equivalents of PTP and further reaction at 60*g* for 5 minutes, we were able to synthesize fully protected DNA dimers in good yields (81-90%).

Using resonant acoustic mixing, we were also able to successfully scale up the reaction from 0.2 mmol scale first to a 1 mmol scale then to a 2 mmol scale and were able to isolate the products in good yield (74% and 77%, respectively). We also adapted the strategy in a similar way to **Chapter 2** and were able to synthesize a DNA trimer in good yield (79%).

Not only does the work here represent the first use of resonant acoustic mixing for the synthesis of nucleic acids, it represents one of the first uses of resonant acoustic mixing for any bond-forming reactions, of which there are only a handful of publications. Similarly to **Chapters 2** and **3**, the solvent volume was reduced by up to 90% during reactions, but the use of column chromatography for purification presents a challenge for this strategy. However, the demonstrated scalability of resonant acoustic mixing presents potential for this strategy, while it is not clear how straightforward scaling of vibration ball milling would be.

6.1.4: Development of an approach for PEG-supported DNA H-phosphonate coupling and purification using thermal control (Chapter 4)

The second part of this chapter focused on the development of a completely new method for the synthesis of oligonucleotides on a PEG support. Given the large volumes of solvent consumed during purification of the previous strategies, we developed a strategy that could reduce the solvent consumption during purification. Taking advantage of the physical properties of PEG, we developed a synthesis cycle where a nucleoside-PEG conjugate could be melted at elevated temperatures, followed by conducting the reaction in solution. Once the reaction was complete, cooling the reaction allowed for the nucleoside-PEG conjugate to precipitate, leaving all other reagents in solution, and the reaction was purified by filtration. In contrast to other strategies using soluble supports for oligonucleotide synthesis, this approach relied almost entirely on controlling the temperature for purification, with minimal solvents required.

We synthesized the PEG-nucleoside and determined that it maintained the physical properties of PEG, and we were able to melt it at 75°C. We subjected the PEG-nucleoside to multiple rounds of heating and cooling to determine its stability and found no evidence of degradation after four such cycles. To synthesize oligonucleotides, we started with removal of the 5′DMTr protecting group. Monitoring the reactions by ^{1}H NMR, we found detritylation was quantitative following this strategy with no evidence of the DMTr group being present after purification by filtration. Using the same modified H-phosphonate approach, we found coupling to be highly efficient (99% by ^{1}H NMR) and recovery of the product was also very high (98%). Analysis of the product by ^{31}P NMR also indicated the exclusive formation of the desired dimer. The cycle was repeated and a trimer was synthesized, although the yield of the second coupling was slightly lower (93%).

The strategy developed here represents a completely new method for the synthesis of oligonucleotides. Initial coupling was nearly quantitative, but dropped slightly when moving to a the trimer, but with some further optimization we expect the average coupling yield to remain very high. Detritylation was also highly effective and found to be quantitative on both the monomer and dimer. Importantly, this strategy required only very small volumes of solvent to yield the desired short oligonucleotides in high yield, purity, and recovery. We also expect this

method to be straightforward to scale up due to the liquid-phase reaction conditions amenable to batch reactors.

6.1.5: Analysis of the sustainability of the methods developed compared to traditional methods for oligonucleotide synthesis (Chapter 5)

This chapter focused on analyzing and quantifying the sustainability of the three methods developed in this thesis. We performed analogous solution-phase reactions to those performed by VBM, RAM, and TCOS, as well as analyzing some reactions from the literature to compare our methods. We focused primarily on the process mass intensity, or PMI, of the solvents consumed during the different strategies as a metric of the sustainability. We generally ignored the masses of reagents as they were more or less the same across all the strategies.

Our analysis showed that VBM (4502), RAM (3911), and our solution-phase (4280) reaction resulted in extremely large PMI values. However, Bonora's strategy which also used a PEG support for oligonucleotide synthesis in solution, also resulted in a very large PMI (3073) due to the large volumes of solvent used during precipitations. Reese's strategy, using the modified H-phosphonate approach in solution, but no soluble support, resulted in a large PMI (906), but still significantly less than by VBM, RAM, our solution-phase, or Bonora's strategy. However, we found TCOS to have by far the lowest PMI (220) compared to the other strategies, due to the reduction of solvent used during the reaction and the avoidance of solvents during purification, where temperature was the main driving force based on careful solvent choice. Compared to large-scale solid-phase synthesis (200), all methods still resulted in higher PMI values.

We noted that the consumption of solvent is likely not linear with the scale and thus skewed the PMI analysis in favor of the larger-scale methods (Reese, SPOS). When we ignored the solvent consumption required for column chromatography and recalculated the PMI for our solution-phase method (107), VBM (70), RAM (60), and Reese's method (252), we found Reese's strategy to be much higher than all three of our methods. We also looked at another large-scale solution-phase synthesis of oligonucleotide, done by Biogen, and found their PMI (62) to confirm that scaling up actually reduced the average PMI. Despite this, TCOS still compared favorably to those other methods while operating at a small scale.

Based on this analysis, we determined that for VBM and RAM to be viable approaches for oligonucleotide synthesis, column chromatography must be avoided. The use of column chromatography skyrocketed the PMI of these two methods, and the adoption of soluble supports with these strategies may be viable to improve the PMI. We also expect that scaling up the different methods could help to improve the PMI as our analysis of different strategies at larger scale consistently resulted in lower PMI values.

6.2: List of publications and patents

1. McKenzie, L. K.; El-Khoury, R.; **Thorpe, J. D.**; Damha, M. J.; Hollenstein, M. Recent progress in non-native nucleic acid modifications. Chemical Society Reviews 2021, 50 (8), 5126-5164

2. **Thorpe, J. D.**; O'Reilly, D.; Friščić, T.; Damha, M. J. Mechanochemical synthesis of short DNA fragments. Chemistry–A European Journal 2020, 26 (41), 8857-8861.

3. A method for the synthesis of oligonucleotides. **Thorpe, J. D.**; O'Reilly, D.; Friščić, T.; Damha, M. J. Provisional US patent filed in May 2021.

6.3: Publications and patents in preparation

1. Thermally Controlled Oligonucleotide Synthesis (TCOS). **Thorpe, J. D.**; Filipponi, P.; Haber, J.; Damha, M. J.

2. Synthesis of short oligonucleotides by mechanochemistry. **Thorpe, J. D.**; Friščić, T.; Damha, M. J.

3. Resonant acoustic mixing (RAM) for the synthesis of short DNA fragments. **Thorpe, J. D.**; Marlyn, J.; Damha, M. J.

4. Recent advances in the chemical synthesis of oligonucleotides. **Thorpe, J. D.**; Damha, M. J.

5. Report of invention for RAM synthesis of short DNA fragments in preparation.

6. Report of invention for TCOS in preparation.

6.4: List of conference presentations

1. “Towards Developing Greener Methods for Oligonucleotide Synthesis.” **Thorpe, J. D**.; Damha, M. J. Oligonucleotide Therapeutics Society Webinar. Virtual talk. March 2023.

2. “Mechanochemistry: Reducing the Solvent Footprint of Oligonucleotide Synthesis”. **Thorpe, J. D**.; Damha, M. J. 18th Annual Meeting of the Oligonucleotide Therapeutics Society. Poster. October 2022.

3. “Scalable Synthesis of DNA and RNA Oligomers Using Mechanochemistry”. **Thorpe, J. D**.; Damha, M. J. 17th Annual Meeting of the Oligonucleotide Therapeutics Society. Virtual talk. October 2021. *Best talk award, Next-Gen Session.*

4. “Scalable Synthesis of DNA Building Blocks and Oligomers Using Mechanochemistry”. **Thorpe, J. D**.; Damha, M. J. XXIV International Roundtable on Nucleosides, Nucleotides, and Nucleic Acids. Virtual poster. August 2021.

5. “Scalable Synthesis of DNA Building Blocks Using Mechanochemistry”. **Thorpe, J. D**.; Friščić, T.; Damha, M. J. 104th Canadian Chemistry Conference and Exhibition. Virtual poster. June 2021.

6. “Greener synthetic approaches to DNA and RNA building blocks”. **Thorpe, J. D**.; O'Reilly, D.; Friščić, T.; Damha, M. J. 102nd Canadian Chemistry Conference and Exhibition. Short talk. June 2019.